Investigating the Structure and Function of PEPITEM, a Novel Inhibitor of T cell Transmigration

By

Bonita Harriet Radha Apta

A thesis submitted to

The University of Birmingham

for the degree of

DOCTOR OF PHILOSOPHY

School of Clinical and Experimental Medicine

College of Medical and Dental Sciences

University of Birmingham

October 2015

UNIVERSITY OF
BIRMINGHAM

University of Birmingham Research Archive

e-theses repository

This unpublished thesis/dissertation is copyright of the author and/or third parties. The intellectual property rights of the author or third parties in respect of this work are as defined by The Copyright Designs and Patents Act 1988 or as modified by any successor legislation.

Any use made of information contained in this thesis/dissertation must be in accordance with that legislation and must be properly acknowledged. Further distribution or reproduction in any format is prohibited without the permission of the copyright holder.

Abstract

Peptide inhibitor of trans-endothelial migration (PEPITEM) is a B cell-secreted peptide which inhibits T cell trafficking across cytokine-stimulated endothelium. This homeostatic mechanism is lost in autoimmune and chronic inflammatory diseases, leading to inappropriate T cell trafficking with pathological consequences, e.g. in type-1 diabetes and rheumatoid arthritis. We aimed to investigate the structure and function of PEPITEM *in vitro* and *in vivo* to establish its pharmacokinetics, therapeutic potential, and underlying molecular mechanisms.

The efficacy of PEPITEM was verified, showing the same regulatory control of T cell trafficking as previously reported. Nuclear magnetic resonance (NMR) studies revealed PEPITEM to be a linear peptide lacking secondary structure. Intravenous administration of radiolabelled native PEPTEIM in wild-type mice showed rapid clearance by the renal circulation, conferring a circulatory half-life of <2 minutes. Common conjugation strategies employed to modify PEPITEM, e.g. PEGylation, did not affect peptide function, demonstrating its potential for therapeutic development. The evolution of PEPITEM from its parent protein, 14-3-3ζ was investigated. PEPITEM is probably cleaved from 14-3-3ζ by matrix metalloproteinase 9 extracellularly after exocytosis from B cells. Interestingly, this generates a 17aa peptide which requires additional proteolytic processing to evolve a smaller biologically active pharmacophore.

These observations add to our current knowledge of the PEPITEM paradigm, which appears central to regulated trafficking of T cells. Future work will formulate new PEPITEM versions with suitable pharmacological profiles, and screen them for function *in vitro* and *in vivo* to develop suitable therapeutic agents.

Acknowledgements

I would firstly like to thank my Supervisor Professor G. Ed Rainger for allowing me the opportunity to work on this exciting project, for patiently guiding me thorough my PhD and, annoyingly, for always being right.

Additionally I thank my Co-Supervisor Dr. Trish Lalor for all the advice and support which you have been so kind as to give me.

Naturally I thank the BBSRC for their generous funding throughout my PhD.

I express my gratitude to Dr. Helen McGettrick, Dr. Myriam Chimen and Dr. Matthew Harrison for your endless help over the last 3 years.

I am grateful for the help of Dr. Carrie Willcox, Dr. Mark Jeeves, Dr. Gillian Grafton and Dr. Ashley Martin, who have generously spared their time for me.

I thank the Conner lab for all the help with troubleshooting, and for your comments, which were much appreciated.

Thank you to all of my colleagues in the IBR that have contributed to this project, and to those, especially Kab, Hafsa, Jas, Lewis, Phil and Arjun, that have made my PhD an unforgettable experience.

Emma, I don't have to say anything for you to know how glad I am to have a best friend like you. And Mike, thank you for putting up with me and my strange habits!

Last but certainly not least, I thank my family for always encouraging, supporting and inspiring me. Mum and Dad, I dedicate this to you.

Contents

List of Figures

List of Tables

List of Abbreviations

14-3-3 β/ε/γ/η/σ/t/ζ	14-3-3 beta/epsilon/gamma/eta/sigma/tau/zeta
^{1}H	Proton
^{3}H	Tritiated
AA	Arachidonic acid
ACN	Acetonitrile
AF680	Alexafluor 680
ANOVA	Analysis of variance
APC	Allophycocyanin
apoE	Apolipoprotein E
AQ	Adiponectin
AR1/2	Adiponectin receptors 1 and 2
BCR	B cell receptor
Breg	Regulatory B cell
BSA	Bovine serum albumin
BSE	Bovine spongiform encephalopathy
CAM	Cell adhesion molecule
CD	Cluster of differentiation
CDH15	Cadherin 15/ M cadherin
CDPA	Citrate phosphate dextrose adenine
CI	Calcium ionophore
CID	Collision-induced dissociation
CDJ	Creuzfeldt-Jakob's disease
COX	Cyclooxygenase
CSF	Cerebrospinal fluid
CT	Threshold cycle
CTL	Cytotoxic T cells
CVD	Cardiovascular disease
Da	Daltons
DAMPs	Danger associated molecular patterns
DC	Dendritic cells
dH_2O	Distilled water
dNTPs	Deoxyribonucleotide triphosphate
DP_2	Prostaglandin receptor 2
DPM1	Disintegrations per minute
EC	Endothelial cells
ECD	N-(3-dimethylaminopropyl)-N'-ethylcarbodiimide hydrochloride
EDTA	Ethylenediaminetetraacetic acid
EIC	Extracted ion chromatogram
EPA	Eicosapentaenoic acid
ETD	Electron Transfer Dissociation
FCS	Foetal calf serum
FFPE	Formalin-fixed paraffin embedded
FITC	Fluorescein isothiocyanate

FoxP3	Forkhead box P3
GLP-1	Glucagon-like peptide-1
GPCR	G-protein coupled receptor
H&E	Haematoxylin and eosin
HDBEC	Human dermal blood microvascular endothelial cells
HDMEC	Human dermal microvascular endothelial cells
HEVs	High endothelial venules
HFD	High fat diet
HIS	Histidine tag
HLA	Human leukocyte antigen
H^N	Amide proton
HPLC	High performance liquid chromatography
HUVEC	Human umbilical vein endothelial cells
ICAM-1	Intracellular adhesion molecule-1
IFN-γ	Interferon gamma
Ig	Immunoglobulin
IL	Interleukin
IP	Intraperitoneal
iTreg	Induced regulatory T cell
IV	Intravenous
IVIS	*In vivo* imaging system
JAM	Junctional adhesion molecule
kDa	Kilodaltons
LFA-1	Lymphocyte function-associated antigen-1
LN	Lymph node
LPS	Lipopolysaccharide
m/z	Mass / charge ratio
MALT	Mucosa-associated lymphoid tissue
MHC I/II	Major histocompatibility complex I/II
MMP	Matrix metalloproteinase
NHS	N-hydroxysuccinimide
NK	Natural killer cell
NMR	Nuclear magnetic resonance spectroscopy
NOE	Nuclear Overhauser effect
NS	Not significant
NTA	Nitrotriacetic acid
nTreg	Natural regulatory T cell
$p/s/cm^2/sr$	Photons per second per centimetre squared per steradian
PAMP	Pathogen associated molecular pattern
PBL	Peripheral blood lymphocytes
PBMC	Peripheral blood mononuclear cells
PBS	Phosphate buffered saline
PECAM-1	Platelet endothelial cell adhesion molecule-1
PE-Cy7	Phycoerythrin Cyanine 7
PEG	Polyethylene glycol

PEPITEM	Peptide inhibitor of trans-endothelial migration
PGD_2	Prostaglandin D_2
PIC	Protease inhibitor cocktail
PMN	Polymorphonuclear leukocytes
PNAd	Peripheral lymph node addressin
PROSPER	Protease substrate specificity webserver
PRRs	Pattern recognition receptors
PSGL-1	P-selectin glycoprotein ligand-1
qPCR	Quantitative PCR
RA	Rheumatoid arthritis
RBC	Red blood cell
RDI	Reverse D-isomerisation
RFU	Relative fluorescence units
RIPA	Radioimmunoprecipitation assay buffer
RMSD	Root-mean-square deviation
ROE	Rotating-frame NOE
ROESY	Rotating frame Overhauser Effect Spectroscopy
ROI	Region of interest
ROS	Reactive oxygen species
RU	Response units
S1P	Sphingosine 1 phosphate
S1P1/4	Sphingosine 1 phosphate receptors 1 and 4
S1PK1/2	Sphingosine 1 phosphate kinase 1 and 2
S1PR1-5	Sphingosine 1 phosphate receptors 1 to 5
SA	Streptavidin
SCID	Severe combined immunodeficiency
SCR	Scrambled peptide
SDS-PAGE	Sodium dodecyl sulfate polyacrylamide gel electrophoresis
SEM	Standard error of the mean
SLOs	Secondary lymphoid organs
SPNS2	Spinster homolog 2
SPR	Surface plasmon resonance
T1D	Type 1 Diabetes
Tcm	Central memory T cell
Tem	Effector memory T cell
TFA	Trifluoroacetic acid
TGFβ	Transforming growth factor beta
T_H1	T helper 1
T_H2	T helper 2
TLR4	Toll like receptor 4
T_M	Memory T cell
TNF-α	Tumour necrosis factor alpha
TOCSY	Total Correlation Spectroscopy
Treg	Regulatory T cell
TSP-1	Thrombospondin-1
VCAM-1	Vascular cell adhesion protein 1

VE cadherin	Vascular endothelial cadherin
VLA-4	Very late antigen-4
WBC	White blood cell
WT	Wild-type

CHAPTER 1: GENERAL INTRODUCTION

1.1. An overview of the Immune system

As early as 430 BC, the principle of immunity was observed by Athenian historian Thucydides, who noted that only nurses who had successfully recovered from the offending Plague of Athens were able to tend to the sick without subsequent infection (Thucydides *et al.*, 1910). Innovative scientists such as Edward Jenner, Louis Pasteur, Robert Koch and Elie Metchnikoff have since pioneered immunology as we know it today.

In this general introduction, the immune system and the process of inflammation will be explored in the context of both health and disease. This thesis will interrogate the structure, function and pharmacokinetics of a novel peptide termed PEPITEM, which inhibits T cell transmigration. Its relevance in immunity and potential for therapeutic application in immunological disease will be explored.

The immune system is a multifaceted, highly specialised and intricately co-ordinated network of tissues, cells, molecules and proteins. Evolved over millions of years, it works dynamically to provide defence against disease, and this is essential for host survival.

1.1.1. The function of the immune system

The two principle activities of the immune system are recognition and response to malady. Immune recognition is the ability to determine ‘self’ from ‘non-self’. Through this aptitude, the immune system is able to distinguish pathogens such as bacteria or parasites from our own cells, self-molecules from non-self molecules

such as bacterial toxins, and even our own virally infected or cancerous cells, from healthy cells. The immune response is the ability to neutralise a threat to the host. This ability to respond to threats enables us to eliminate pathogens including viruses, bacteria and parasites, neutralise molecules such as toxins and bacterial proteins, and carefully remove our own diseased cells (Owen *et al.*, 2007).

1.1.2. Leukocytes

"Leukocyte" is the collective term for a white blood cell (WBC). Leukocytes, along with red blood cells (RBC) and platelets, are produced in the bone marrow through haematopoiesis. During this process, haematopoietic stem cells can give rise to lymphoid progenitor cells or myeloid progenitor cells, eventually differentiating down several lineages (Figure 1.1). While the lymphoid lineage produces B and T lymphocytes and natural killer (NK) cells , the myeloid lineage results in erythrocytes, platelets, basophils, eosinophils, neutrophils and monocytes. Both lineages have the capacity to produce dendritic cells (DC), (Owen *et al.*, 2007).

1.1.3. Innate and adaptive immunity

The immune system can be separated into two distinct yet allied systems; innate and adaptive immunity. The main differences are summarised in Table 1.1. The innate immune system can be considered the first line of defence, which kicks into action immediately following an insult. Although specificity is limited, innate immunity is crucial for defence against bacterial pathogens. This is highlighted in

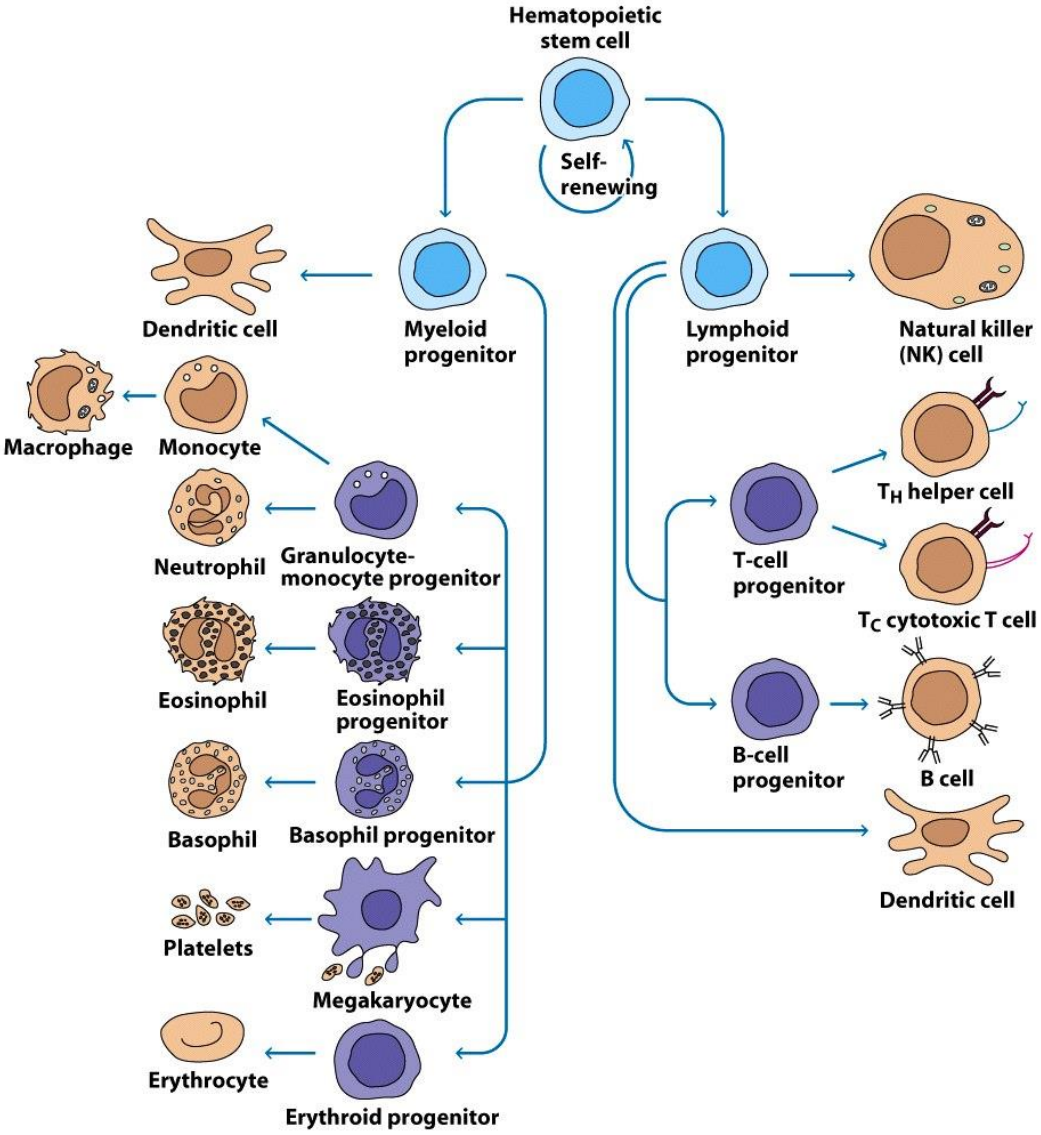

Figure 1.1. Leukocyte production by haematopoiesis.
Self-renewing hematopoietic stem cell progenitors can differentiate down the myeloid or lymphoid lineages. These discrete lineages can give rise to a number of cell types, each with their own specific immunological functions. Adapted from Owen *et al.* (2007).

Table 1.1. Innate vs Adaptive Immunity.
The immune system can be divided into two distinguished parts. Here, the main differences between these two allied systems are compared. Adapted from Owen *et al.* (2007).

Feature:	Innate immunity:	Adaptive immunity:
Response time	Hours	Days
Main components	Physical barriers, phagocytes	Lymphocytes
Soluble factors	Cytokines, complement, acute phase proteins	Cytokines, antibodies
Specificity	Limited	Diverse and improving
Response to 2^{o} infection	Same as response to initial infection	Faster, more specific

diseases such as chronic granulomatous disease, where phagocytic cells including neutrophils have a genetic defect in the oxidative pathway used to generate reactive oxygen species (ROS), such as hydrogen peroxide (Owen *et al.*, 2007). This defect leads to an inability to kill phagocytosed pathogens, and therefore persistent bacterial and fungal infections. The innate immune system responds to antigens through a series of pattern recognition receptors (PRRs) which recognise pathogen-associated molecular patterns (PAMPs) and danger-associated molecular patterns (DAMPs). These molecular patterns are highly conserved structural motifs expressed by pathogens or released following damage for PAMPs and DAMPs respectively (Newton and Dixit, 2012).

The adaptive immune system supports the innate immune system with a more tailored immune response. This response, although slower, is more specific and thus

more effective at clearing pathogens. In adaptive immunity, B cells and T cells play a central role and this will be discussed further in sections 1.2 and 1.3. The importance of adaptive immunity is emphasised by research in athymic “nude” mice, which under normal living conditions have a high mortality rate. This is due to the lack of thymus (Flanagan, 1966), and thus T cells (De Sousa *et al.*, 1969), leading to a deficiency in cell-mediated immunity and antibody production.

Antigen presenting cells (APC) bridge innate and adaptive immunity. They provide a means by which the innate immune compartment can communicate with the adaptive compartment, activating T cells and B cells and initiating the adaptive immune response (Owen *et al.*, 2007). Ultimately, for a fully functional immune system, both the innate and adaptive counterparts are required.

1.2. T cells

T cells form an essential part of adaptive immunity, providing cell-mediated defence against disease. With a whole host of T cell subsets, these lymphocytes are dedicated to the eradication of a multitude of diseases and the regulation of immune responses. Here, the role of T cells will be explored in more detail.

1.2.1. Generation

T cells originate in the bone marrow from haematopoietic progenitor cells, and differentiate down a lymphoid lineage before migrating to the thymus, a primary lymphoid organ. Here, they mature and are educated by the thymic stroma through positive and negative selection. During this process, T cells are tested according to

their integral ability to distinguish self from non-self, thus ensuring self-tolerance (Moroy and Karsunky, 2000, Owen *et al.*, 2007).

Upon maturation, T cells express the T cell receptor (TCR) cluster of differentiation 3 (CD3), and either the co-receptor cluster of differentiation 4 (CD4) or cluster of differentiation 8 (CD8). They are released into the periphery as naïve T cells where they recirculate every 12-24 hours (Owen *et al.*, 2007). These T cells are poor at responding to antigen, but are able to migrate well to lymphoid organs such as lymph nodes.

Naïve T cells circulate continuously between the lymphatic system consisting of complex structures where immune cell trafficking, meetings and surveillance takes place. The lymphatic system comprises a network of vessels and capillaries which carry fluid called lymph formed when plasma, under blood pressure, leaves capillaries, permeates tissues and then drains into lymphatic vessels and is eventually returned to the blood. This extensive network of vessels connects lymphoid organs, allowing movement of T cells and other WBC between the lymph and the blood. Naïve T cells express adhesion molecule L-selectin (CD62L), C-C chemokine receptor type 7 (CCR7) and the β2 integrin lymphocyte function-associated antigen 1 (LFA-1). Expression of these molecules aids specific homing to the glycoprotein peripheral node addressin (PNAd), chemokine (C-C motif) ligand 21 (CCL21) and intercellular adhesion molecule-1 or 2 (ICAM-1/2) respectively, expressed by post-capillary high endothelial venues (HEVs), facilitating entrance to lymph nodes (Weninger *et al.*, 2001).

1.1.2. Activation and recruitment

During circulation, T cells continuously survey the body for specific antigens. Antigen presenting cells such as DCs and macrophages constitutively take up antigen from inflamed tissue, process them, and bring them back to secondary lymphoid organs (SLOs) such as lymph nodes (LNs), the spleen and mucosa-associated lymphoid tissue (MALT), where T cell traffic is frequent. Antigen-specific T cells recognise cognate non-self antigens presented to them by APCs in the context of major histocompatibility complex (MCH) class I and II for $CD8^+$ and $CD4^+$ T cells respectively. Subsequent activation is triggered via two signals – (i) through the binding of CD3 to an MHC-antigen complex, and (ii) through the binding of co-stimulatory molecule CD28 on T cells to cognate receptors on activated APCs such as CD86 or CD80 (Jensen, 2007). Following activation, T cells up-regulate the expression of proliferation-promoting cytokine interleukin (IL)-2, undergo clonal expansion and differentiate into memory and effector cells. Memory T cells and effector T cells have distinct trafficking patterns achieved through differential expression of specific cell adhesion molecules such as selectins (Ley and Kansas, 2004). This enables T cells to be recruited to the right place at the right time, and perform desired effector or regulatory functions.

1.1.3. T cell subsets and function

Following activation, T cells can be divided in to 2 main groups; effector T cells and memory T cells. These subsets have specific functions, and their characteristics reflect this. Other T cell subsets include regulatory T cells, and their functions will be discussed below.

1.1.3.1. Effector T cells

Effector T cells conduct specialist functions and can be further divided into $CD4^+$ T helper (T_H) cells (T_H1 or T_H2), and $CD8^+$ cytotoxic T cells (CTL). T_H1 play a key role in cell-mediated immunity and CTL activation, and can polarise the immune response towards defence against pathogens through the secretion of IL-2, interferon gamma (IFN-γ) and tumour necrosis factor alpha (TNF-α), (Owen *et al.*, 2007). These cytokines are then able to activate other leukocytes such as neutrophils and macrophages (Broere *et al.*, 2011). On the other hand, T_H2 provide the response to extracellular pathogens and provoke allergic responses through secretion of IL-3, IL-4, IL-5 and IL-6, and are able to co-ordinate humoral immunity through the activation of B cells (Owen *et al.*, 2007). CTL possess cytotoxic killing activity and are important in the removal of damaged or virus infected cells by their ability to recognise abnormal self-antigens presented to them in MHC class I-antigen complexes. Following recognition of a damaged cell e.g. a cancer cell, CTLs destroy the target cell either though cell lysis via the release of cytotoxic proteins, or through the induction of apoptosis mediated by the binding of CTL Fas ligand to target cell Fas receptors (Owen *et al.*, 2007).

1.1.3.2. Memory T cells

Following the restoration of homeostasis, most T cells undergo apoptosis. However, a small proportion remain and differentiate into memory T cells (Kaech *et al.*, 2002). This memory T cell (T_M) population of antigen-experienced cells have the capacity to mount faster and more specific secondary immune responses following

subsequent recognition of the same antigen. These cells can be divided into two types with distinct functions; central memory (T_{CM}) and effector memory T cells (T_{EM}).

T_{CM} reside in secondary lymphoid organs and despite having limited effector function, are capable of expert proliferation and differentiate into effector cells in response to antigen. Reflecting this, these cells have high expression of L-selectin and C-C chemokine receptor type 7 (CCR7), required for re-circulation, and can produce pro-proliferative cytokine IL-2 but are poor at producing pro-inflammatory cytokine IFN-γ (Kaech *et al.*, 2002). Conversely, T_{EM} occupy the periphery, and possess advanced effector functions in inflamed tissues in response to antigen (Sallusto *et al.*, 2004). Again, this is reflected by the low expression of L-selectin and the absence of CCR7. Instead, these cells are highly capable of producing IFN-γ, but poor at producing IL-2 (Kaech *et al.*, 2002).

1.1.3.3. Regulatory T cells

Regulatory T cells (T_{reg}), as the name suggests, represent a population of T cells which regulate the function of many immune cells and play an important role in the maintenance of self-tolerance within the immune system. T_{regs} can be induced in the periphery (iT_{reg}) following activation, or develop naturally in the thymus (nT_{reg}), and recognise self-antigens to facilitate the maintenance of self-tolerance (Pacholczyk and Kern, 2008). They express the surface marker CD25 (Sakaguchi *et al.*, 1995) also present on activated T cells, but a more specific marker of T_{reg} is the transcription factor forkhead box P3 (FoxP3, Hori *et al.* (2003)). Upon activation, T_{reg} suppress other T cells (Tang and Bluestone, 2008) by mopping up available pro-proliferative cytokine IL-2 produced during inflammation, secreting anti-inflammatory

cytokines such as IL-10 and transforming growth factor beta (TGF-β), and inducing apoptosis in responding T cells (Shevach, 2009). T cells can also act indirectly on T cell performance by down-modulation of APC function, for example by, suppressing antigen presentation (Sakaguchi *et al.*, 2009).

1.3. B cells

B cells, defined by their expression of the B cell receptor (BCR), play a fundamental role in the humoral immune response, with their primary functions being to produce antibody and serve as APCs. The role B cells play in adaptive immunity will be explored in more detail here.

1.3.1. Generation

B cells, like T cells, are derived from haematopoietic progenitor cells in the bone marrow. However, unlike T cells, B cells remain there during initial stages of maturation. The generation of B cells requires the unique microenvironment provided by the bone marrow stroma, which supports the maturation of B cells through the secretion of cytokines such as IL-7 (Engel *et al.*, 2011).

Developing B cells express surface antibodies in the form of surface immunoglobulin (Ig) IgM (Engel *et al.*, 2011). This Ig is produced through the rearrangement of the genes coding for the heavy chain and light chains of the Ig to produce a unique, functional BCR complex, capable of recognising antigen presented by APCs in MHC I (Owen *et al.*, 2007). During development, deletion of

auto-reactive B cells by negative selection occurs in the bone marrow, mediated by the stroma and helps to prevent autoimmunity (Engel *et al.*, 2011). However evidence has suggested that B cells can also arrest and re-arrange the light chain genes of their B cell receptor (Shevach, 2009). After successful passage of this checkpoint, B cells are released into the periphery at a rate of approximately 5 million per day, and begin to circulate, maturing into naïve B cells expressing CD19, IgM, and, after entering SLOs, IgD on their surface (Engel *et al.*, 2011, LeBien, 2000).

1.3.2. Activation and recruitment

Naïve or resting B cells can be activated in a thymus-dependent or thymus independent manner; that is, in the presence or absence of T cells respectively. An example of the latter is the activation of B cells by lipopolysaccharide (LPS), a component of the cell wall of gram-negative bacteria. LPS binds both its receptor toll-like receptor 4 (TLR4) and the BCR on the B cell surface. The ligation of these two receptors causes the subsequent activation of the B cell and differentiation into short-lived plasma cells which secrete IgM, but are low-affinity and cannot generate memory cells (Fagarasan and Honjo, 2000). Despite this, these B cells are integral to fast immune responses against pathogens.

T cells play an essential role in B cell responses to antigen, which occur in SLO such as LN (Engel *et al.*, 2011). Following the recognition of specific antigen by the BCR, the BCR-antigen complex is internalised by receptor-mediated endocytosis (Owen *et al.*, 2007). It is subsequently processed into smaller peptides, which are presented at the membrane as peptide-MHC II complexes. The co-stimulatory molecule B7 is also up-regulated, as well as MHC II. This initial signal causes the B

cells to migrate to follicles in the periphery of SLOs (Engel *et al.*, 2011), where they interact with T_H to become fully activated.

Initially, antigen-specific TCR on T cells recognises cognate antigen presented by the B cell in the context of MHC II. This interaction, along with the ligation of B cell CD80/CD86 to T cell CD28 as described in section 1.1.2, activates the T_H cell. Once activated, T_H cells express the ligand for B cell costimulatory molecule CD40 (CD40-L), (Noelle *et al.*, 1992). Interaction of B cell CD40 with T cell CD40L provides a second signal to the B cell (Engel *et al.*, 2011), which begins to up-regulate receptors for T_H1 cytokines such as IL-2, IL-4 and IL-5 (Owen *et al.*, 2007). The activated T_H cell secretes these cytokines, which bind to the B cell and stimulate complete B cell activation, inducing proliferation and differentiation into effector B cells (Engel *et al.*, 2011). These short-lived B cells secrete IgM and IgG (Owen *et al.*, 2007).

Some of the activated B cells form germinal centres within follicles (Engel *et al.*, 2011). The importance of germinal centres in the humoral immune response is highlighted by the fact that three key processes take place there. The first of these processes is affinity maturation, where rapid B cell division and somatic hypermutation of B cell Ig genes leads to the production of B cells with high-affinity membrane Ig (MacLennan *et al.*, 2003, Owen *et al.*, 2007). Class switching subsequently occurs, where B cell Ig can improve further through changing the isotype of the constant region of the antibody, improving the biological effector activity of the antibody while maintaining antigen specificity (Owen *et al.*, 2007). Finally, germinal centres support the vital process of B cell differentiation into plasma and memory cells (MacLennan *et al.*, 2003). This is influenced heavily by T_H, and the cytokines that they secrete such as IL-2, IL-4 and IL-5 (Owen *et al.*, 2007).

1.3.3. B cell subsets and function

Like T cells, B cells can be subdivided into an effector subset cells known as plasma cells, and a memory subset. The functions of these cells will be outlined here.

1.4.3.1. Plasma B cells

Both short-lived and long-lived plasma cells have been identified in mice and humans, depending on the context of B cell activation and interactions with T_H (Bortnick and Allman, 2013). The primary role of these effector B cells is to produce large amounts of high affinity antibodies. Upon differentiation, plasma cells migrate to the medullary cord and secrete antibodies into the lymph (Shapiro-Shelef and Calame, 2005). Antibody function is primarily mediated by their binding affinity to a specific epitope. Through this interaction, antibodies are able to bind specifically to their target antigen, triggering a series of down-stream effects. These include immobilisation, neutralisation and opsonisation of pathogens, antibody mediated cytotoxicity and activation of other compartments of the immune system including the complement system and effector cells (Owen *et al.*, 2007).

1.4.3.2. Memory B cells

Formed within germinal centres after a primary immune response, memory B cells are capable of existing for long periods of time, recirculating between peripheral lymphoid tissues via vascular and lymphatic vessels (Crotty *et al.*, 2003, Tangye and Tarlinton, 2009). This subset of B cells classically express CD19 and CD27, and respond efficiently to antigens. Compared to naïve B cells, memory B cells express much higher levels of co-stimulatory molecules such as CD80 and CD86, needed for

complete T cell activation (Good *et al.*, 2009). Central to their role, memory B cells possess the capacity to rapidly proliferate and differentiate into antibody-secreting plasma cells following re-exposure to a previously encountered antigen. Succeeding this secondary immune response, these antigen-experienced B cells are more specialised at producing antibodies, which are of high affinity due to affinity maturation (Engel *et al.*, 2011).

1.1.4.2. Regulatory B cells

The existence of immunosuppressive B cells has been speculated for some years, however studies defining this controversial subset have been more recent. Regulatory B cells (B_{reg}) represent a B cell subset with suppressive or regulatory functions. Like T_{reg}, B_{reg} are also important in maintaining self-tolerance. As a consequence of class switching, B_{reg} express additional Ig on their surface including IgG, IgA and IgM (Owen *et al.*, 2007). Although B_{reg} have been identified in mice (Mauri and Ehrenstein, 2008), the existence of a counterpart in humans continues to be debated (Jamin *et al.*, 2008). One such way by which B_{reg} have been speculated to regulate immune responses is through the production of anti-inflammatory cytokine IL-10 (Yang *et al.*, 2013).

1.4. T cell trafficking in inflammation

In order to fulfil their immunological roles, T cells must be capable of selective migration to sites of inflammation in tissues, facilitated by the expression of a variety

of cell adhesion molecules. T cell trafficking during inflammation involves a multi-step paradigm, summarised in Figure 1.2, known as the leukocyte adhesion cascade. This is similar for neutrophils, monocytes and lymphocytes, and enables leukocyte extravasation out of the vasculature (Schmidt *et al.*, 2013). There, they perform a number of functions leading to the elimination of any hazards, and the resolution of inflammation.

1.4.1. T cell extravasation at sites of inflammation.

Endothelial cells lining post-capillary venules express a diverse range of cell adhesion molecules and chemokines to orchestrate the recruitment of T cells during inflammation (Aird, 2005). The main stages in T cell recruitment from the blood can be summarised into several sequential steps. These steps are tissue specific, and involve different cell adhesion molecules depending on the context and tissue in which migration is occurring.

(i) Capture from flow

T cell capture by endothelial cells is highly dependent on cytokines such as TNF-α and IFN-γ (Springer, 1995), secreted primarily by WBC during inflammation. Effector and memory T cells circulate in the blood during an inflammatory response and are subsequently captured by cytokine-activated endothelium. In this process, initial margination of cells occurs due to the physiological and kinetic properties of flowing blood; the larger RBC accumulate in the centre of the lumen, forcing the smaller T cells towards the periphery (Munn *et al.*, 1996). This facilitates close-proximity interactions between T cell and endothelial cell adhesion molecules,

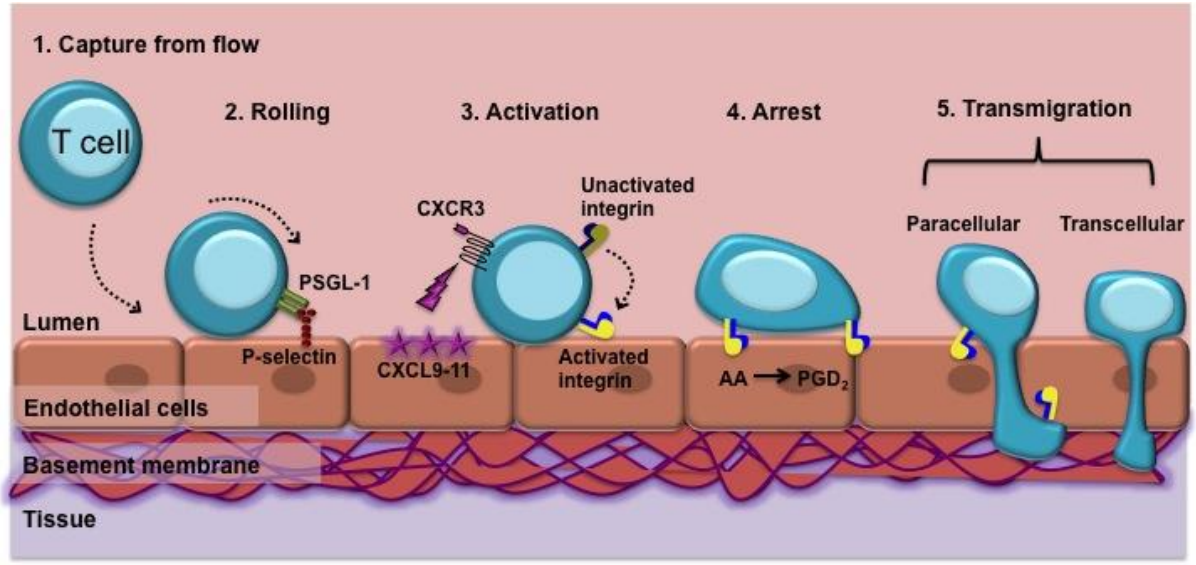

Figure 1.2. T cell recruitment and transmigration.
Initially, T cells are recruited from flow and roll along the endothelium via selectin-mediated interactions. For example, activated T cells use PSGL-1 to roll on endothelial cell P-selectin (Ley and Kansas, 2004). T cells undergo chemokine-driven integrin activation through inside-out signalling, and arrest on the endothelium. Following a final signal from PGD_2 and engagement of DP_2, T cells cross the endothelial cell layer and move into the tissue by paracelluar or transcelluar migration.

allowing the proceeding steps in the cascade.

(ii) Rolling

When in close proximity to inflamed vascular endothelium, T cells roll along the surface of the blood vessel. This phenomenon is mediated by a group of cell adhesion molecules known as selectins, which bind a family of mucin-like cell adhesion molecules, such as P-selectin glycoprotein-1 (PSGL-1), via their lectin domain (Ley, 2003). Several selectins are involved in T cell rolling, including E-selectin, P-selectin and L-selectin. E-selectin and P-selectin are both expressed on the surface of endothelial cells, and were originally identified on endothelial cells and platelets respectively. P-selectin plays a key role in mediating T cell capture and

rolling (Luscinskas *et al.*, 1995b), whereas E selectin is essential for T_M cell adhesion (Shimizu *et al.*, 1991). L-selectin expression is exclusive to leukocytes, but is not present on effector memory T cells (Ley *et al.*, 2007, Springer, 1994, von Andrian *et al.*, 1993). Selectins bind their ligands with low affinity leading to the rapid breaking and re-forming of weak bonds between the molecules. These low affinity interactions enable rolling to occur and are important in reducing velocity, allowing sufficient time for the leukocyte to examine endothelial cell moieties such as chemokines (Schmidt *et al.*, 2013). Mounting evidence has suggested that very late antigen-4 (VLA-4) is also able to support T cell rolling on vascular cell adhesion molecule-1 (VCAM-1), (Alon *et al.*, 1995, Johnston *et al.*, 1996, Luscinskas *et al.*, 1995b).

(iii) Activation

Upon sensing an appropriate signal from the endothelium, T cells will become activated and cease to roll. Activation signals occur through the binding of chemokines, synthesised by inflamed endothelial cells, to receptors on the surface of T cells. Chemokines are a group of chemoattractant cytokines of around 8 to 16kDa, and are comprised of 4 families classified by the position of two conserved cysteine residues within the amino acid sequence; C, CC, CX3C and CXC (Rollins, 1997). IFN-γ, a cytokine commonly produced at the site of inflammation, induces the expression of chemokines CXCL9, CXCL10 and CXCL11 on the endothelial cell surface (Mazanet *et al.*, 2000, Piali *et al.*, 1998). These chemokines are able to bind to the G-protein coupled receptor (GPCR) CXCR3, expressed highly on the surface of effector and memory T cells (McGettrick *et al.*, 2009, Piali *et al.*, 1998), and GPCR signalling in turn leads to T cell activation.

(iv) Arrest

Chemokine binding to T cell GPCRs induce a rapid intracellular signalling cascade leading to a change in conformation of T cell transmembrane receptors known as integrins. Through a process known as “inside out signalling”, structural changes in T cell integrin LFA-1 render it active, facilitating high-affinity binding to the endothelial cell ligand VCAM -1 (Hogg *et al.*, 2011, Ley *et al.*, 2007). This strong binding interaction leads to T cell arrest and firm adhesion on the endothelial cell surface.

(v) Transmigration

In the final stage of the leukocyte adhesion cascade, T cells initially migrate on the surface of the endothelium (Middleton *et al.*, 2002). Recent evidence demonstrated the requirement of T_M cells for a final signal, which is provided by endothelial cell prostaglandin D_2 (PGD_2) binding to the D-prostanoid receptor (DP_2) on the T_M surface (Ahmed *et al.*, 2011).

Other mechanisms regulating this final step in T cell migration have been suggested in the literature. For example, IL-15 has been attributed to enhanced T cell activation and transmigration *in vitro* (Sancho *et al.*, 1999) and *ex vivo* in T cells from multiple sclerosis (MS) patients (Broux *et al.*, 2015). Matrix metalloproteinase (MMP) activation in T cells, for example through Wnt signalling (Wu *et al.*, 2007), also facilitates T cell migration by permitting passage through the basement membrane. Interestingly, the prostaglandin analogue PGD_3 was shown to inhibit neutrophil transmigration via antagonism of the DP_2 receptor in neutrophils (Tull *et al.*, 2009), however this same mechanism has not yet been established in T cells.

The process of transmigration, whereby T cells cross the endothelial cell layer via diapedesis, can occur in two different ways. The most common of these ways is known as paracellular migration, where T cells migrate between gaps in cells via tight junctions, and use endothelial cell adhesion molecules such as PECAM-1, LFA-1, junctional adhesion molecules (JAMs) and vascular endothelial (VE)-cadherin (Ley *et al.*, 2007, Muller, 2003). The less common way, termed transcellular migration, is where T cells migrate directly through the endothelial cells via formation of vesiculo-vacuolar organelles, creating intracellular endothelial cell channels (Ley *et al.*, 2007, Millan *et al.*, 2006).

1.4.2. Memory T cell recruitment to inflamed tissues

Antigenic stimulation of naïve T cells leads to the reinstatement of homeostasis, and the generation of T_{EM} and T_{CM}. T_{EM} circulate in the periphery, providing immune surveillance of tissues, while T_{CM} reside in SLOs, waiting for their cognate antigen (Kaech *et al.*, 2002). During inflammation, T_M are recruited to the tissues by adhesion molecules up-regulated on inflamed vascular endothelial cells following cytokine activation. Enrichment of T_M subsets during inflammation has been reported both *in vivo* during peritoneal inflammation (Roberts *et al.*, 2009), and *in vitro* (Ahmed *et al.*, 2011, Chimen *et al.*, 2015).

As briefly mentioned previously, the generation of PGD_2 from arachidonic acid (AA) by EC cyclooxygenases (COX), and its receptor DP_2 on the surface of T cells, has been implicated in the migration of $CD4^+$ T_M cells across inflamed endothelial cells (Ahmed *et al.*, 2011). PGD_2 binding to DP_2 enhanced $CD4^+$ T_M cell trafficking following activation by chemokine receptor CXCR3. Evidence supporting this model

of T_M cell trafficking includes the observation of decreased inflammatory responses following DP_2 inhibition in mouse models of allergic inflammation (Stebbins *et al.*, 2010).

1.5. The role of T cells in autoimmune and chronic inflammatory diseases

The primary role of T cells in inflammation is to respond to the presence of non-self material known as antigens. The T cell response is a highly complex biological response involving an impressive multitude of inflammatory mediators and immune cells under tight regulation. Under normal physiological circumstances, T cell trafficking is beneficial to the elimination of the antigenic trigger and the resolution of acute inflammation. However, when this highly co-ordinated system fails, disease can result.

1.5.1. Chronic inflammation

Chronic inflammation occurs when acute inflammation does not resolve and persists for long periods of time. During this process, an accumulation of leukocytes such as T cells occurs in tissues due to excessive trafficking, local proliferation or delayed egress. Once in the tissues, inflammatory cells release a multitude of mediators causing a continuous cycle of inflammation, cell recruitment and activation. Ultimately, tissue damage results which in turn leads to the development of a variety of chronic inflammatory diseases, usually with a T cell element. Often, T cell

mediated chronic inflammation is tissue specific (Luster *et al.*, 2005), highlighting the ability of T cells to home distinctively to specific tissues. The aetiology of chronic inflammatory disease remains a subject of fierce debate. However most speculate the cause to be dysregulation of pro-inflammatory or anti-inflammatory processes that regulate the extent of inflammation and resolution. For example, perhaps dysregulation in the production of IL-10, a key anti-inflammatory cytokine (Kubo and Motomura, 2012), or the suppressive function of T_{reg} (Lindley *et al.*, 2005).

1.5.2. Type 1 Diabetes

Type 1 Diabetes (T1D) is an autoimmune endocrine disorder resulting from the inability of pancreatic beta cells to produce the metabolic hormone insulin (Daneman, 2006). Currently affecting around 400,000 people in the UK (Juvenile Diabetes Research Foundation, 2010), T1D is characterised by an increased blood glucose level which can be life threatening if left untreated.

It is widely agreed that the pathogenesis of T1D is due to insulitis and subsequent beta cell destruction, mediated by the infiltration of auto-reactive T cells specific for a self-antigen, which to date is still unknown. Evidence supporting this includes the identification of $CD4^+$ and $CD8^+$ T cells in insulitic lesions (Figure 1.3),(Imagawa *et al.*, 1999), however the presence of B cells and macrophages has also been reported (Itoh *et al.*, 1993). Many popular hypotheses involve a viral element, with some scientists suggesting pro-autoimmune infection triggering autoimmunity, and others implicating molecular mimicry of human antigens (Filippi and von Herrath, 2008). Contributing factors to the onset of T1D include the failure of

T_{reg} to suppress $CD8^+$ T cells through T_{reg} expression of TGF-β (Lindley *et al.*, 2005), or the sensitivity of T cells to TGF-β (Gregori *et al.*, 2003, Lawson *et al.*, 2008).

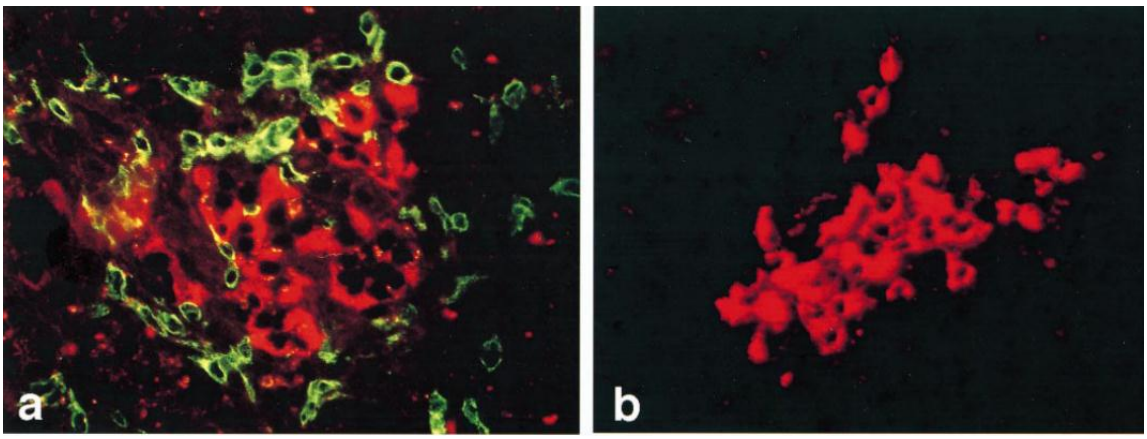

Patient with T1D Healthy control

Figure 1.3. Infiltration of T cells into pancreatic islets in type 1 diabetes. A section of the pancreatic islets from (a) a patient with T1D and (b) a healthy control. Insulin is stained in red and T cells are stained in green, identified by cluster of differentiation 3 (CD3). Infiltration of T cells can be seen in the pancreas of the type 1 diabetes patient leading to insulitis and autoimmune destruction of beta cells, however T cells are absent in the healthy control. (Imagawa *et al.* (1999) copyright license number: 2814290215519).

1.5.3. Rheumatoid Arthritis

Rheumatoid Arthirits (RA) is a chronic autoimmune disease involving persistent synovial inflammation. Affecting between 0.5 and 1% of adults, RA can lead to decreased mobility resulting from joint damage (Scott *et al.*, 2010). Like T1D, RA is also triggered by an unknown antigen recognised by autoreactive T cells, leading to excessive immune cell trafficking. $CD4^+$ T cells play a primary role in the

establishment of RA, and have been found in the synovium along with the presence of autoantibodies (Komatsu and Takayanagi, 2012). The involvement of both T_{EM} and T_{CM} under the regulation of the T cell mitogen IL-12, has been implicated in the pathogenesis of RA (Kohem *et al.*, 1996, Zhang *et al.*, 2005). Furthermore, synovial inflammation is exacerbated through immune cell production of IL-1, IL-6 and TNF-α, facilitating the continuous recruitment and activation of immune cells (Komatsu and Takayanagi, 2012, Scott *et al.*, 2010).

1.5.4. Atherosclerosis

Atherosclerosis is one of the most prevalent cardiovascular diseases (CVD) in the UK, resulting from accumulation of lipid within the arterial walls. Atherosclerosis involves a complex multi-factorial process initially involving endothelial cell activation, inflammation and the recruitment of leukocytes (Falk, 2006). Macrophages phagocytose deposited lipids, becoming foam cells and contributing to the atherosclerotic plaque. T cells also contribute to the development and maintenance of chronic inflammation in atherosclerosis. The involvement of both T_H1 and T_H2 responses in atherosclerosis has been examined (Ait-Oufella *et al.*, 2009), with T cells playing an important part in the progression of disease. T_H1 cells predominate, contributing to the exacerbation of inflammation through the production of high levels of pro-inflammatory cytokines such as IFN-γ, sustaining the inflammatory response through the further recruitment of monocytes and DCs, thus progressing plaque formation (Mallat *et al.*, 2007). Atherosclerotic plaques are susceptible to rupture due to arterial shear stress, which can lead to coronary complications such as stroke, and even death.

1.6. PEPITEM: a novel inhibitor of T cell transmigration

T cell recruitment during inflammation is normally highly regulated, controlled by antigen specificity, T_{reg} and regulatory cytokines. From early on, T cells are controlled for auto-reactivity by negative selection in the thymus. However, during certain diseases including those discussed above, T cell trafficking can become dysregulated, causing excessive migration of T cells into tissues with pathological consequences. Recently, our laboratory has demonstrated that B cells regulate T cell trafficking in response to adiponectin stimulation (Chimen *et al.*, 2015). This homeostatic mechanism, mediated by a peptide termed Peptide Inhibitor of Trans-Endothelial Migration (PEPITEM), represents a novel paradigm and forms the basis on which this thesis centres. Here, PEPITEM and its molecular mechanism will be discussed in further detail.

1.6.1. Anti-inflammatory properties of Adiponectin

Adiponectin is an adipokine primarily secreted by adipocytes (Ouchi *et al.*, 2011). The adiponectin receptors, AdipoR1 (AR1) and AdipoR2 (AR2), represent ubiquitously expressed GPCRs capable of binding globular and full length adiponectin respectively (Yamauchi *et al.*, 2003). Adiponectin plays an important role in energy homeostasis, metabolism and the regulation of insulin sensitivity. Physiological levels of adiponectin vary between 3 and 30µg/ml, but generally are high (Arita *et al.*, 1999, Ouchi *et al.*, 2011). However, adiponectin levels are severely decreased in obesity and the protective roles of adiponectin against obesity-related diseases have been demonstrated by the correlation of low levels of adiponectin with

higher risk of CVD, metabolic syndrome and type II diabetes (Kadowaki and Yamauchi, 2005, Ouchi *et al.*, 2011, Rabe *et al.*, 2008).

Adiponectin has pleiotropic effects within the immune system (Kadowaki *et al.*, 2006, Ouedraogo *et al.*, 2007) and is capable of exerting anti-inflammatory effects and mediating immune responses, such as the inhibition of TNF-α production and the stimulation of anti-inflammatory cytokine IL-10 production by macrophages (Ouchi *et al.*, 2011). Conversely, adiponectin has also been reported to exhibit pro-inflammatory effects through the induction of pro-inflammatory cytokines including IL-6, IL-8 and TNF-α by monocytes and macrophages (Haugen and Drevon, 2007, Peake and Shen, 2010, Tsatsanis *et al.*, 2005) . Perhaps the differences in adiponectin function may be attributed to the different forms of adiponectin (Neumeier *et al.*, 2006), or indeed the inflammatory context.

The importance of adiponectin in inflammation is demonstrated by studies in adiponectin-deficient mice, who were found to have greater levels of the pro-inflammatory cytokines TNF-α and IL-6, reversible by the addition of exogenous adiponectin (Ouchi *et al.*, 2011). These mice were also more susceptible to vascular diseases such as atherosclerosis, and involve chronic inflammatory infiltrates (Matsuda *et al.*, 2002, Okamoto *et al.*, 2002). Furthermore, increased rolling and adhesion of leukocytes has been reported in adiponectin-deficient mice, along with the upregulation of key endothelial cell adhesion molecules involved in leukocyte trafficking (Cao *et al.*, 2009, Ouedraogo *et al.*, 2007). However, the mode of action of these effects remains unclear, and the immunological role of adiponectin has not yet been fully established.

1.6.2. Sphingosine-1-phosphate in T cell trafficking

Sphingosine-1-phosphate (S1P) is a sphingolipid produced in the cytosol through the phosphorylation of sphingosine by the enzymes sphingosine kinase 1 and sphingosine kinase 2 (SPHK1/2), which are expressed by vascular endothelial cells (Hla *et al.*, 2001). It has a short half-life in plasma of 15 minutes (Venkataraman *et al.*, 2008). S1P is exported across the EC membrane into the blood by the S1P transporter protein spinster homolog 2 (SPNS2), where it exerts its effects by binding to one of five GPCRs (S1PR1–S1PR5). However, S1P signalling is mainly limited to S1PR1 and S1PR4 in T lymphocytes (Reviewed by Garris *et al.* (2014)).

The major role of S1P has been well reported, regulating the egress of recirculating lymphocytes from secondary lymphoid organs such as LN into efferent lymphatics (Matloubian *et al.*, 2004). However recent studies have revealed the ability of S1P to inhibit T cell migration from tissues into afferent lymphatics, mediated by high levels of S1P in tissues during inflammation (Ledgerwood *et al.*, 2008, Roviezzo *et al.*, 2011). Furthermore, the role of S1P in T cell trafficking is highlighted by the effect of deletion of endothelial cell SPNS2 in mice, which resulted in dysregulated lymphocyte trafficking (Fukuhara *et al.*, 2012).

Although high SPHK expression has been reported in high endothelial venules, not much research has been done into other vascular beds (Pham *et al.*, 2010). Interestingly, sphingosine kinase activity has been reported to be induced in endothelial cells by adiponectin through the activation of nuclear factor kappa beta (NF-κβ) (Kase *et al.*, 2007).

Mounting evidence for the role of S1P in T cell trafficking has led to the development of pharmacological agent Fingolimod in 2010, an immunomodulatory

S1P receptor agonist used in the treatment of multiple sclerosis (MS), (U.S. Food and Drug Administration, 2010).

1.6.3. PEPITEM; a novel inhibitor of T cell transmigration

In 2015, using a well-characterised *in vitro* model of transmigration, Chimen and colleagues described PEPITEM for the first time, initially observing that adiponectin treatment of lymphocytes inhibited their transmigration across cytokine-stimulated human umbilical vein endothelial cells (HUVEC), (Chimen *et al.*, 2015). However, the fact that few T cells expressed adiponectin receptors implied that adiponectin was not performing this effect through direct interaction with T cells. On the other hand, B cells do express adiponectin receptors, and depletion of B cells from the *in vitro* model of transmigration freed lymphocytes from adiponectin-mediated inhibition, suggesting that adiponectin acted directly on B cells. The analysis of supernatants from adiponectin-stimulated B cells revealed that a B cell-secreted agent was regulating the trafficking of T cells across inflamed endothelium. Through proteomic screening using mass spectrometry, the mystery agent was identified as PEPITEM, named Peptide Inhibitor of Trans-Endothelial Migration, according to its function. Further investigations found that PEPITEM inhibited the transmigration of T lymphocytes, but not monocytes or neutrophils (Chimen *et al.*, 2015).

PEPITEM is a 14-amino acid peptide, proteolytically derived from its parent protein, 14-3-3 zeta (14-3-3ζ). PEPITEM represents an exciting and novel adiponectin-mediated paradigm for the regulated trafficking of T cells, beginning with

the binding of adiponectin to its receptors on the surface of B cells. Following this interaction, B cells are stimulated to release PEPITEM which interacts with cadherin-15 (CDH15), a cell adhesion molecule expressed on the surface of endothelial cells, triggering an intracellular signalling cascade involving the phosphorylation of sphingosine to S1P by SPHK1. S1P is subsequently released by the endothelium, and binds to its receptors S1PR1/4 on the surface of T cells. This binding alters the activation state of integrin LFA-1, inhibiting T cell transmigration across the endothelium (Figure 1.4). However, much still remains to be determined about PEPITEM, such as its pharmacokinetics and plasma concentration *in vivo* in healthy individuals, but also the export mechanism and amount secreted by B cells following adiponectin stimulation.

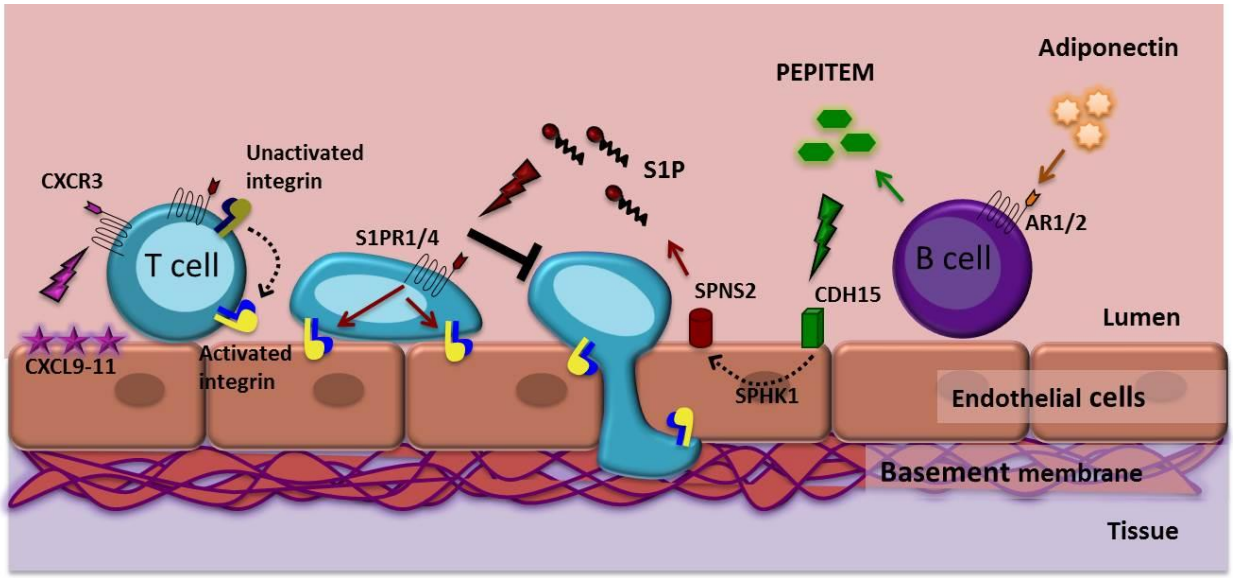

Figure 1.4. Novel homeostatic regulation of T cell migration during inflammation.
In the current model of T cell recruitment, T cells are recruited by inflamed endothelial cells and arrest on the endothelium, preparing to transmigrate. Chimen *et al*. (2015) described a novel paradigm in the regulation of T cell migration. Initially, B cells are stimulated by adiponectin to release PEPITEM. Through interaction with CDH15, PEPITEM induces the endothelial cell synthesis and release of S1P by sphingosine kinase-1 (SPHK1). S1P binds to its receptors on the T cell surface, inhibiting transmigration.

1.6.4. 14-3-3ζ is the parent protein of PEPITEM

The 14-3-3 family of proteins in mammals consists of seven isoforms; beta (β), epsilon (ε), gamma (γ), eta (η), sigma (σ), tau (τ), and zeta (ζ), classified based on their chromatographic elution profiles. 14-3-3 alpha (α) and delta (δ) represent the phosphorylated forms of β and ζ respectively (Fu *et al.*, 2000). Remarkably, these proteins are highly conserved between all eukaryotic cells and are 100% homologous between mammalian and avian species. Expressed in almost all mammalian tissues (Celis *et al.*, 1990), this family of dimeric proteins were demonstrated to interact with binding partners via a phosphorylated serine motif (Muslin *et al.*, 1996). The location of PEPITEM in 14-3-3ζ protein spans residues 28 to 41 (Chimen *et al.*, 2015). This positioning makes PEPITEM accessible to other molecules at the protein's outer surface, and potentially reflects a requirement for interaction with other proteins, for example with proteases enabling proteolytic cleavage of PEPITEM from 14-3-3ζ (Figure 1.5).

14-3-3 proteins interact with a large number of intracellular proteins, with reports suggesting interaction with over 200 ligands (Pozuelo Rubio *et al.*, 2004), modulating their function (Fu *et al.*, 2000) and regulating various cellular processes including protein trafficking, the cell cycle, DNA repair, apoptosis, differentiation, cell adhesion and motility (Bridges and Moorhead, 2005, Dougherty and Morrison, 2004, Fu *et al.*, 2000, Wilker and Yaffe, 2004). As a result of this varied function, it is no surprise that altered expression or function of 14-3-3 proteins can manifest as disease, and associations between 14-3-3 isoforms and human diseases are beginning to emerge.

a)

------**PEPITEM**------

1- MDKNELVQKAKLAEQAERYDDMAACMK **SVTEQGAELSNEER** NLLSVAYKNVVGARRSSWRVVSS
IEQKTEGAEKKQQMAREYREKIETELRDICNDVLSLLEKFLIPNASQAESKVFYLKMKGDYYRYLAEVAA
GDDKKGIVDQSQQAYQEAFEISKKEMQPTHPIRLGLALNFSVFYYEILNSPEKACSLAKTAFDEAIAELDT
LSEESYKDSTLIMQLLRDNLTLWTSDTQGDEAEAGEGGEN -245

b)

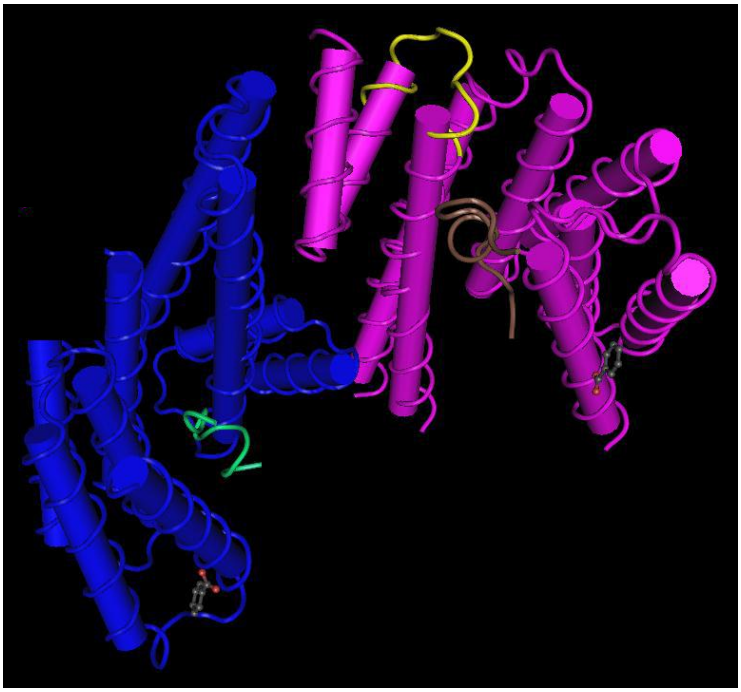

Figure 1.5: The amino acid sequence and crystal structure of 14-3-3ζ
(a) The 14-3-3ζ isoform is composed of 245 amino acids. The position of PEPITEM is located from residues 28 to 41, highlighted in red. (b) The crystal structure of a 14-3-3ζ dimer, with each monomer (blue and pink) consisting of 9 anti-parallel α-helices. In this structure taken from Ottmann *et al.* (2007), the 14-3-3ζ dimer is shown binding hydrophobically to the exoenzyme S peptide (highlighted in green and brown). The dimer has been modelled to demonstrate the exposed PEPITEM residues (highlighted in yellow).

A role for 14-3-3 proteins has been established in human cancer and some 14-3-3 binding partners have been identified as products of oncogenes (Lodygin and Hermeking, 2005), or are involved in processes which impact tumour growth, such as the cell cycle and apoptosis, supporting this connection. 14-3-3σ is down-regulated in breast carcinoma, consistent with hypermethylation of the 14-3-3σ gene, suggestive of gene silencing (Ferguson *et al.*, 2000, Umbricht *et al.*, 2001). Furthermore, the 14-3-3ζ isoform has been identified in the secretome of tumour associated monocytes and macrophages from ascites of patients with epithelial ovarin cancer (Kobayashi *et al.*, 2009).

In addition to cancer, 14-3-3 proteins have also been correlated with neurological diseases (Layfield *et al.*, 1996), consistent with their high expression in the brain. For example, several isoforms of 14-3-3 are upregulated in the brain in Alzheimer's disease (Wilker and Yaffe, 2004), and in down syndrome patients (van Heusden, 2005). Additionally, the gene encoding 14-3-3ε is consistently deleted in patients with Miller-Dieker syndrome (van Heusden, 2005). 14-3-3 isoforms have also been identified in cerebrospinal fluid (CSF) from individuals with Creuzfeldt-Jakob's disease (CJD) and cattle with bovine spongiform encephalopathy (BSE), (van Heusden, 2005), and are currently being tested as diagnostic markers for these prion diseases.

Currently, none of the 14-3-3 isoforms have been directly implicated in the regulation of T cell trafficking. However, some studies have suggested a function for 14-3-3β and 14-3-3ζ in cell spreading (reviewed by Mhawech (2005)). Reports have identified the binding of 14-3-3β to β1 integrin, assisting cell spreading and migration (Han *et al.*, 2001, Rodriguez and Guan, 2005). 14-3-3ζ can also mediate integrin signaling through binding to the integrin signaling adaptor Cas (Garcia-Guzman *et al.*,

1999) in fibroblast cell lines and T cells (Nurmi *et al.*, 2006). 14-3-3 interaction with the signaling protein apelin-13 in HUVEC was shown to increase monocyte adhesion (Li *et al.*, 2010), however this study had limitations due to the use of the THP-1 monocyte cell line which may not resemble primary monocytes *in vivo*, and ECV304 endothelial cells which are not considered to resemble HUVEC.

Despite these studies, the role of 14-3-3ζ in immunity remains unclear. Its expression has been confirmed in monocytes, $CD4^+$ and $CD8^+$ T cells, B cells and NK cells (Su *et al.*, 2004). 14-3-3 proteins have been shown to mediate T cell function through binding to pathways involved in T cell stimulation or activation (Di Bartolo *et al.*, 2007, Liu *et al.*, 1996, Meller *et al.*, 1996). Conversely, one study revealed that interaction of 14-3-3θ with protein kinase C (PKC) inhibited T cell activation (Meller *et al.*, 1996). However, this area of study has been scarcely researched and provides no indication of 14-3-3 isoforms giving rise to functionally active peptides regulating the immune system, and the importance of this protein in the PEPITEM pathway remains to be examined.

1.6.5. PEPITEM; a therapeutic agent?

Chronic inflammation encompasses a large range of clinical diseases affecting many organs of the body. Most, if not all, have a T cell element. The PEPITEM paradigm represents a homeostatic, lymphocyte-specific regulatory pathway which may be compromised in disease, and holds therapeutic potential for diseases resulting from inappropriate T cell trafficking across inflamed endothelium. Indeed recently it has been shown that the expression of adiponectin receptors 1 and 2 on B cells as well as PEPITEM production diminishes with age, suggestive of immune

senescence of this homeostatic pathway. Chimen *et al.* (2015) showed that inhibition of T cell trafficking was dysregulated in chronic inflammatory diseases including T1D and RA, with circulating levels of PEPITEM in patient serum reportedly reduced when compared to healthy donors. Moreover, regulation could be re-established using exogenous PEPITEM both *in vitro* and also *in vivo* using animal models of chronic inflammation.

The use of PEPITEM in T cell-mediated diseases represents a more specific therapeutic agent than adiponectin or S1P. Adiponectin is highly pleotropic, regulating a host of homeostatic processes, including lipid and glucose metabolism. Therefore, the use of adiponectin to inhibit T cell transmigration during inflammation may result in a variety of off-target effects on metabolism. Similarly, S1P regulates T cell trafficking within LN and mediates T cell egress from SLOs (Cyster, 2005). Again, using S1P as a therapeutic agent may cause significant and undesirable effects on immune function. The potential of PEPITEM development as a treatment for chronic T cell-mediated immune disease must now be addressed.

1.7. Aim and objectives

The PEPITEM paradigm represents a highly novel and innovative area of biomedical science, contributing not only to the basic biology of human beings, but also to the knowledge of chronic inflammatory diseases, and how we may treat them. However, much remains to be discovered regarding the basic biology of PEPITEM and its related paradigm. For example, adiponectin stimulates B cells to secrete PEPITEM, although the rate of PEPITEM production remains unknown. While much

is known about the structure of the parent protein 14-3-3ζ, currently nothing is known about the structure of PEPITEM other than its amino acid sequence.

When considering the use of PEPITEM to treat T-cell mediated chronic inflammatory diseases, it is essential to understand the pharmacokinetics of the peptide first, and optimise the appropriate dose for administration in animal models.

Additionally, many of the steps in the PEPITEM paradigm have not yet been fully elucidated, including the mechanism of PEPITEM release from B cells. Furthermore, it is unclear how PEPITEM is processed from its parent protein 14-3-3ζ, into a functional 14 amino acid peptide.

We aim to investigate further the molecular mechanisms underlying the PEPITEM paradigm, and whether it can be exploited to treat T cell-mediated inflammatory disease. We intend to do this using the following specific objectives:

1. Confirm the reproducibility of PEPITEM-mediated inhibition of PBL transmigration *in vitro*
2. Examine the structure of PEPITEM and its interactions, and investigate the development of a high-throughput assay for PEPITEM function *in vitro*
3. Assess the potential of PEPITEM development for therapeutic use in the treatment of chronic T cell-mediated immune disease
4. Determine the role of 14-3-3ζ in the PEPITEM paradigm.

CHAPTER 2: MATERIALS AND METHODS

2.1. Materials

Table 2.1. List of main reagents used.

Reagent	Manufacturer	Catalogue number	Working concentration	Application
EDTA	Sigma-Aldrich	93302	1x	Cell culture, cell sorting
Histopaque 1077	Sigma-Aldrich	10771	1x	PBMC isolation
Histopaque 1119	Sigma-Aldrich	11191	1x	PBMC isolation
PBS without calcium or magnesium	Sigma-Aldrich	P4417	1x	cell sorting, flow cytometry
Medium M199	Gibco Invitrogen	31150	1x	Cell culture, PBL assays
Fetal calf serum (FCS)	Sigma-Aldrich	F9665	20% v/v	Cell culture
Gentamycin	Gibco	G1272	35 µg/ml	HDBEC cell culture
Trypsin (cell culture grade)	Gibco Invitrogen	25200056	2.5mg/ml	HDBEC cell culture
TNF-α	R&D systems	210-TA-010	100U/ml	Cell culture
IFN-γ	Peprotech	300-02	10ng/ml	Cell culture
Adiponectin	Enzo Life Sciences	ALX-522-063	10µg/ml	PBL assays
BSA Fraction V	Sigma-Aldrich	A7030	0.15% w/v	Cell culture, PBL assays
Formaldehyde	Sigma-Aldrich	F1635	2-10% v/v	PBL assays, confocal microscopy, histology
DSC-18 columns	Sigma-Aldrich	52602-U	N/A	Mass spectrometry
Acetonitrile	VWR Chemicals	23595.328	1x	Mass spectrometry
Trifluoroethanoic acid	Sigma-Aldrich	302031	0.1-1% v/v	Mass spectrometry
Water (HPLC grade)	Merck Millipore	100030	1x	Mass spectrometry
Formic acid	Sigma-Aldrich	zero6450	1% v/v	Mass spectrometry
RNeasy Mini Kit	Qiagen	74104	n/a	RNA extraction
Ethanol	Fisher Scientific	BP2818	70-100% v/v	RNA extraction, DNase treatment
RNase-free dH_2O	Qiagen	129112	1x	RNA extraction
Random primers	Promega	C1181	0.5µg	Reverse transcription
dNTP	Promega	U1201	10mM	Reverse transcription
Trypsin (sequencing grade)	Promega	V5111	1x	Mass spectrometry
Promocell media	Promocell	C-220202	N/A	HDBEC cell culture
14-3-3ζ	SignalChem	Y92-30N-20	20ng/ml	PBL assay, western blotting
14-3-3ζ -His	Fitzgerald	80R-1064	25µg/ml	PBL assay, Biacore
CDH15-FC	R&D	4096-MC-050	12.5-200µg/ml	Biacore
Thrombospondin-1	R&D	3074-TH	10-100µg/ml	Biacore
CD19 microbeads	Miltenyi Biotech	130-050-301	n/a	Cell sorting
RQ1 RNase-Free DNase	Promega	M6101	1U	DNase treatment
Phenol/chloroform/isoamyl alcohol (25:24:1)	Sigma-Aldrich	S77617	1x	RNA purification
NaAc	Sigma Aldrich	S7899	3M	RNA purification
M-MLV Reverse transcriptase (with buffer)	Promega	M1701	200U	Reverse transcription
PVDF membrane	Millipore	IPVH00010	n/a	Western blotting
ECL	G E Healhcare	RPN2109	N/A	Western blotting

EC medium MV3h	Promocell	C-22020	1x	HDBEC cell culture
RNasin Plus RNase Inhibitor	Promega	N2111	25U	Reverse transcription
Protease inhibitor cocktail	Sigma Aldrich	P2714-1BTL	1:100	Western blotting
CryoSFM	Promocell	C-29912	N/A	Cell Culture
Penicillin/streptomycin	Gibco	10378016	100U/ml and 100µg/ml	Jurkat T cell culture
RPMI	Gibco Invitrogen	21875	1x	Jurkat T cell culture
GM6001	Santa Cruz	SC-203979	10nM	PBL assay
CD19 microbeads	Milteni Biotech	130-050-301	N/A	PBL assay
PBL with /without calcium and magnesium	Sigma Aldrich	D8662/D5773	1x	PBL assay
B cell enrichment kit	Stem Cell	19054	n/a	B cell isolation
Hbs-P buffer	GE Healthcare	BR100368	1x	Biacore
CaCl2	Sigma Aldrich	C1016	5mM	Biacore
EDC	GE Healthcare	BR-1000-50	0.4M	Biacore
NHS	sigma	130672	0.1M	Biacore
Streptavidin	sigma	S-4762	0.5mg/ml	Biacore
Ethanolamine-HCL	BIAcore life sciences	BR-1006-33	1M	Biacore
CDH15	R&D	4096-MC	25µg/ml	Biacore
Fluo 4 NW Calcium Assay Kit	Invitrogen	F36206	N/A	Calcium Flux assay
Calcium Ionophore	Santa Cruz	74267-27-9	0-1µM	Calcium flux assay
S1P	Cayman chemicals	62570	0-100µM	Calcium flux assay
Scintillant	Perkin Elmer	1200-437	1x	Radioactivity counting
CPDA	Sigma Aldirch	C4431	1x	Blood collection
Oil Red O	Sigma Aldrich	O0625	N/A	Histology
DPX mounting media	Leica Biosystems	3808600ED	1x	Histology
Isopropanol	Sigma Aldrich	W292907	70-100% v/v	Histology

Table 2.2. List of PEPITEM derivatives used.
All peptides were synthesised by Alta biosciences, Birmingham, UK, except tritiated PEPITEM, which was synthesised by Cambridge Biosciences. *Glycine was not D-isomerised as it does not have an enantiomer.

Peptide ID	Peptide sequence	Working concentration	Application
Native PEPITEM (Pure synthesis)	SVTEQGAELSNEER	20ng/ml	Migration assay
Scrambled PEPITEM	TAVLENSREGESQE	20ng/ml	Migration assay
PEPITEM-AF680	SVTEQGAELSNEER-AF680	100µg/ml	IVIS imaging
^{3}H PEPITEM	SVTEQGAELSNEER (tritiated)	0.1-10ng	Mass spectrometry, *in vivo* pharmacokinetics
Biotinylated PEPITEM	BIOTIN-SVTEQGAELSNEER	25µg/ml	Biacore
Biotinylated scrambled	BIOTIN-TAVLENSREGESQE	25µg/ml	Biacore
Native PEPITEM (crude synthesis)	SVTEQGAELSNEER	2-200ngml	Migration assay
Alanine substitutions	AVTEQGAELSNEER	20ng/ml	Migration assay
Alanine substitutions	SATEQGAELSNEER	20ng/ml	Migration assay
Alanine substitutions	SVAEQGAELSNEER	20ng/ml	Migration assay
Alanine substitutions	SVTAQGAELSNEER	20ng/ml	Migration assay
Alanine substitutions	SVTEAGAELSNEER	20ng/ml	Migration assay
Alanine substitutions	SVTEQAAELSNEER	20ng/ml	Migration assay
Alanine substitutions	SVTEQGAALSNEER	20ng/ml	Migration assay
Alanine substitutions	SVTEQGAEASNEER	20ng/ml	Migration assay
Alanine substitutions	SVTEQGAELANEER	20ng/ml	Migration assay
Alanine substitutions	SVTEQGAELSAEER	20ng/ml	Migration assay
Alanine substitutions	SVTEQGAELSNAER	20ng/ml	Migration assay
Alanine substitutions	SVTEQGAELSNEAR	20ng/ml	Migration assay
Alanine substitutions	SVTEQGAELSNEEA	20ng/ml	Migration assay
N-term peg	352 PEG -SVTEQGAELSNEER	20ng/ml	Migration assay
N/C block	Acetyl – SVTEQGAELSNEER - amide	20ng/ml	Migration assay
D isomer	REENSLEAG*QETVS (D amino acids)	20ng/ml	Migration assay
C-terminal PEG	SVTEQGAELSNEER-352 PEG-amide	20ng/ml, 1.75µg/ml	Migration assay, Mouse model of atherosclerosis
C-terminal PEG scrambled	TAVLENSREGESQE-352 PEG-amide	1.75µg/ml	Mouse model of atherosclerosis

Table 2.3. List of antibodies used in flow cytometry, western blotting, confocal microscopy and Biacore.

Reagent	Manufacturer	Catalogue number	Working concentration	Application
CD3-PECy7 (conjugated)	eBioscience	25-0031	1:50	Flow cytometry
CD19-APC (conjugated)	eBioscience	17-1093	1:50	Flow cytometry
14-3-3ζ (unconjugated)	R & D	MAB2669	1:2000/12µg/ml	Western blot,/ Confocal microscopy
Goat anti-mouse-FITC (conjugated)	Dako	F0479	1:30	Confocal microscopy
Donkey anti-mouse HRP (conjugated)	Santa Cruz	SC-2318	1:2000	Western blot
Anti-human IgG (unconjugated)	Abcam	Ab109489	25µg/ml	Biacore

Table 2.4. TaqMan gene expression assays used for real-time qPCR.
All primers were purchased from Invitrogen.

Target Gene	Catalogue number
18s	Hs03003631_g1
ICAM-1	Hs0016932_m1
VCAM-1	Hs00365486_m1
CXCL9	Hs00171065_m1
CXCL10	Hs00171042_m1
CXCL11	Hs00171138_m1
14-3-3ζ	Hs03044281_g1

2.2. Methods

2.2.1. Gene measurement

2.2.1.1. RNA extraction

Total mRNA from human dermal blood microvascular endothelial cells (HDBEC), or lymphocytes was extracted using the RNeasy Minikit (Qiagen) according to manufacturer's instructions. Initially, cells were lysed in RLT buffer, 70% v/v ethanol was added and each sample was vortexed to disrupt cell membranes. The sample was then added to a spin column for centrifugation at 15,000x g. Appropriate buffers were added and the flow-through discarded as per the manufacturers protocol. mRNA was eluted from the spin column using RNAse-free dH_2O and the RNA concentration was determined using Nanodrop Spectrofluorimeter 3300 (LabTech). RNA was subsequently stored at -80^{o}C until further use.

2.2.1.2 DNase treatment

Genomic material was removed from mRNA following isolation. 1µg RNA samples were treated with 1 unit RNAse-Free DNAse (Promega) as per manufacturer's instructions and incubated at 37^{o}C for 30 minutes before being transferred to ice for 5 minutes. 150µl dH_2O and 200µl phenol/chloroform/isoamyl alcohol were added to the reaction and vortexed before centrifugation at 15,000x g for 5 minutes at 4^{o}C. The top layer of the reaction was transferred to a fresh tube. 15µl 3M pH 5.5 NaAc and 375µl 100% v/v ethanol was added to the reaction,

vortexed and incubated at -80^{o}C for 2 hours. The reaction was defrosted until viscous and centrifuged at 15,000x g for 15 minutes at 4^{o}C. Supernatant was removed and the pellet was re-suspended in RNase-free dH_2O.

2.2.1.3 Reverse transcription

Isolated mRNA was converted to cDNA by reverse transcription. 0.5µg of random primers (Promega) were annealed to 1µg RNA by incubation at 70^{o}C for 5 minutes, and then transferred immediately to ice. A master mix of 5µl M-MLV 5x buffer, 5µl 10mM dNTPs, 25U RNasin Plus RNase Inhibitor, 200U M-MLV reverse transcriptase (all Promega) and dH_2O to 25µl per reaction was added to each tube and incubated at 37^{o}C for 1 hr. For each reverse transcription, a negative control was included by omitting reverse transcriptase from the master mix. All cDNA was stored at -20^{o}C.

2.2.1.4 Real-time qPCR

Quantitative PCR (qPCR) was performed on a 7500 HT Real Time PCR Machine (Applied Biosciences). All qPCR was performed in duplicate reactions. In each reaction, 10µl of Taq Universal Master Mix (Invitrogen), 1µl of TaqMan gene expression assay kit (Invitrogen, see table 2.4) and 1µl of mRNA along with water to a final volume of 20µl was added to each well of a 96 well qPCR plate. 18S was used as an endogenous control. All TaqMan gene expression kits utilised FAM reporter-labelled probes. qPCR employed 40 cycles of: 50°C for 2 minutes, 95°C for 10 minutes, 95°C for 15 seconds, 60°C for 1 minute, with the final holding at 10°C. Gene

expression was calculated relative to endogenous 18s expression using the ΔΔCt method. Results are expressed as fold change relative to 18S.

2.2.2. Protein expression

2.2.2.1. Generation of lysates for western blotting

Cell pellets were lysed in RIPA buffer (pH 8.0) containing protease inhibitor cocktail (PIC; Sigma-Aldrich) used according to manufacturer's instructions and incubated for 30 minutes at 4^{o}C with agitation. Lysates were centrifuged to remove debris at 15,000x g for 5 minutes and supernatant was transferred to a fresh Eppendorf. Lysates were stored at -20^{o}C until ready for use.

2.2.2.2. Generation of supernatants for western blotting

B cells were isolated as described in section 2.2.4.2 and stimulated with or without 10µg/ml adiponectin (Enzo Life Sciences) for 1 hour at room temperature with agitation. Cells were pelleted at 600x g for 10 minutes and supernatant was transferred to a fresh Eppendorf. A vacuum centrifuge was used to lyophilise supernatant samples before incubation with RIPA buffer (pH 8.0) containing PIC. Samples were stored at -20^{o}C until ready for use.

2.2.2.3. SDS-PAGE and western blotting for protein

Samples were diluted 1:1 in 2x Lamelli buffer and 20µl of each lysate was electrophoresed on 8% polyacrylamide gels for 1 hour at 200V before being transferred onto PVDF membranes (Millipore) for 1 hour at 100V. Membranes were blocked in 20% w/v non-fat powdered milk in PBS tween (0.1% v/v) for 1 hour at room temperature with agitation. After washing with PBS tween (0.1% v/v), membranes were then incubated with primary antibody (see table 2.3) diluted in PBS tween (0.1% v/v) at 4^{o}C overnight with agitation. Membranes were washed with PBS tween (0.1% v/v) and incubated with secondary antibody (see table 2.3) diluted in PBS tween (0.1% v/v) at room temperature for 1 hour with agitation. After final washes with PBS tween (0.1% v/v), chemifluorescence was detected using the ECL kit (G E Healthcare). X-ray film was exposed to the membrane for 2-5 minutes and developed using a Compact X4 Xograph imaging system. Antibody specificity was confirmed using 10ng recombinant 14-3-3ζ protein. HeLa cell lysates of undetermined protein concentration were used as an additional positive control.

2.2.2.4. Flow cytometry

1x10^{5} cells were transferred into a 5ml polypropylene tube (BD Falcon). Cells were pelleted at 400 x g for 5 minutes and re-suspended in 100µl PBS containing BSA (0.15% w/v, PBSA). Cells were stained with antibody (see table 2.3) for 20 minutes in the dark at 4^{o}C. Tubes were topped up to 4ml with cold PBSA, pelleted at 400g for 5 minutes, re-suspended in 300µl PBSA and kept on ice in the dark until ready for cytometry. Flow cytometry was performed using a CyAn flow cytometer (Dako) with Summit software. At least 10,000 total events were acquired per sample

where possible. Flow cytometry plots were created using Flow Jo software employing the gating strategy described in section 6.2.

2.2.2.5. Confocal microscopy

$2.5x10^4$ HDBEC were seeded in a µ-Slide (Ibidi) and stimulated with 100U/ml TNF-α + 10ng/ml IFN-γ for 24 hours. Cells were fixed in 2% v/v formaldehyde and blocked with rabbit serum (Sigma Aldrich) for 30 minutes. HDBEC were stained with primary antibody (see table 2.3) overnight at 4^oC with agitation. Cells were then washed in PBS and stained for 1 hour with secondary antibody (see table 2.3). For negative controls, the primary antibody was omitted and PBS used it its place. Cells were stained with bisBenzimide (1µg/ml, Sigma Aldrich) for 5 minutes before being washed for a final time. Images were captured using confocal microscopy, with an inverted Zeiss LSM-510 UV confocal microscope at x20 or x40 magnifications.

2.2.3. In vitro adhesion and migration assays

2.2.3.1 Cell culture

Human dermal blood microvascular endothelial cells (HDBEC, PromoCell) were cultured in low-serum medium 2% w/v (Endothelial cell growth medium; PromoCell) with 35µg/ml gentamycin (Gibco). At passage 4, cells were frozen down in CryoSFM (PromoCell) and stored in liquid nitrogen. Prior to use, cells were thawed at 37^oC and cultured in a $25cm^2$ cell culture flask. After 24 hours the media was replaced.

Jurkat T cells were cultured in 25cm^2 cell culture flask with RPMI (Gibco) supplemented with 10% v/v FCS, 100U/ml penicillin and 100µg/ml streptomycin (all Sigma-Aldrich).

2.2.3.2. PBL isolation

Peripheral blood mononuclear cells (PBMC) were isolated from the whole blood of healthy donors collected in EDTA (Sigma-Aldrich) using a two-step density gradient created with Histopaque 1119 and Histopaque 1077 (Sigma-Aldrich). Adherent monocytes were removed by seeding PBMC onto tissue culture plastic for 30 minutes and incubating at 37^{o}C (Rainger *et al.*, 2001). The remaining peripheral blood lymphocytes (PBL) were then re-suspended at 1x10^6 cells/ml in M199 (Life Technologies) with 0.15% w/v bovine serum albumin (BSA; Sigma-Aldrich). Blood was collected under approval from the University of Birmingham Local Ethical Review Committee (ERN_07-058).

2.2.3.3. Static adhesion and migration assay

HDBEC were seeded at 1x10^5 per well in 12 well plates and left to adhere. After 24 hours, confluent endothelial cell (EC) monolayers were cytokine-stimulated with 100U/ml TNF-α and 10ng/ml IFN-γ for 24 hours at 37^{o}C. PBL were treated with 10µg/ml adiponectin for 1 hour at room temperature with agitation and washed before use. For peptide treatment of PBL, peptides (see Table 2.2) were added to PBL immediately before use. Prior to addition of PBL, EC were washed with M199 BSA (0.15% w/v) to remove residual cytokines and treatments. 1x10^6 PBL, different lymphocyte fractions or Jurkat T cells were added to each well and incubated at 37^{o}C.

After 6 minutes, EC were washed with M199 BSA (0.15% w/v) to remove non-adherent PBL. Cells were fixed with 2% v/v formaldehyde (Sigma-Aldrich) and imaged using an inverted bright field microscope (Zeiss) at x20 magnification.

To examine the effect of EC pre-treatment with 14-3-3ζ on transmigration, recombinant 14-3-3ζ (20ng/ml) was incubated with EC in M199 BSA (0.15% w/v) containing 100U/ml TNF-α and 10ng/ml IFN-γ for 1 hr before or immediately before performing the migration assay.

The broad-spectrum matrix metalloproteinase inhibitor GM6001 was used to investigate the cleavage of 14-3-3ζ into PEPITEM. GM6001 (Santa Cruz, 10nM) was pre-incubated with EC in M199 BSA (0.15% w/v) containing 100U/ml TNF-α and 10ng/ml IFN-γ and also with PBL for 1 hr prior to migration. After all treatments, EC were washed and the transmigration assay was performed as previously described.

2.2.3.4. Analysis

PBL migration was imaged and analysed using ImagePro 6.2 software (Media Cybernetics). Adherent and migrated PBL from microscope images were counted and the average from 8 randomly selected fields was taken. The number of adherent cells was calculated by multiplying the calibrated microscope field by the surface area of EC in mm^2 and dividing this by the known total number of PBL added, to obtain the percentage of the PBL that had adhered. This was used to calculate the percentage of transmigrated PBL. Adherent cells were classed as phase-bright and surface adherent. Transmigrated cells were classed as phase-dark and appeared spread under the endothelial cell monolayer (Figure 2.1).

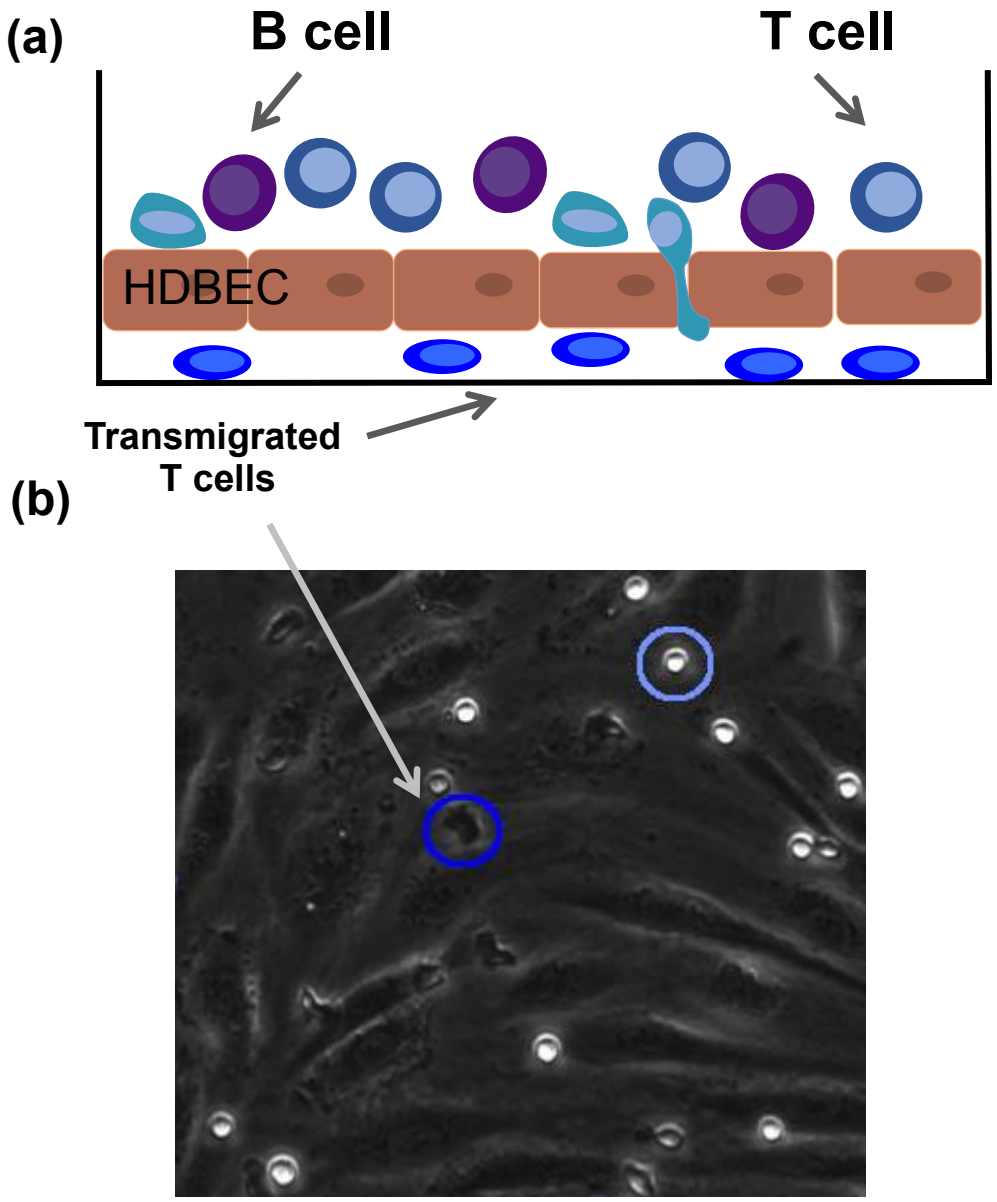

Figure 2.1. Diagrammatic representation of *in vitro* T cell transmigration assay. (a) Schematic of *in vitro* transmigration assay. HDBEC are grown to confluence and cytokine stimulated before the addition of PBL, including B cells and T cells. In this assay, it is the T cells that predominantly transmigrate. (b) Example of a field of view imaged using an inverted light microscope. Firmly adherent phase bright PBL (light blue) remain round and on top of the endothelium, while transmigrated phase dark PBL (dark blue) appear underneath the endothelial cell layer appearing flattened and irregularly shaped.

2.2.4. Cell sorting

2.2.4.1. T cell isolation

PBL were isolated from healthy donors as previously described. B cells were depleted using CD19 beads (Miltenyi Biotec) according to manufacturer's instructions. $9x10^6$ PBL were incubated with 80µl MACs buffer (1x PBS, 2mM EDTA, 5mg/ml BSA), and 20µl CD19 magnetic beads at 4^oC for 20 minutes. Cells were then washed and re-suspended in 500µl MACs buffer. Magnetic LD columns (Miltenyi Biotec) placed in a MidiMACS Separator magnet (Miltenyi Biotec) were rinsed with 1ml MACs buffer before addition of cells for magnetic separation. 1ml MACs buffer was added, and this step was repeated for maximum elution. Flow cytometry was used to confirm B cell depletion, and purity of at least 99% $CD3^+$ T cells was deemed acceptable.

2.2.4.2. B cell isolation

PBMC were isolated as previously described and B cells were enriched using an EasySep kit (StemCell) and following manufacturer's instructions. Human antibody cocktail was incubated with PBMC at 50µl per $1x10^7$ cells for 10 minutes at room temperature in a 15ml centrifuge tube. Magnetic beads were added to the solution at 75µl per $1x10^7$ cells for 5 minutes at room temperature. The total volume was brought to 9ml with MACs buffer and the tubes were placed in an EasySep magnet (StemCell) for 5 minutes at room temperature. Enriched cells were then poured off into a fresh 15ml centrifuge tube, re-incubated in the magnet for 5 minutes

and poured into a final 15ml centrifuge tube to enhance purity. Flow cytometry was used to confirm B cell enrichment and purity of at least 95% was deemed acceptable.

2.2.5. Identification of PEPITEM in samples

2.2.5.1. Demonstrating the production of PEPITEM from 14-3-3ζ

10µl of recombinant 14-3-3ζ protein (100µg/ml, Fitzgerald) re-suspended in PBS was aliquotted into Eppendorf tubes giving 10µg/tube. 40µg/ml HPLC-grade trypsin (Promega) prepared in in 10% v/v acetonitrile (ACN, VWR chemicals), 90% v/v HPLC dH_2O and 0.1% v/v TFA (trifluoroacetic acid, Sigma-Aldrich) was used to digest the 14-3-3ζ protein for 1 h at 37°C. As described in section 2.2.5.2 and 2.2.5.3, samples were purified on C18 columns with 10-100% v/v ACN + 0.1% v/v TFA as the final elution, and analyzed using mass spectrometry and database searching.

2.2.5.2. Preparation of samples for mass spectrometry

All samples were spiked with 10ng tritiated (^3H) PEPITEM (Alta Biosciences) as an internal mass standard for relative intensity quantification by mass spectrometry. C-18 solid phase extraction columns (Supelco, Sigma-Aldrich) were used to purify samples. Initially, columns were conditioned with 1ml 100% ACN + 0.1%v/v TFA. Columns were then washed with 1ml HPLC-grade dH_2O (Sigma-Aldrich) + 0.1% TFA to equilibrate. Samples containing 0.1% v/v TFA were added to the column and, like all additions, were allowed to percolate by gravity. Columns were washed again with 1ml dH_2O + 0.1% v/v TFA, and finally eluted with 1ml 10-

100% ACN. Eluent containing purified samples was collected in Eppendorf tubes, dried in a vacuum centrifuge at 37^{o}C and re-suspended in 30µl 2% v/v ACN containing 0.1% v/v formic acid (Sigma-Aldrich).

2.2.5.3. Mass spectrometry

10µl of each purified sample was analysed by liquid chromatography–tandem mass spectrometry (LC-MS/MS) as illustrated in Figure 2.2. A gradient of 2−36% v/v ACN in 0.1% v/v formic acid over 30 min at 350nl/min was run in a Dionex Ultimate 3000 HPLC system. The initial low concentration of solvent enables peptides to bind to the column before being eluted by the increasing solvent gradient. This facilitates peptide separation on the basis of hydrophobicity, with highly hydrophobic peptides being retained longer on the column. The HPLC instrument was connected to an Electron Transfer Dissociation (ETD) amazon ion-trap mass spectrometer (Bruker) with a nanospray source. Here, samples were sprayed into the mass spectrometer and electrostatic attraction of the sample now in gas-phase draws the peptides into the ion-trap. This separates the ions basis of their mass to charge ratio (m/z). A mass spectrometry survey scan from 350 to 1,600 m/z was performed and the five ions of highest intensity per survey scan were selected for fragmentation by ETD, usually at the peptide bond. M/z is then determined, and this process is named MS/MS. Raw data was processed using the Bruker ProteinScape software package to select peaks which were subsequently searched using the Mascot search engine (version 2.1) with the SwissProt protein database.

Endogenous and synthetic ^{3}H PEPITEM elute at the same position on the gradient owing to their identical chromatographic properties, enabling comparison in the same mass spectrum. However, due to their different physical properties, these versions were resolved as separate peaks within this mass spectrum (Table 2.5), thereby allowing a comparison of intensity of 10ng radiolabelled standard within extracted ion chromatograms (EIC) to endogenous PEPITEM in samples. Within the field of analytical science, this method of quantification is time-honoured (Eidhammer *et al.*, 2012).

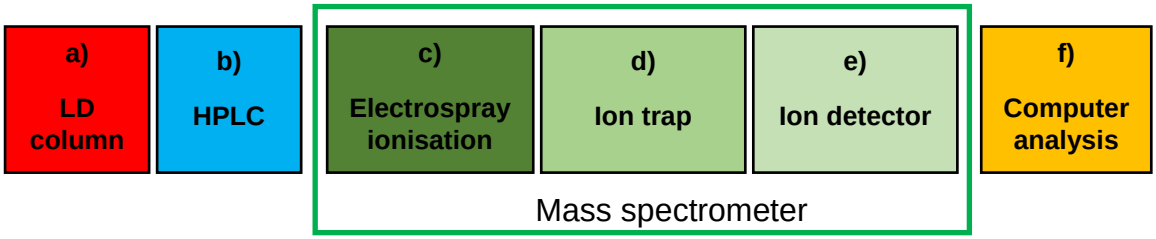

Figure 2.2. Schematic representation of the proteomic approach employed to detect PEPITEM in biological samples.
(a) Initially, peptides were purified on C18 LD columns. (b) Peptides were then separated based on hydrophobicity using HPLC. (c) The sample exits the HPLC system and enters the mass spectrometer, where the peptides are subsequently given charge by electro-spray ionisation and (d) separated by m/z in an ion trap. (e) Finally, ions are detected and their abundance measured, (f) and the data analysed via computer.

Table 2.5. M/z of endogenous and ^{3}H PEPITEM.
Quantification was made possible owing to the different m/z of radiolabelled (^{3}H) PEPITEM and endogenous PEPITEM.

PEPITEM VERSION:	TOTAL SIZE (m/z)
Endogenous PEPITEM	774.88 ± 0.05
Radiolabelled (^{3}H) PEPITEM standard	780.88 ± 0.05

2.2.6. Investigating PEPITEM interactions using Biacore binding assays

Biacore binding assays monitor real-time molecular interactions by utilising the principle of surface plasmon resonance (SPR) (Figure 2.3). All Biacore assays were performed with the kind help of Dr. Carrie Willcox (University of Birmingham Cancer sciences, UK) using a Biacore 3000 SPR system (G E Healthcare). HBS-P buffer (GE Healthcare) containing 5mM $CaCl_2$ was used for all reagent dilutions and binding experiments, except when using a Sensor Chip NTA cassette (GE Healthcare), where $CaCl_2$ was omitted. Regeneration of the chips as described by the manufacturer was carried out between all experiments.

To test biotinylated PEPITEM binding to recombinant CDH15, a Sensor Chip CM5 cassette (GE Healthcare) was first activated with EDC (0.4M N-(3-dimethylaminopropyl)-N'-ethylcarbodiimide hydrochloride, G E Healthcare) mixed 1:1 with NHS (0.1M N-hydroxysuccinimide, Sigma-Aldrich). Streptavidin (0.5mg/ml,

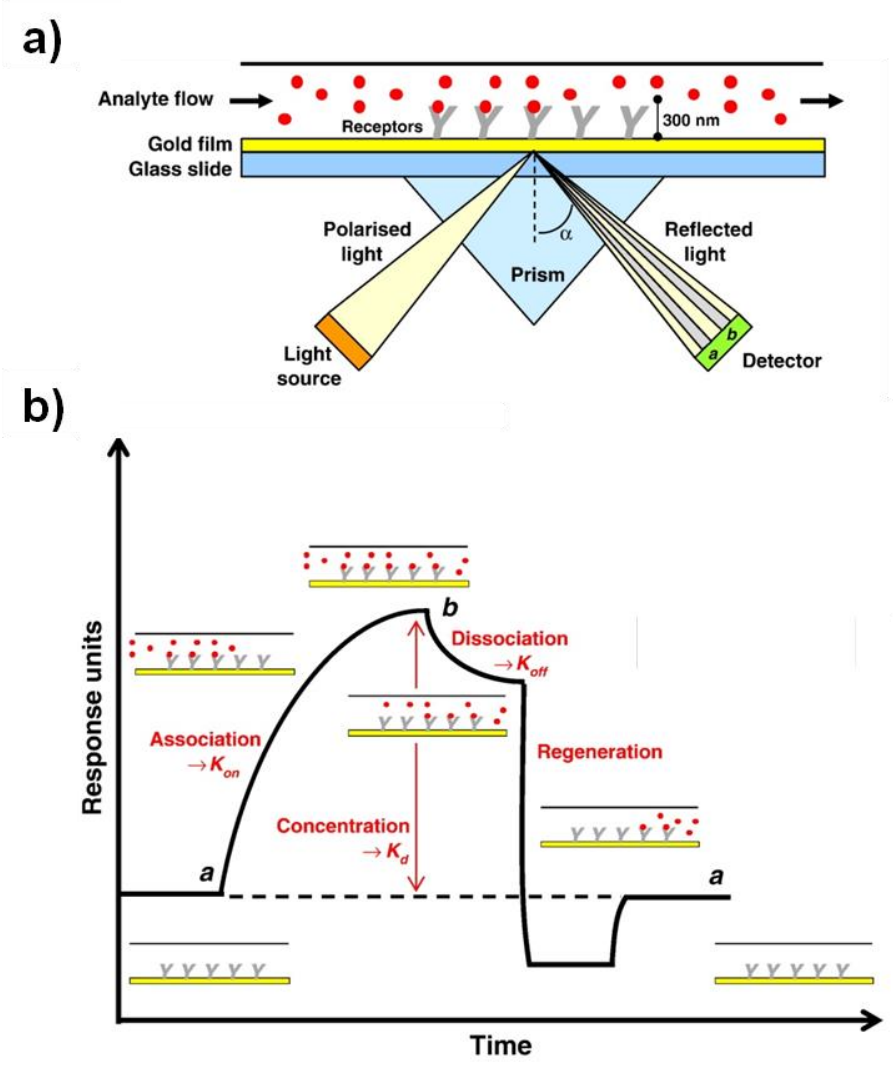

Figure 2.3. Surface plasmon resonance in BIAcore binding assays.
(a) The receptor molecule is immobilised on the sensor surface while analyte ligand solution is injected into the flow cell. Polarised light is directed from a laser through a prism to the sensor surface. The refraction of light off the surface at particular angle, known as the incidence angle (α), causes light absorption and oscillation or "resonance" of electrons also known as surface plasmons on the chip surface. This causes a decrease in intensity of the reflected light detected, which varies following binding interactions at the surface. (b) Illustration of BIAcore sensorgram measuring changes in SPR. Interactions between immobilised molecules, such as receptors, with injected cognate ligand alters the refractive index at the surface, increasing resonance measured as response units (RU). An association phase represents binding site engagement by ligand (k_{on}). When saturation is achieved, the maximum RU can be used to measure binding affinity (K_D). Following cessation of ligand injection, a dissociation phase follows where (k_{off}). The sensorchip surface can then be regenerated ready for the next investigation. (Adapted from Patching (2014)).

Sigma-Aldrich) was coupled to the chip and unreacted esters were then blocked with 1M ethanolamine-HCl (Biacore Life Sciences). 25µg/ml N-terminal biotinlyated PEPITEM or Scrambled control was then immobilised onto the chip at 5µl/min. 12.5-100µg/ml (0.10-0.82µM) recombinant CDH15 or 50µg/ml (0.30µM) recombinant thrombospondin-1 (both R & D) was subsequently flowed over the chip at 10µl/min.

To test binding in the opposite orientation, 25µg/ml anti-human IgG antibody (Abcam) was immobilised onto a CM5 Sensor Chip cassette following activation as previously described. FC-tagged CDH15 (25µg/ml, R & D) was immobilised onto the chip at 5µl/min. A solution of 10-50µg/ml (6.7-33.33µM) PEPITEM and 10-50µg/ml (0.06-0.30µM) TSP-1 (pre-incubated at 37^{o}C for 1 hr to promote potential complex formation) was then flowed over at 10µl/min.

Finally, to investigate any interactions between 14-3-3ζ and potential binding partners, a Sensor Chip NTA cassette (G E Healthcare) was regenerated with nickel(II)chloride solution and 14-3-3ζ-His tagged recombinant protein (25µg/ml, Fitzgerald) was immobilised at 5µl/min. 50-100µg/ml TSP-1 (0.30-0.60µM) or 50-200µg/ml CDH15 (0.80-1.60µM) was flowed over at 10µl/min.

Blank flow cells or scrambled PEPITEM were used as controls in case of any non-specific binding. Binding was measured in response units (RU) and the data traces were analysed using BiaEvaluation software (G E Healthcare).

2.2.7. Examining PEPITEM structure using Nuclear Magnetic Resonance Spectroscopy

Nuclear magnetic resonance (NMR) occurs when the nuclei of atoms are placed into a stable magnetic field and subsequently exposed to a second oscillating magnetic field. NMR spectroscopy is based on the principle that subatomic particles i.e. protons, neutrons and electrons, have "spin". In ^{1}H, commonly used for NMR investigations, two energy states (*m*) are possible, $m = +½$ (a) and $m = -½$ (β), as depicted in Figure 2.4. The difference in energy states gives rise to a population difference with more nuclei in the lower energy state. This gives rise to a single signal.

All NMR investigations were performed with the help of Dr. Mark Jeeves at the HWB-NMR facility, University of Birmingham. 1.2mg PEPITEM (>90% purity) was initially dissolved into 50mM sodium phosphate buffer. 50mM 5N NaOH was added until PEPITEM was dissolved. The pH of the solution adjusted to pH 6.0 by addition of 5M HCl. The final salt and PEPITEM concentrations were determined based on the amount of NaOH and HCl added. A final solution of 5mM PEPITEM in a 50mM sodium phosphate buffer containing 50mM sodium chloride at pH 6.0 was used for NMR investigations.

NMR data was collected on a Bruker 600 MHz spectrometer equipped with a 1.7mm triple resonance cryogenic probe as summarised in Figure 2.5. A one dimensional 1H spectrum was collected to assess peptide purity and solubility. A two dimensional TOCSY (Total correlation spectroscopy) spectrum was collected using a spin-lock mixing period of 100 ms to identify nuclei in the same spin system. Two ROESY (Rotating frame nuclear Overhauser effect spectroscopy) spectra were

collected using mixing times of 100 and 200 ms in order to generate distance restraints for structural determination.

Data was processed using NMRpipe (Delaglio *et al.*, 1995) and analysed using CcpNmr Analysis (Vranken *et al.*, 2005). Structures were calculated using Crystallograpy and NMR System (CNS) software (Brunger, 2007). Structural alignment and figures were created using PyMOL software (Schrödinger).

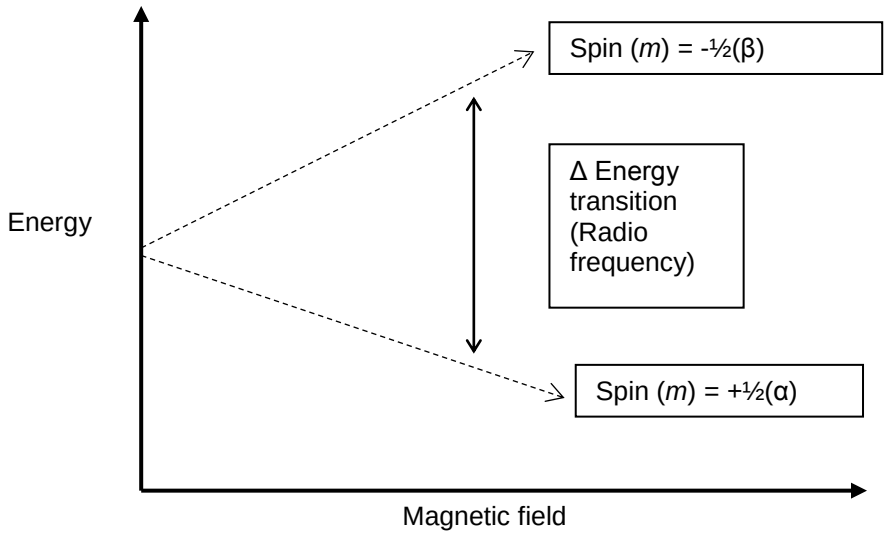

Figure 2.4. ^{1}H spin states in an external magnetic field.
Depending on the strength of the external magnetic field, nuclei absorb and re-emit electromagnetic energy at a specific frequency. ^{1}H nuclei take on either a low energy (α) or high-energy (β) state. Nuclei with lower energy spin in alignment with the external magnetic field, whereas nuclei with higher energy spin against the external magnetic field. (Adapted from Keeler (2013)).

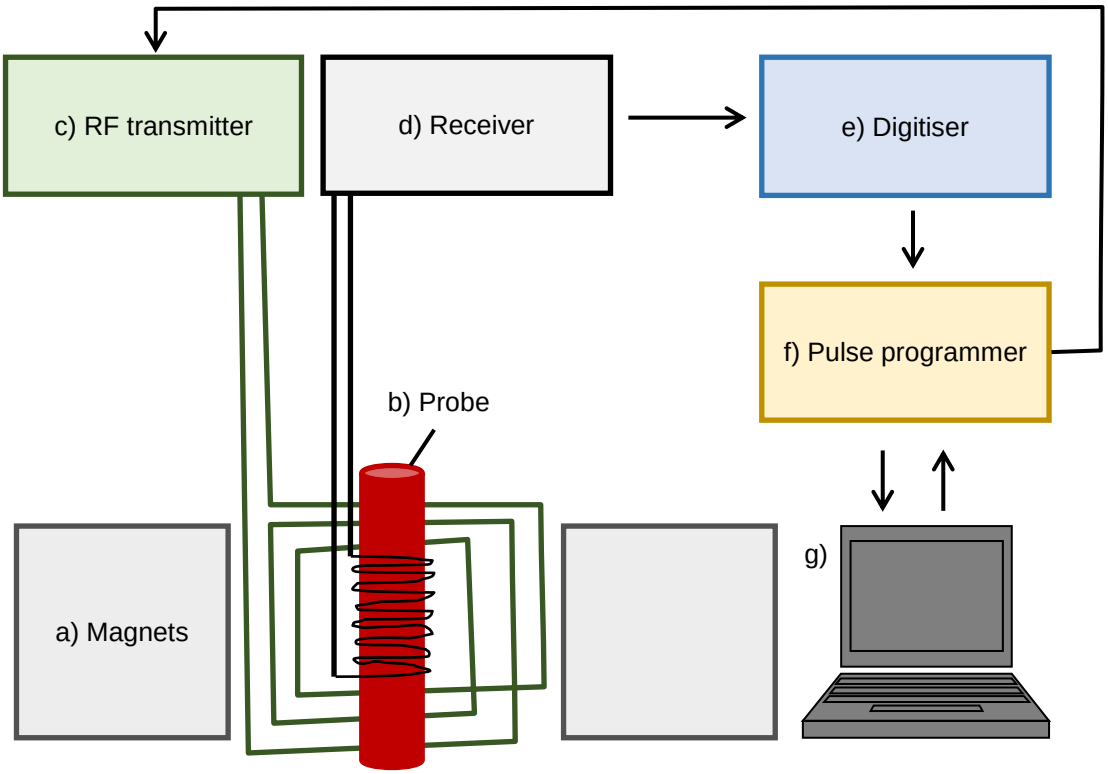

Figure 2.5. Schematic of NMR spectrometer.
A stable magnetic field is generated using (a) a 600MHz magnet. (b) A 1.7mm triple resonance cryogenic probe was used to excite the sample placed in it and detect magnetisation. (c) A transmitter generated short pulses of radio frequency (RF) energy and (d) a receiver amplified small NMR signals from the probe. (e) A digitiser converts these signals from voltage into binary numbers. (f) Pulse programmer hardware controls spectrometer function, delivering precise pulses. Finally, (g) a computer controls the whole experiment and facilitates data processing (Adapted from Keeler (2013)).

2.2.8. Intracellular calcium flux assay

HDBEC were seeded at $5x10^3$ per well in a 96-well clear bottom black-sided assay plate (Greiner Bio One) and grown to confluence. HDBEC were stimulated with 100U/ml TNF-α and 10ng/ml IFN-γ for 24 hours at 37^oC. Calcium flux was measured

using a Fluo-4 NW Calcium Assay Kit (Invitrogen) according to manufacturer's instructions. Briefly, calcium dye was reconstituted with HEPES buffer solution, and 2.5mM probenecid was added to prevent calcium leakage. Cells were washed with 100µl warm PBS without calcium and magnesium, and then incubated with the calcium dye solution for 30 minutes at 37^{o}C in the dark followed by 30 minutes at room temperature in the dark.

A compound plate containing 270µl per well of each treatment was prepared so that the final concentration once injected into the assay plate was as follows: calcium ionophore (0-10^{-6}M, Sigma-Aldrich), sphingosine-1-phosphate (S1P; 0-10^{-1}M, Cayman Chemicals), PEPITEM or scrambled peptide (0-10^{-1}mg/ml). 50µl of each compound was injected into the respective wells of the assay plate. The plate was read at room temperature every 2 seconds for 180 seconds per well using a FlexStation plate reader (Molecular Devices, E_{ex} 488nM, E_{em} 525nM) with SoftMax Pro software (Molecular Devices). To calculate percentage maximal increase in relative fluorescent units (RFU), data was normalised by subtracting the average baseline reading before treatment (measured over the first 12 seconds) from the maximal RFU after treatment, and then dividing by the average baseline. Data represents the mean of 4 experiments all performed in triplicate.

2.2.9. *In vivo* studies using PEPITEM

2.2.9.1. Mice

Apolipoprotein E-deficient (apoE$^{-/-}$) C57BL/6 mice (Jackson Laboratories) and wild-type (WT) BALB/c mice (bred in-house) were nurtured

[redacted] under specific pathogen-free (SPF) conditions. All animals were fed a normal chow diet (LabDiet) unless otherwise stated. All experiments were performed in accordance with United Kingdom Home Office regulations. To study the *in vivo* effects of PEPITEM in a model of atherosclerosis, 6 week-old apoE$^{-/-}$ C57BL/6 mice were placed on a high fat diet containing 0.15% w/w supplementary cholesterol (HFD, Special Diet Services) for a further 6 weeks. Weights of all mice used in this study were recorded weekly and before procedures. All tissue was collected under the appropriate home office (40/3659) and PIL (40/10768) licenses.

2.2.9.2. In vivo pharmacokinetics of PEPITEM

Initially, varying concentrations of ^{3}H PEPITEM were spiked into mouse blood *in vitro* and measured by scintillation counting to test optimal detection of radioactivity. Several ratios of ^{3}H PEPITEM:scintilllant were also measured to determine optimal measurement conditions.

Male 8-10-week old WT C57BL/6 mice were weighed and injected intravenously (IV) via the tail vein with 100µl radiolabelled (^{3}H) PEPITEM at 1ng/g. After 2-60 minutes, mice were anaesthetised with isofluorane and culled by cardiac puncture followed by cervical dislocation. Approximately 800µl blood was collected into CDPA and centrifuged at 15,000x g for 10 minutes. Serum was transferred into a fresh Eppendorf. 50µl of serum was placed into scintillation counting tubes in triplicate with 2ml of Optiphase Hisafe 3 scintillant cocktail (Perkin Elmer) per tube, and counted using a Packard Tri-Carb 2500TR scintillation counter. Samples were counted for 10 minutes and radioactivity was measured as disintegrations per minute

(DPM1). Quench correction was automatically applied using internal ^{3}H standards. For time point 0, mice were not injected but instead culled as described above for baseline radioactivity measurements. For 100% radioactivity measurements, mice were not injected. Instead, whole blood was collected and spiked with 1ng/g ^{3}H PEPITEM prior to RBC removal by centrifugation and processed as described above.

2.2.9.3. Determining the endpoint of PEPITEM in vivo.

PEPITEM was conjugated to SAIVI Alexa Fluor 680 dye (Life Technologies) via the amide group by Alta Biosciences, Birmingham, UK, according to manufacturer's instructions. Initially, the conjugated peptide was tested *in vitro* for functionality using the adhesion assay described in section 2.2.3. Optimum dosage for *in vivo* imaging was determined using a black 96-well plate and 0-150µg PEPITEM-AF680 diluted in PBS.

100µg of PEPITEM-AF680 was injected IV via the tail vein into 3 male 6-8 week old BALB/c mice, which were fasted 16 hours prior to imaging to minimise dietary autofluorescence. 3 age and sex-matched mice were injected with PBS as a control. After 15 minutes, mice were sacrificed by schedule 1 procedure. All major organs (stomach, gut, liver, heart, lungs, spleen, and kidney) were excised immediately and arranged in a petri dish. Organs were imaged using an *In Vivo* Imaging System (IVIS Spectrum, Perkin Elmer) using 675nm excitation filters and 720nm emission filters. Regions of interest (ROIs) were set for each organ and fluorescent signal was measured as radiant efficiency using Living Image software (Perkin Elmer). Data was normalised to the ROI area using the sum of the radiance from inside the ROI divided by the number of pixels, and background was subtracted.

Data is expressed as photons per second per centimetre squared per steradian (p/s/cm^2/sr).

2.2.9.4. In vivo effects of PEPITEM in apoE$^{-/-}$ mice on high fat diet

6 male C57BL/6 mice were fed HFD for 6 weeks. In addition from 6 weeks of age, mice received intra-peritoneal (IP) injections of 1.75mg/ml C-terminal PEGylated PEPITEM or C-terminal PEGylated scrambled control in 200µl sterile PBS twice a week for 6 weeks (350µg/injection). After 6 weeks, mice were culled by cardiac exsanguination under isofluorane anaesthesia. Approximately 200µl blood was collected in CPDA (Sigma Aldrich) for blood counts, and the rest was stored in an Eppendorf tube at -80^{o}C for serum analysis later. Liver, hearts and all major organs were collected for future analysis.

2.2.9.5. Tissue preparation and histology.

Livers were fixed in 10% v/v formaldehyde for 24 hours, paraffin embedded and sectioned into 4µm sections using a microtome. Hearts were frozen and cryosectioned into 6µm cross-sections of the aortic root, ensuring visibility of the bicuspid valves. Sections were mounted on Xtra glass slides (Leica Biosystems, UK).

Standard histological assessment of tissue morphology was performed using haematoxylin and eosin (H&E) staining of formalin-fixed paraffin embedded (FFPE) tissue sections. De-waxed sections were stained using a routine protocol. Sections were raised in dH_2O, stained in Mayers haemotoxylin for 4 minutes, incubated in 0.3% v/v acid alcohol for 30 seconds and stained in eosin for 2 minutes with intermittent 5 minute incubations in dH_2O between each step. Sections were then dehydrated

rapidly in alcohol, cleared and mounted in DPX mounting media (all Leica Biosystems).

Oil red O staining was performed to visualise lipid accumulation within the aortic root. Frozen sections were allowed to equilibrate to room temperature. Gently, sections were then fixed in 4% v/v formaldehyde for 10 minutes, submerged in dH_2O, rinsed in 70% v/v isopropanol (Sigma-Aldrich) and incubated in Oil red O solution (Sigma-Aldrich), for 30 minutes. Oil Red O solution and was prepared fresh using 0.5g in 100ml isopropanol. Sections were then briefly submerged in 70% v/v isopropanol and then in PBS before allowing to air dry at room temperature. Stained sections were imaged using brightfield microscopy and subsequently analysed using Image J software.

2.3. Statistical analysis

All data are expressed as mean ± standard error of the mean (SEM) unless otherwise specified. Differences were analysed using GraphPad Prism statistical software package (GraphPad software Inc., USA), by linear regression analysis, unpaired t-test or by one way analysis of variance (ANOVA), followed by post-hoc analysis for multiple group comparison either to the control (Dunnett) or between all conditions (Bonferroni). The Kolmogorov-Smirnov normality test was used to test for normal distribution. $P \leq 0.05$ was considered statistically significant.

CHAPTER 3: EXAMINING PEPITEM INHIBITION OF PBL TRANSMIGRATION *IN VITRO*

3.1. Introduction

T cell trans-endothelial migration represents a complex physiological response to non-self or altered-self antigens. This tightly-controlled and multi-step paradigm is essential for the elimination of the antigenic trigger, and ultimately the resolution of acute inflammation.

Although released by a multitude of white blood cells (WBC), TNF-α is predominantly produced by activated macrophages and T cells. IFN-γ is the classical T cell cytokine, crucial for the orchestration of the adaptive immune response (Frucht *et al.*, 2001, Sen, 2001). These pro-inflammatory cytokines are able to activate endothelial cells (EC) during inflammation, an essential step for the recruitment and transmigration of immune cells from the circulation and into the tissues where they are required. TNF-α is able to induce ICAM-1 and VCAM-1 expression in EC, increasing the adhesion of both lymphocytes and polymophonuclear cells (PMN). On the other hand, IFN-γ induces only ICAM-1 expression in EC and increases adhesion of lymphocytes but not PMN (Thornhill *et al.*, 1991). However, *in vivo*, it is more likely that EC will be subject to stimulation by a combination of cytokines as opposed to individual ones.

The synergistic use of TNF-α and IFN-γ to induce recruitment and transmigration of T cells has been validated in a number of studies (Ahmed *et al.*, 2011, McGettrick *et al.*, 2009, Piali *et al.*, 1998). Of the PBL recruited by TNF-α and IFN-γ stimulated EC, $CD4^+$ and $CD8^+$ $CD45RA^-/RO^+$ memory T cells predominantly migrate, however exact proportions have varied between experiments (Ahmed *et al.*, 2011, Brezinschek *et al.*, 1995, McGettrick *et al.*, 2009, Pietschmann *et al.*, 1992).

In chronic inflammation, the regulatory mechanisms underlying selective recruitment of immune cells and preferential migration of T lymphocytes are dysregulated. This results in persistent T cell trafficking into inflamed tissues. Such inappropriate T cell trafficking can manifest with pathological consequences, highlighted by diseases such as rheumatoid arthritis (RA) and type 1 diabetes (T1D) (Imagawa *et al.*, 1999, Komatsu and Takayanagi, 2012).

Lipid mediators are synthesised from lipid precursors released from cell membranes, via conserved biosynthetic enzymes. The bioavailability of fatty acids has been previously shown to regulate both T cell and neutrophil migration (Ahmed *et al.*, 2011, Tull *et al.*, 2009). Following integrin activation, T cells receive a final signal from PGD_2, which binds to the PGD_2 receptor (DP_2) on the T cell surface, promoting migration. The availability of different fatty acids, for example, eicosapentaenoic acid (EPA), can also effect leukocyte migration. EPA can act as alternative substrate for COX enzymes, generating a PGD_2 analogue, PGD_3 which can subsequently antagonise the DP_2 receptor (Tull *et al.*, 2009).

More recently, our lab identified a novel pathway in the homeostatic regulation of T cell trafficking (Chimen *et al.*, 2015). T cell trafficking is dysregulated in chronic inflammatory diseases and recent findings suggested that this is due, at least in part, to impairment of the adiponectin-PEPITEM axis as a result of decreased expression of B cell adiponectin receptors (Chimen *et al.*, 2015).

In this chapter, the reproducibility of results previously obtained in our lab will be initially evaluated to ensure comparability between historical and new experiments. The data presented here suggested this was indeed the case.

3.2. Results

3.2.1 Establishing optimal cytokine concentrations for lymphocyte adhesion and transmigration across endothelium.

The *in vitro* transmigration assay first described by McGettrick *et al.* (2009) was developed in our lab for measuring the migration of T cells across cytokine stimulated endothelium. This well-established technique was central to the research conducted by Chimen *et al.* (2015). In succession of this original research, the *in vitro* migration assay forms a key part in the generation of fresh data to be described in this thesis. Therefore, the reproducibility of the recruitment and transmigration of PBL under static conditions was initially investigated to ensure historical comparability, as variables such as new investigators or reagent batches can cause undesired discrepancies in results.

HDBEC were stimulated for 24 hours with varying concentrations of pro-inflammatory cytokines, TNF-α and IFN-γ. The adhesion and migration of PBL from healthy donors was assessed using the *in vitro* transmigration assay. Unstimulated EC were unable to support the substantial recruitment and transmigration of PBL, with the adhesion of only 32 cells/mm^2/1x10^6 and the transmigration of just 2% PBL (Figure 3.1a). However, stimulation with increasing concentrations of TNF-α + 10ng/ml IFN-γ lead to an increase in both adhesion and transmigration of PBL.

EC stimulated with 100U/ml TNF-α + 10ng/ml IFN-γ demonstrated significant recruitment of 181 cells/mm^2/1x10^6 PBL, and transmigration of 37% PBL compared to the unstimulated control.

Again in experiments where EC were stimulated with 100U/ml TNF-α + 10ng/ml IFN-γ, adhesion was increased from 7 cells/mm^2/1x10^6 to 197 cells/mm^2/1x10^6, and transmigration from 0% to 41% (Figure 3.1b), however increasing the concentration of IFN-γ to 100ng/ml did not lead to an additive effect, with the number of adherent cells being 190mm^2/1x10^6 and transmigration at 43%.

To further confirm the ability of EC to recruit PBL, gene expression of key endothelial cell adhesion molecules and chemokines involved in the recruitment and migration of T cells were measured as evidence of endothelial cell activation after EC treatment with the confirmed optimal concentrations of 100U/ml TNF-α and 10ng/ml IFN-γ. Cytokine stimulation lead to an increase in relative gene expression of ICAM-1 and VCAM-1 (Figure 3.2a), and the IFN-γ inducible chemokines CXCL9-11 (Figure 3.2b). These data demonstrated the ability for 100U/ml TNF-α and 10ng/ml IFN-γ to induce EC cell adhesion molecules and chemokine expression, and thus facilitate the transmigration of PBL.

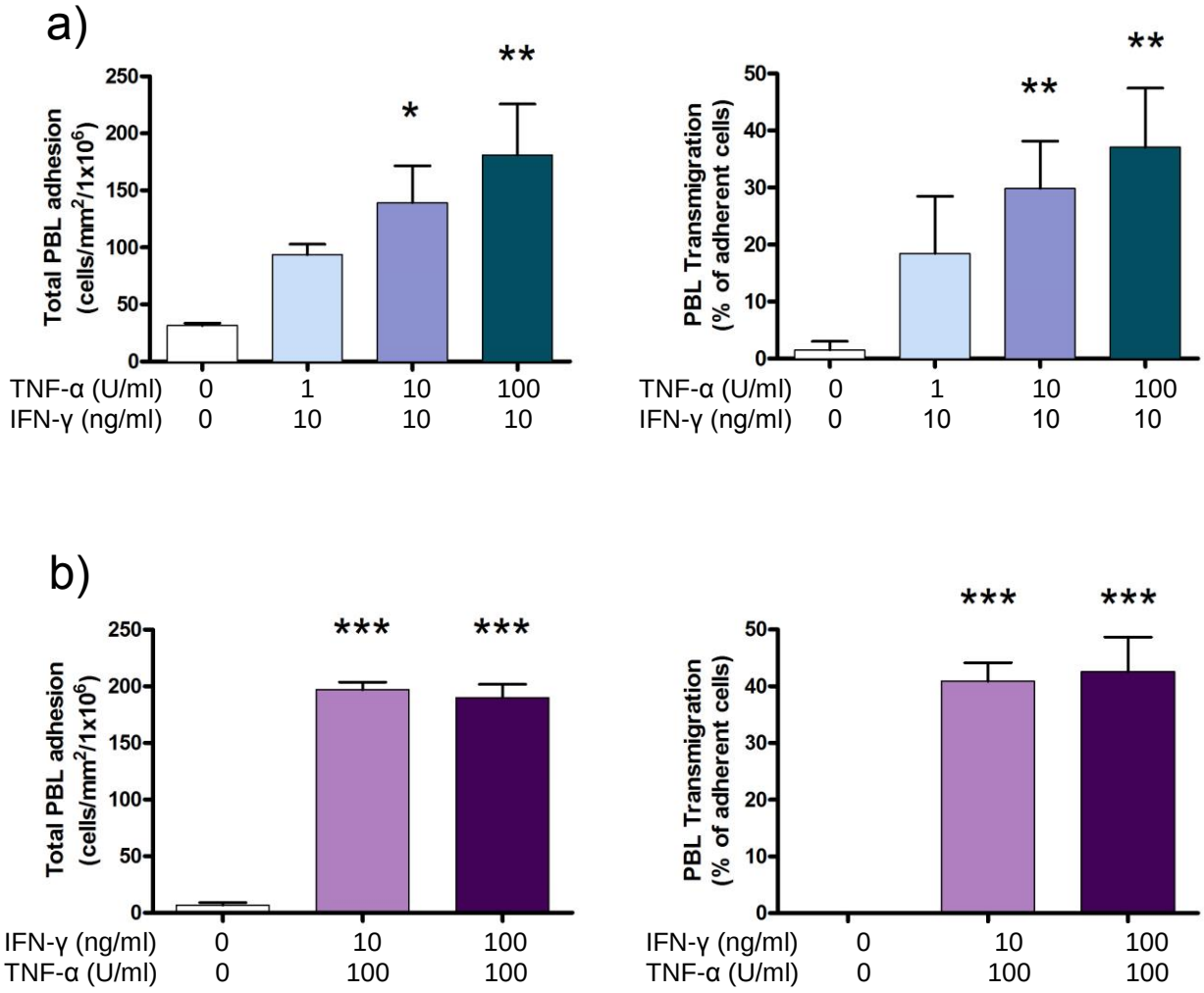

Figure 3.1. The effects of TNF-α and IFN-γ on PBL adhesion and migration. HDBEC were synergistically stimulated with varying concentrations of TNF-α and IFN-γ. The levels of PBL total adhesion and transmigration across the endothelium were assessed under static conditions. (a) EC were stimulated with increasing concentrations of TNF- α, or (b) IFN-γ. Data represents mean ± SEM of 3 independent experiments, analysed by one-way ANOVA with Dunnett's post-test compared to unstimulated controls (Clear bars). *P≤0.05, **P≤0.01 and ***P≤0.001.

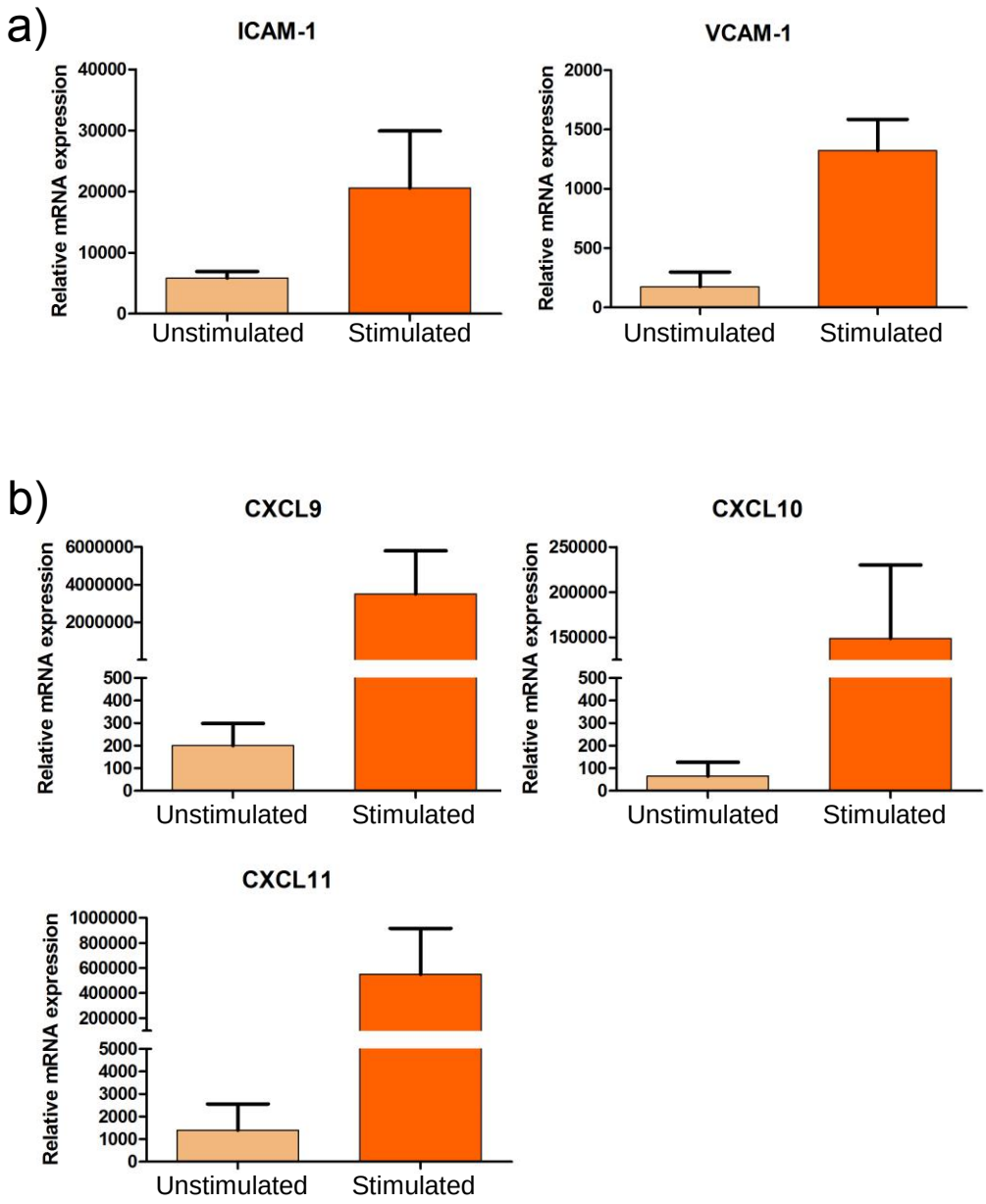

Figure 3.2. Chemokine and cell adhesion molecule expression in HDBEC following cytokine stimulation.
HDBEC were stimulated with 100U/ml TNF-α + 10ng/ml IFN-γ for 24 hours. mRNA was isolated and converted to cDNA. The expression of (a) cell adhesion molecules and (b) chemokines was measured by qPCR, relative to the endogenous control 18S. Data represent mean ±SEM of 2 independent experiments.

3.2.2. Investigating the reproducibility of the inhibitory effects of Adiponectin and PEPITEM *in vitro*, and the involvement of exogenous lipids.

After confirming optimal cytokine conditions for the *in vitro* migration assay, we next assessed the reproducibility of the inhibitory effects of adiponectin and PEPITEM first described by Chimen *et al.* (2015).

Adiponectin (AQ) was used at 10µg/ml, validated initially in preliminary experiments (data not shown), while PEPITEM was synthesised and tested at 10ng/ml and 20ng/ml for inhibitory function. AQ or PEPITEM treatment did not significantly affect adhesion (Figure 3.3a). Conversely, a significant decrease in transmigration was observed for adiponectin and PEPITEM-treated conditions. While 10µg/ml adiponectin reduced PBL transmigration from 33% to 17%, the addition of 10ng/ml and 20ng/ml of PEPITEM to the migration assay decreased PBL transmigration to 20% and 19% respectively. 20ng/ml scrambled peptide exhibited similar levels of transmigration as the control (34% compared to 33% respectively), demonstrating that the inhibitory effect is specific to PEPITEM.

To determine the effectiveness of PEPITEM inhibition of PBL transmigration at different extents of inflammation, EC were stimulated with 10-100U/ml TNF-α + 10ng/ml IFN-γ for 24 hours. The adhesion and transmigration of PBL across the endothelium was measured following the addition of 20ng/ml PEPITEM (Figure 3.3b). Consistent with Figure 3.1a, increasing TNF-α concentrations increased both adhesion and transmigration of PBL. Again, PEPITEM did not affect the adhesion of

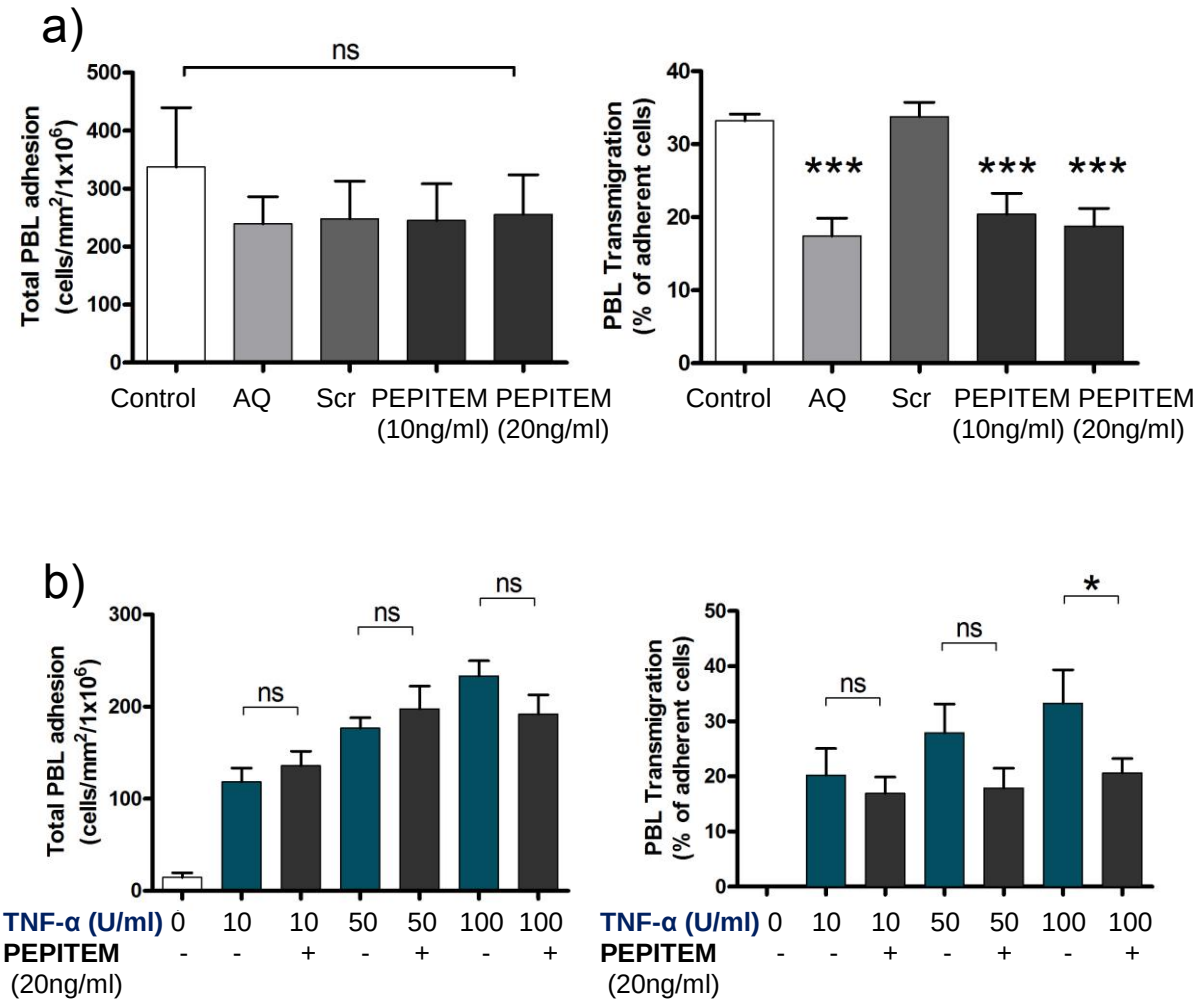

Figure 3.3. Inhibition of PBL transmigration across cytokine-stimulated endothelium by adiponectin and PEPITEM.
HDBEC were (a) stimulated with 100U/ml TNF-α + 10ng/ml IFN-γ for 24 hours. PBL adhesion and transmigration was examined following treatment with 10μg/ml adiponectin (AQ) or 10-20ng/ml PEPITEM or scrambled (Scr) control. (b) EC were stimulated with 0-100U/ml TNF- α + 10ng/ml IFN-γ before examining the effects of 20ng/ml PEPITEM on PBL adhesion and transmigration. *P≤0.05, ***P≤0.001, ns=not significant by one way ANOVA followed by Dunnett's or Bonferroni post-tests. Data represent mean ± SEM of ≥3 experiments.

PBL. However, PEPITEM treatment lead to the significant inhibition of PBL transmigration across EC stimulated with 100U/ml TNF-α + 10ng/ml IFN-γ (21% migration compared to 33%), but not at lower TNF-α concentrations.

Fatty acids are common precursors for the synthesis of cell mediators. PGD_2 is a prostanoid derived from the fatty acid arachidonic acid via COX enzymes (O'Banion, 1999). PGD_2 has previously been shown to mediate memory T cell transmigration across cytokine-simulated endothelium (Ahmed *et al.*, 2011). Therefore, the availability of fatty acid precursors has the potential to interfere with T cell migration in our *in vitro* migration assay. To certify that the inhibitory effect of PEPITEM was not influenced by the presence of exogenous fatty acids present in media and BSA, the assay was repeated in the presence or absence of fatty acids.

No significant differences in adhesion were noted between treatments in the presence (Figure 3.4a) or absence (Figure 3.4b) of exogenous fatty acids. Adiponectin and PEPITEM maintained their abilities to significantly inhibit PBL transmigration across cytokine-stimulated EC. The presence or absence of fatty acids did not significantly affect the inhibitory properties of AQ and PEPITEM (Figure 3.4c), with adiponectin inhibiting transmigration by 51% and 64%, and PEPITEM inhibiting PBL transmigration by 58 and 65% with and without fatty acids respectively.

Interestingly, in the absence of fatty acids, fewer PBL were recruited under control conditions (221cells/mm^2/1x10^6 compared to 303cells/mm^2/1x10^6 in the presence of fatty acids). Similarly, fewer PBL transmigrated in the absence of fatty acids (19%) compared to with fatty acids (28%).

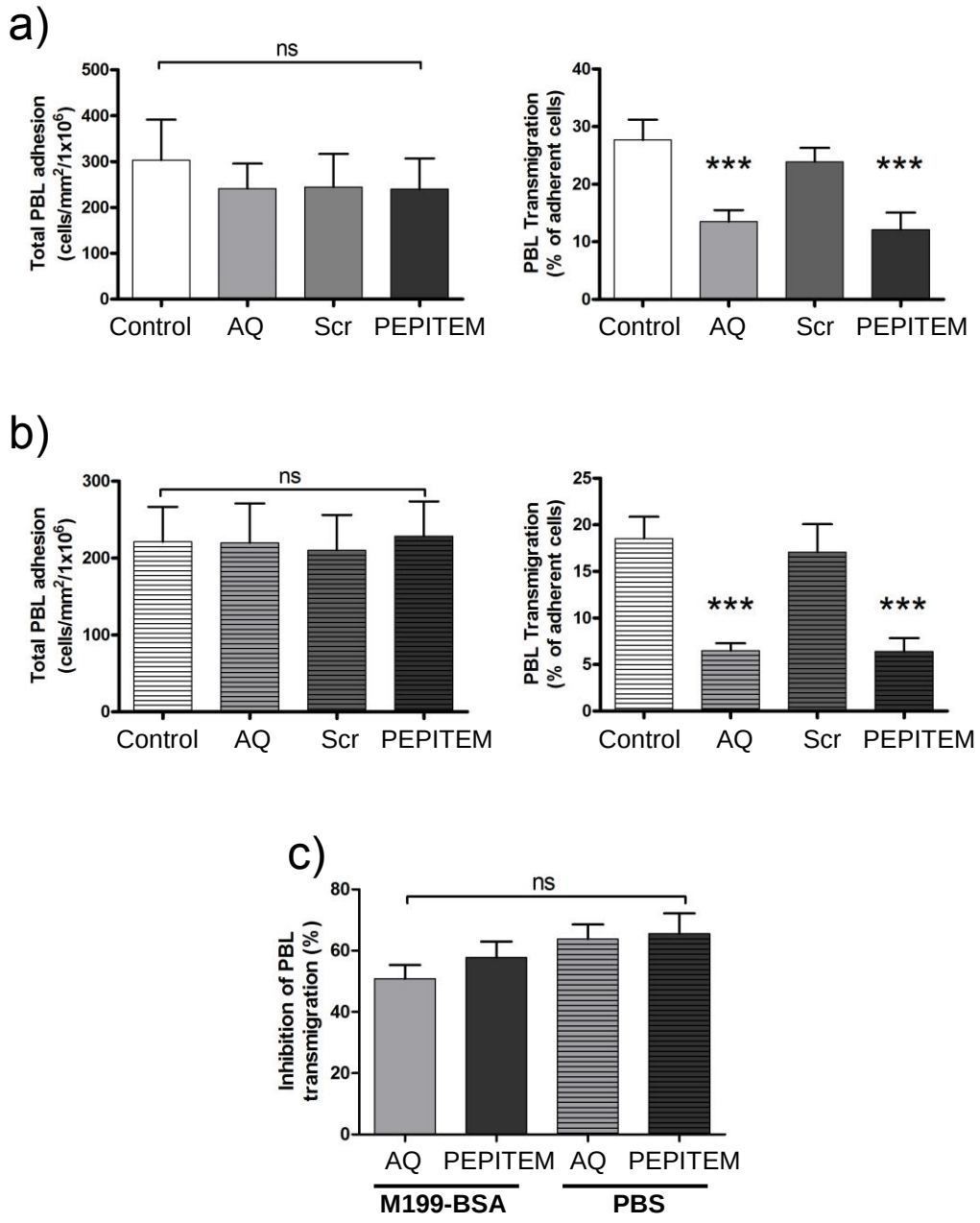

Figure 3.4. The effect of exogenous fatty acids on the inhibitory function of PEPITEM.

PBL adhesion and transmigration across cytokine-stimulated HDBEC following treatment with 20ng/ml PEPITEM or 10µg/ml adiponectin (AQ) was examined in the presence or absence of exogenous lipids using either (a) M199 + 0.15% w/v BSA, or (b) PBS with Ca^{2+} + Mg^{2+}. (c) The percentage inhibition of PBL transmigration by PEPITEM and AQ was compared in M199-BSA or PBS. ***P≤0.001, ns=not significant by one way ANOVA followed by Dunnett's or Bonferroni post-test. Data expressed as mean ±SEM of 4 independent assays. a) and b) represent matched data sets.

These data confirmed the effects of adiponectin and PEPITEM reported previously, and implies that while the absence of fatty acids decreased PBL recruitment and transmigration, it did not affect the ability of adiponectin or PEPITEM to inhibit PBL transmigration.

3.2.3. Tryptic release of PEPITEM from 14-3-3ζ protein.

14-3-3ζ is a highly conserved and ubiquitous protein. However currently, little is known about the production of PEPITEM by B cells, or the cleavage of PEPITEM from 14-3-3ζ.

To demonstrate proteolytic release of PEPITEM from 14-3-3ζ *in vitro*, recombinant 14-3-3ζ protein was digested for 1 hour at 37^{o}C with HPLC-grade trypsin. Samples were purified on C18 columns and eluted with increasing concentrations of ACN which in turn decreases column retention. Samples were analysed by mass spectrometry and database searching as described.

No PEPITEM was detectable in samples eluted with 10% ACN (Table 3.1), indicated by the lack of PEPITEM score and the lack of identification of the peptide fragment sequence of PEPITEM. Unfortunately, some samples became lost during transit to the mass spectrometry facility, however PEPITEM was detected in all measured samples eluted with 20% v/v ACN and above. The same 14-amino acid sequence was detected in all measured samples and the m/z ratio for the parent ion was consistently 774.88. The PEPITEM scores indicate a significant match between the mass of the peptide from mass spectrometry analysis and the real mass of the fragment stored in the database. While the score varied between 86.8 and 111.2, the

scores all remained highly significant as scores ≥30 are considered statistically significant according to the software manufacturer. These data show the ability of PEPITEM to be enzymatically produced from 14-3-3ζ protein.

Table 3.1. Enzymatic release of PEPITEM from its parent protein 14-3-3ζ. Recombinant 14-3-3ζ was incubated for 1 hour at 37^{o}C with HPLC-grade trypsin. Following purification, samples were eluted with increasing percentages of acetonitrile (ACN). Samples were analysed by mass spectrometry with Mascot database searching. The PEPITEM score represents the score given by the search engine indicating the quality of the match between the mass of the peptide from mass spectrometry analysis and the real mass in the database. Scores ≥30 indicate significant matches.

Sample ID	Elution	PEPITEM found	PEPITEM score	Sequence
1	10% ACN	NO	-	-
2	20% ACN	YES	111.2	SVTEQGAELSNEER
3	30% ACN	YES	98.4	SVTEQGAELSNEER
4	40% ACN	SAMPLE LOST	-	-
5	50% ACN	YES	107.4	SVTEQGAELSNEER
6	60% ACN	YES	106.3	SVTEQGAELSNEER
7	70% ACN	YES	88.5	SVTEQGAELSNEER
8	80% ACN	YES	107.9	SVTEQGAELSNEER
9	90% ACN	YES	86.8	SVTEQGAELSNEER
10	100% ACN	SAMPLE LOST	-	-

3.3. Discussion

Lymphocyte migration has been studied *in vitro* under both static and flow conditions. Human umbilical vein endothelial cells (HUVEC), which are macrovascular in origin, and human dermal microvascular endothelial cells (HDMEC), which are microvascular in origin, have been used to study T cell trafficking *in vitro* (Ahmed *et al.*, 2011, Chimen *et al.*, 2015, Luscinskas *et al.*, 1995a, McGettrick *et al.*, 2009). We chose to employ the use of human dermal blood microvascular endothelial cells (HDBEC), as they more closely replicate *in vivo* conditions, being of microvascular origin. T cell recruitment occurs mostly in the peripheral microvasculature such as post-capillary venues, with some exceptions, for example, in the lungs where recruitment occurs in capillaries. The use of both HUVEC and HDMEC has been validated by Chimen *et al.* (2015) to investigate the inhibitory effects of AQ and PEPITEM on PBL transmigration. HDBEC resemble the same population of dermal-derived microvascular EC cells as HDMEC, with the batch used here consisting of a purified population of blood microvascular EC. This was confirmed by PromoCell with immunohistochemical staining and flow cytometry using EC marker PECAM-1 (99% positive), lymphatic EC marker podoplanin (99.7% negative) and stromal cell marker CD90 (96% negative), (PromoCell, 2015).

In order to confirm the reproducibility of PBL transmigration *in vitro* using HDBEC, pro-inflammatory cytokines TNF-α and IFN-γ were examined for their ability to facilitate the recruitment and transmigration of PBL by EC. While EC treated with increasing concentrations of TNF-α exhibited an increasing trend of both PBL

adhesion and recruitment, IFN-γ reached a maximal effect at 10ng/ml, with PBL adhesion and migration across stimulated EC remaining essentially the same as treatment with 100ng/ml IFN- γ. These observations are consistent with other reports using 100U/ml TNF-α + 10ng/ml IFN-γ to study PBL transmigration (Chimen *et al.*, 2015, McGettrick *et al.*, 2009).

TNF-α and IFN-γ mediate EC upregulation of key molecules such as E-selectin, P selectin, ICAM-1 and VCAM-1, required for leukocyte recruitment and migration (Bahra *et al.*, 1998, Bevilacqua *et al.*, 1989, Lidington *et al.*, 1999). Additionally, IFN-γ induces the chemokines CXCL9-11 which are key for T lymphocyte migration. These chemokines represent ligands for the T cell chemokine receptor CXCR3 (Cole *et al.*, 1998, Loetscher *et al.*, 1996). Following ligand binding to CXCR3, integrin activation is triggered via inside out signalling, and permits T cell firm adhesion required for subsequent trans-endothelial migration (Hogg *et al.*, 2011).

To confirm endothelial cell activation and upregulation of these key molecules in HDBEC following cytokine stimulation, we examined mRNA expression by qPCR. Indeed following 24hr stimulation, these adhesion molecules and chemokines were all upregulated in HDBEC, of which CXCL9-11 demonstrated the greatest increase in mRNA expression. Here, we confirm that 100U/ml TNF-α + 10ng/ml IFN-γ provides adequate stimulation of HDBEC to facilitate the measurement of PBL transmigration in our *in vitro* transmigration assays.

Although others have used flow-based assays to study the behaviour of PBL *in vitro*, the static adhesion assay used here has been validated previously by

Chimen *et al.* (2015) who saw no difference in the inhibitory function of AQ between flow and static conditions. We wished to validate the reproducibility of this recently published work demonstrating that AQ and PEPITEM significantly inhibits the transmigration of PBL. In that study, both HUVEC and HDMEC were used however here, we use HDBEC. Nevertheless, our findings were consistent with that of Chimen *et al.* (2015), displaying significant levels of inhibition by both AQ and PEPITEM.

Interestingly, studies have demonstrated preferential recruitment of $CD45RA^{-}/RO^{+}$ memory T cells under static conditions following EC stimulation with TNF-α + IFN-γ (Ahmed *et al.*, 2011, Lichtman *et al.*, 1997, McGettrick *et al.*, 2009, Pietschmann *et al.*, 1992). Additionally, Chimen *et al.* (2015) revealed that PEPITEM-mediated inhibition was mainly of $CD4^{+}$ and $CD8^{+}$ memory T cells. Therefore, in subsequent chapters, though we refer to PBL we may assume that it is the memory T cells forming the majority of transmigrating PBL, and also the majority of PBL inhibited by these agents.

No difference in inhibition of PBL transmigration was seen between 10ng/ml and 20ng/ml PEPITEM. We therefore used 20ng/ml PEPITEM in subsequent experiments to ensure that maximal inhibition could be observed and measured. Remarkably, PEPITEM demonstrated enhanced inhibitory function at higher levels of inflammation, modelled using 10-100U/ml TNF-α + 10ng/ml IFN-γ in section 3.2.2. Although inhibition of PBL transmigration was observed at 50U/ml TNF-α, this was not deemed statistically significant. Perhaps the interacting receptor on the EC, thought to be CDH15 (Chimen *et al.*, 2015), is not upregulated sufficiently by low concentrations of TNF-α, leading to a reduction in intracellular signalling and in turn, a decrease in S1P production required to inhibit T cell transmigration (see Figure 1.4). Chimen *et al.* (2015) reports upregulation of CDH15 in HDMEC only at 100U/ml

TNF-α + 10ng/ml IFN-γ by immunohistochemical staining and real-time qPCR. CDH15 expression needs to be quantified following EC stimulation with increasing concentrations of TNF-α to address this possibility. Additionally, It would be interesting to see if PEPITEM retains its inhibitory function when stimulating EC with different concentrations and combinations of cytokines such as IL-4, which is known to recruit PBL (Thornhill *et al.*, 1991).

Fatty acids and lipids are present in both media and BSA, although the amount probably varies between batches. Fatty acids and lipids typically present in media include free (i.e. unesterified) fatty acids, triglycerides, phospholipids and cholesterol (Brunner *et al.*, 2010), while the majority of lipid impurities in serum albumin are free fatty acids (Chen, 1967). The bioavailability of fatty acids such as arachidonic acid, required for the biosynthesis of PGD_2, has been shown to affect both T cell and neutrophil migration (Ahmed *et al.*, 2011, Tull *et al.*, 2009). For this reason, we investigated the effect of exogenous fatty acids on PEPITEM function to ensure that the inhibitory effect we saw was independent of this.

Lack of exogenous fatty acids still led to significant AQ or PEPITEM inhibition of PBL transmigration, and this did not significantly differ in the presence or absence of fatty acids. These data imply that fatty acid availability does not influence the inhibitory effect that we see in the PEPITEM paradigm.

Interestingly, a reduction in adhesion and transmigration of PBL was noted in the absence of exogenous fatty acids. Fatty acids serve as fuel for cells, and also constitute cellular components such as membrane phospholipids as well as precursors for bioactive lipid mediators. Cells require nutrients contained in media for

energy and component synthesis, including fatty acids and glucose, to enable basic cellular functions and promote growth. The reduction in adhesion and transmigration seen in conditions absent of such nutrients (i.e. in PBS only) may reflect the lack of substrates available to support the energy requirements of cell adhesion and migration. Additionally, the reduction in transmigration may be attributed in part to the lower numbers of PBL recruited in the first place. Although PGD_2 promotes T cell transmigration, it is unlikely that absence of fatty acids lead to a reduction in PGD_2 synthesis by EC and reduced T cell transmigration due to the short 6-minute incubation of PBL with EC. In light of these results, the volume of media M199 and concentration of BSA will be kept consistent to minimise variability in PBL adhesion and migration.

Finally, PEPITEM was shown to be cleavable from 14-3-3ζ recombinant protein *in vitro* using HPLC-grade trypsin. In all measured samples eluted with 20% v/v ACN or more, a fragment belonging to the 14-3-3ζ protein was correctly identified by mass spectrometry and the 14-amino acid sequence was confirmed as PEPITEM. Vascular EC such as HUVEC have been shown to express trypsin (Koshikawa *et al.*, 1997) but currently, the mechanisms surrounding the release of PEPITEM from 14-3-3ζ *in vivo* are unknown. Investigations into the protease(s) responsible for the cleavage of 14-3-3ζ into PEPITEM are required to elucidate this process.

3.4. Conclusions

Like others, we show that synergistic stimulation of EC with TNF-α and IFN-γ is sufficient to simulate EC to express important cell adhesion molecules and

chemokines, resulting in the significant recruitment and migration of PBL. We confirm that in our assays, 100U/ml TNF-α and 10ng/ml IFN-γ were optimal for our studies. Additionally, synergistically stimulation of EC with TNF-α + IFN-γ was more physiological relevant, mimicking multiple cytokine stimulation seen *in vivo.*

Here, we reiterate the inhibitory effects of AQ and PEPITEM on PBL transmigration. This is important as the reproducibility of AQ and PEPITEM inhibition is key to the subsequent work presented here. Interestingly, the effect of PEPITEM was greater when there is more inflammation, modelled using increased concentrations of TNF-α. We have also shown that while adhesion was reduced, the AQ-PEPITEM axis was not dependent on exogenous lipids.

Finally, we have demonstrated the ability for PEPITEM to be released from the 14-3-3ζ parent protein. This finding is interesting as it raises questions about the production of PEPITEM by B cells; How does it occur? Where does it occur? What regulates this process? These questions will be addressed in subsequent chapters.

CHAPTER 4: INVESTIGATING PEPITEM STRUCTURE, INTERACTIONS AND HIGH-THROUGHPUT MEASUREMENT OF FUNCTION

4.1. Introduction

A physiological role for PEPITEM had not been specified until earlier this year (Chimen *et al.*, 2015). Prior to this, the only mention of this peptide in the literature has been as a tryptic peptide used for identifying 14-3-3ζ protein in mass spectrometry samples (Kobayashi *et al.*, 2009, Mohammad *et al.*, 2013). Though one study reported the PEPITEM sequence as a peptide presented by human leukocyte antigen (HLA)-DQ8, transgenically expressed in NOD mice (Suri *et al.*, 2005), this study detailed only that this peptide is naturally processed and preferentially presented by APCs.

Due to its originality, the structure of PEPITEM has not yet been elucidated. PEPITEM represents 14 amino acids located at residues 28 to 41 in the 14-3-3ζ protein. These residues are not covert, but instead appear exposed on the protein surface (Figure 1.5). The relevance of this is uncertain, but it may have some physiological bearing on subsequent processing into PEPITEM. Although PEPITEM appears linear as part of 14-3-3ζ, it is unknown what conformation it takes following enzymatic release.

Nuclear magnetic resonance spectroscopy (NMR) is a powerful tool for studying the chemical structure of molecules. It exploits the absorption and emission of radio frequency energy by protons subject to a magnetic field. The Nuclear Overhauser effect (NOE) is a quantum phenomenon which occurs following the magnetisation of a proton affecting its spin (Figure 2.4), influencing the spin of another nearby proton approximately 4-5 angstroms (Å) apart and causing an

increase or decrease in chemical shift, differing according to a proton's local chemical environment. This series of interactions or "coupling" between protons along the length of a peptide can occur through bonds or through space, creating detectable NMR signals. These signals convey spatial information about protons used to decipher the structure and stereochemistry of molecules (Jacobsen, 2007).

The related ROE (rotating-frame NOE) is used in mid-sized molecules (1000-3000 Da) where the conventional NOE is close to zero. The use of the rotating frame negates the effect of the tumbling rate of the peptide meaning that even when the NOE is zero the ROE is not.

Amino acids are made up of separate chemical groups each with their own spin system. Total correlation spectroscopy (TOCSY) exploits the scalar coupling between protons to provide us with information about the chemical shift of protons within the same spin system of an amino acid following magnetism. Associations between spin systems within an amino acid provide information about intra-residue interactions (Keeler, 2013). Rotating-frame nuclear Overhauser effect spectroscopy (ROESY) provides through-space information via ROEs. Often used when examining small peptides, ROESY delivers information about through-space associations of protons within the context of the rotating frame (Jacobsen, 2007, Keeler, 2013). This gives overlapping information with the TOCSY as protons in the same spin system are usually close in space but also give information about protons on different residues which lie within 5 Å of each other.

In addition to a lack of understanding of the structure of PEPITEM, little is known about the interactions which take place on the EC surface leading to

PEPITEM-mediated EC synthesis and secretion of sphingosine-1 phosphate (S1P). Chimen *et al.* (2015) identified the EC-borne receptor for PEPITEM using biotinlyated PEPITEM as “bait” in a pull-down assay with EC lysates, followed by mass spectrometry of bound candidates. Cadherin 15 (CDH15) was recognised as the strongest match by Mascot database searching, however interestingly, thrombospondin-1 was also identified, but demonstrated a much lower Mascot match (unpublished observations). CDH15 is a transmembrane glycoprotein belonging to the cadherin superfamily of proteins. Originally identified in skeletal muscle, CDH15 (aka M-cadherin) is involved in cell-cell interactions and its expression has been demonstrated in endothelial cells (Chimen *et al.*, 2015). Thrombospondin-1 (TSP-1) is a matricellular glycoprotein with numerous physiological roles. As well as being involved in cell adhesion, TSP-1 plays a role in immune regulation and interacts with a wide range of proteins (reviewed by Lopez-Dee *et al.* (2011) and Resovi *et al.* (2014)).

Compellingly, knockdown experiments targeting EC CDH15 abrogated the inhibitory effects of PEPITEM on T cell transmigration, suggesting a central role in the paradigm (Chimen *et al.*, 2015). Although S1P kinase 1 (SPHK1) was subsequently identified downstream of cell-surface interactions, it remains unclear what connects CDH15 to that pathway.

Biacore binding assays provide a means to measure ligand-receptor interactions and involve measurement of surface plasmon resonance (SPR). The refraction of a light source off a solid phase chip at particular angle, known as the incidence angle, causes the oscillation or “resonance” of electrons also known as surface plasmons on the chip surface (Figure 2.3). Interactions of immobilised molecules with ligands cause a detectable change in SPR recorded in the Biacore

sensorgram, providing kinetic information about binding events. Disappointingly, previous interrogation of PEPITEM interactions with CDH15 conducted through Biacore binding assays was inconclusive and lacked appropriate controls (Chimen *et al.*, 2015).

The *in vitro* migration assay represents a validated functional read-out for the measurement of inhibition of PBL transmigration by PEPITEM. Nevertheless, this assay requires multiple blood donors for the fresh isolation of PBL, which is time consuming. Jurkat T cells are an immortalised T cell line used in the investigation of T cell biology. Jurkat T cells have previously been used to study T cell transmigration *in vitro* (Kitani *et al.*, 1998, Ma and Ma, 2014, Ticchioni *et al.*, 2002), and would eliminate the need for fresh PBL in transmigration assays.

Many studies into receptor agonists and antagonists utilise calcium signalling assays, which enable high-throughput measurement of drug-induced calcium signalling, for example via GPCR. (An Haack *et al.*, 2011, Luo *et al.*, 2011, Valentine and Tigyi, 2012). These plate-based assays are high-throughput and would eliminate the time consuming and highly subjective job of analysing surface adherent and transmigrated cells in the migration assay.

S1P is a sphingolipid produced by endothelial cells in response to PEPITEM stimulation (Chimen *et al.*, 2015), and is also involved in T cell egress from lymph nodes (Pham *et al.*, 2008). S1P released from EC in the PEPITEM paradigm binds to the surface of T cells via the S1P receptors 1 and 4 (S1PR1/4), leading to the inhibition of T cell transmigration. However, S1P has also been reported in the literature to bind to S1P receptors expressed by EC, and lead to intracellular calcium flux (Itagaki *et al.*, 2007, Seol *et al.*, 2005). If this secondary feature could be

exploited, the time-consuming analysis process following migration assays could be eliminated, along with the requirement for fresh PBL altogether.

In this chapter, we initially investigate the chemical structure of PEPITEM and important amino acids within its sequence. We employ Biacore binding assays to investigate potential interactions of PEPITEM or 14-3-3ζ with CDH15 and TSP-1. Finally, we attempt to develop a high-throughput assay for measuring the effect of PEPITEM.

Here, evidence is presented suggesting that PEPITEM is an unstructured peptide with no individually crucial amino acids. Our data may indicate that PEPITEM and 14-3-3ζ do not interact directly with CDH15 or thrombospondin-1 in our *in vitro* binding assays, and PEPITEM was not capable of eliciting a measurable intracellular calcium response in EC.

4.2. Results

4.2.1. Exploring the structure of PEPITEM using NMR.

Our current knowledge of PEPITEM portrays this peptide as 14-amino acids long, some residues of which are charged. However we are not currently aware if this peptide has any secondary structure, or consistent conformations following release from 14-3-3ζ.

To examine the structure of PEPITEM, we utilised NMR spectroscopy to study the possible conformation of PEPITEM *in vitro*. Initially, the protons in each amino

acid were “assigned” i.e. associated to their unique chemical shift (ppm) using the TOCSY spectra. Each point labelled in Figure 4.1 represents a proton within PEPITEM. The labelsdenote the amino acid which the proton is assigned to (e.g. 9Leu is Leucine at 9th amino acid position). Next, the TOCSY and ROESY spectra were overlaid allowing discrimination between intra-residue cross peaks and inter-residue signals, and providing structural information. Stronger cross peaks in the spectra indicate closer proximity of protons. Intra-residue cross peaks illustrated in Figure 4.1 are displayed as the assignment and the proton (H) detected in that residue, followed by the intra-residue proton it interacts with respectively. (e.g. 5GlnH, Hba). Where necessary, proton nomenclature (e.g. a/α, b/β, g/γ) represents their position in the amino acid residue, and where there are two protons attached to a heavy atom they are differentiated by a following “a” or “b”. Inter-residue cross peaks are labelled as the proton assigned to the amino acid, followed by the proton in another residue it interacts with e.g. 9LeuH 7AlaHb.

In the overlaid TOCSY and ROESY spectra, we observed amide proteins along the x-axis with cross peaks to the aliphatic H$^{\alpha}$ protons on the y-axis between 3.6 and 4.5 ppm. Methyl protons were located between 0.5 and 1.3 ppm on the y-axis, with the rest of the protons located in the central portion between 1.4 and 3.4 ppm. Many intra-residue assignments were made, for example between protons in Glu at the 13th residue (13GluH,Hbb - x=8.2ppm y=2.0ppm). Some inter-residue NOEs were noted, for example between the 2nd and 5th residues (5GlnH 2ValHgb - x=8.4ppm y=0.5ppm). These are better illustrated in Figure 4.2, which maps all inter-residue distance restraints within the PEPITEM sequence. No long range ROEs were seen between amino acids more than 3 residues apart, however the presence of

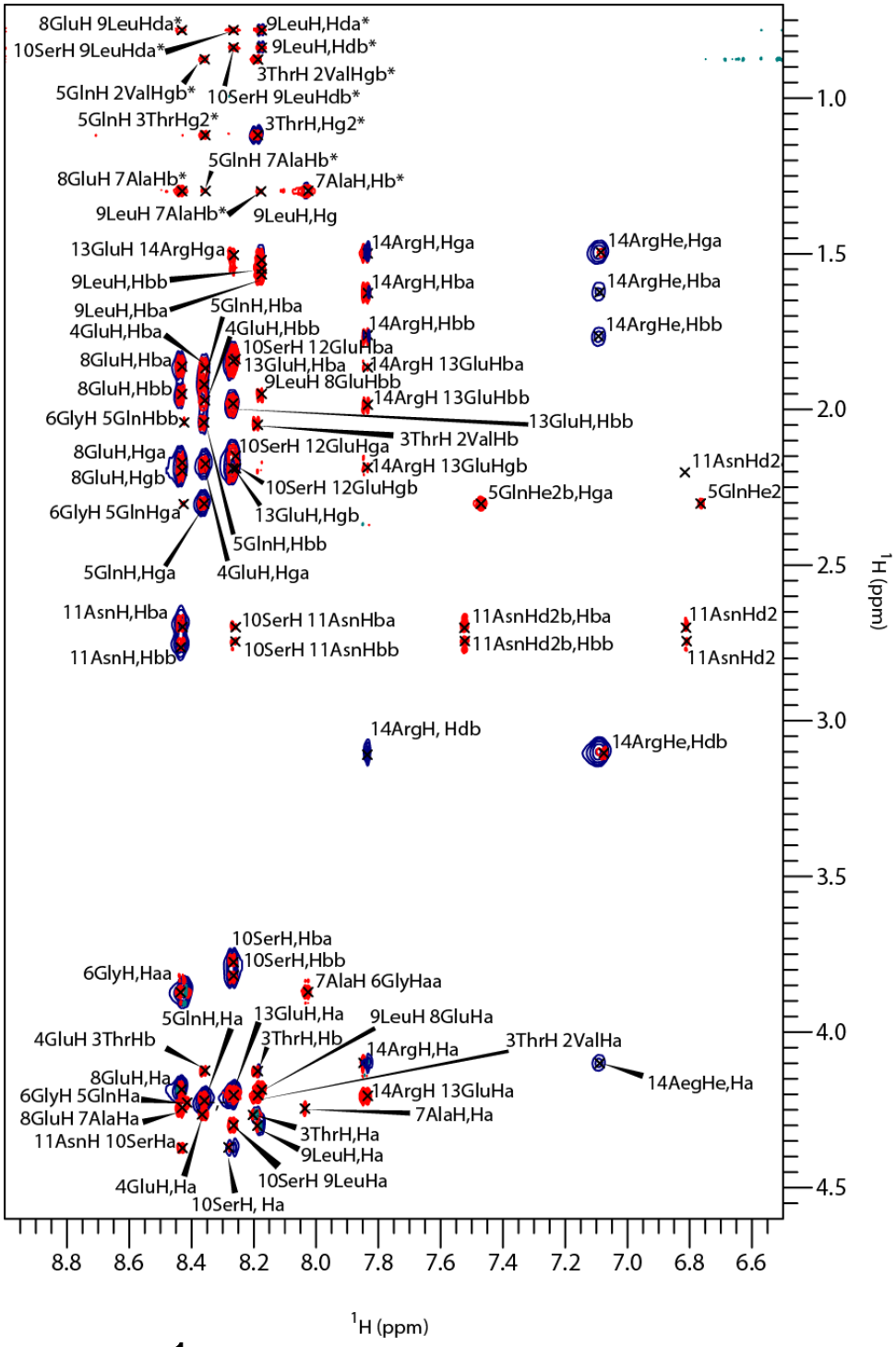

Figure 4.1. 2D ^{1}H NMR spectrum of PEPITEM acquired at 600MHz. A region within the overlaid TOCSY (blue) and ROESY (red, tm=200ms) spectra of PEPITEM showing cross-peaks between amide protons in the x-dimension and aliphatic protons between 3.6-4.5ppm, and methyl assignments between 0.5-1.3ppm in the y dimension. The TOCSY spectrum gives inter-residue peaks and the ROESY spectrum gives both intra and inter-residue peaks via through space interactions. ^{1}H chemical shift is reported in the x and y dimensions as parts per million (ppm). Labelling represents the position and amino acid assigned to the proton followed by an associated proton. * = methyl groups with 3 equivalent protons.

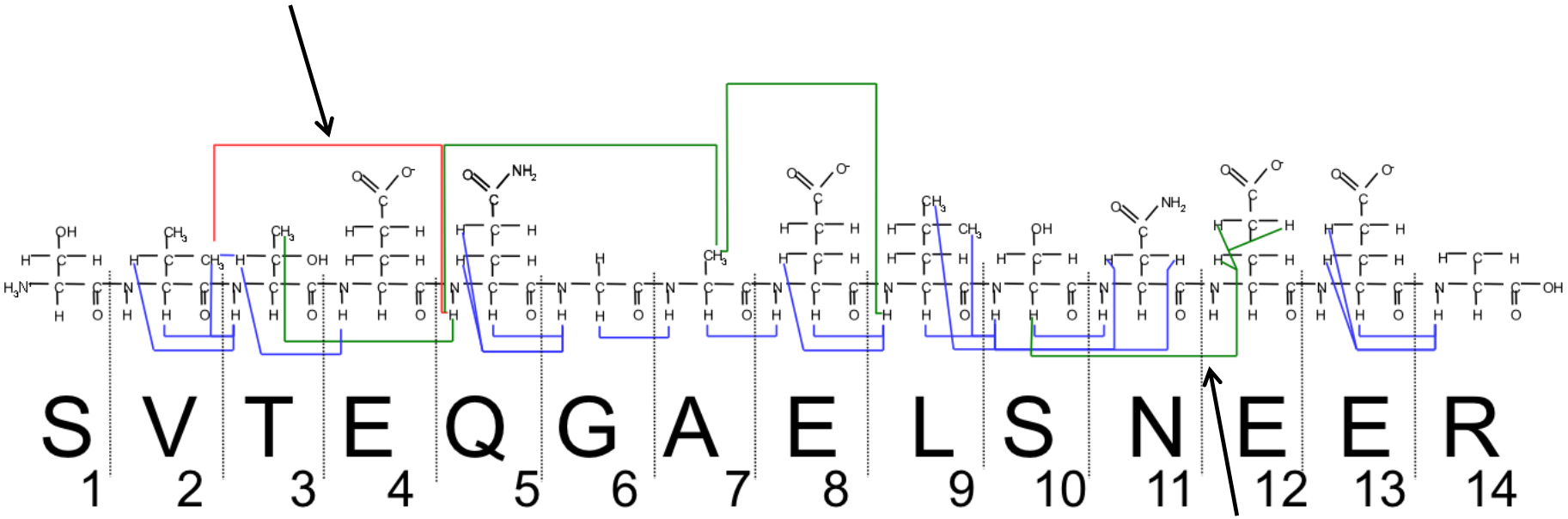

Figure 4.2. Diagrammatic representation of inter-residue associations between protons in PEPITEM.
The position of each amino acid in the PEPITEM sequence can be represented as i. There are several close-range associations (ROEs) between neighbouring amino acids along the length of the peptide sequence (i to i+1 ROEs) connected by blue lines. Three i to i+2 ROEs are shown in green, and one medium-range i to i+3 ROE is connected by a red line. Arrows indicate potential hinge regions.

ROEs between the residues 2 and 5, and 10 and 12 may suggest the existence of hinge-like structure, which roughly corresponds to the loop regions in 14-3-3ζ.

With NMRpipe software,we next produced 100 predicted conformers of PEPITEM which met the NMR-derived structural information obtained in figure 4.1. We then performed structural alignments using PyMOL softwareof the 20 lowest energy structures defined by chemical characteristics of the NMR data. Initially, we aligned the conformers along the whole length of the peptide (Figure 4.3a), in which conformer structure was fairly inconsistent throughout. Alignment of the first 5 N-terminal residues demonstrated random movement and considerable flexibility in the 20 conformers (Figure 4.3b). Finally, we aligned PEPITEM with the last 5 C-terminal residues (Figure 4.3c). These residues aligned reasonably well, and flexibility of the rest of the chain could then be seen.

The root mean squared deviation (RMSD) for these 20 structures was calculated by pairwise alignment of conformers, followed by calculation of the distance of each atom from the mean structure. This was squared, rooted, and the sum of distances of each conformer was divided by the total number of atoms giving the RMSD for PEPITEM. The average RMSD was 2.945 Å for the backbone atoms and 4.157 Å for all atoms, showing little convergence of the 20 structures.

We further interrogated the structure of PEPITEM by examining whether particular amino acids in the PEPITEM structure could be attributed to its function. We performed single alanine substitutions along the length of the peptide sequence, as alanine is a charge-neutral amino acid, and charged residues often impart

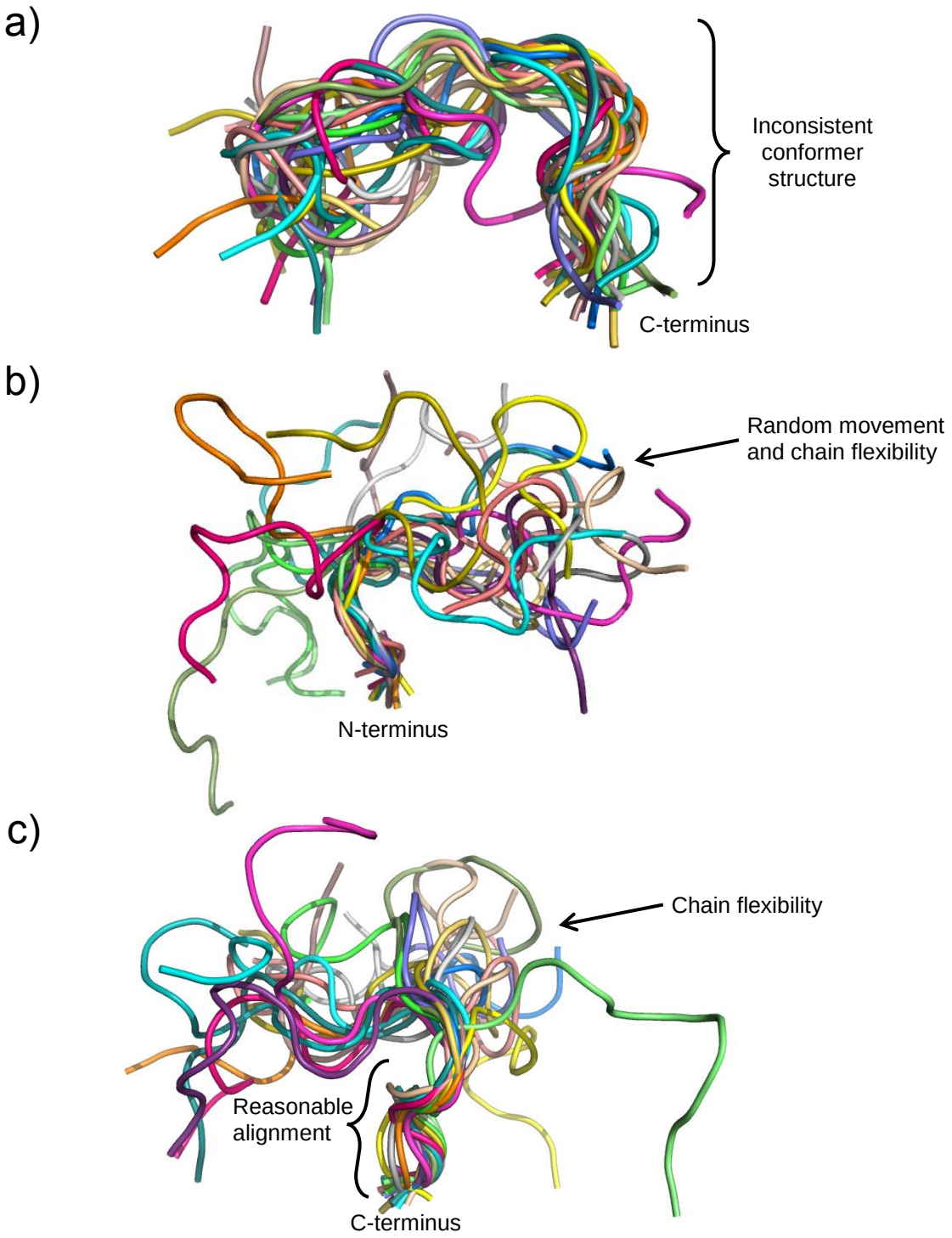

Figure 4.3. 3D alignment of PEPITEM conformers.
Structural alignment of 20 conformers with the lowest energy was performed using PyMOL software. Alignment was performed (a) along the whole length of PEPITEM, (b) using the first 5 N-terminal residues of PEPITEM, or (c) using the final 5 C-terminal residues. Each separate colour is representative of each individual conformer of the peptide which were in agreement with the NMR data.

structure and therefore function. We then screened each peptide at 20ng/ml for function using the *in vitro* migration assay. Alanine substitution at position 7 represents native PEPITEM as it has an alanine residue naturally at this position. None of these PEPITEM variants significantly affected PBL adhesion (Figure 4.4). Interestingly, the closer the alanine substitution to the C-terminus, the more PEPITEM function was reduced, however this was not statistically significant compared to residue 7, and all peptides retained inhibitory function of between 21 - 45%.

These data confirmed the absence of secondary structure of PEPITEM, and lack of singly crucial residues.

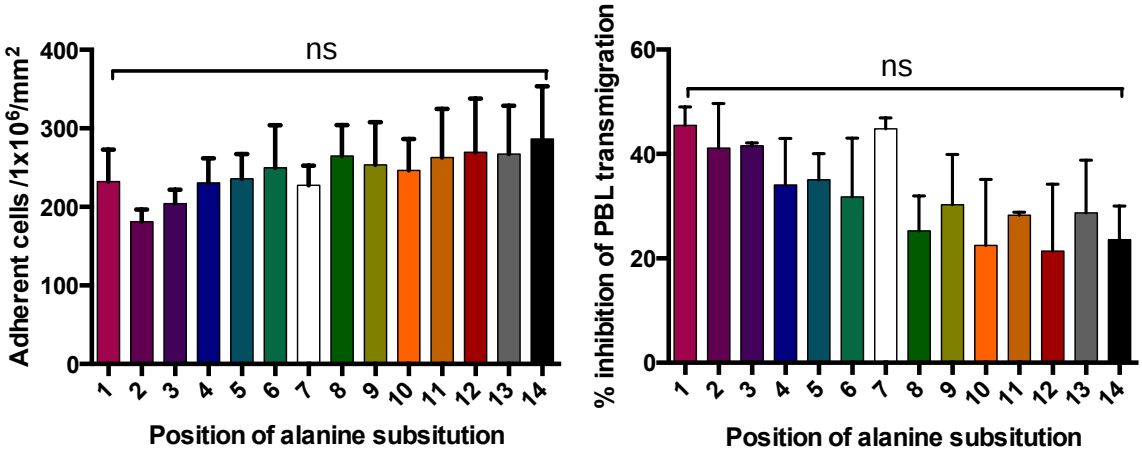

Figure 4.4. The effect of alanine substitutions on PEPITEM function. PEPITEM versions were synthesised with the substitution of alanine at each of the 14 amino acid residues in turn, except residue 7 which has a naturally occurring alanine and therefore represents native PEPITEM. Peptides were tested at 20ng/ml for inhibitory function using the *in vitro* migration assay. Data is expressed as percentage inhibition of transmigrated PBL. ns = not statistically significant analysed by one way ANOVA with Dunnett's post- test. N=3-6.

4.2.2. Examining the interactions of PEPITEM, 14-3-3ζ, CDH15 and TSP-1 in Biacore binding assays.

A role for CDH15 in the PEPITEM paradigm was recently demonstrated by Chimen *et al.* (2015). Previous binding experiments warranted further interrogation and validation. Therefore, we sought to perform additional binding assays to elucidate any binding interactions *in vitro* between PEPITEM, 14-3-3ζ, CDH15 or TSP-1 using the Biacore 3000 system.

N-terminal biotinlyated PEPITEM and scrambled control peptide were bound to a streptavidin-coated CM5 Sensor chip, and increasing concentrations of CDH15 were flowed over for 1 minute (Figure 4.5). While an increase in RU was observed during the injection of all concentrations of CDH15 over the PEPITEM-immobilised flow-cell, this was also the case for injections over flow cells immobilised with scrambled peptide or streptavidin alone. Figure 4.5a illustrates the increase and subsequent drop in response units (RU) seen on the Biacore sensorgram across all flow cells after injection of the highest concentration of CDH15 (100µg/ml). Following the injection and initial increase in RU, all conditions dropped almost back to baseline, although remained slightly higher. SPR for PEPITEM was 0.87 RU before injection of 100µg/ml CDH15, and 4.27 RU after (Figure 4.5b).

TSP-1 has been previously identified as a potential binding partner of PEPITEM in addition to CDH15. We investigated the involvement of TSP-1 in the binding of PEPITEM to the EC surface. First, we flowed TSP-1 over immobilised PEPITEM. Similar to CDH15, we saw an increase in RU after the initial injection,

followed by a decrease almost back down to baseline (Figure 4.6a) and this trend was also seen in control (SA and Scr) conditions (Figure 4.6b).

Next, we investigated whether TSP-1 and PEPITEM interact with CDH15 as a complex. Therefore, we initially promoted potential complex formation between TSP-1 and a PEPITEM using concentration ratios of 1:5 (10µg/ml TSP-1 with 50µg/ml PEPITEM) or 5:1 (50µg/ml TSP-1 with 10µg/ml PEPITEM). After injection of either solution, the trend of increasing RU following followed by a decrease back to roughly baseline was seen again (Figure 4.7a). On closer examination of the RU, injection of 50µg/ml TSP-1: 10µg/ml PEPITEM induced some non-specific interaction with the blank flow cell (Figure 4.7b).

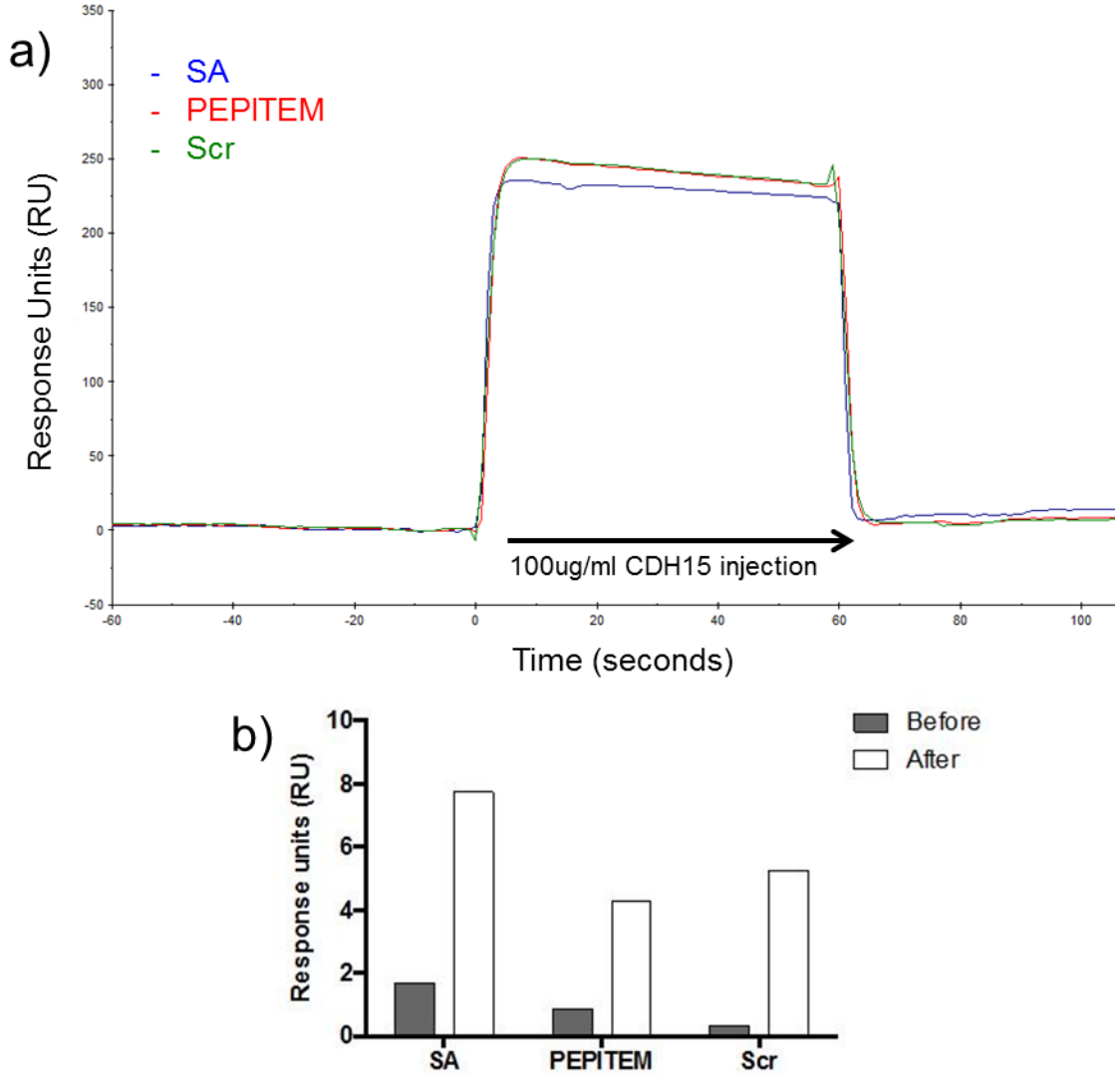

RU:	Before	After
SA	1.66	7.74
PEPITEM	0.87	4.27
Scr	0.32	5.24

Figure 4.5. Studying *in vitro* interactions between immobilised PEPITEM and CDH15.
N-terminal biotinlyated PEPITEM, scrambled peptide (Scr) or streptavidin alone (SA) was immobilised to a CM5 Sensor Chip. Between 12.5-100µg/m (equivalent to 0.10-0.82µM)l recombinant CDH15 was injected (a) Representative Biacore sensorgram following injection of 100µg/ml CDH15 and (b) quantification of response units (RU) before (grey) and after (white) injection of 100µg/ml CDH15. Data represents 1 experiment

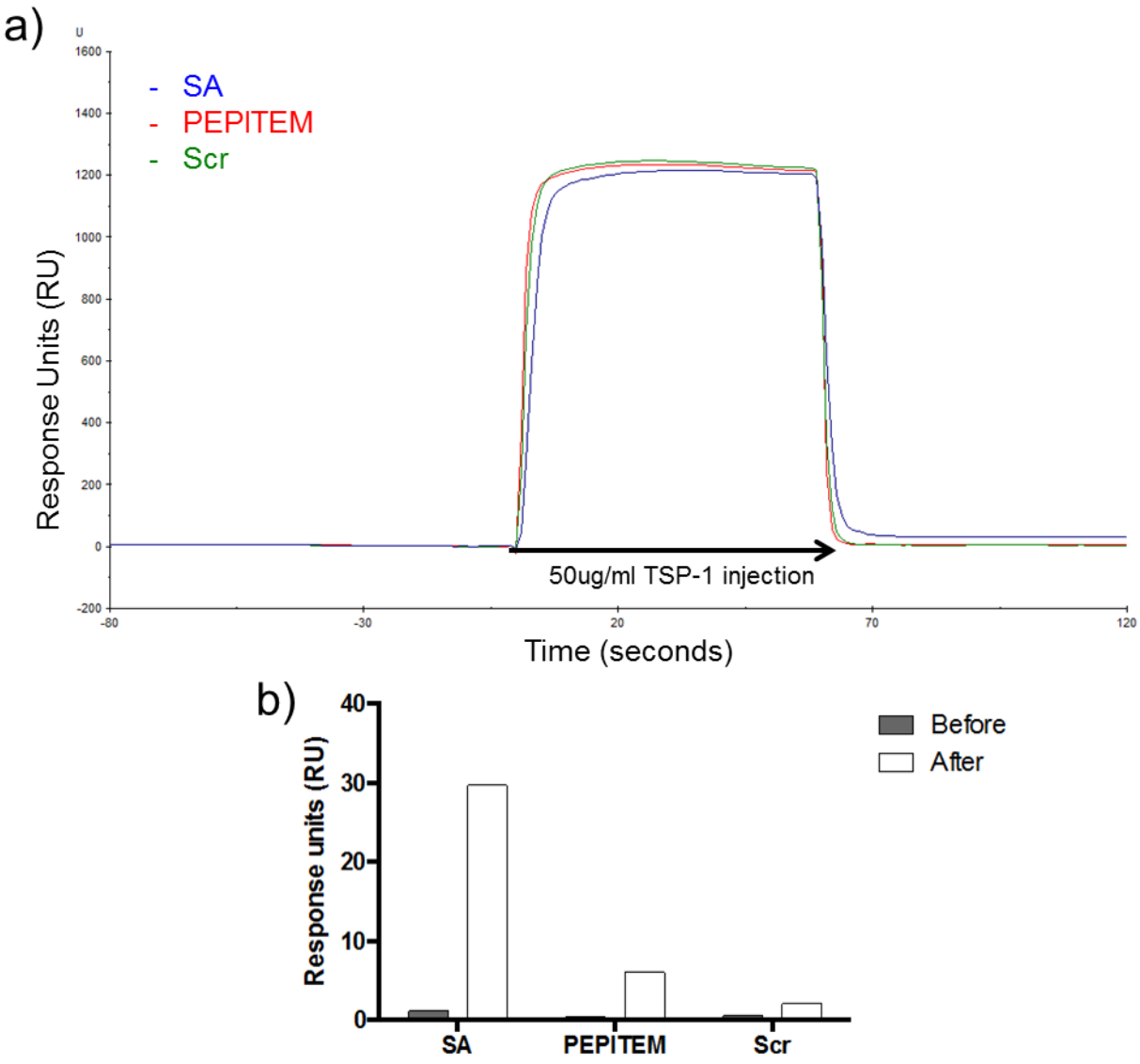

RU:	Before	After
SA	1.11	29.68
PEPITEM	0.35	5.97
Scr	0.47	2.00

Figure 4.6. Investigating PEPITEM interactions with TSP-1 using Biacore. N-terminal biotinlyated PEPITEM, scrambled peptide (Scr) or streptavidin alone (SA) was immobilised to a CM5 Sensor Chip. 50µg/ml (equivalent to 0.30µM) TSP-1 was flowed over for 1 minute. (a) Representative Biacore sensorgram following injection of 50µg/ml TSP-1 and (b) quantification of response units (RU) before (grey bar) and after (white bar) TSP-1 injection. Data represents 1 experiment.

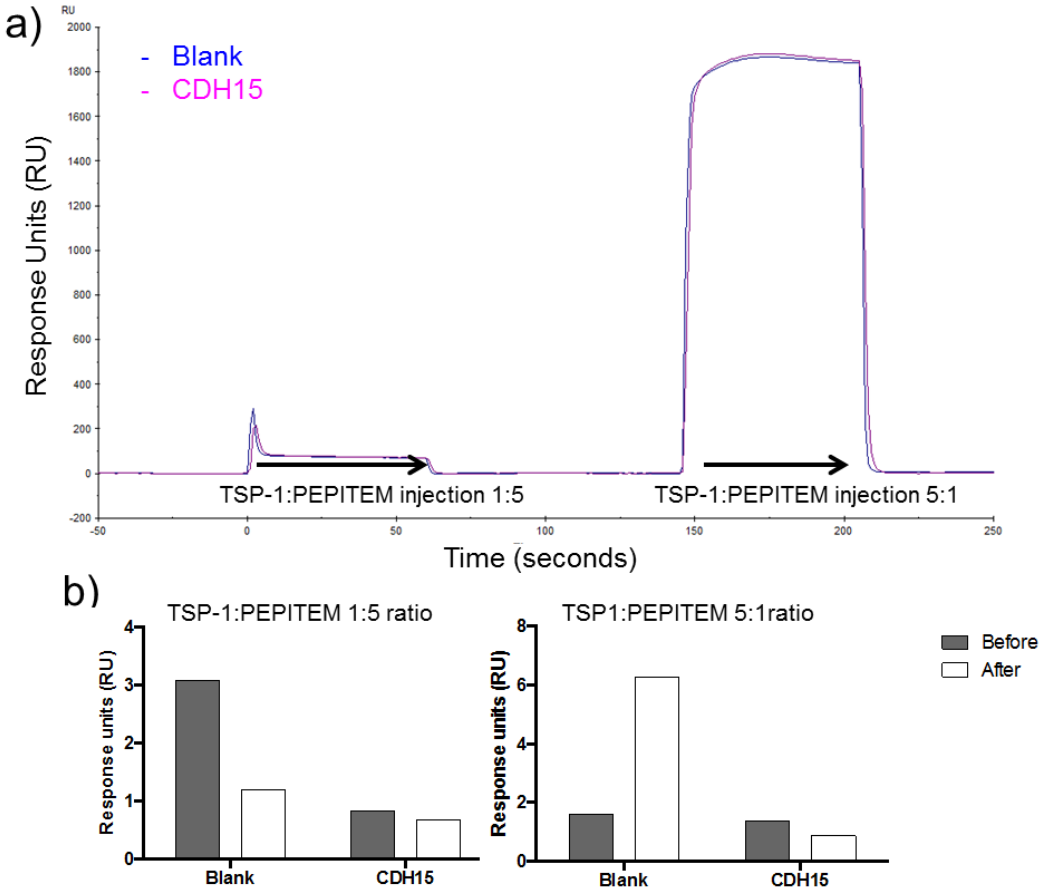

RU:	Before	After
Blank	3.08	1.19
CDH15	0.84	0.68

RU:	Before	After
Blank	1.61	6.28
CDH15	1.36	0.88

Figure 4.7. Examination of CDH15 interactions with TSP-1-PEPITEM complexes *in vitro*.
PEPITEM and TSP-1 at concentration ratios of 1:5 (10µg/ml TSP-1 equivalent to 0.06µM with 50µg/ml PEPITEM equivalent to 33.33µM), or 5:1 (50µg/ml TSP-1 equivalent to 0.30µM with 10µg/ml PEPITEM equivalent to 6.7µM) were flowed over immobilised CDH15 or a blank flow-cell for 1 minute. (a) Representative Biacore sensorgram following injection of PEPITEM-TSP-1 solutions (b) quantification of response units (RU) before (grey bar) and after (white bar) injection. Data represents 1 experiment.

Finally, as 14-3-3ζ is the parent protein of PEPITEM, we investigated the potential interaction of 14-3-3ζ with CDH15 or TSP-1. The N-term biotinlyated PEPITEM had previously been checked for function *in vitro* (Chimen *et al.*, 2015), demonstrating that biotinlyation did not affect receptor interactions. However, to investigate 14-3-3ζ interactions, we utilised a histidine-tagged 14-3-3ζ protein (14-3-3ζ-His). Initially, we investigated what effect this may have upon the inhibition of PBL transmigration, since PEPITEM can be enzymatically cleaved from the parent protein. Surprisingly, while 14-3-3ζ-His did not affect adhesion, we saw a significant decrease in PBL transmigration from 27% in the control to 17% with 14-3-3ζ-His treatment (Figure 4.8). Clearly this finding may be important in elucidating the molecular mechanism behind PEPITEM function, and requires addressing in subsequent chapters.

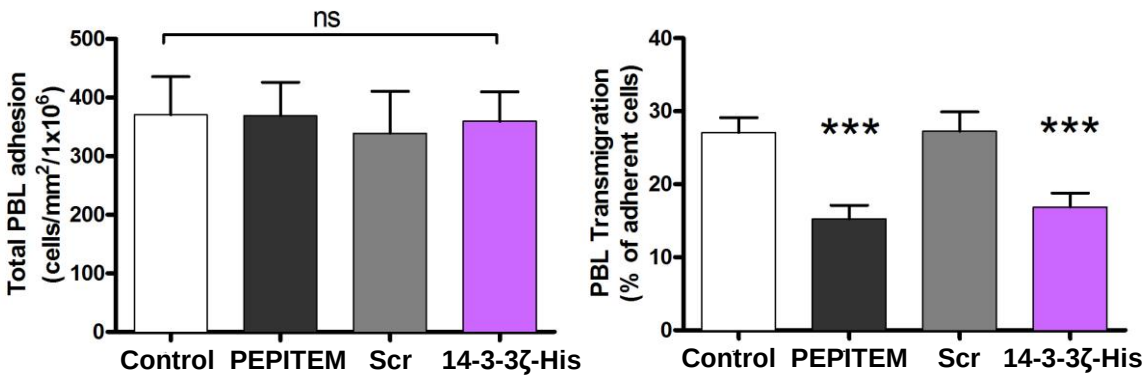

Figure 4.8. The effect of histidine tagging of 14-3-3ζ on PBL transmigration.
20ng/ml Scrambled peptide (Scr), PEPITEM or 14-3-3ζ-His was tested in the *in vitro* migration assay to assess its effect on PBL transmigration across cytokine-stimulated endothelium. Data represents mean ± SEM of 5 independent experiments. ***P≤0.001 using one way ANOVA followed by Dunnett's post-test. Ns = not significant.

Following the realisation that recombinant 14-3-3ζ-His inhibits PBL transmigration, we immobilised 14-3-3ζ-His to a nickel chip and injected TSP-1 or CDH15. Figure 4.9a shows the Biacore sensorgram following injection of the highest concentrations of TSP-1 (100µg/ml) and CDH15 (200µg/ml). In keeping with previous Biacore observations, there was an increase followed by a decrease in RU after each injection, however when quantified, this returned to a higher RU value than prior to injection in both blank and 14-3-3ζ-His immobilised flow cells (Figure 4.9b).

Together, these data implied that while 14-3-3ζ-His can inhibit PBL transmigration, no interactions between PEPITEM, 14-3-3ζ or CDH15 and TSP-1 were evident.

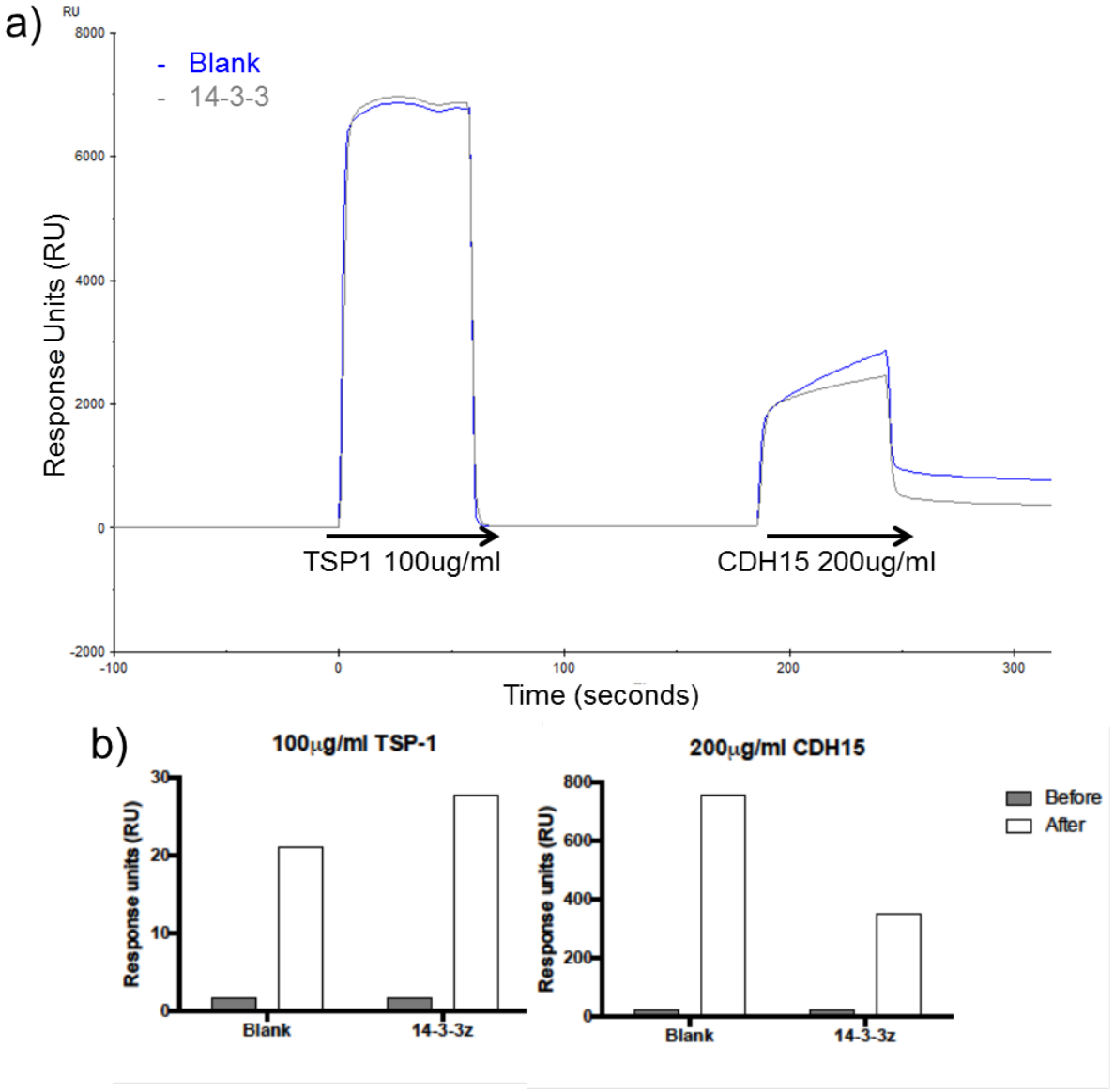

RU:	Before	After
Blank	1.68	21.02
14-3-3ζ	1.72	27.74

RU:	Before	After
Blank	24.34	752.74
14-3-3ζ	23.40	352.07

Figure 4.9. Exploring 14-3-3ζ interactions with CDH15 and TSP-1. 50-100µg/ml (0.30-0.60µM) TSP-1 or 50-200µg/ml (0.80-1.60µM) CDH15 were flowed over immobilised 14-3-3ζ-His or a blank flow cell. (a) Representative Biacore sensorgram following injections of 100µg/ml TSP-1 followed by 200µg/ml CDH15 and (b) quantified response units (RU) prior to (grey) and after (clear) injections. Data represents 1 experiment.

4.2.3. Development of a high-throughput assay for measuring PEPITEM function.

The current use of the migration assay requires multiple blood donations, PBL isolation and lengthy data-analysis. We initially investigated the potential of using Jurkat T cells, an immortalised T cell line, as a substitute for PBL to reduce experiment time, reagents, and to standardise our assays.

Jurkat T cells were examined for adhesion and transmigration across cytokine-stimulated EC. Initial observations under control conditions were unexpected (Figure 4.10a). It was immediately obvious that substantially more Jurkat T cells were surface adherent compared to PBL from a healthy donor. Upon quantification of adhesion and transmigration (Figure 4.10b), indeed a significantly higher level of Jurkat T cells were adherent (4120 cells/mm^2/1x10^6) compared to previous observations, which were usually in the low hundreds. Furthermore, very few Jurkat T cells transmigrated (less than 1% transmigrated cells), and this was unaffected by treatment with PEPITEM. These data strongly suggested the inappropriateness of the use of Jurkat T cells to examine the function of PEPITEM.

We next sought to exploit S1P-induced intracellular calcium flux as a secondary effect of PEPITEM to indirectly measure its function. To investigate whether calcium flux was a viable means to use as a read-out of PEPITEM function, we employed a simple plate-reader based assay in 96-well format using the fluorescent calcium indicator Fluo-4. Here, calcium flux would be detected as an increase in relative fluorescence units (RFU) in response to different concentrations of ligand. We first tested the calcium response of HDBEC in this assay using

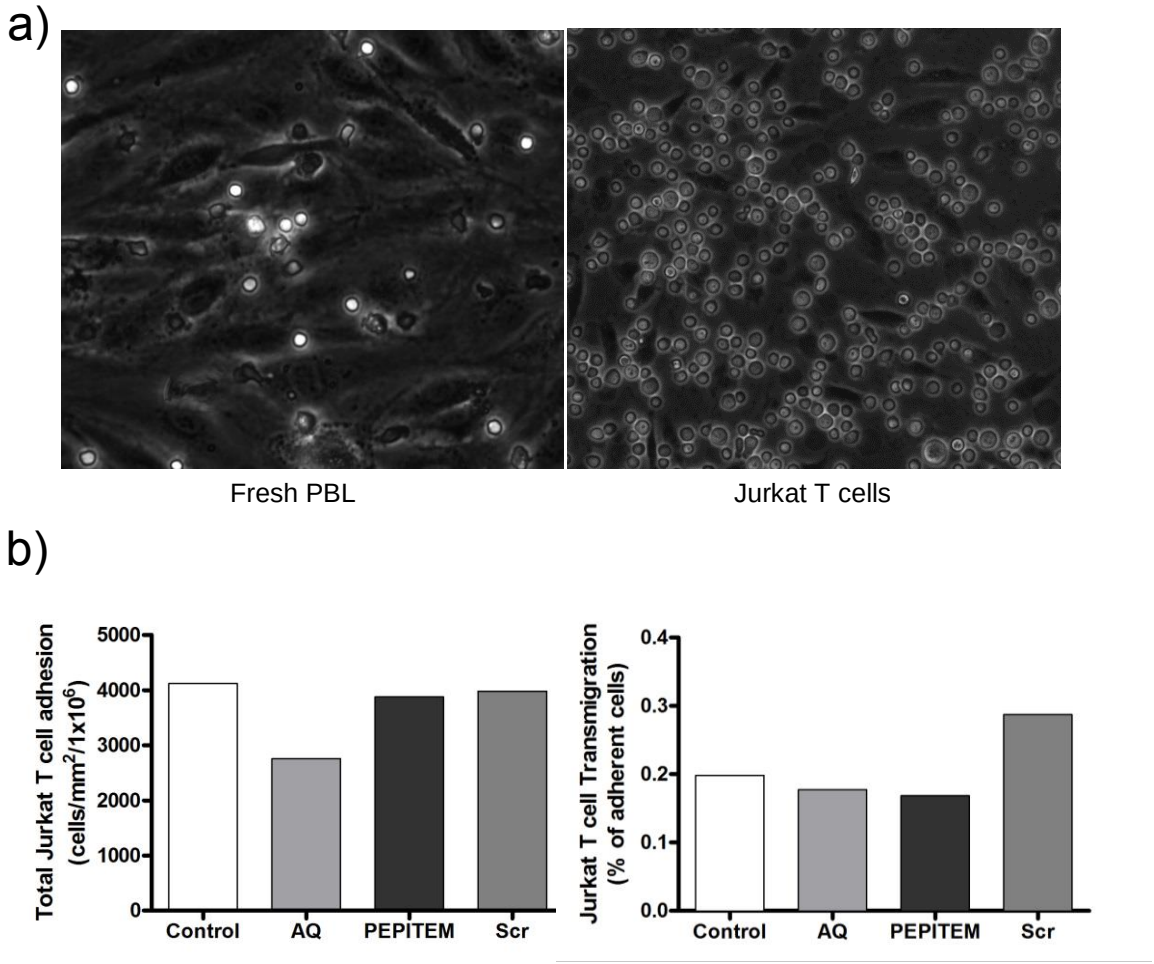

Figure 4.10. The use of Jurkat T cells to study PBL transmigration *in vitro*.
Jurkat T cells were added to cytokine-stimulated HDBEC before washing, fixing and imaging. Some Jurkat T cells were pre-incubated with 10µg/ml adiponectin (AQ) 1 hour prior to migration, or some wells were treated with 20ng/ml PEPITEM or scrambled (Scr) immediately before migration. (a) Images acquired by phase contrast microscopy were used to compare control conditions between Jurkat T cells and freshly isolated PBL. (b) Adherent and transmigrated Jurtkat T cells were counted. Data is from 1 experiment.

calcium ionophore, an agent known to causes mass intracellular calcium release. In the raw traces, responses were seen above 10^{-9}M, and at 10^{-6}M the response was almost saturated (Figure 4.11a). When we converted this to percentage increase in RFU compared to baseline, increasing calcium ionophore concentrations positively correlated with an increase in the maximal RFU response (4.11b), and the deviation from zero was statistically significant.

As a positive control, we then confirmed that S1P was a viable ligand to induce calcium flux in HDBEC. Indeed, S1P elicited an obvious increase in RFU responses above 10^{-1}M (Figure 4.12a), and again we observed positive correlation of S1P concentration with maximal RFU response which was statistically significant from zero (Figure 4.12b).

Subsequently, we tested the ability of PEPITEM (Figure 4.13a) or scrambled control (Figure 4.13b) to induce calcium flux in HDBEC. No obvious increase in RFU was noticeable at any concentrations in the raw traces even at the highest concentration of 10^{-2}mg/ml PEPITEM or scrambled peptide. Unexpectedly, scrambled peptide treatment of HDBEC induced a statistically significant increase in RFU when calculated as percentage increase, but not PEPITEM treatment (Figure 4.13c), however the differences between the slopes were not statistically significant. Notably, negligible percentage increases in RFU between 8% and 14% were detected and seemed to increase at higher concentrations of either peptide.

These data suggested that PEPITEM did not induce high enough levels of S1P to induce a measurable calcium flux.

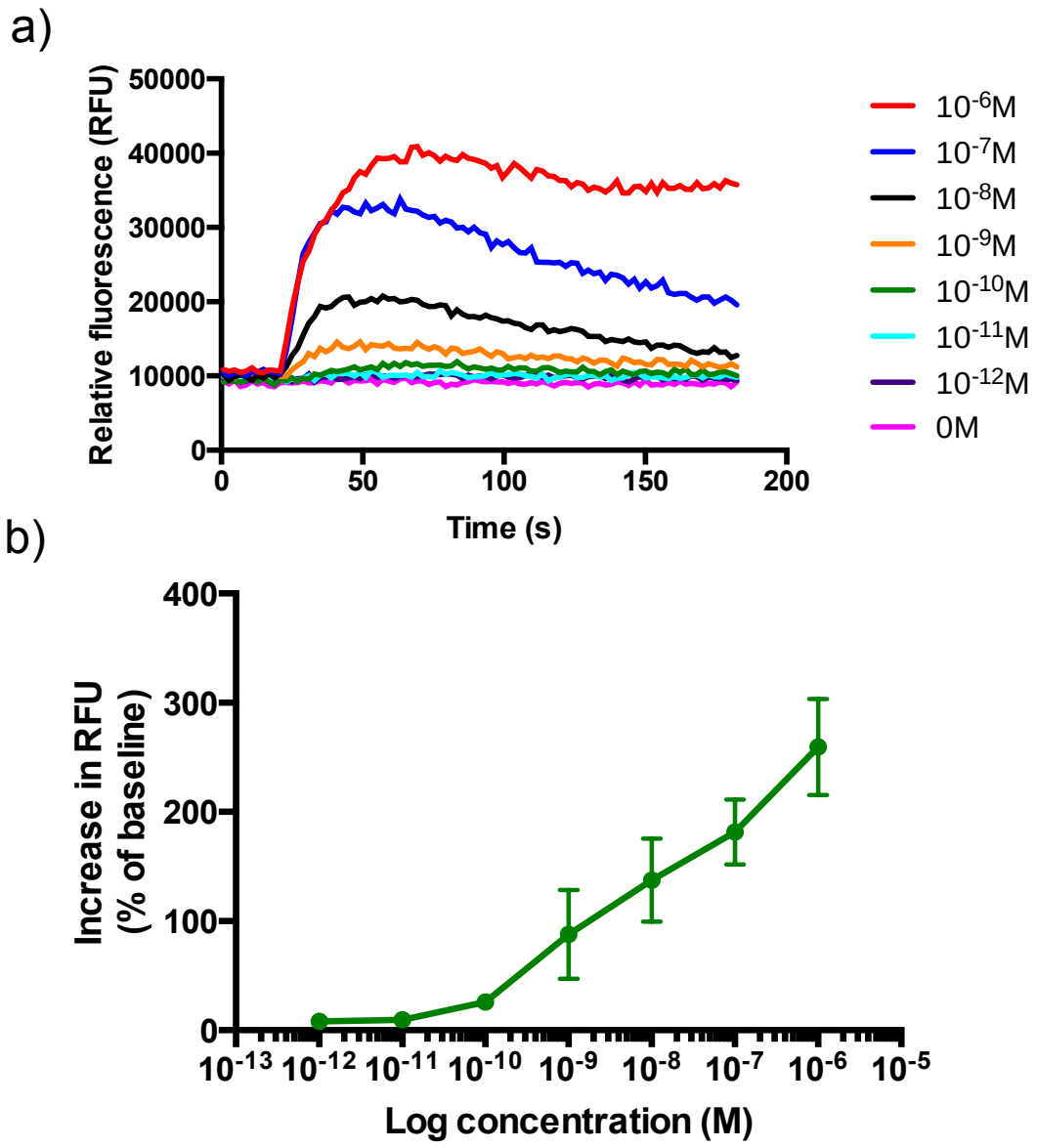

Figure 4.11. Calcium ionophore-induced intracellular calcium flux
Cytokine-stimulated HDBEC were loaded with Fluo-4 calcium dye prior to treatment with 0-10^{-6}M calcim ionophore. Calcium flux was measured using a FlexStation plate reader over 180 seconds. (a) Representative trace of calcium flux following calcium ionophore treatment. (b) Percentage maximal increase in RFU following treatment with calcium ionophore ($P \leq 0.0001$). Data is mean ± SEM of 4 independent experiments with linear regression analysis.

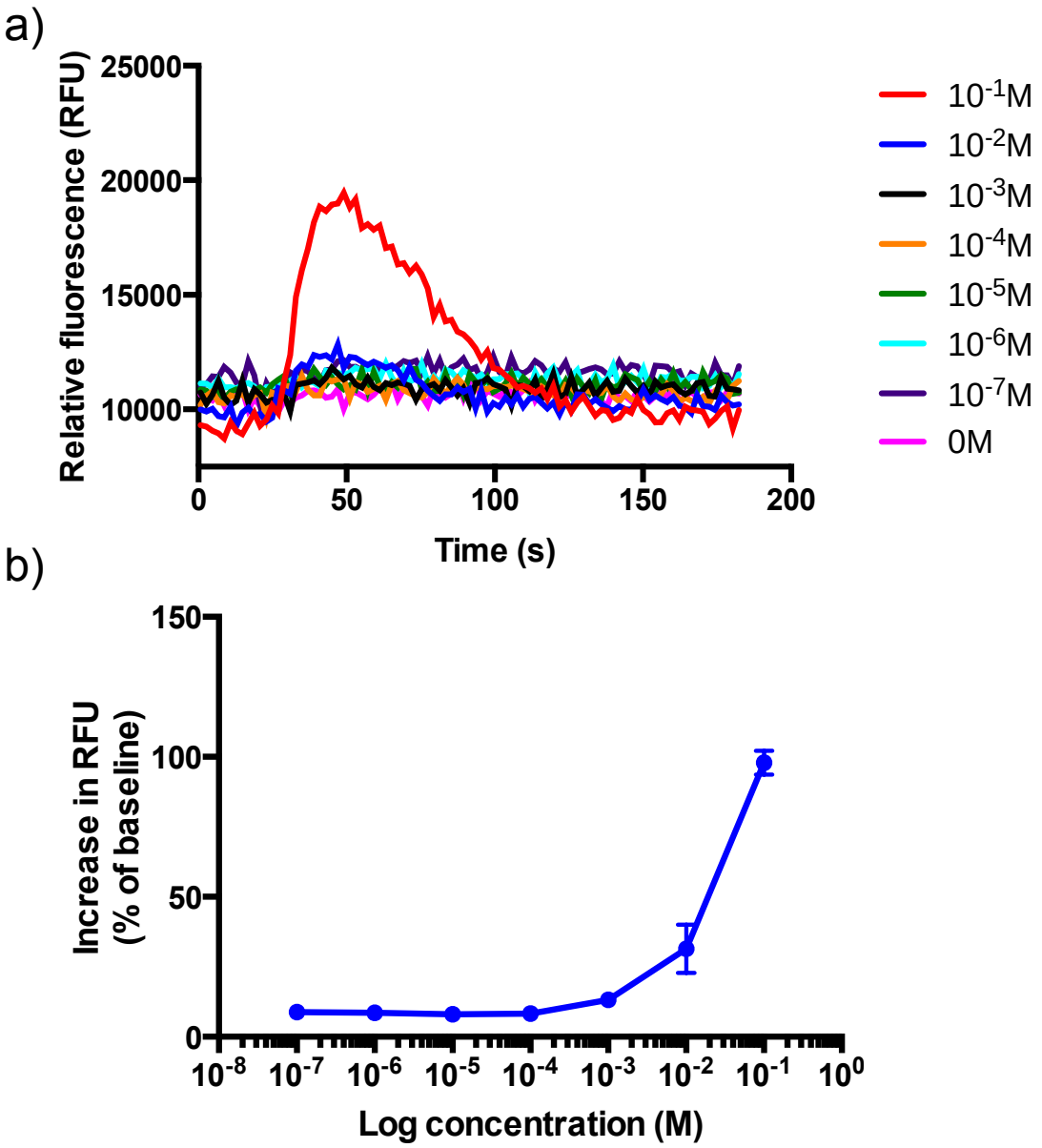

Figure 4.12. Calcium flux in HDBEC following S1P treatment.
Cytokine-stimulated HDBEC were loaded with Fluo-4 calcium dye prior to treatment with 0-10^{-1}M S1P. (a) Representative trace of calcium flux following S1P treatment. (b) Percentage maximal increase in RFU following treatment with S1P. Data is represented as mean ± SEM of 4 independent experiments. Linear regression analysis was performed, P≤0.0001.

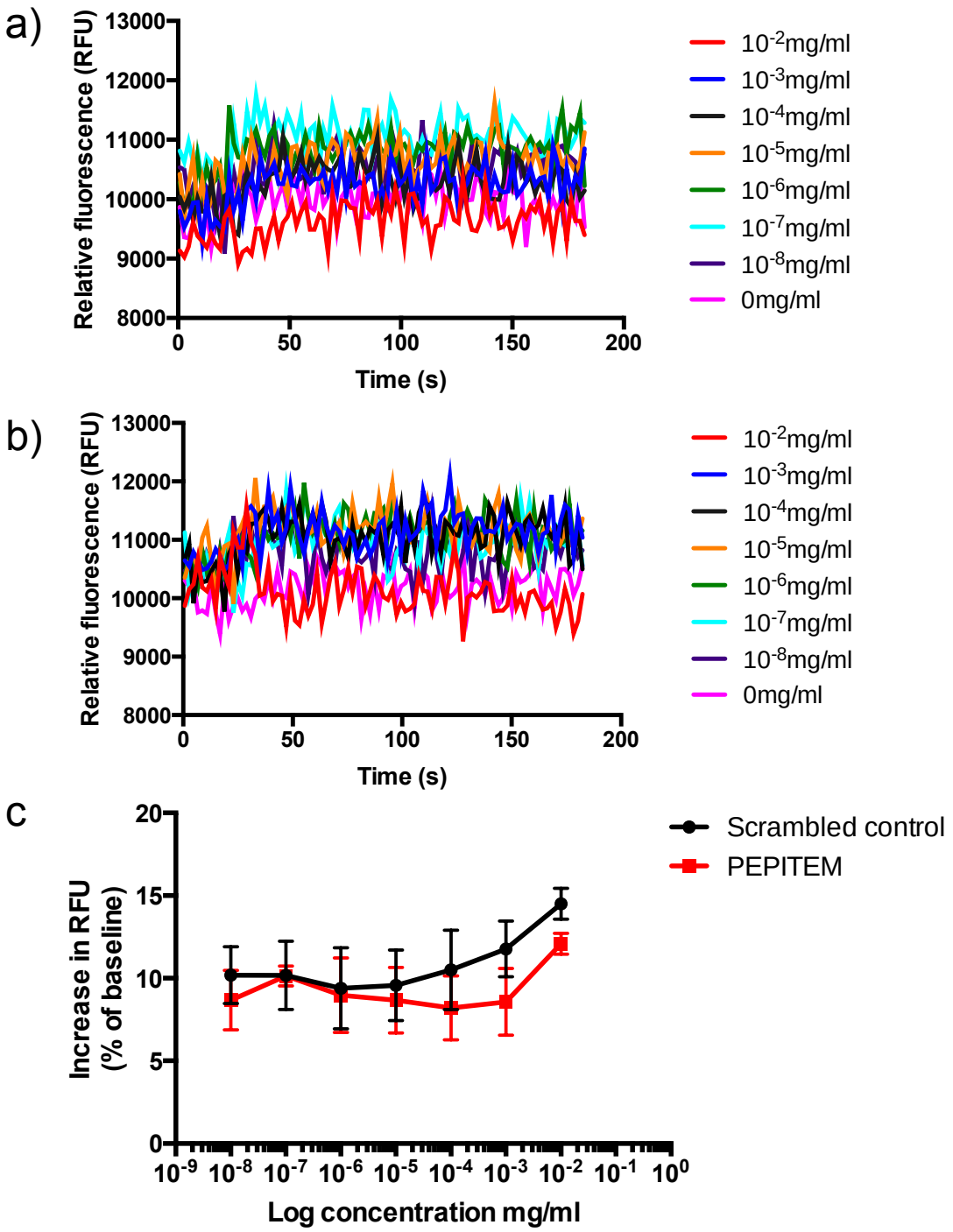

Figure 4.13. Intracellular calcium flux in response to PEPITEM treatment. Cytokine-stimulated HDBEC were loaded with Fluo-4 dye and treated with increasing concentrations of PEPITEM or Scrambled peptide. Fluorescent signal measured using a FlexStation plate reader over 190 seconds. Representative traces of calcium flux following (a) PEPITEM or (b) Scrambled peptide treatment. (c) Percentage maximal increase in RFU following PEPITEM (P=0.0655) or Scrambled treatment (P=0.03). N=4. Mean ± SEM. Data was analysed by linear regression. P=0.6434 between slopes.

4.3. Discussion

Due to the novelty of PEPITEM, little information about its function is available in the literature, and nothing has been published about its structure other than as part of 14-3-3ζ. Additionally, there are no known published interactions of PEPITEM except with CDH15, but this requires further investigation. In this chapter, we examined PEPITEM structure using NMR, and investigated binding interactions using Biacore. Finally, we assessed the potential of developing a higher throughput assay for PEPITEM function utilising Jurkat T cells, or intracellular calcium flux indirectly induced by PEPITEM.

We employed the use of NMR to determine the structure of PEPITEM. TOCSY and ROESY spectra identified several inter-residue interactions between amino acids one, two and three residues away. However absence of consecutive adjoining of H^{α} protons to H^{N} (amide protons) 3 residues apart confirmed a lack of alpha helices, and indeed there was no evidence of secondary structure.

The 14 residues corresponding to the PEPITEM sequence in 14-3-3ζ are located between the second and third alpha helices of the protein, and are prominent on the surface of the protein (Figure 1.5). Interestingly, some medium-range interactions at either end of the sequence between residues 2 and 5, and residues 10 and 12 roughly corresponded to these loop regions in 14-3-3ζ, however not enough NOEs were measured to be certain of this association. Perhaps these regions have some importance in the cleavage of PEPITEM from its parent protein.

Modelling of the top 20 conformers demonstrated some structure at the C terminus when the last 5 residues were aligned. This was because there were slightly

more NOEs detected in this region, meaning that the structure is slightly better defined. Despite these residues aligning reasonably well, the rest of the chain appeared highly flexible. Calculation of the average RMSD demonstrated that there is little convergence of the top 20 conformers, and supported observations of very little secondary structure within the peptide.

Possibly the biggest limitation was one which was unavoidable. PEPITEM is a small peptide of approximately 1.5kDa. Often, short peptides are indeed linear and can take many conformations affected by the environment they are in. Moreover, PEPITEM may only adopt a stable conformation upon receptor binding. Here, we used a pH 6 buffer for investigations for good signal to noise ratio, as lower pH reduce the exchange rate of H^N. While pH 6 does not resemble *in vivo* conditions, since the blood has a pH of 7.35-7.45 (NHS, 2015) and this is the environment where T cells begin trans-endothelial migration, using pH in this range would likely only give very small signals from the H^N, compromising our analysis. Therefore, it is difficult to accurately predict the conformation PEPITEM will take *in vivo.*

Alanine substitution at any given residue did not reveal any significant differences in the inhibitory function of PEPITEM, determined using the *in vitro* migration assay. This suggests that no amino acids are individually essential for function. However, a subtle reduction in inhibitory function was noted towards the C-terminus. This was an interesting observation because there are several charged residues at this terminus absent from the N-terminus, and NMR spectroscopy suggested more structure in this region. Perhaps more than one residue must be substituted to significantly alter PEPITEM function. It would be exciting to investigate whether alanine substitution of all charged residue simultaneously at the C-terminus abrogates PEPITEM function.

Together, these data tells us that there is no secondary structure, besides possible hinge regions at either end corresponding with loops in 14-3-3ζ.

Biacore binding assays can provide information about molecular interactions by measuring differences in SPR. Interaction of CDH15 and PEPITEM was suggested by Chimen *et al.* (2015) and briefly investigated using a Biacore T200 system.

An increase in RU during the injection of all molecules was observed across experiments, and was followed by a prompt decrease. This is due to the injection of increased protein or peptide concentrations and buffer components giving signal during injection. This signal was not accumulating in the flow cell and therefore the signal dropped off again at the end of injection. Equivalent signals were observed over all flow cells in each experiment, indicative of no specific binding interactions, and any rises in RU were negligible. In some investigations, control flow cells demonstrated the highest increase in RU after injection, again supporting a lack of binding interactions. Therefore, it can be concluded that no interactions were observed between CDH15, PEPITEM, 14-3-3ζ and TSP-1 in these investigations.

Chimen *et al.* (2015) reported a key role for CDH15 in PEPITEM function, however Biacore experiments were not comprehensive in that study. The binding assays were performed using a Biacore T200 system, whereas here, a Biacore3000 system was employed, and may not be as sensitive to small changes in SPR. It is also possible that a lack of interaction between PEPITEM or 14-3-3ζ with CDH15 and TSP-1 was due to the use of recombinant proteins, which, depending on expression models used in production, may mis-fold or aggregate. If this is the case, binding

interactions would be hindered by protein conformations unrecognisable to their ligands. Membrane preparations are commonly used in Biacore studies to investigate interactions between membrane proteins, which take on particular conformations in the lipid bilayer and facilitate interactions. When studying PEPITEM interactions in the future, it would be advisable to consider membrane preparations as an alternative to recombinant proteins.

Buffer choice can also affect protein conformation. The same buffer conditions used by Chimen *et al.* (2015) were also employed in our studies. However this may not mimic *in vivo* conditions occurring during PEPITEM binding to EC, and therefore a range of buffers must be tested during further investigations.

We considered the possibility of binding interactions at the EC surface occurring as part of a larger complex, and therefore tested different concentration ratios of PEPITEM with TSP after incubation at 37^{o}C. We saw no indication of specific binding interactions. If repeated, molar ratios of PEPITEM and TSP-1 should be used as PEPITEM is much smaller than TSP-1 and equivalent concentrations would not yield an equivalent number of molecules.

Surprisingly, 14-3-3ζ-His inhibited PBL transmigration to the same extent as PEPITEM, and this requires further investigate to confirm that this wasn't due to the presence of a histidine tag.

Finally we investigated the use of a high-throughput assay to measure PEPITEM function *in vitro*. When we substituted PBL for Jurkat T cells, adhesion and transmigration was not comparable to previous data using PBL. Substantially higher numbers of Jurkat T cells became surface adherent, but did not transmigrate. Other

people have shown migration of Jurkat T cells *in vitro*, but those studies typically employed the use of chemotactic chambers or transwell filters for longer periods of time, in the presence of chemotactic agents (Kitani *et al.*, 1998, Ma and Ma, 2014, Ticchioni *et al.*, 2002). Furthermore, Jurkat T cells have been reported to possess a defect in the integrin LFA-1 (Mobley *et al.*, 1994), required for T cell firm adhesion and subsequent transmigration. Indeed since they are a cancer cell line, it is questionable how much they resemble *in vivo* primary T cells. We therefore turned our attention to exploiting indirect S1P-induced intracellular calcium flux in EC as a measurement of PEPITEM function. PEPITEM was found at 1.5ng/ml in the serum of healthy donors by Chimen *et al.* (2015) and we have demonstrated inhibitory function at 20ng/ml *in vitro*. While calcium ionophore and S1P were able to induce dose-dependent calcium flux in EC, PEPITEM did not do so even at levels much higher than those seen in human serum or used *in vitro.* The low percentage increases in RFU in PEPITEM and scrambled treatments was likely due to an increase in optical path-length as a result of the addition of these substances into the assay plate. This is probably the case as no such increases were observed in the raw data traces at any concentration.

Since the synthesis of S1P has been suggested by Chimen *et al.* (2015) as a result of PEPITEM binding, we can conclude that intracellular calcium flux indirectly induced by PEPITEM was not measurable, and perhaps the assay was not sensitive enough. Indeed Chimen *et al.* (2015) demonstrated significant inhibition of PBL transmigration by S1P at 10^{-7}M, however no intracellular calcium flux was detected at this concentration *in vitro*, highlighting these sensitivity issues. It is possible that the concentration of S1P that PEPITEM induces is small as it acts locally, since high concentrations would be detrimental due to pleotropic effects elsewhere in the body.

To utilise calcium flux as a measurement of PEPITEM function, the sensitivity of the assay needs to be greatly improved. The sensitivity of the assay is ultimately determined by the dissociation constant (*Kd)* of the dye for calcium. Therefore, another possible approach might be to use a dye with a lower *Kd* than Fluo-4. Alternatively, since calcium signalling can be specifically localised within a cell, changes can sometimes be detected using confocal microscopy but not using the FlexStation. Using confocal microscopy, however, would not be as high-throughput. Alternatively, other features leading to S1P production such as SPHK1 activity could be measured following PEPITEM treatment and evaluated as a means to assess PEPITEM function.

4.4. Conclusions

In this chapter, we confirmed that PEPITEM is a simple, unstructured linear peptide with high flexibility, and no individually essential amino acids. While we revealed a lack of interaction between PEPITEM or 14-3-3ζ and CDH15 or TSP-1 *in vitro*, Chimen *et al.* (2015) demonstrated a key role for CDH15 and this requires further investigation. The measurement of PEPITEM function by way of indirect S1P-induced intracellular calcium flux was not sensitive enough to detect changes in intracellular calcium following PEPITEM treatment, and we remain unsure about the levels of S1P induced. Development of a high throughput assay would be advantageous to PEPITEM research as it would provide an invaluable means of testing large numbers of PEPITEM derivatives which may hold therapeutic use in the future. Moreover, investigations into EC surface interactions which occur following

PEPITEM binding would prove key to a comprehensive understanding of this novel paradigm.

CHAPTER 5: THE PHARMACOKINETICS OF PEPITEM AND ITS DERIVATISED PEPTIDES

5.1. Introduction

Autoimmunity, Crohn's disease, multiple sclerosis, type I diabetes (T1D), atherosclerosis and rheumatoid arthritis (RA) are just a handful of examples of chronic inflammatory diseases, which usually are T cell driven. For example in T1D and RA, T cell infiltration occurs in the pancreas and joint synovium respectively (Imagawa *et al.*, 1999, Komatsu and Takayanagi, 2012) and is followed by tissue destruction. Since PEPITEM is a potent inhibitor of T cell trafficking, it represents an attractive agent with therapeutic potential. PEPITEM has been tested in a range of animal models of disease including peritonitis and uveitis (Chimen *et al.*, 2015) and demonstrated reduced T cell trafficking into inflamed tissues. However, there are currently several obstacles in front of the development of PEPITEM for therapeutic use. The pharmacokinetics of PEPITEM are currently unknown, including its plasma concentration across the population, and the amount released by B lymphocytes under adiponectin stimulation. Furthermore, the optimal dose of PEPITEM *in vivo* has not yet been fully established.

Peptides are an attractive prospect for drug therapies and arguably have several advantages, including higher affinity to their target and lower toxicity compared to small molecule drugs typically less than 500 Daltons (Da) in size, which have more side effects and lower specificity due to their small size (Craik *et al.*, 2013). However, there are some problems which restrict the use of peptides as drug therapeutics.

Here, we use the word "protease" to define enzymes which break down both proteins and peptides, and this term is recognised as interchangeable with the term

“peptidase” (Barrett and McDonald, 1986). Proteases hydrolyse peptide bonds and are ubiquitous *in vivo*. Numerous proteases have important function in a range of biological processes from digestion to apoptosis (Potempa and Pike, 2009). Small peptides are particularly vulnerable to proteases owing to their typically uncomplicated structure, and can undergo enzymatic degradation in the blood, kidneys or liver (Werle and Bernkop-Schnurch, 2006).

Moreover, small peptides of approximately of 5kDa or less experience renal clearance *in vivo*, as the glomerular cut off is usually between 30-70kDa, although this has been widely debated and studies have suggested that other molecular properties such as net charge and molecular dimensions influence this (Duncan, 2003, Fox *et al.*, 2009, Ohlson *et al.*, 2001, Oliver *et al.*, 1992, Ruggiero *et al.*, 2010).

Generally, this means that peptides are likely to have a short *in vivo* half- life. Indeed the size of PEPITEM is just 1.5kDa and this presents a major problem, as effective therapeutic agents require significant availability and exposure for substantial effectiveness. This is particularly important in the treatment of chronic inflammatory disease, where inflammation is persistent.

Pharmaceutical modifications have been used to increase peptide stability and half-life *in vivo*. Common modifications include the addition of polyethylene glycol (PEG) polymers to peptides, which can promote increased water solubility and can even reduce immunogenicity (Veronese and Pasut, 2005). PEG repeats can also increase the molecular weight (MW) of peptides reducing the likelihood of renal filtration. Addition of N or C terminal PEG repeats can also provide some relief from exopeptidases by blocking the termini, further increasing stability (Veronese and

Pasut, 2005, Werle and Bernkop-Schnurch, 2006). It is possible that the addition of PEG to a peptide may hinder its function, and it is therefore important to test PEG derivatives.

N-terminal acetylation or C-terminal amidation can also prevent degradation by endopeptidases and exopeptidases, and the usage of uncommon amino acids, for example, in their D-isomeric form, can also prevent protease recognition and subsequent degradation, increasing stability (Landon *et al.*, 2004, Werle and Bernkop-Schnurch, 2006). An advantage of D-isomerisation of all amino acids but in reversed sequence (reverse D-isomerisation, RDI) can reduce recognition by proteases but retain receptor-ligand interactions through maintaining the position of the adjuncts of each residue. Again these modifications may change the peptide's biological activity.

To determine the action of agents *in vivo*, appropriate mouse models of chronic inflammation must first be used. The apolipoprotein E-deficient (apoE $^{-/-)}$ mouse is a commonly used mouse model of atherosclerosis (Meir and Leitersdorf, 2004). This is due to similarities between atherosclerosis in humans, and induced disease in mice, with comparable morphology and progression (Nakashima *et al.*, 1994, Plump *et al.*, 1992). High fat diet (HFD) can also be used to accelerate disease progression in this model. We now know that atherosclerosis is an inflammatory disease exacerbated by T cells (Reviewed in section 1.5.4). Previous studies suggested the alleviation of disease by certain anti-inflammatory drugs (Paul *et al.*, 2000, Reis *et al.*, 2000). Furthermore, transfer of $CD4^+$ T cells from $apoE^{-/-}$ mice into $apoE^{-/-}/SCID^{-/-}$ mice accelerated atherosclerotic lesion progression (Zhou *et al.*, 2000),

suggesting a role for T cells in the establishment of atherosclerosis. Chimen *et al.* (2015) demonstrated inhibition of $CD4^+$ T cells by PEPITEM, but PEPITEM has not yet been tested in a mouse model of atherosclerosis.

In this chapter, we examine whether common pharmacological modifications affect PEPITEM function *in vitro* before investigating the pharmacokinetics and localisation of the native form *in vivo.* We also assess the ability of PEPITEM to reduce plaque burden in an $apoE^{-/-}$ model of atherosclerosis.

Here, we provide evidence that common pharmaceutical modifications do not affect PEPITEM function *in vitro* and may be useful further down the line in development. In agreement with literature of short peptides to date, PEPITEM has a short circulating half -life and is cleared by the kidneys. Finally, we find that intraperitoneal (IP)-treatment of $apoE^{-/-}$ mice on HFD with PEPITEM for 6 weeks did not reduce plaque severity.

5.2. Results

5.2.1. Assessing the effect of common pharmaceutical modifications on PEPITEM function *in vitro.*

To assess the effect of common pharmaceutical modifications on the function of PEPITEM, derivitised peptides were synthesised by way of a small-scale epi-scan array, yielding crude, unpurified peptides. Such arrays, though more economically viable for the production of large variations of peptides, can leave behind impurities

or contaminants as a result of the synthesis process. Modifications included the addition of N- or C- terminal 352MW PEG repeats (N- or C- PEG), N and C terminal acetylation and amidation (N/C block), and reverse D-isomerisation (RDI).

Initially we compared the function of purified and crude native PEPITEM in the *in vitro* migration assay. Both pure and crude peptides demonstrated no significant difference in function, with 20ng/ml of pure and crude PEPITEM significantly reducing PBL transmigration to 23% and 22% respectively, compared to the control (37%, Figure 5.1a). After testing each peptide modification at 20ng/ml, we saw no effect on PBL adhesion, and none of the modifications significantly enhanced or hindered PEPITEM function *in vitro*, exhibiting between 30 and 35% inhibition of PBL transmigration (Figure 5.1b).

These data suggest that PEPITEM can be modified to improve its stability *in vivo* without reducing its efficacy.

5.2.2. Investigating the *in vivo* pharmacokinetics of PEPITEM.

Small peptides are known for having short half-lives *in vivo*. To establish the longevity of exogenous PEPITEM in the circulation, we first needed to be able to detect it in plasma. A tritiated version of PEPITEM (^{3}H PEPITEM) was synthesisd allowing the detection of PEPITEM through the measurement of radioactivity.

a)

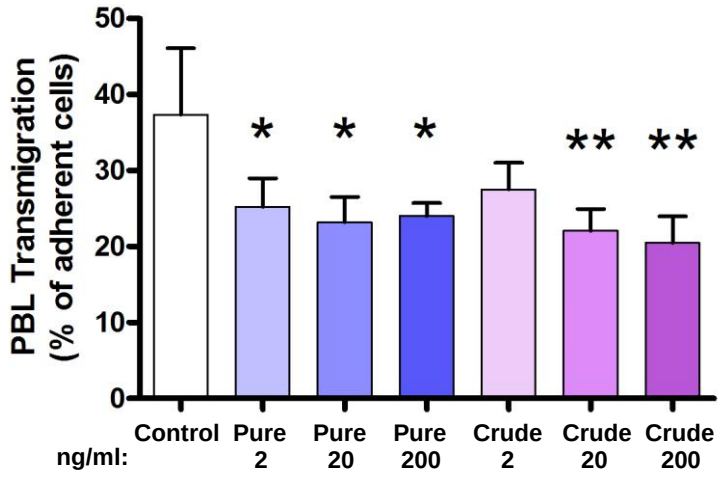

b)

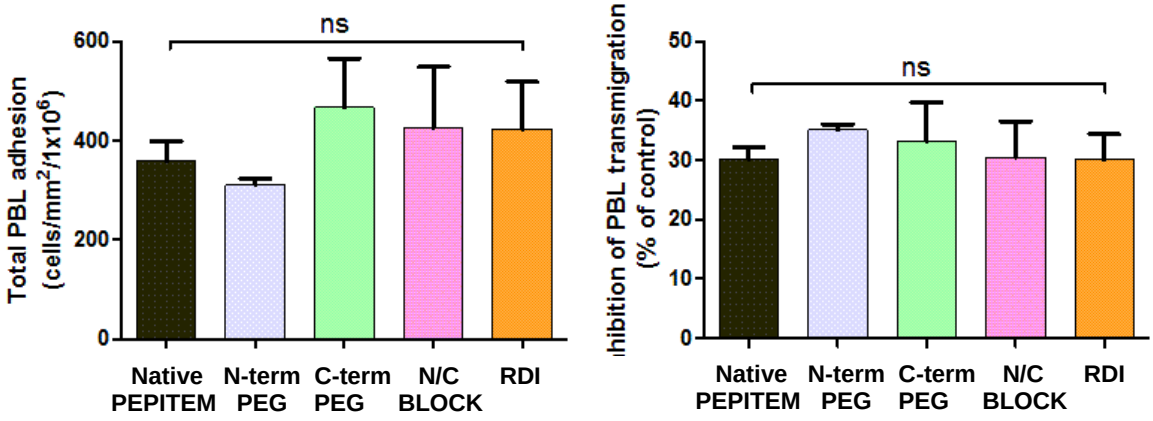

Figure 5.1. The effect of PEPITEM modifications on the inhibition of PBL transmigration.
Peptide derivatives were synthesised by crude array and assessed using the *in vitro* migration assay. (a) Native PEPITEM synthesised by crude array was compared to native PEPITEM synthesised more purely at 2-200ng/ml (b) modified peptides were assessed for PEPITEM function at 20ng/ml. *P<0.05, **P=0.01, ns= not significant analysed by way ANOVA with Dunnett's post-test. Data represent mean ± SEM of 3 independent experiments.

We first performed a dilution of ^{3}H PEPITEM from 0.1ng to 10ng in increasing volumes of scintillant liquid to determine optimal conditions for the detection of radioactivity by scintillation counting (Figure 5.2a). No differences were observed in radioactivity counts (Disintegrations per minute, DPM1) between different volumes of scintillant, and radioactivity remained detectable at all concentrations. Therefore, to utilise a minimal amount of radioactive substance while maintaining sensitivity, 1ng ^{3}H PEPITEM and 2ml scintillant was chosen for future experiments.

Cardiac puncture is an appropriate method for *ex-vivo* assessment of the blood. Occasionally, red blood cells may become lysed during cardiac exsanguination and centrifugation, causing the release of haemoglobin. Due to the presence of double bonds in haemoglobin molecules, the potential for signal quench during scintillation counting was possible. To check whether RBC lysis affected the detection of radioactivity, mouse plasma samples with and without visible amounts of haemoglobin were spiked with 0.1ng or 1ng ^{3}H PEPITEM (Figure 5.2b). The presence of visible haemoglobin did not hinder the detection of radioactivity by scintillation counting, confirming the reliability of the signal between samples.

After establishing optimal conditions for the detection of radioactivity in plasma, 1ng/g ^{3}H PEPITEM was injected into mice via the tail vein for 2 to 60 minutes, and plasma was examined for radioactivity by scintillation counting. After 2 minutes, only 1062 DPM1 was detected compared to 20046 DPM1 at 0 minutes, representing a significant decrease in radioactivity (Figure 5.3). Radioactivity counts further decreased to 332 DPM1 and 266 DPM1 after 30 and 60 minutes respectively. These data therefore imply rapid clearance and low retention of PEPITEM in circulation following IV injection.

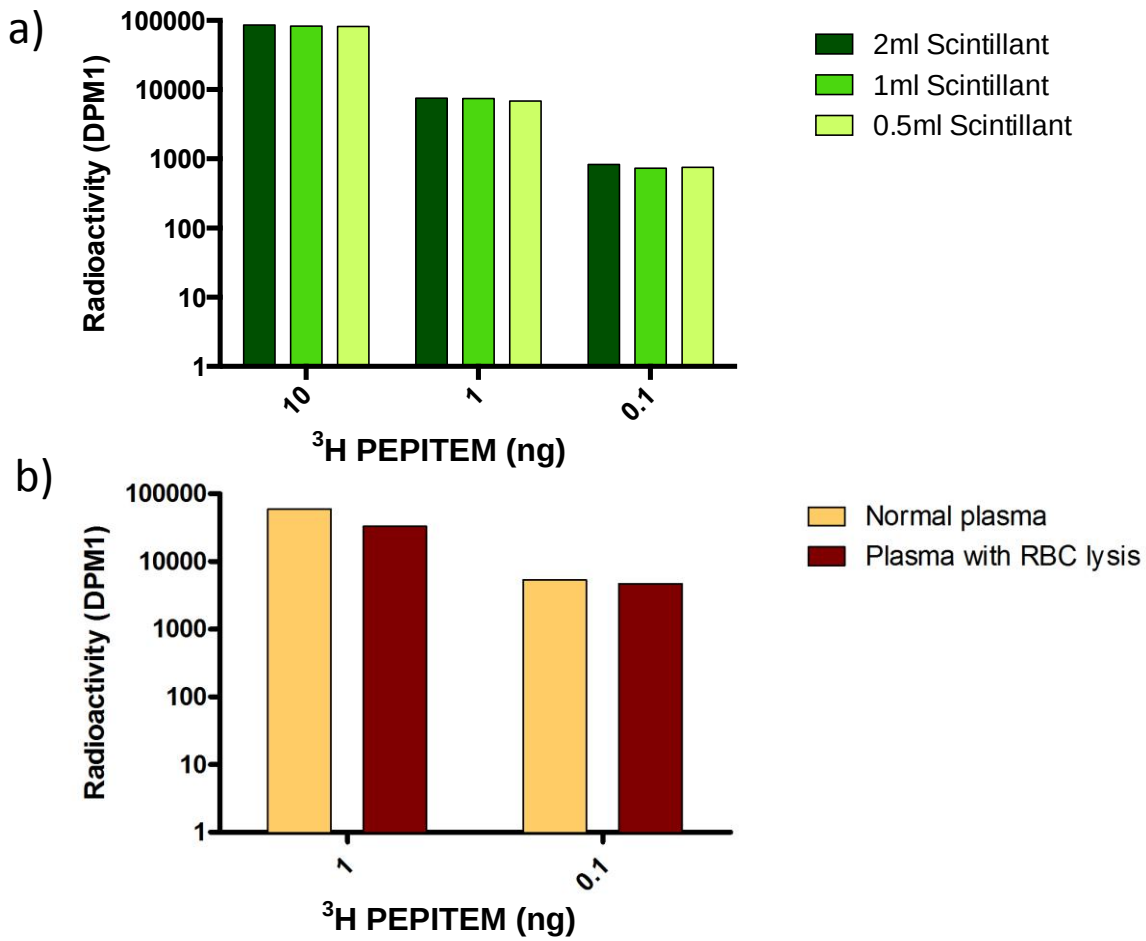

Figure 5.2. Determining optimal conditions for the detection of radioactive PEPITEM in serum.
(a) Initially, 0.1-10ng ^{3}H PEPITEM was spiked into 0.5-2ml scintillant. (b) The effect of haemoglobin on the reliability of the signal of 0.1 or 1ng radioactive PEPITEM was then confirmed. Radioactivity was detected using a scintillation counter and signal is expressed as DPM1. Data represents 1 experiment.

With PEPITEM being much smaller than the renal filtration cut off, we investigated whether this short circulating half-life could be attributed to clearance by the kidneys. PEPITEM was conjugated to alexafluor-680 fluorescent dye to enable us to track it *in vivo* via fluorescence. Upon testing the fluorescently-labelled PEPITEM (PEPITEM-AF680) *in vitro* utilising the migration assay, we confirmed that PEPITEM-AF680 did not affect PBL adhesion and retained the ability to inhibit T cell

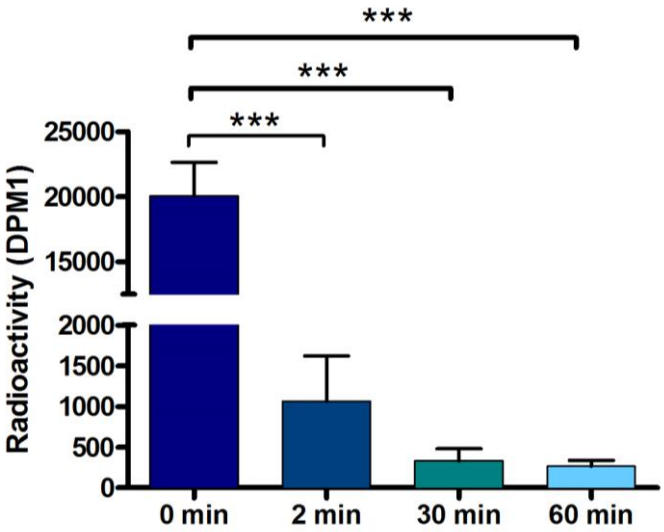

Figure 5.3. The *in vivo* pharmacokinetics of PEPITEM.
1ng/g ^{3}H PEPITEM was injected via the tail vein of C57BL/6 mice. Blood was extracted after 2, 30 or 60 minutes and assessed for radioactivity by scintillation counting. Radioactivity at 0 minutes was determined by spiking 1ng/g ^{3}H into collected blood before centrifugation and measurement of radioactivity. Data expressed as radioactive counts (DPM1), and represents mean ± SEM of 3-6 mice. P≤0.001 by one way ANOVA followed by Dunnett's post-test.

trafficking significantly, and PBL transmigration was reduced from 30% in the control to 16% (Figure 5.4). This level of inhibition was similar to PEPITEM (18% PBL transmigration).

We established the optimal concentration of 100µg/ml for the detection of PEPITEM-AF680 imaging using the *In Vivo* Imaging System (IVIS), (data not shown). 100µg/ml of PEPITEM-AF680 was injected into BALB/c mice for 15 minutes to allow enough time for a detectible PEPITEM-AF680 fluorescent signal to accumulate in any given organ(s). Animals were sacrificed and organs were excised for *ex-vivo* imaging using the *IVIS.* Localised fluorescence was clearly observable in the kidneys, stomach and gut 15 minutes post-injection of PEPITEM-AF680 (Figure 5.5), and when quantified, kidney fluorescent intensity was $7.1x10^{7}$p/s/cm^{2}/sr in control mice,

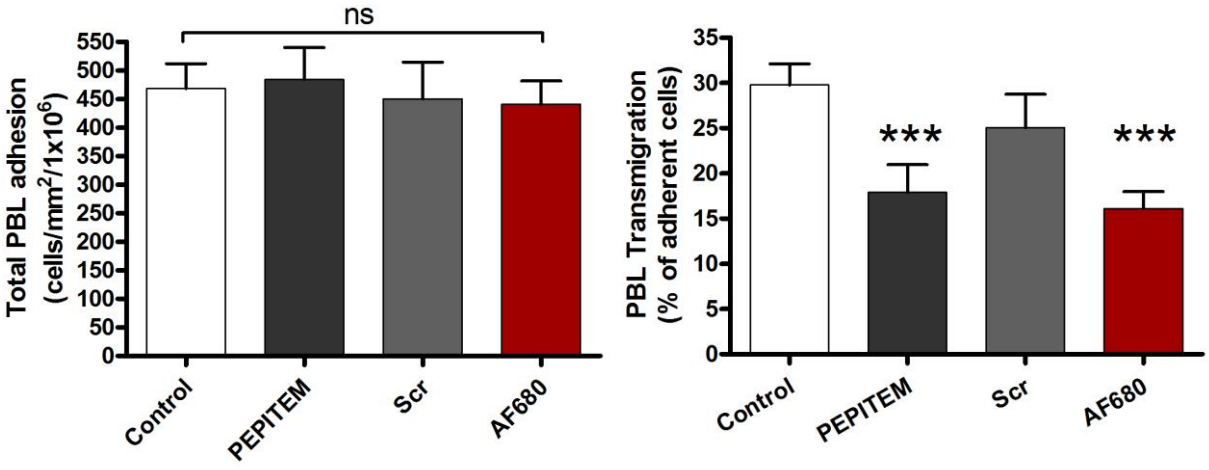

Figure 5.4. Inhibition of PBL transmigration by a PEPITEM-AF680 conjugate.
PEPITEM was conjugated to Alexa-fluor 680 dye via the amide bond. 20ng/ml PEPITEM-AF680 was tested alongside 20ng/ml native PEPITEM or Scrambled for function in the *in* vitro migration assay**.** Data represents mean ± SEM of 8 independent experiments, and was analysed by one way ANOVA with Dunnett's post-test. ***P≤0.001, ns=not significant.

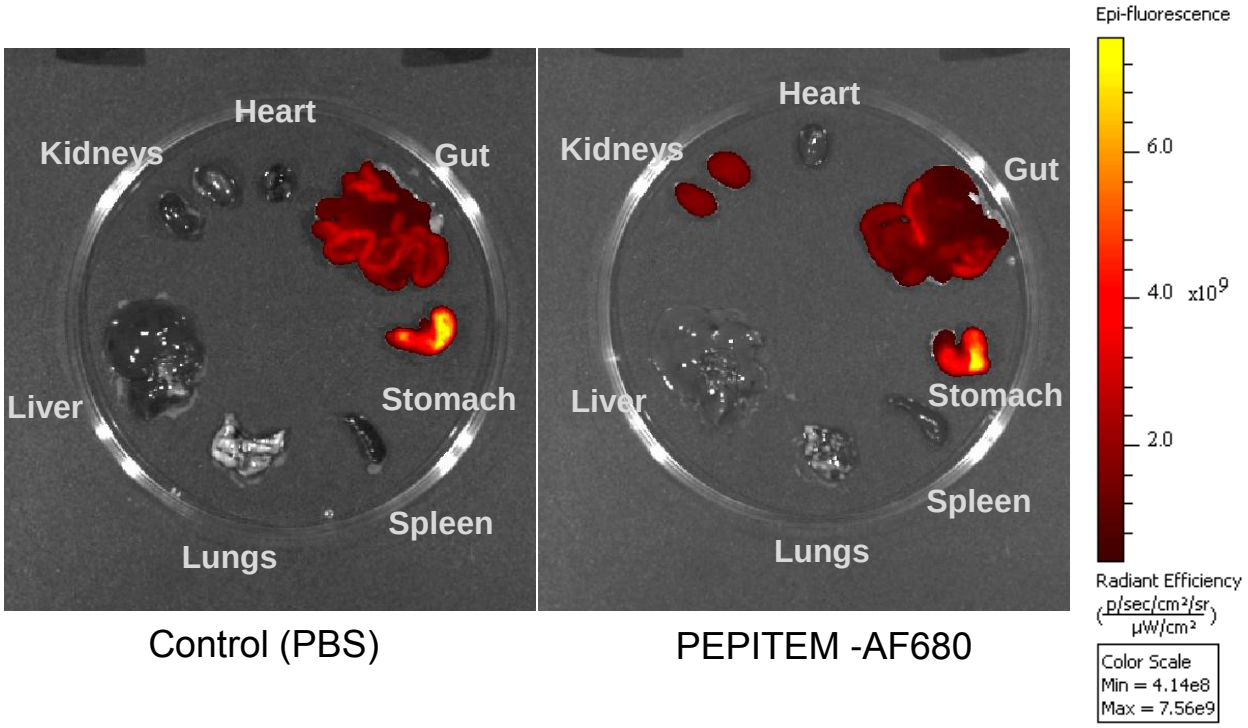

Figure 5.5. IVIS imaging of organs following injection of PEPITEM-AF680 into BALB/C mice
(a) PBS control or (b) 100µg/ml PEPITEM-AF680 was injected IV into BALB/c mice. Organs were imaged *ex-vivo* after 15 minutes. Representative images taken using the IVIS Spectrum Imager, with 3 mice per group. Fluorescence is expressed radiant efficiency (p/s/cm^2/sr).

and $1.9x10^9$p/s/cm^2/sr in PEPITEM-AF680-treated mice, and was significantly different (Figure 5.6). Higher levels of fluorescence were also observed in the spleen, lungs and heart of PEPITEM-AF680-treated mice, but these increases were much smaller than that seen in the kidneys. High levels of autofluorescence were notable in the stomach and gut of the control group, however the fluorescent intensity was not higher in PEPITEM-AF680-treated mice. Calculation of the percentage increase in fluorescence following PEPITEM-AF680 treatment compared to the PBS control mice revealed the largest increase in fluorescent signal localised mainly in the kidney, and the lack of increase in the stomach and gut (Figure 5.7). This is indicative of rapid renal clearance of PEPITEM from the circulation *in vivo*.

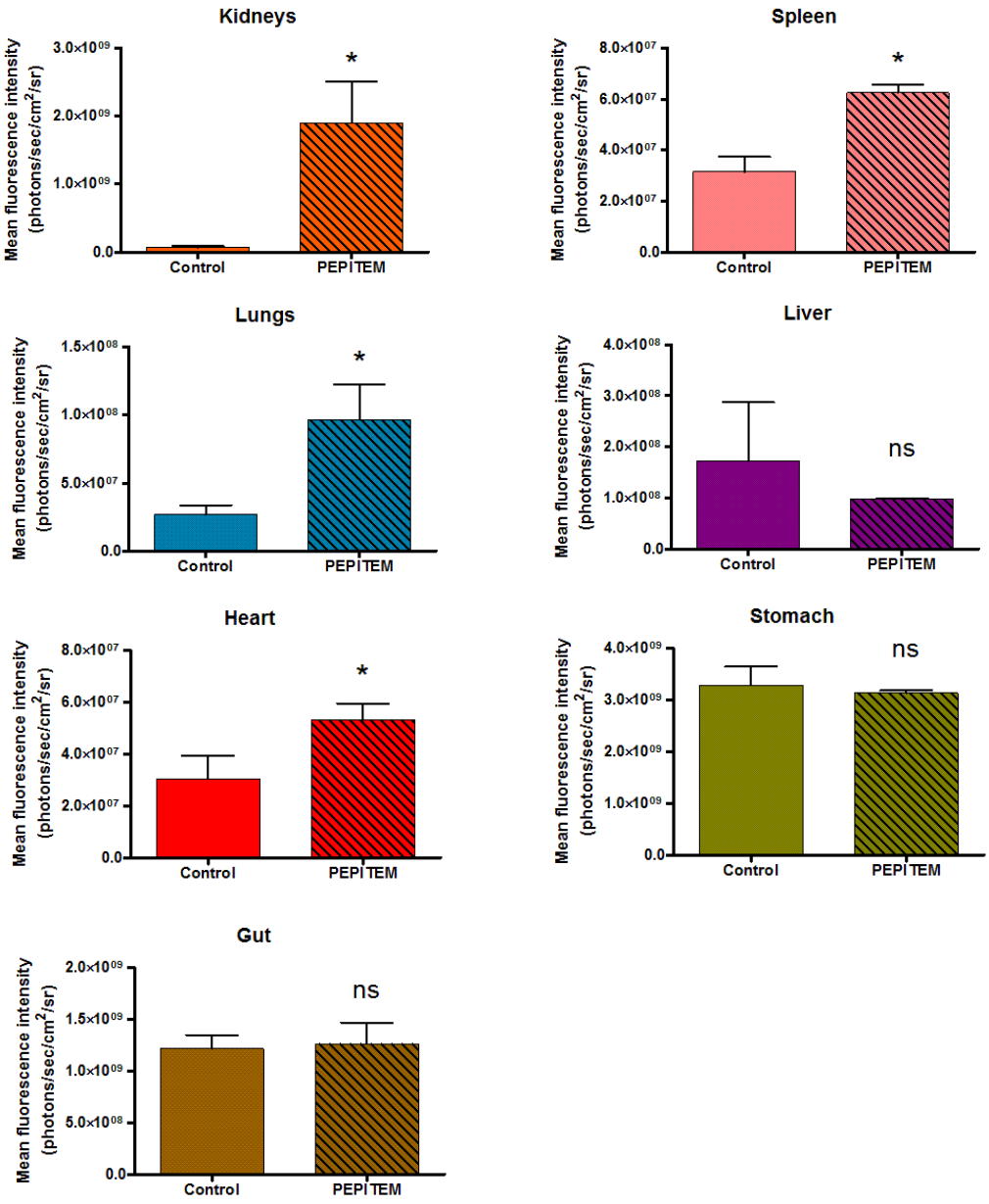

Figure 5.6. Organ fluorescence following injection of PEPITEM-AF680 into BALB/c mice.
100µg/ml PEPITEM-AF680 or PBS control was injected IV into BALB/C mice. After 15 minutes, organs were excised and imaged for fluorescence. Mean fluorescence intensity of each organ was measured representing the average fluorescent counts divided by the number of pixels in each ROI. *P≤0.05 and ns=not significant by unpaired t-test. N=3 mice per group. Data expressed as mean ± SEM.

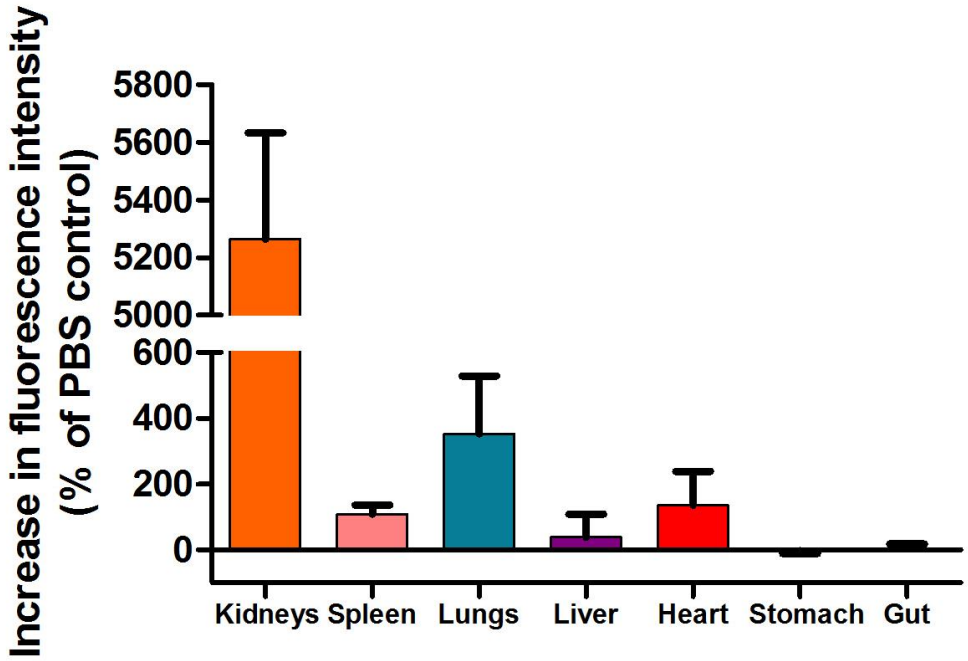

Figure 5.7. The organ distribution of PEPITEM-AF680 *in vivo*. PEPITEM-AF680 or PBS control was injected IV into BALB/c mice. After 15 minutes, organs were excised and imaged for fluorescence. The increase in fluorescence of each organ from mice treated with PEPITEM-AF680 was calculated from the data in Figure 5.6, by dividing the increase in fluorescence by the fluorescence in PBS control mice. N=3.

5.2.3. Investigating the effect of PEPITEM in a mouse model of atherosclerosis.

Atherosclerosis is characterised by plaque formation in the artery wall in an inflammatory environment, and T cells have been shown to exacerbate it. We investigated whether treatment of apoE$^{-/-}$ mice with PEPITEM administered via intraperitoneal (IP) injection could reduce atherosclerotic plaque burden *in vivo*. We selected C-terminal PEG PEPITEM for increased stability as it demonstrated no significant difference in inhibitory function in *in vitro* migration assays, and may aid stability of the C-terminus which alanine substitution data suggested might be important for function.

Mice on HFD were treated twice a week with 1.75mg/ml PEPITEM or scrambled control for 6 weeks. Hearts were isolated and the aortic root was examined for plaque burden. Mice in both control and PEPITEM groups demonstrated plaque formation in the aortic root bicuspid valves (Figure 5.8a). However, plaque burden did not differ between groups, exhibiting 11.8% and 11.9% plaque burden for control and PEPITEM treatment respectively. Since previous studies reported inflammation and steatosis in the liver of apoE$^{-/-}$ mice on HFD, we examined the liver of control and PEPITEM-treated mice. No signs of inflammation or steatosis were seen in either group (Figure 5.9).

These experiments suggested that PEPITEM treatment for 6 weeks did not alleviate plaque burden in a mouse model of atherosclerosis.

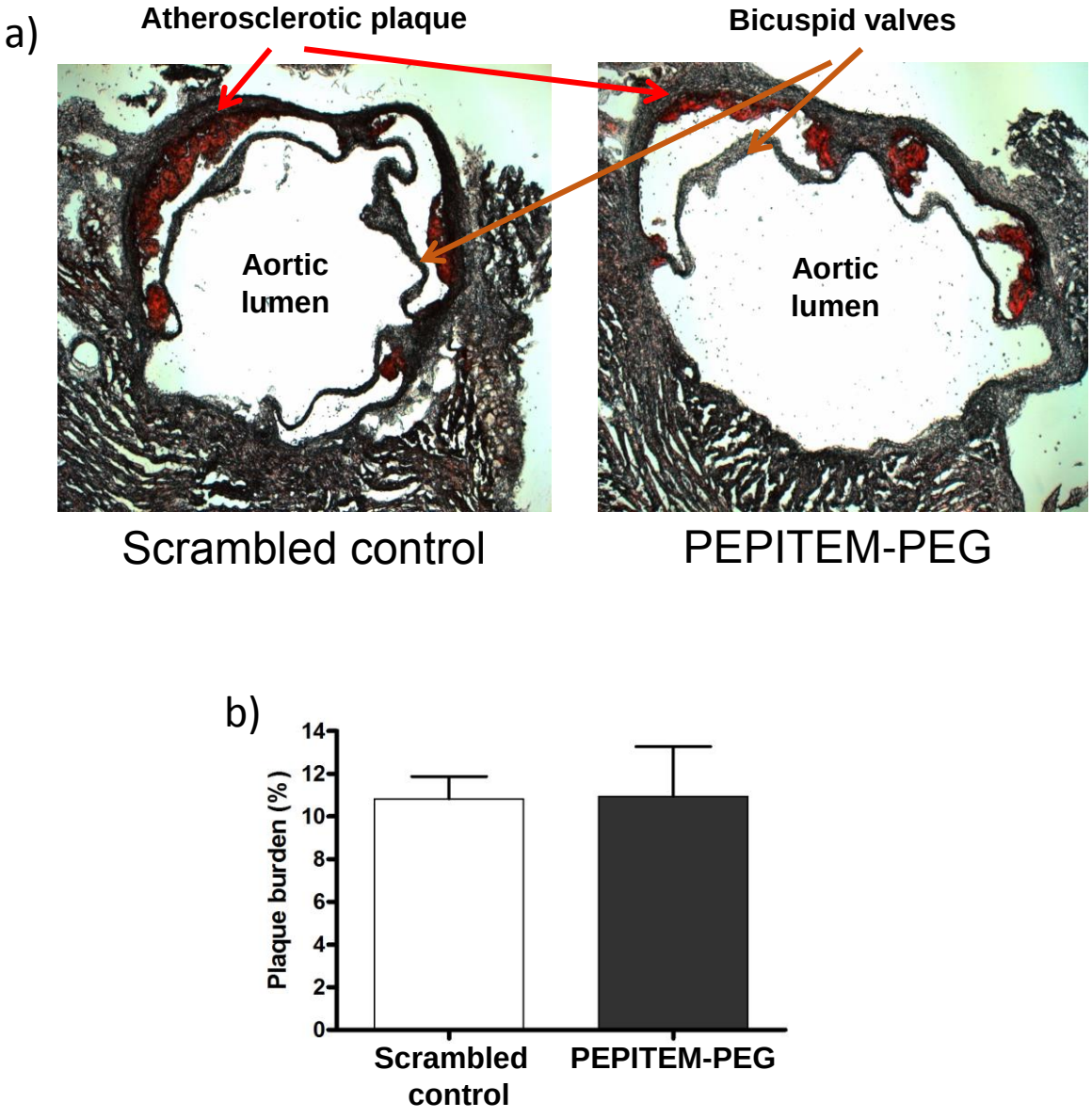

Figure 5.8. Plaque burden in apoE$^{-/-}$ mice on HFD following treatment with PEPITEM-PEG.
C57BL/6 mice were treated for 6 weeks with PEPITEM-PEG or scrambled control. (a) Heart sections were observed for plaque formation in the aortic root, imaged by light microscopy. (b) Percentage plaque burden (stained red with Oil red O) was quantified using image J. Data represent mean ± SEM of 2 and 3 mice for scrambled control and PEPITEM-PEG groups respectively.

Scrambled Control

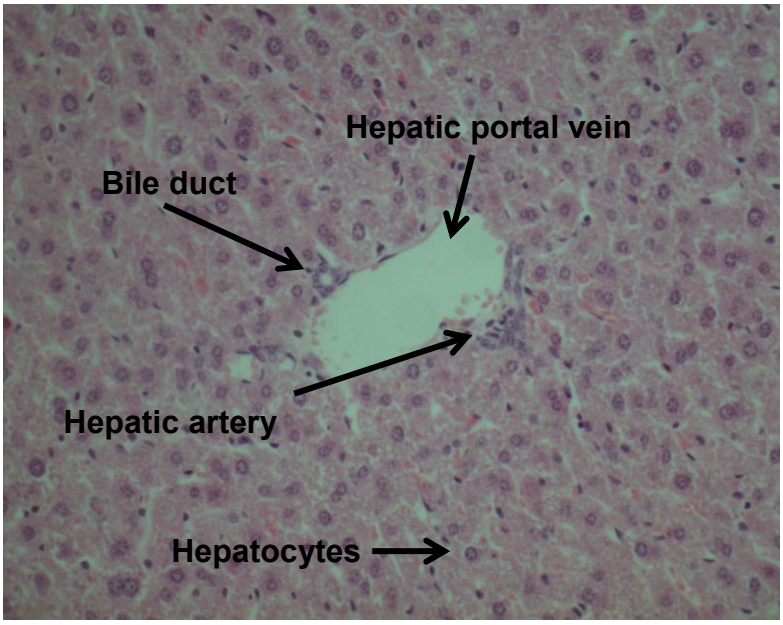

PEPITEM-PEG

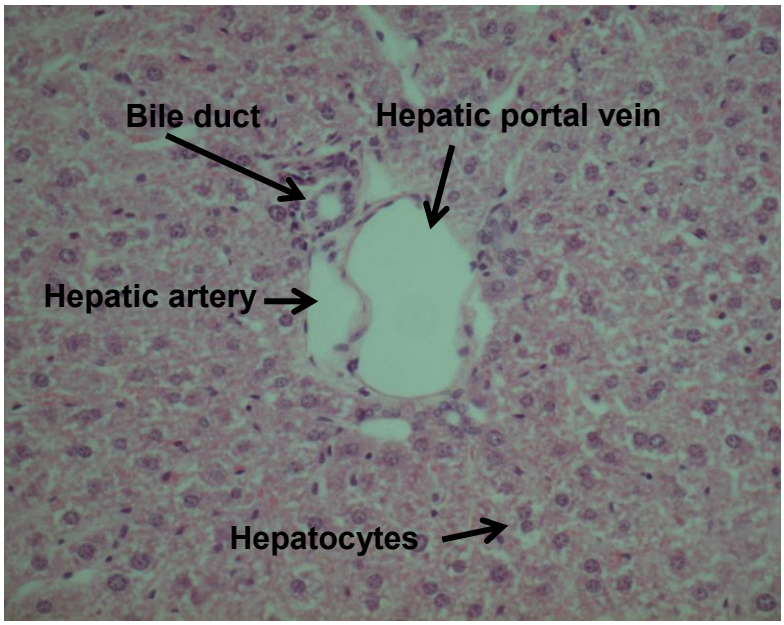

Figure 5.9. Liver histology of apoE$^{-/-}$ mice on HFD following 6 weeks of PEPITEM-PEG treatment.
Representative H&E-stained liver sections from C57BL/6 mice treated for 6 weeks with scrambled control or PEPITEM-PEG. Images were acquired by brightfield microscopy.

5.3. Discussion

The high potency of PEPITEM and its specificity to memory T cells (Chimen *et al.*, 2015) make PEPITEM a desirable candidate for development into a therapeutic agent against a wide range of T cell-mediated chronic inflammatory diseases.

There are numerous ways available for peptide modification and this is common practice in the pharmaceutical industry. We tested several common modifications in this chapter to examine any effects on PEPITEM function and thus their plausible use to increase peptide stability during future development. None of the modifications significantly affect the ability of PEPITEM to inhibit PBL transmigration *in vitro*. Initially we tested the effect of the addition of N or C terminal 352Da PEG repeats, as larger PEGs become increasingly expensive and we were unsure what effect addition of synthetic polymers to these termini would have on function. The fact that addition of PEG to either termini did not affect function means their use is a possibility in the future as a strategy to increase solubility or stability if necessary. Additionally, adjusting the size of PEG is an option if increased molecular weight is required. N-terminal acetylation and C-terminal amidation of PEPITEM could also be employed as a preventative measure for recognition by exopeptidases. The reverse D-isomerised peptide, representing the PEPITEM amino acid sequence in reverse order using D-amino acids, represents the use of amino acid isomers rare in nature which are not easily recognised by proteases, again preventing degradation. Similarly, this variant did not affect PEPITEM function.

These data suggested that PEPITEM can be modified to improve its stability *in vivo* without reducing its effectiveness at inhibiting PBL transmigration. This could

prove valuable further down the line in development for increasing peptide half-life, or for studying PEPITEM biology, for example by conjugation to a fluorescent dye as utilised in this chapter. Economically, crude synthesis of large numbers of modified peptides did not affect PEPITEM function and remains a cost-effective option for screening large numbers of modified peptides.

Besides degradation by proteases, PEPITEM faces potential clearance from the circulation by the kidneys due to its small size of just 14 amino acids (1.5kDa). We employed the use of radiolabelled PEPITEM to measure PEPITEM presence in plasma. Disappointingly but perhaps expectedly, ^{3}H PEPITEM demonstrated rapid clearance from the circulation of C57BL/6 mice, the majority of which occurred in under 2 minutes. The bi-exponential reduction observed was similar to results obtained following injection of inulin, a fructose polymer of approximately 5kDa (Qi *et al.*, 2004) . A further decline in the presence of ^{3}H PEPITEM occurred at 30 minutes. However, residual radioactivity remained after 60 minutes suggesting that PEPITEM may be held in a compartment interchangeable with the plasma, such as organs. The cardiac output in mice is 5-10ml/min and is approximately 20 times faster than in humans. Therefore, we cannot be certain how fast PEPITEM clearance from the circulation would occur in humans, but in light of these data, it is likely to be cleared quickly and probably by the kidneys.

To investigate the endpoint of PEPITEM *in vivo* and confirm our suspicion of renal clearance, we conjugated PEPITEM to AF680 and initially checked for function *in vitro*. Unsurprisingly, since earlier modifications to either termini did not affect PEPITEM function, PEPITEM-AF680 still significantly inhibited PBL transmigration.

We next investigated the endpoint of PEPITEM *in vivo*. Baseline levels of fluorescence were present in all organs after 15 minutes, demonstrated by the control group. Furthermore, high levels of autofluorescence were detected in the organs of the GI tract, with the stomach exhibiting the highest levels of fluorescence of any organ including the kidneys in both control and PEPITEM-AF680-treated groups. This did not differ between groups, however since the autofluorescence was so high, it may not have been possible to detect smaller increases in fluorescent signal above this. Therefore we are unable to conclude if PEPITEM enters the stomach or gut *in vivo*. High levels of autofluorescence in these organs was most likely due to the chow diet, which consists highly of alfalfa and thus autofluorescent chlorophyll (Inoue *et al.*, 2008). This was confirmed by imaging a chow pellet, which was highly fluorescent (data not shown). Higher fluorescence levels was also seen in the heart, spleen and lungs of PEPITEM-AF680 treated animals compared to the control group. This was in agreement with the pharmacokinetic data, which suggested the sequestration of small levels of radioactivity in, probably in plasma-interchangeable tissue.

The most dramatic difference in autofluorescence was seen in the kidneys of PEPITEM-AF680 treated mice. These data were highly suggestive of the majority of PEPITEM-AF680 being cleared from the circulation by the kidneys. We suspected this was highly likely, as peptides <5kDa are often rapidly cleared and PEPITEM is only 1.5kDa. The second largest difference in fluorescence was noted in the lungs. Other than the kidneys, the lungs receive a significant fraction of the cardiac output. This may explain the presence of fluorescence in the lungs of PEPITEM-AF680 treated mice, however the mechanism of PEPITEM absorption by the lungs is unknown. Unfortunately, it is possible that some of the dye molecules may have been

cleaved off. To confirm this in the near future, radioactivity will be measured in all major organs collected following the pharmacokinetics experiment, and ^{3}H PEPITEM organ distribution will be compared to PEPITEM-AF680 distribution.

Together, these data imply that PEPITEM has a short *in vivo* half-life, leaving the circulation rapidly mainly due to renal clearance, however some residual PEPITEM may be retained in other organs.

The half-life of PEPITEM must be increased in order to deliver a suitable therapeutic agent for the treatment of T cell-mediated chronic inflammatory diseases. This can be achieved by increasing its molecular weight, perhaps using higher molecular weight PEG or conjugation to larger inexpensive proteins such as albumin, which is not readily filtered by the kidneys (Leger *et al.*, 2004). The issue of stability may then be addressed using the modifications tested in this chapter. One example where drug modification has led to a successful increase in *in vivo* half-life is the erythropoiesis-stimulating drug Hematide, which is modified with PEG (Stead *et al.*, 2006). Additionally, conjugation to albumin has extended the half-life of a glucagon-like peptide 1(GLP-1) analogue termed CJC-1131, in clinical trials (Giannoukakis, 2003).

We next investigated the effect of intra-peritoneal delivery of native PEPITEM in an apoE$^{-/-}$ mouse model of atherosclerosis through examination of atherosclerotic changes in the aortic root. In these preliminary data, no difference in plaque burden in the aortic root was observed in mice receiving PEPITEM treatment compared to control groups. Chimen *et al.* (2015) had previously demonstrated the ability of PEPITEM to alleviate T cell trafficking in mouse models of Salmonella infection and

Sjögren's syndrome, by delivering PEPITEM to mice at 100µg/day IP for up to 4-5 days. We therefore chose a dose of 700µg/week, and separated this into two 350µg injections in order to observe effects after 6 weeks HFD, whist complying with animal ethics. However two injections per day may not have been as efficient as daily delivery. It is unclear whether the similarities in plaque burden between groups is because the model is not sensitive to PEPITEM, or because of low therapeutic coverage resulting from two doses per week compared to daily doses. Furthermore, while we now know PEPITEM undergoes rapid clearance from the circulation, it is uncertain if delivery into the peritoneum makes PEPITEM susceptible to peptidases in the tissue.

PEPITEM specifically inhibits the trans-endothelial migration of memory T cells (Chimen *et al.*, 2015). Stemme *et al.* (1992) reported that 64% of T cells located in plaques are of the $CD45RO^{+}$ memory phenotype, but it was unclear if these cells were differentiating into memory cells in the tissue, or whether they were being selectively recruited from the blood. While atherosclerosis involves a T cell element, it is also recognised as a multifactorial disease, with complex involvement of other cell types such as monocytes (Reviewed by Hansson *et al.* (2002)). Plaque formation occurred in our mouse model of atherosclerosis, but it is unclear if the model used was sensitive enough to detect small differences in treated mice as a result of inhibiting T cell trafficking into the plaque. Indeed the extent of involvement of T cells in atherosclerosis has been questioned for some time. Zhou *et al.* (2000) reported recruitment of $CD4^{+}$ T cells to atherosclerotic lesions following allogenic transfer to $apoE^{-/-}/Scid^{-/-}$ mice. The presence of $CD4^{+}$ T cells exacerbated plaque burden in this model. Conversely, while Dansky *et al.* (1997) confirmed the presence of T cells in

atherosclerotic lesions, they concluded that lymphocytes play only a minor role in atherosclerosis and are not essential for atheroma formation in apoE$^{-/-}$ mice.

High fat diet can be used to accelerate atherosclerosis in apoE$^{-/-}$ mice. However, placing mice on a high fat diet also induces steatosis, with studies reporting the deposit of lipids and inflammation in the liver as early as 7 weeks post-high fat feeding (Schierwagen *et al.*, 2015, Tous *et al.*, 2005). Interestingly, while mice experienced plaque formation, no lipid deposits or abnormal morphology was observed in either group after 6 weeks of HFD. It is possible that 6 weeks of HFD feeding may not be sufficient to induce chronic lipid deposition, and perhaps may lead us to not see any difference in plaque burden following PEPITEM treatment, as atherosclerosis might not have been severe enough to demonstrate any potential effects of inhibition of T cell trans-endothelial migration with PEPITEM in this context.

In summary, these experiments suggested that after 6 weeks of PEPITEM treatment, there was no difference in plaque burden. Small group numbers limited this investigation and unfortunately, one individual was also culled due to health issues. As there is much variability among living things, a repeat of this experiment with greater animal numbers is necessary, perhaps with an extended high-fat feeding time, and a revised treatment plan after establishing a peptide with a longer *in vivo* half-life.

5.4. Conclusion

Effective therapeutics have long half-lives *in vivo*. They are not rapidly cleared by the kidneys, and are not degraded readily by proteases. PEPITEM is a good candidate as a therapeutic agent for the treatment of chronic inflammatory disease, and has potential for modification to address any stability issues it may have. However, its current use as a therapeutic is hampered by fast renal clearance reducing its availability and exposure, and therefore its effectiveness as a treatment.

Many diseases are T cell mediated or have a T cell element which may exacerbate symptoms, including RA, atherosclerosis, and T1D. PEPITEM function was not altered by modification *in vitro*, but it didn't last long in circulation and was cleared by the kidneys within minutes, with lesser amounts residing in other organs.

We must now focus on increasing the *in vivo* half-life of PEPITEM by investigating methods used previously by others to produce successful drug treatments. These new versions of PEPITEM must then be tested *in vitro* for function, and *in vivo* for effectiveness using appropriate mouse models of chronic inflammation.

CHAPTER 6: THE ROLE OF 14-3-3ζ IN THE PEPITEM PARADIGM

6.1. Introduction

Present in all eukaryotes, 14-3-3 proteins are highly conserved. They are capable of dimer formation and interaction with more than 200 ligands (Pozuelo Rubio *et al.*, 2004). 14-3-3 has been identified as a modulator of numerous cellular processes required for the normal function of cells (reviewed in section 1.6.4), and has been associated with a range of diseases, particularly neurological conditions, for example Alzheimer's disease (Berg *et al.*, 2003). 14-3-3 proteins are primarily considered as intracellular trafficking proteins with numerous functions (Fu *et al.*, 2000). However some studies report 14-3-3 being present in extracellular environments. For example, 14-3-3 isoforms have been detected in cerebrospinal fluid (CSF) of patients suffering from Creutzfeld–Jakob disease (CJD) (Zerr *et al.*, 1998). Despite several associations with disease, a direct role for 14-3-3 in inflammation remains elusive and there is no clear biological function for extracellular 14-3-3 isoforms.

Recently, 14-3-3ζ and other isoforms of the 14-3-3 family of proteins were identified in the exosomes of B cells (Buschow *et al.*, 2010). Exosomes are cell-derived vesicles, containing cargo of proteins, lipids and RNA (Raposo and Stoorvogel, 2013). Having such important roles in other cellular functions, we considered whether 14-3-3 plays a role in the homeostatic mechanism identified by Chimen *et al.* (2015), involving B cell production of PEPITEM. PEPITEM represents amino acids 28 to 41 of the 27kDa 14-3-3ζ protein. Enzymatic release of PEPITEM from 14-3-3ζ protein has been demonstrated in Chapter 3. We also showed that 14-3-3-His can inhibit PBL transmigration to the same extent as PEPITEM, however it

was not clear if that effect was due to 14-3-3ζ alone, or interference from the histidine tag.

Though Chimen *et al.* (2015) demonstrated the presence of PEPITEM in B cell supernatants following AQ stimulation, it remains unclear how PEPITEM is released by B cells, or whether it is released first as 14-3-3ζ, and then subsequently cleaved into PEPITEM extracellularly by proteases.

In this chapter, we examine the role of 14-3-3ζ in the function of PEPITEM. Initially, 14-3-3ζ recombinant protein was tested it in the *in vitro* migration assay for the ability to inhibit PBL transmigration in the absence of the histidine tag. Preliminary investigations were undertaken to examine the protein and mRNA expression of 14-3-3ζ in B cells and EC. Ultimately, we investigated the role of proteases in the inhibitory function of 14-3-3ζ.

Here, we describe the ability of 14-3-3ζ to inhibit PBL transmigration independent of B cells. We provide evidence that suggests B cells secrete 14-3-3ζ constitutively, and that matrix metalloproteases (MMPs) may play an important role in the release of PEPITEM from its parent protein, adding an additional layer of complexity to this already multifaceted homeostatic paradigm.

6.2. Results

6.2.1. The effect of 14-3-3ζ protein on PBL transmigration *in vitro.*

Since PEPITEM can be enzymatically released from 14-3-3ζ, and 14-3-3ζ-His elicited inhibitory function, we investigated whether using 14-3-3ζ recombinant protein in our *in vitro* migration assay would yield similar results compared to treating EC with PEPITEM. No difference in PBL adhesion was observed (Figure 6.1), however the addition of 14-3-3ζ in the migration assay showed significant ability to inhibit the transmigration of PBL across EC, reducing it from 25% in the control, to 14%. This was comparable to PBL transmigration seen following PEPITEM treatment (12%).

We considered the involvement of B cells in the effect of 14-3-3ζ, perhaps as the source of proteases releasing PEPITEM from 14-3-3ζ, and leading to the inhibition of PBL transmigration. To determine whether the effect of 14-3-3ζ required the presence of B cells, B cells were depleted from PBL preparations through negative selection. Flow cytometry was used to confirm the purity of samples post-depletion. PBL were first gated on by size using SSC and FSC (Figure 6.2a). Next, doublets were removed (Figure 6.2b) and $CD3^+$ T cells or $CD19^+$ B cells were gated on (Figure 6.2c and 6.2d). Typically, $CD3^+$ T cells made up the majority of the sample, with B cells representing approximately 3% of total PBL (Figure 6.3a). However post-depletion, $CD3^+$ T cells were enriched, and the presence of less than 1% $CD19^+$ B cells was deemed acceptable (Figure6.3b). Typically, T cell purity was 99.5%.

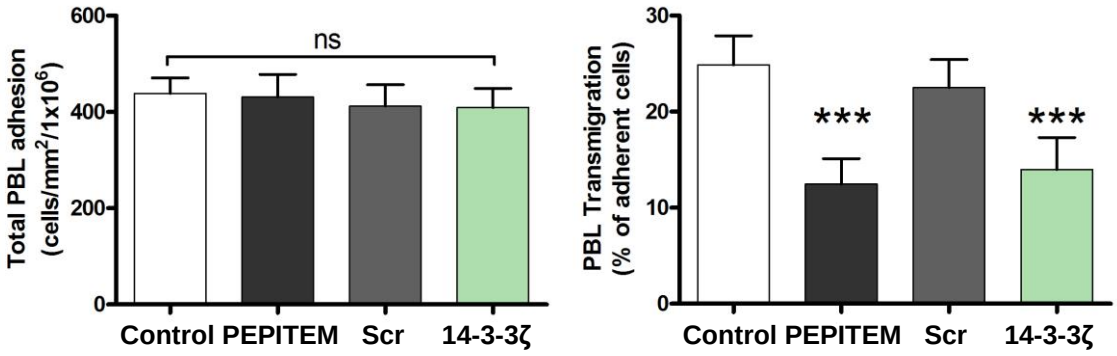

Figure 6.1. Inhibition of PBL transmigration by 14-3-3ζ.
PBL were added to cytokine-stimulated-EC with 20ng/ml 14-3-3ζ, PEPITEM or scrambled peptide (Scr). Adherent and migrated cells were assessed by phase contrast microscopy. Data represents mean ± SEM of 9 independent experiments, and was analysed by one way ANOVA with Dunnett's post-test. ***P<0.001, ns= not significant.

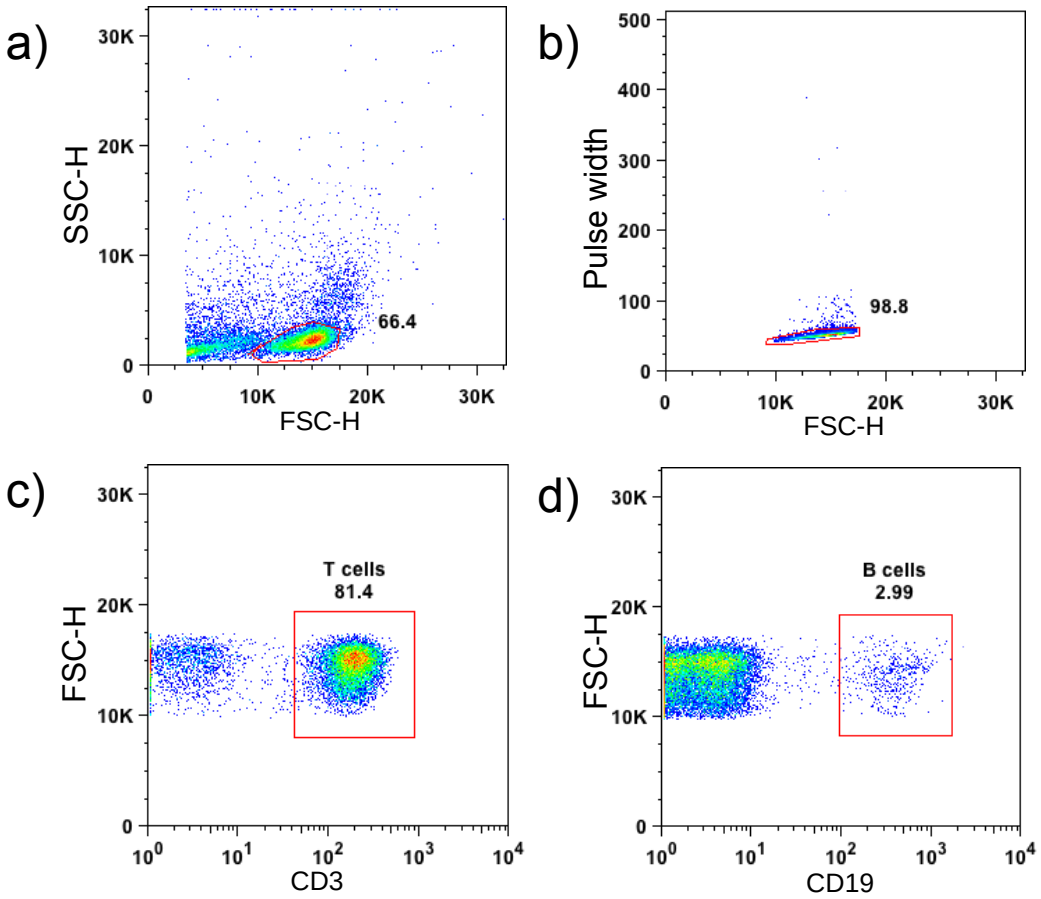

Figure 6.2. Gating strategy for the identification of PBL and PBMCs by flow cytometry.
Representative flow cytometry plots demonstrating the gating approach for the assessment of T or B cells. PBL or PBMC were isolated from healthy donors. (a) Initially, the PBL populations were gated on based on size using forward scatter (FSC-H) and side scatter (SSC-H). (b) Doublet cells were gated out using FSC-H against Pulse width. (c) T cells were identified as a $CD3^+$ population, while (d) B cells were identified as $CD19^+$ cells.

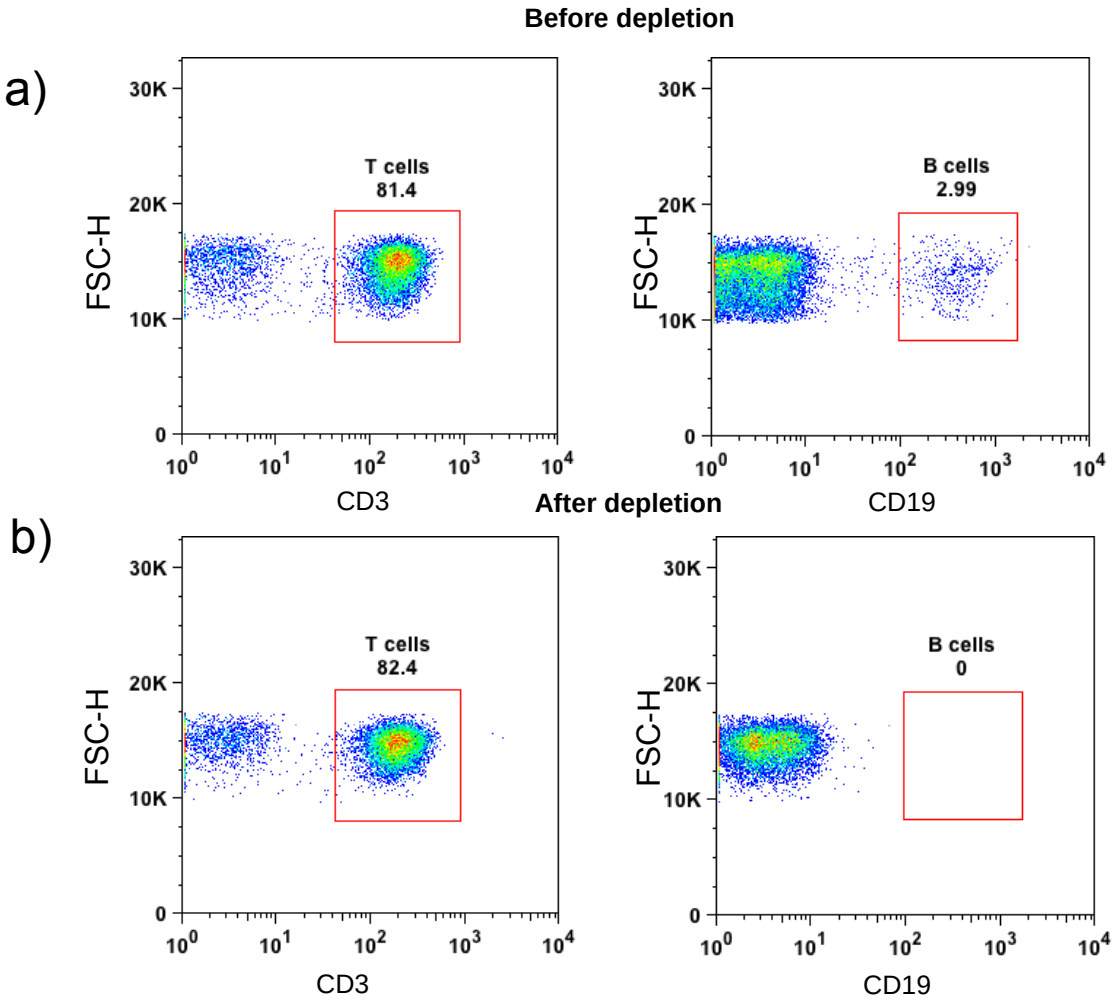

Figure 6.3. Assessment of B cell depletion from PBL preparations using flow cytometry.
Representative flow cytometry plots illustrating the gating strategy employed to confirm B cell absence. B cells were depleted from isolated PBL by negative selection magnetic beads. Flow cytometry was used to assess T cell enrichment (a) before and (b) after B cell depletion. Preparations containing <1% B cells were deemed acceptable, however typically there were <0.5%.

After establishing an enriched T cell population consisting of less than 1% B cells, the *in vitro* migration assay was repeated using 20ng/ml 14-3-3ζ recombinant protein. Again, no difference was seen in adhesion. However interestingly, 14-3-3ζ retained its ability to inhibit PBL transmigration in the absence of B cells (Figure 6.4). Control conditions exhibited 27% transmigration, and 14-3-3ζ treatment reduced this to 15%, which was similar to PEPITEM treatment (14%).

We next investigated whether the inhibitory effects of 14-3-3ζ were dependent on direct interaction with PBL in the *in vitro* migration assay. 14-3-3ζ recombinant protein was pre-incubated for 1 hour on cytokine-stimulated EC before washing and performing the migration assay with fresh PBL. Interestingly, while no differences were seen in adhesion, pre-treatment of EC with 14-3-3ζ inhibited PBL transmigration (Figure 6.5). Control conditions saw 30% transmigration, while treatment with PEPITEM, 14-3-3ζ, or pre-incubation with 14-3-3ζ reduced this to 20, 20 and 21% migration respectively.

These data suggest that 14-3-3ζ can inhibit PBL transmigration. Whether this is directly as a protein or indirectly as PEPITEM remains unknown.

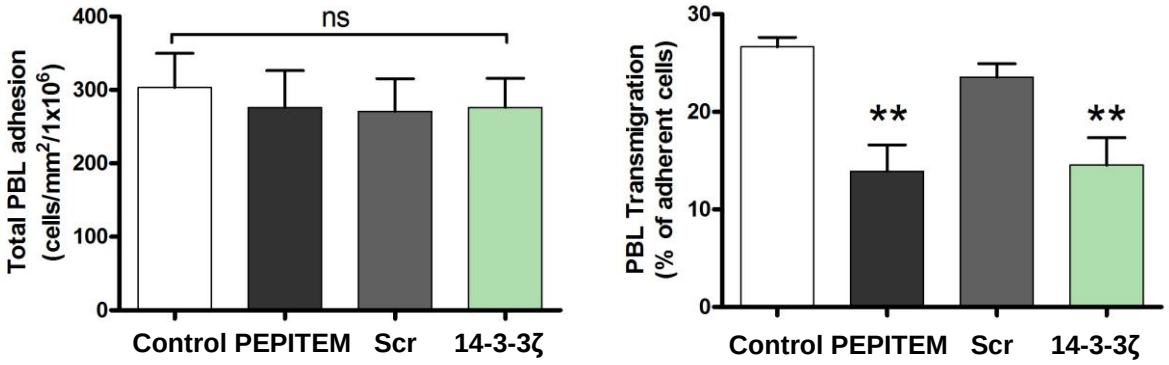

Figure 6.4. The effect of 14-3-3ζ on PBL transmigration following B cell depletion.
B cells were depleted using magnetic beads and purity was confirmed by flow cytometry. PBL and 20ng/ml 14-3-3ζ, PEPITEM or Scrambled peptide (Scr) were simultaneously added to cytokine-stimulated EC and recruitment and migration were observed. **P<0.01 analysed by one way ANOVA with Dunnett's post-test. Ns = not statistically significant. Data representative mean ± SEM of 4 separate experiments.

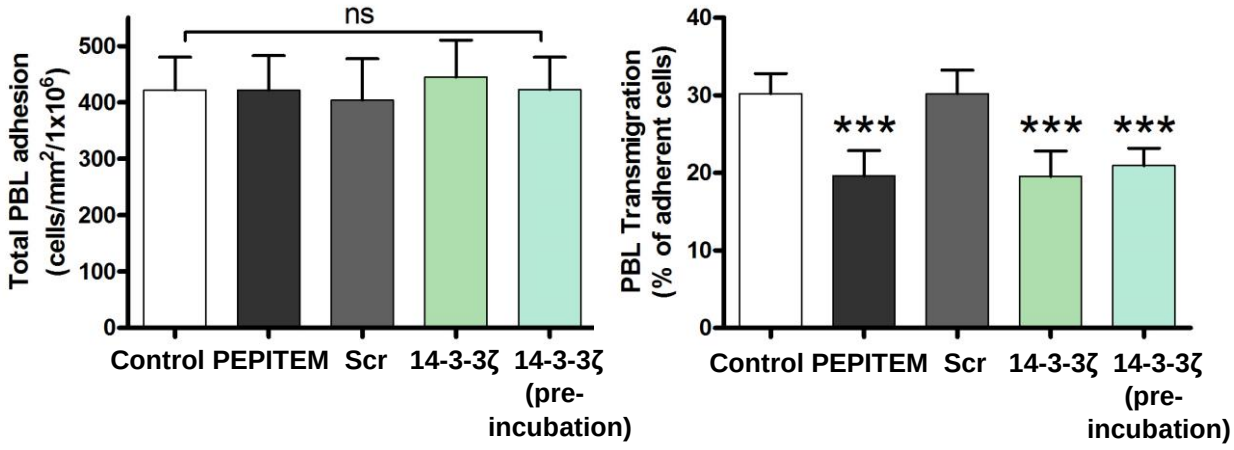

Figure 6.5. The effect of 14-3-3ζ pre-incubation with EC on PBL transmigration.
Cytokine-stimulated EC were pre-incubated with 20ng/ml 14-3-3ζ for 1 hour before EC were washed and the migration assay performed. Data was analysed by one way ANOVA with Dunnett's post-test, and represent 7 independent experiments. ****P<0.001, ns=not statistically significant. Data expressed as mean ± SEM.

6.2.2. 14-3-3ζ expression by lymphocytes and endothelial cells.

Chimen *et al.* (2015) demonstrated the presence of PEPITEM in B cell supernatants following B cell stimulation with AQ. However, the mechanisms of PEPITEM production from B cells remain unknown, and it is not clear whether PEPITEM is secreted as 14-3-3ζ before extracellular processing into PEPITEM. We performed preliminary investigations to identify whether B cells secrete 14-3-3ζ in response to AQ stimulation.

B cells were first enriched from PBL by depleting $CD19^-$ cells. Flow cytometric analysis of processed samples was conducted, and B cell enrichment was confirmed (Figure 6.6). B cell purity of at least 95% was deemed acceptable, however purity was typically 96%.

Following 1 hour incubation of B cells with or without AQ, B cell supernatants were lyophilised and examined for the presence of 14-3-3ζ protein via western blot. Recombinant 14-3-3ζ protein confirmed specificity of the antibody, and HeLa cell lysates of unknown protein concentration were used as an additional positive control. Interestingly, 14-3-3ζ protein was detectable in supernatants from both unstimulated and AQ stimulated samples (Figure 6.7a). Upon quantification of protein signal intensity by densitometry, 14-3-3ζ appeared to be produced in equivalent amounts in both unstimulated and AQ stimulated B cells (Figure 6.7b).

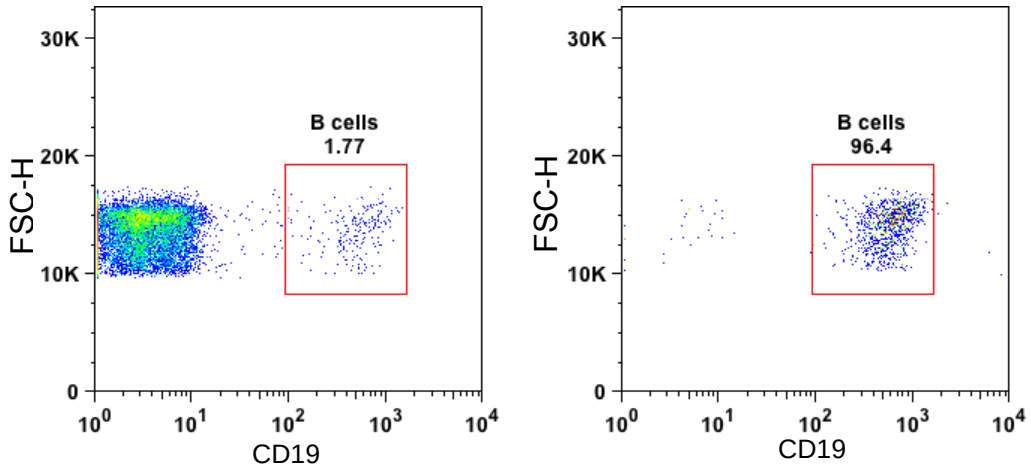

Figure 6.6. Confirmation of B cell enrichment from PBMC.
Representative flow cytometry plots demonstrating the enrichment of B cells. PBMC were isolated from healthy blood and B cells were depleted. Flow cytometry was performed and the purity of $CD19^+$ cells measured. B cell purity >96% was deemed acceptable.

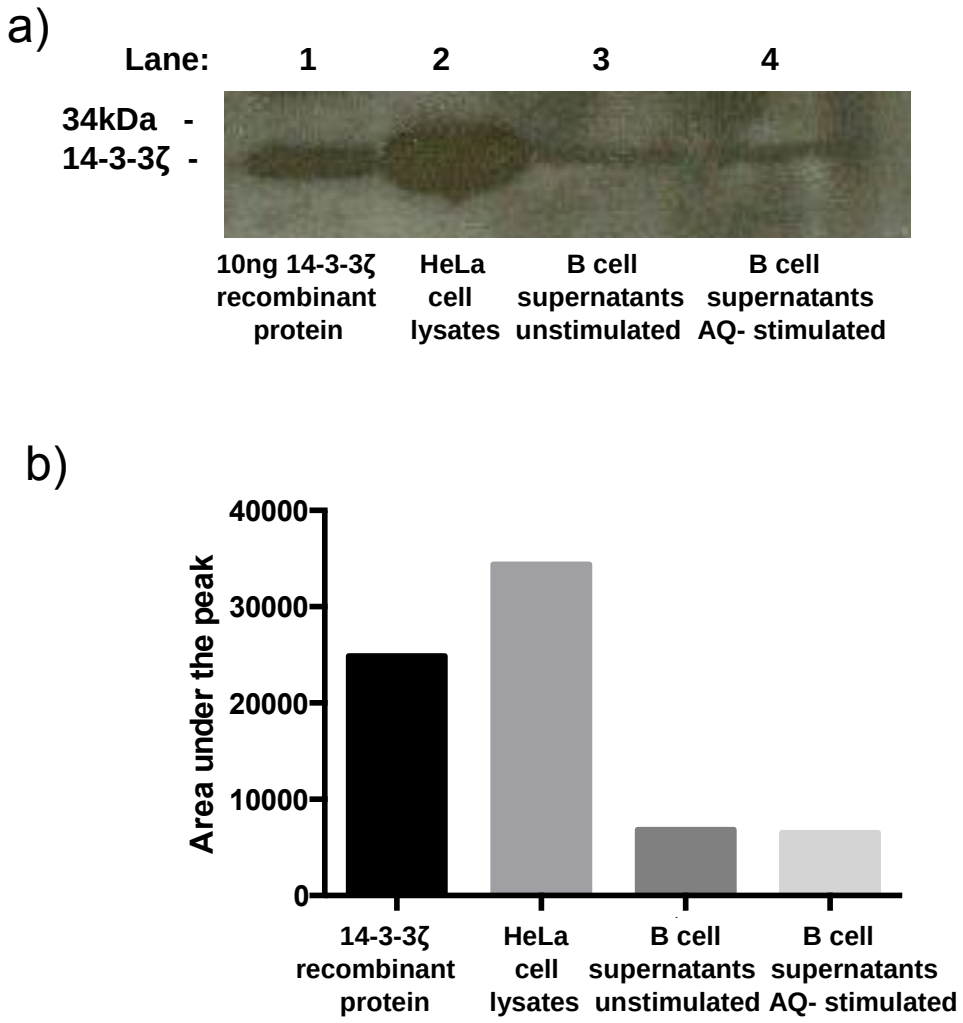

Figure 6.7. 14-3-3ζ protein expression in B cell supernatants.
B cells enriched from PBMC were stimulated with or without 10µg/ml adiponectin for 1 hour. Cells were pelleted and supernatants interrogated for 14-3-3ζ protein by western blotting. (a) blotting for 14-3-3ζ (b) densitometry of western blot using area under the curve method. Data is from 1 experiment.

We subsequently assessed mRNA expression in lymphocytes and endothelial cells. Preliminary data showed the relative expression of 14-3-3ζ in B cells to be much higher than in HeLa cells, B cell-depleted PBL, or HDBEC (Relative expression to 18s: 866, 72, 54 and 23 respectively, Figure 6.8a). 14-3-3ζ expression did not substantially increase in B cells following AQ stimulation (Figure 6.8b), and was not significantly increased in cytokine-treated HDBEC (Figure 6.8c). Stimulated EC also demonstrated the presence of 14-3-3ζ protein assessed by confocal microscopy (Figure 6.9), which appeared highly expressed throughout the cells but not the nuclei.

These preliminary results imply that EC and B cells express 14-3-3ζ protein, and it is possible that 14-3-3ζ is constitutively secreted by B cells. B cells, B cell-depleted PBL and EC also express low levels of 14-3-3ζ mRNA, but B cells express it more highly.

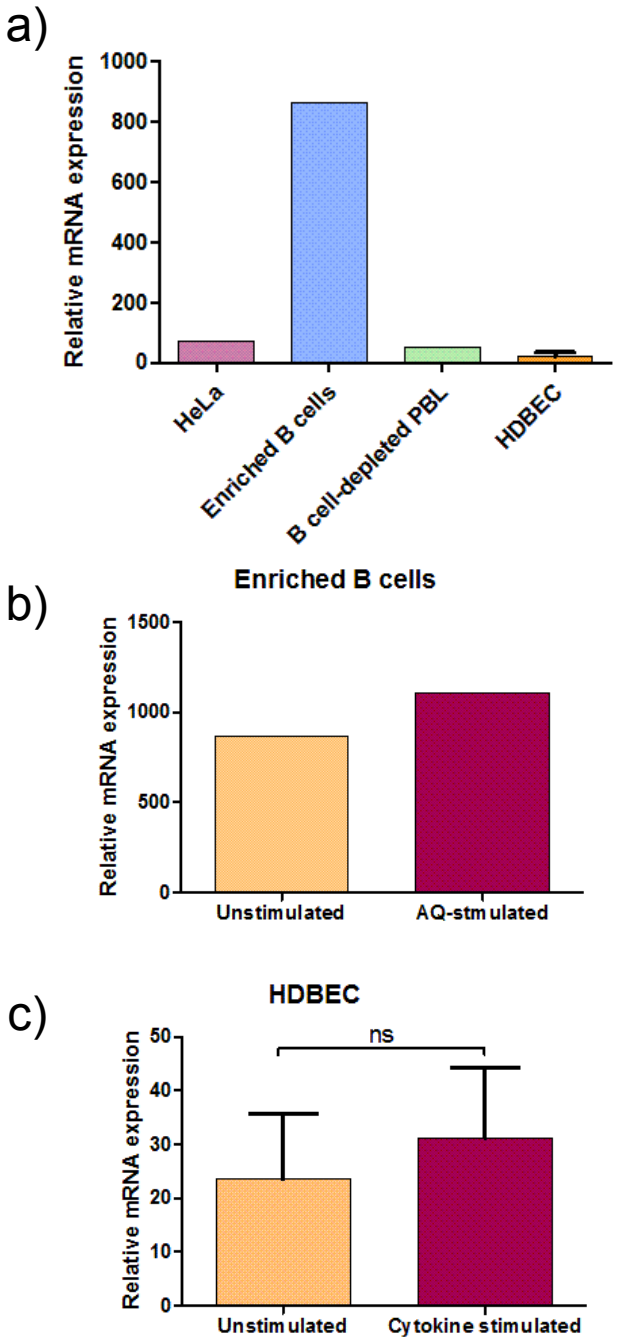

Figure 6.8. Assessment of 14-3-3ζ gene expression in lymphocytes and HDBEC by qPCR

(a) 14-3-3ζ mRNA expression in B cells, B cell-depleted PBL and EC. HeLa mRNA was used as a positive control (n=1). (b) 14-3-3ζ expression in isolated B cells stimulated with or without 10µg/ml AQ (n=1). (c) 14-3-3ζ expression in HDBEC stimulated with or without TNF-α + IFN-γ (n=4, ns= not significant by Mann-Whitney t-test).

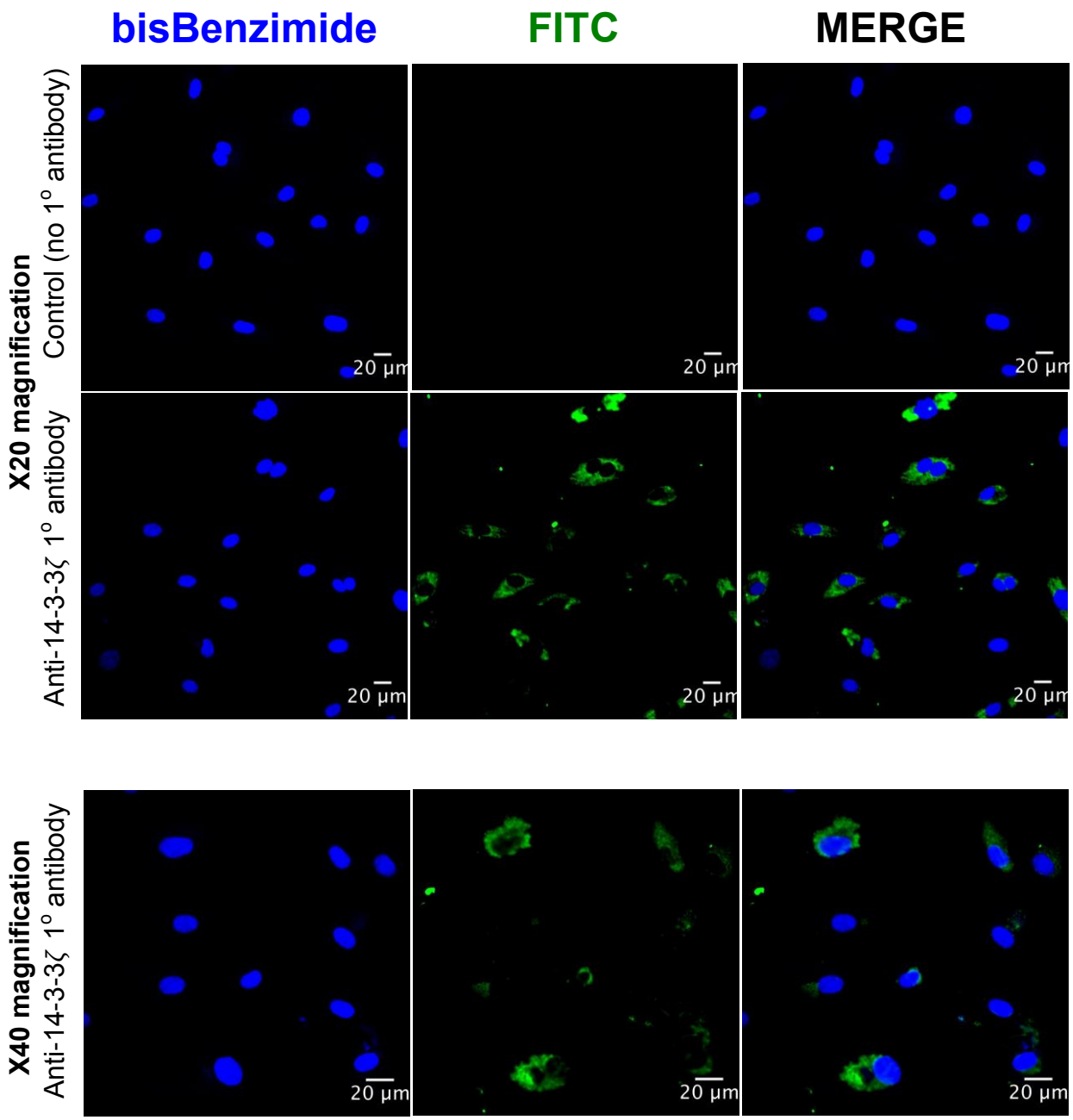

Figure 6.9. Expression of 14-3-3ζ protein HDBEC.
EC were grown in Ibidi µ-slides, cytokine-stimulated and fixed with formaldehyde. 14-3-3ζ was stained using mouse anti-human 14-3-3ζ primary antibody, followed by an anti-mouse-FITC secondary. Nuclei were stained with bisBenzimide and images were acquired using an inverted Zeiss LSM-510 UV confocal microscope.

6.2.3 Investigating the role of proteases in 14-3-3ζ function.

The suggestion from preliminary data that B cells may constitutively secrete 14-3-3ζ protein suggests that the regulation of PEPITEM production may be mediated by extracellular proteases from PBL or EC. Therefore, we investigated the role of proteases in 14-3-3ζ-mediated inhibition of PBL transmigration.

MMPs are an abundant family of proteases expressed by a variety of cells, including PBL and EC (Abraham *et al.*, 2005, Di Girolamo *et al.*, 1998, Hanemaaijer *et al.*, 1993). The role of MMPs in T cell migration has been reported in several studies (Brundula *et al.*, 2002, Faveeuw *et al.*, 2001, Marracci *et al.*, 2002). We investigated the role of MMPs in the paradigm using a broad spectrum protease inhibitor, GM6001. Following pre-treatment of both PBL and EC with the inhibitor, the *in vitro* migration assay was performed, and surface adherent and transmigrated PBL were subsequently analysed.

A small reduction in adhesion was noted following treatment with the GM6001+ 14-3-3ζ or GM6001+ PEPITEM, but not following treatment with the inhibitor alone (Figure 6.10). PEPITEM and 14-3-3ζ significantly inhibited PBL transmigration, and excitingly, this inhibition was lost following treatment with the GM6001+ 14-3-3ζ or GM6001+ PEPITEM. PBL transmigration was comparable to the control which was 41%, compared to 36.6% or 37.2% in 14-3-3 and PEPITEM treated conditions respectively.

We next submitted the amino acid sequence of 14-3-3ζ to PROSPER, an online database to identify predicted proteases *in silico* (Figure 6.11a, Song *et al.* (2012)). Of the proteases that did not cleave in the centre of the PEPITEM sequence,

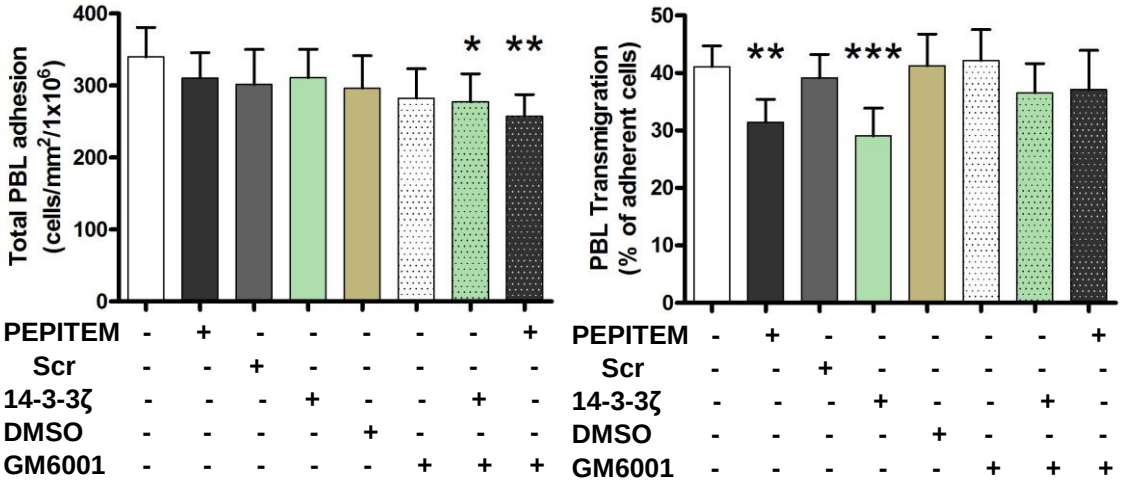

Figure 6.10. The effect of MMP inhibition on 14-3-3ζ and PEPITEM function. EC and PBL were treated with MMP broad-spectrum inhibitor, GM6001 (10nM) for 1 hour prior to performing migration assay. Immediately before migration, PEPITEM, scrambled peptide (Scr) or 14-3-3ζ (all 20ng/ml) were added to PBL. Data represents mean ± SEM of 6 independent experiments, analysed by one way ANOVA with Dunnett's post-test. *P≤0.05, ** P≤0.01, P≤0.001.

a)

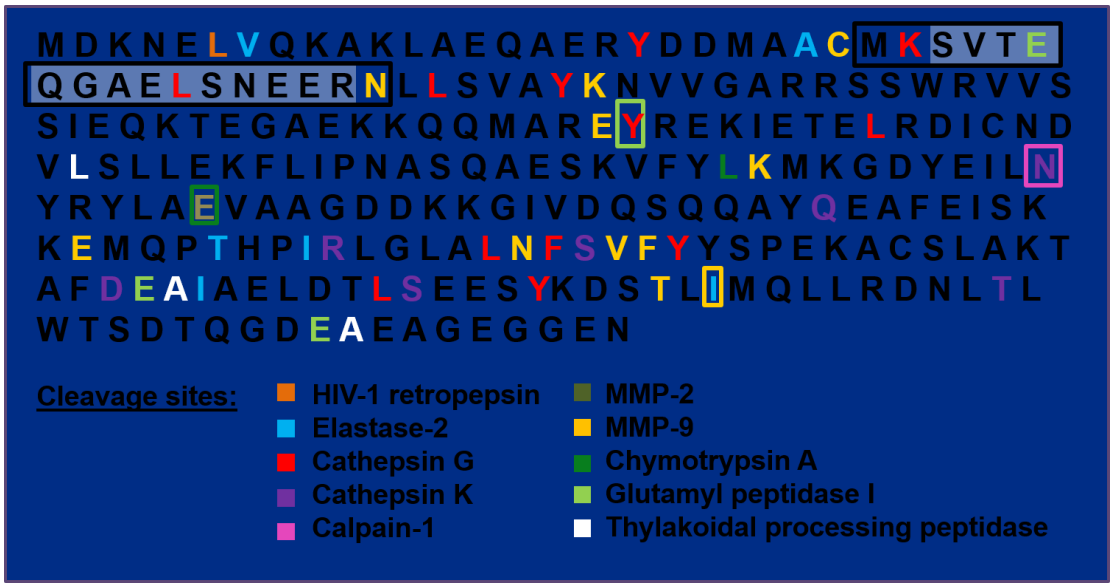

b)

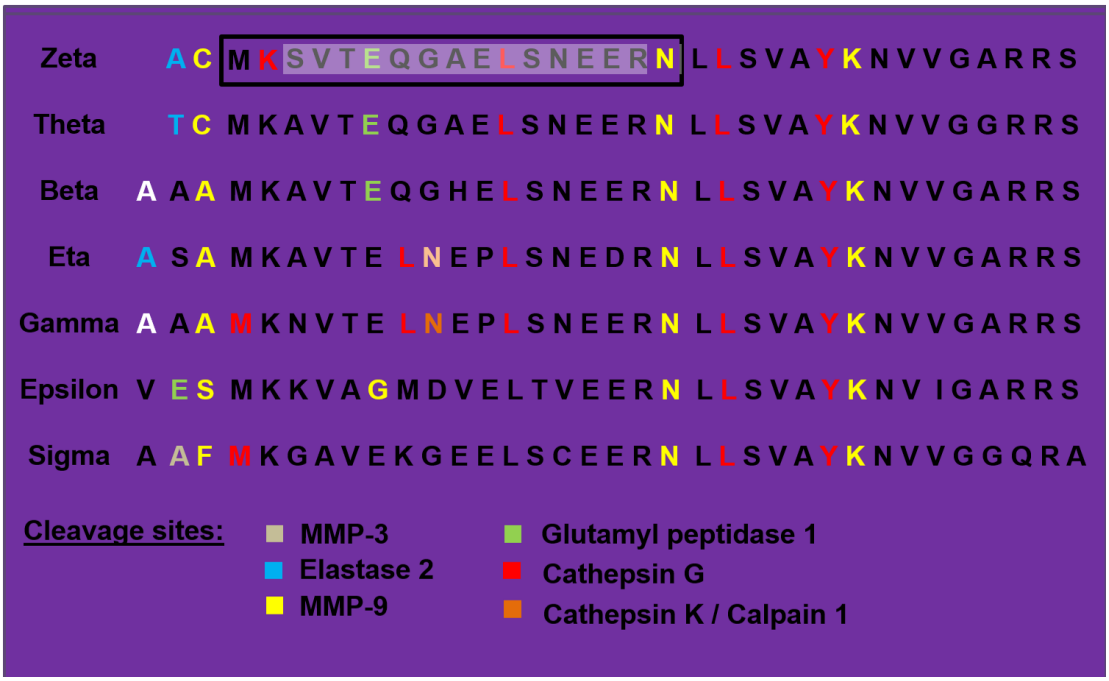

Figure 6.11. *In silico* analysis of predicted protease cleavage sites in 14-3-3ζ protein.
(a) Human 14-3-3ζ protein sequence was entered into PROSPER, and analysed for the presence of protease cleavage sites. (b) Alignment of the seven 14-3-3ζ isoforms, highlighting conserved protease cleavage sites. The original PEPITEM sequence is highlighted in white, with the new 17aa product designated by a black box.

matrix metalloproteinase 9 (MMP-9, yellow residues) was identified as a potential protease involved in the release of PEPITEM from its parent protein. Proteases predicted to cleave within the PEPITEM sequence included cathepsin G (red residues) and glutamyl peptidase I (green residues). Furthermore, when we submitted all 14-3-3 isoforms to PROSPER, we noticed that several cleavage sites were conserved at the same residues between 14-3-3 family members (Figure 6.11b). While MMP-9 and cathepsin G cleavage sites were present in all 14-3-3 isoforms, glutamyl peptidase I was present in four family members. The relevance of these apparently conserved protease recognition sites is currently unknown.

Together these results suggested a role for MMPs in the PEPITEM paradigm, however confirmation of the involvement of MMP-9 and the role of the other identified proteases is required.

6.3. Discussion

After the surprising finding that 14-3-3ζ-his inhibits PBL transmigration *in vitro*, we investigated the role of 14-3-3ζ in the PEPITEM paradigm.

We first tested whether the inhibition of PBL migration by 14-3-3ζ-His was due to the presence of a histidine tag. Indeed 14-3-3ζ significantly inhibited PBL migration to the same extent as PEPITEM. We considered whether the 14-3-3ζ protein itself was inhibiting PBL trafficking, or whether 14-3-3ζ was first being processed into PEPITEM, maybe by B cells. Chimen *et al.* (2015) previously demonstrated the release of PEPITEM by B cells. In the view that extracellular 14-3-3ζ inhibits PBL

transmigration, the processing of 14-3-3ζ is likely to be occurring outside of B cells to give rise to the PEPITEM detected in B cell supernatants, and not intracellularly.

14-3-3ζ was used at 20ng/ml (0.72nM) in the migration assay, where we observed significant inhibition of PBL transmigration. Although the same concentration of PEPITEM was used, PEPITEM is much smaller in size than 14-3-3ζ protein. This means that there would have been fewer molecules of 14-3-3ζ but more molecules of PEPITEM, where 20ngml PEPITEM is equivalent to 13.3nM, and yet inhibition was observed with both treatments. PEPITEM significantly inhibits PBL transmigration at concentrations as low as 0.1ng/ml, equivalent to 0.07nM (Chimen *et al.*, 2015). This may explain why 20ng/ml 14-3-3ζ still induced inhibition of PBL transmigration.

We next investigated whether 14-3-3ζ-mediated inhibition of PBL required the presence of B cells, since PEPITEM was found in supernatants of isolated B cells, suggesting that they can process 14-3-3ζ into PEPITEM independently of other cell types. We depleted B cells from PBL preparations and examined transmigration *in vitro*. Indeed the presence of B cells was not necessary for 14-3-3ζ mediated inhibition of PBL transmigration. Assuming that 14-3-3ζ is processed into PEPITEM extracellularly, these data suggested that EC or T cells may also facilitate this process.

Chimen *et al.* (2015) demonstrated that 1 hr pre-incubation with PEPITEM on EC before performing the migration assay inhibited PBL transmigration. We considered whether this was also true for 14-3-3ζ, and certainly it was. These results imply that extracellular 14-3-3ζ is capable of inhibition of PBL transmigration by first interacting directly with the EC. Perhaps the involvement of EC proteases was

required for the release of PEPITEM from 14-3-3ζ protein. Unfortunately while these investigations suggested that extracellular 14-3-3ζ inhibits PBL transmigration, they do not tell us whether EC is processing 14-3-3ζ into PEPITEM itself, or if PBL are affecting 14-3-3ζ after their addition to the EC.

In preliminary investigations, we examined the secretion of 14-3-3ζ by B cells following stimulation with AQ. 14-3-3ζ protein expression in B cell supernatants in both unstimulated and AQ-stimulated conditions was detected by western blot. Interestingly, 14-3-3ζ is known to dimerise (Fu *et al.*, 2000). However due to western blot methodology, we were unable to determine whether 14-3-3ζ in B cell supernatants was a monomer or a dimer, but this can be confirmed in future using native, SDS-free conditions. Quantification of protein by densitometry suggested similar protein levels in the supernatant of stimulated and unstimulated B cells, implying constitutive secretion of 14-3-3ζ protein of less than 10ng in 1 hour, as this was the concentration of recombinant 14-3-3ζ protein ran as a positive control. While there is a chance that 14-3-3ζ was found in B cell supernatants as a consequence of release following apoptosis, this is unlikely as experiments performed by other members of our lab have previously confirmed that B cells do not undergo apoptosis after 1 hour at room temperature.

The 14-3-3 family of proteins including the 14-3-3ζ isoform have been detected in the exosomes of B cells (Buschow *et al.*, 2010), suggesting that externalisation of 14-3-3ζ proteins represents an active secretory mechanism in immunity. However this requires careful investigation, as the B cells used in the study in question were an Epstein–Barr virus-transformed human B-cell line RN (HLA-

DR15), and it is unclear how closely these cells resemble healthy human B cells. Exosomes from B cells isolated from healthy donors must now be examined for the presence of 14-3-3ζ, to evaluate the likelihood of 14-3-3ζ export from B cells via exosomes.

Upon preliminary analysis of 14-3-3ζ expression in mRNA isolated from negatively selected B cells, PBL preps following B cell depletion or EC, B cells expressed 14-3-3ζ more highly, supporting our hypothesis that B cells are the cell type responsible for 14-3-3ζ secretion and therefore PEPITEM production in this paradigm, although this requires further validation due to the small sample size. In addition to 14-3-3ζ mRNA, endothelial cells were also seen to express 14-3-3ζ protein diffusely. Again this demonstrated the specificity of the process of 14-3-3ζ secretion by B cells, as EC have the potential for 14-3-3ζ secretion, yet they do not autoregulate this pathway and therefore must not secrete 14-3-3ζ.

AQ stimulation did not increase 14-3-3ζ production by B cells, suggesting that B cells are constitutively expressing 14-3-3ζ. If this is indeed the case, the release of PEPITEM from 14-3-3ζ may well be regulated by proteases, under AQ control. MMPs are a family of proteases which are known to degrade extracellular matrix molecules. 14-3-3 proteins have been identified in the literature as up-regulators of MMPs, and have been associated with inflammatory diseases. For example, 14-3-3σ has been shown to upregulate MMP-1 in fibroblasts (Asdaghi *et al.*, 2012, Ghahary *et al.*, 2004), and levels of extracellular 14-3-3η in the joints and serum of RA patients correlated positively with MMP expression (Maksymowych and Marotta, 2014). Furthermore, numerous studies have reported the involvement of MMPs in T cell migration both *in vitro* and *in vivo* (Brundula *et al.*, 2002, Faveeuw *et al.*, 2001, Marracci *et al.*, 2002).

We examined the involvement of MMPs in the inhibitory function of 14-3-3ζ using the broad spectrum MMP inhibitor GM6001. A reduction in adhesion following treatment with the inhibitor and 14-3-3ζ or PEPITEM was noted. It is possible that the GM6001 inhibitor exhibited a minor effect on PBL recruitment, as the conditions treated with it represented the lowest adhesion. Even so, transmigration was expressed as a percentage of adherent cells to account for this discrepancy. Pre-incubation of EC and PBL with GM6001 abolished function of 14-3-3ζ, suggesting the requirement of MMPs for subsequent processing into PEPITEM for the inhibition of PBL transmigration. Unexpectedly, MMP inhibition also abrogated the ability of PEPITEM to inhibit PBL transmigration. *In silico* analysis using the online protease specificity prediction server, PROSPER, identified potential protease cleavage sites within 14-3-3ζ. MMP-9 cleavage sites flanked the PEPITEM sequence and were absent within the PEPITEM sequence itself. Indeed studies have demonstrated the expression of MMPs, including MMP-9, in human B cells, as well as T cells (Abraham *et al.*, 2005, Di Girolamo *et al.*, 1998, Trocmé *et al.*, 1998). Furthermore, MMP-9 expression has been reported in endothelial cells (Taraboletti *et al.*, 2002), and is upregulated following stimulation with TNF-α (Hanemaaijer *et al.*, 1993, Mackay *et al.*, 1992, Nelimarkka *et al.*, 1998). If MMP-9 does indeed cleave 14-3-3ζ into PEPITEM, this may explain why EC pre-treatment with 14-3-3ζ was able to significantly inhibit PBL transmigration.

The peptidases cathepsin G and glutamyl peptidase I were predicted to cleave at sites located within the PEPITEM sequence. The broad spectrum MMP inhibitor does not inhibit cathepsin G or glutamyl peptidase I, yet both 14-3-3ζ and PEPITEM function was abrogated following treatment with the broad spectrum inhibitor. This

implies that MMPs are required for initial cleavage of 14-3-3ζ, but subsequent proteases, potentially cathepsin G or glutamyl peptidase I, may also be involved which require the initial cleavage from 14-3-3ζ into smaller peptides, recognisable by these proteases, to yield functional peptide(s). Indeed glutamyl peptidase I is an endopeptidase highly expressed in epithelial cells of the intestine and kidney, but also by vascular endothelium (Lojda and Gossrau, 1980). Cathepsin G on the other hand is expressed primarily by cells of the myeloid lineage (Grisolano *et al.*, 1994), which were excluded in our assays, however one study has reported cathepsin G activity associated with T lymphocytes (Delgado *et al.*, 2001). If glutamyl peptidase I is in fact responsible for further PEPITEM processing, it may explain why it requires initial degradation of 14-3-3ζ to recognise its substrate, since this endopeptidase recognises specific motifs at the N-terminus.

Our data suggests an MMP, conceivably MMP-9, is responsible for initial cleavage of 14-3-3ζ into PEPITEM. However the MMP-9 cleavage sites would in fact yield a 17 amino acid product, providing the sequence MKSVTEQGAELSNEERN. Since mass spectrometric methodology involved peptide fragmentation, which always occurs uniformly due to the integral properties of the amino acids within the sequence, it is possible that the 14 amino acids detected previously were actually part of a larger 17 amino acid peptide sequence, MKSVTEQGAELSNEERN. Assuming this cleavage product is yielded from 14-3-3ζ by MMPs, the final possible peptide products cleaved by cathepsin G would be MK, SVTEQGAEL or SNEERN. Potential products yielded by glutamyl peptidase I would be MKSVTE and QGAELSNEERN, and if both proteases were involved, MK, SVTE, QGAEL or SNEERN could be cleaved. Therefore, it is possible that 14-3-3ζ, after initial cleavage

into PEPITEM, is subsequently processed into smaller pharmacophore(s). We must now evaluate which of these peptides are functional *in vitro*.

Many proteins and peptides are known to undergo cleavage into smaller active forms, mediated by proteases. Several examples of this are evident in immunity. A number of different isoforms of the chemokine IL-8 have been identified (Yoshimura *et al.*, 1989), and processing of these isoforms by a number of proteases including MMP-9, increase the activity of IL-8 (Van den Steen *et al.*, 2000). Chemerin, like IL-8, is a chemoattractant protein with immunological function. It too can be cleaved by several proteases, including cathepsin G, into both active and inactive peptides (Kastin, 2013).

14-3-3ζ is the only family member possessing the PEPITEM motif. However, rather interestingly, when all 14-3-3ζ isoforms are aligned, the PEPITEM sequence appears highly conserved with only a few amino acids varying in the sequence. Moreover, predicted MMP-9 protease sites appear conserved among family members, all giving rise to 17 amino acid peptide products following excision. Cathepsin G protease sites also appear conserved between family members, and this may have implications *in vivo* where cells of the myeloid lineage such as neutrophils are present. It raises important questions as to whether PEPITEM is in fact a member of a larger family of peptides derived from the 14-3-3 family of proteins. These peptides, like PEPITEM, may also have biological function, but whether this is in immunity is unknown.

The data presented in this chapter suggests that extracellular processing of 14-3-3ζ must occur via initial involvement of MMPs in the processing of B cell-derived extracellular 14-3-3ζ into PEPITEM, and this initial step appears essential to subsequently yield functional peptides which inhibit PBL transmigration. It is now possible that PEPITEM is a 17 amino acid peptide subsequently processed into smaller peptides, and similar processing steps can be seen elsewhere in inflammation such as in IL-8 or chemerin production.

6.4. Conclusion

The importance of 14-3-3ζ and how it is regulated is now recognised as an integral part of the PEPITEM paradigm. Indeed both 14-3-3ζ and MMPs have been implicated in inflammatory diseases.

The experiments performed in this chapter suggested the secretion of 14-3-3ζ by B cells, as well as an important role for MMPs and other proteases in the PEPITEM paradigm, representing another level of regulation of T cell trafficking. In order to fully comprehend this complex homeostatic pathway, we must now investigate which proteases are involved in the processing of 14-3-3ζ into PEPITEM, and what is their source.

CHAPTER 7 – GENERAL DISCUSSION

7.1 General discussion

In this thesis, I examine the biological and chemical nature of PEPITEM, and investigate the involvement of proteases in the adiponectin-PEPITEM axis.

I initially demonstrated the reproducibility of previous work conducted by Chimen *et al.* (2015) on the ability of adiponectin, and therefore PEPITEM, to inhibit T cell transmigration *in vitro*. I confirmed the simple structure of PEPITEM using NMR, but was unable to demonstrate any binding interactions with CDH15 or TSP-1 using Biacore binding assays. I showed the inability of PEPITEM to elicit measurable calcium flux in endothelial cells, and revealed the short circulating half-life of PEPITEM *in vivo* for the first time. This was found to be mainly due to renal filtration, and highlighted the requirement for further peptide modification in order to develop PEPITEM as a suitable therapeutic for chronic inflammatory diseases. Finally, I uncovered the significance of the 14-3-3ζ protein in the PEPITEM paradigm through demonstration of its secretion by B cells, and the requirement of MMPs for PEPITEM function.

The PEPITEM-adiponectin axis represents a novel, exciting finding and provides insight into the molecular mechanisms underlying the regulation of T cell trafficking. However, due to its novelty, the underlying molecular mechanisms remain to be firmly established. The importance of understanding such mechanisms is highlighted in chronic inflammatory dieses such as T1D and RA, where this homeostatic regulatory pathway is impaired, and T cell trafficking becomes dysregulated.

Current therapies used in the treatment of chronic inflammatory diseases often include the use of antibodies. Rituximab is monoclonal antibody currently used in the

treatment of RA, and is being investigated for the treatment of a range of other chronic inflammatory diseases (Gürcan *et al.*, 2009). Through the recognition of CD20, it specifically depletes B cells believed to exacerbate disease through antibody production. This is interesting as Chimen *et al.* (2015) demonstrated B cell-mediated inhibition of T cell trafficking across inflamed EC. However, Chimen *et al.* (2015) also demonstrated that B cell adiponectin receptor expression, required to elicit PEPITEM production, is impaired in chronic inflammatory diseases including RA and T1D. It has been suggested that certain B cell subsets promote T cell recruitment in mice models of diabetes (Ryan *et al.*, 2010) but it is not known which subsets Rituximab targets (Browning, 2006). PEPITEM is secreted in higher quantitates by plasma cells (Chimen *et al.*, 2015), suggesting plasma cells play a critical role in the regulation of T cell trafficking, however the role of B_{regs} in this context requires further attention.

Anti-CD3 therapies including the monoclonal antibody Teplizumab (Sherry *et al.*, 2011) have been tested in clinical trials and target T cells in T1D, thought to be responsible for the infiltration and subsequent destruction of beta cells in the pancreatic islets. The monoclonal antibody Infliximab is used to target soluble and membrane-bound TNF-α (Scallon *et al.*, 2002), a pro-inflammatory cytokine responsible for the activation and subsequent recruitment of many immune cell types. TNF-α blockers such as Infliximab are currently used in the treatment of number of chronic inflammatory diseases including Crohn's disease and RA.

Unfortunately, the success of these antibody-based therapies has been somewhat limited. Aside from being highly expensive to produce, undesirable side-effects and issues with recurrent infections can occur with these treatments, along with disappointing results over long-term treatment (Chatenoud *et al.*, 1994, Herold *et*

al., 2002, Keymeulen *et al.*, 2005, Pescovitz *et al.*, 2009). There is clearly a requirement for more effective and more specific therapeutic agents.

T cells are involved in a large range of chronic diseases. AQ and S1P are able to inhibit T cell transmigration through the paradigm shared with PEPITEM, however the therapeutic use of these molecules in the inhibition of T cell trafficking is unsuitable, with the exception of the S1P analogue fingolimod, which was approved by the FDA in 2010 for the treatment of multiple sclerosis (MS), (FDA, 2010). Both adiponectin and S1P have pleotropic effects on metabolism and T cell migration respectfully, and are therefore likely to lead to undesirable off-target effects. On the other hand, PEPITEM represents a different therapeutic strategy for the treatment of T cell mediated disease, owing to its specificity to T cells and potency at low concentrations (Chimen *et al.*, 2015). Additionally, as a peptide, it would be more cost effective than current antibody therapies. So far, no toxicity has been associated with PEPITEM in short-term animal studies conducted both here and by Chimen *et al.* (2015), however its long term toxicity is unknown and must be validated.

Unfortunately, like many therapeutics, the use of PEPITEM as a therapeutic agent has limitations highlighted by research presented in this thesis. Perhaps the biggest hurdle for the development of PEPITEM as a therapeutic agent is its rapid renal clearance from the circulation. An effective therapeutic agent requires a long *in vivo* half-life to maximise exposure to its target, and exert intended effects. Many successful therapeutic agents have undergone modification to become appropriate medications, including the erythropoiesis-stimulating drug Hematide, and the

glucagon-like peptide 1 (GLP-1) analogue CJC-1131 (Giannoukakis, 2003, Stead *et al.*, 2006).

When designing a drug, it is important to consider the intended method of delivery. Oral therapy is the most desirable method as it allows non-invasive dosage, which can be managed by the patient. Absorption by the gut and entrance into the blood stream must be considered when modifying PEPITEM to ensure it is efficiency. For certain T cell-mediated skin conditions such as psoriasis, topical treatment with PEPITEM is an option and may require minimal modification for success, facing no opposition from rapid renal clearance. Indeed we must now further modify PEPITEM to suit its requirements *in vivo*, and screen modified peptides *in vitro* using a suitable high-throughput assay. Optimal doses of these modified peptides must then be established using *in vivo* models of chronic inflammation.

The 14-3-3 family of proteins have only briefly been associated with lymphocyte trafficking to date. In the current literature, a role for 14-3-3σ in the regulation of integrin activation in fibroblasts and lymphocytes has been described (Nurmi *et al.*, 2006). Indeed it is intriguing since neither 14-3-3ζ protein nor PEPITEM have been associated with lymphocyte trans-endothelial migration in the literature, and certainly have not been linked to S1P production by endothelial cells.

The evidence presented in this thesis provides new insights into the novel immunological role of extracellular 14-3-3ζ protein. These data suggest that 14-3-3ζ is released from B cells, and PEPITEM is subsequently excised from the parent protein extracellularly by MMP-9. It is likely that PEPITEM undergoes further proteolytic cleavage into smaller bioactive peptides, however this step requires initial

excision of PEPITEM from 14-3-3ζ. Numerous studies have reported the involvement of MMPs in T cell migration both *in vitro* and *in vivo*, however MMP-9-mediated degradation of 14-3-3ζ into a functional immunological peptide is a novel observation.

Fascinatingly, in other 14-3-3 family members, the respective PEPITEM sequence differs only by a few amino acids. *In silico* analysis revealed conserved predicted MMP-9 cleavage sites present in all 7 14-3-3 family members, at the same residues flaking the PEPITEM-like motifs, all of which were 17 amino acids in length. This remarkable similarity suggests that the other PEPITEM-like sequences, once excised, may also have biological activity. It is possible that proteolytic cleavage of the 14-3-3 family members represents an evolutionary trait for the systematic release of functional peptides key to other regulatory paradigms, perhaps associated with their diverse range of functions.

3D constructions of the 14-3-3ζ protein structure demonstrate PEPTEM residues exposed on the protein surface. Presumably, this facilitates cleavage of these residues from 14-3-3ζ. The NMR data presented in this thesis suggested potential hinge regions at either end of PEPITEM, roughly corresponding to the helices which flank the sequence. This flexibility may indeed allow interaction with proteases, and it would be interesting to see if this feature is also present at corresponding residues in the other 14-3-3 isoforms.

It is now clear that 14-3-3ζ signifies yet another level of homeostatic regulation of T cell trafficking in the PEPITEM paradigm, necessary for the prevention of chronic inflammatory disease. The cellular source of proteases and the underlying mechanisms controlling their function must now be investigated.

Chimen *et al.* (2015) studied the effects of PEPITEM on T cell migration and showed that PEPITEM inhibits CD4+ and CD8+ T cells, but not neutrophils or monocytes. Within PBL, B cells were shown to secrete this agent, however other potential sources of PEPITEM were not explored. The research presented in chapter 6 demonstrated the ability of several cell types including epithelial cells (HeLa) and endothelial cells (HDBEC) to express the parent protein 14-3-3ζ. This raises the question of which other cell types may also be able to produce PEPITEM and thus regulate the immune response, and requires more attention.

In summary, this research provides us with additional knowledge about T cell trafficking and the current model of the PEPITEM paradigm, which is illustrated in Figure 7.1. However, many questions remain to be addressed, listed in section 7.2.

Understanding the molecular mechanisms underlying this regulatory process and identifying crucial motifs within the PEPITEM sequence will facilitate the design of modified peptides for therapeutic use. Additionally, although much more complicated than originally comprehended, complete elucidation of the PEPITEM paradigm will prove invaluable to the field of T cell immunology, as it represents a significant homeostatic mechanism crucial for the prevention of disease and appears central to the regulation of T cell trafficking into inflamed tissues.

Our observations to date add to our current understanding of PEPITEM, and with subsequent investigation, the prospect of exploiting PEPITEM for the treatment of T cell-mediated chronic disease looks hopeful.

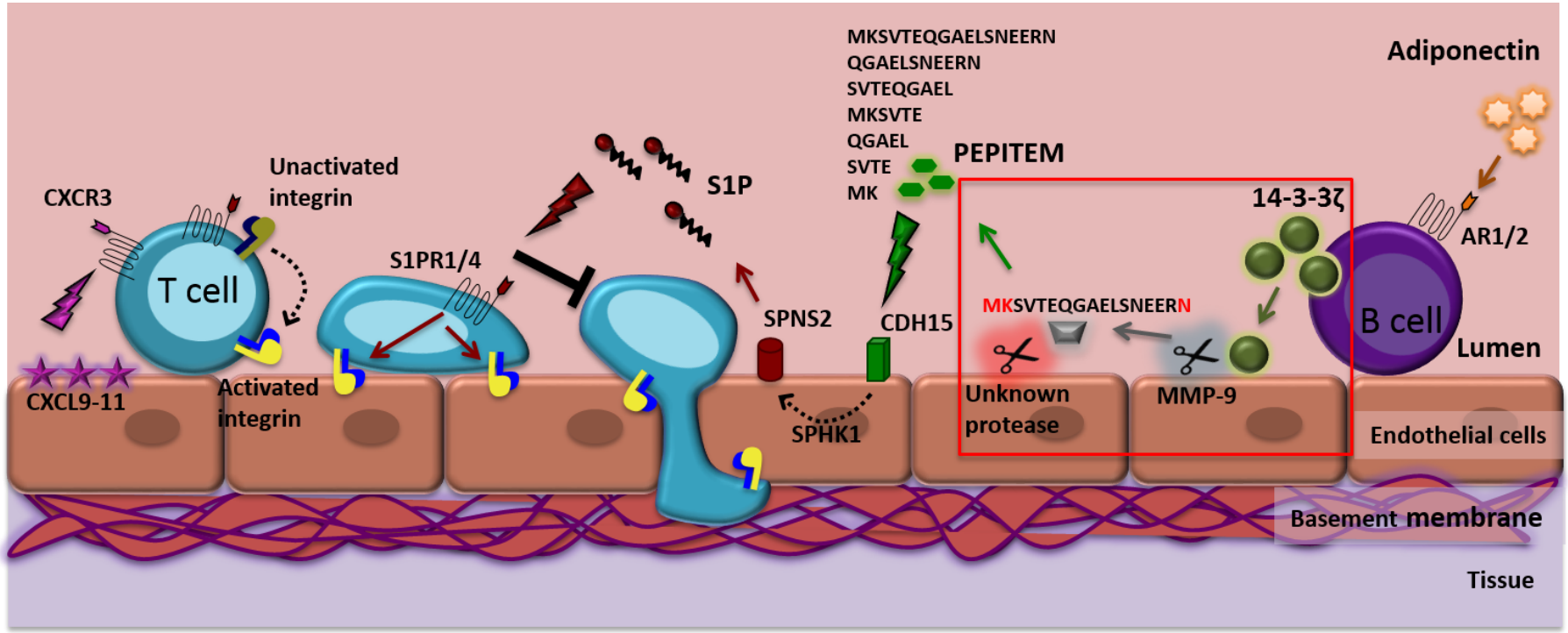

Figure 7.1. PEPITEM: An Updated Paradigm.
T cells are recruited by inflamed endothelial cells and arrest on the endothelium, preparing to transmigrate. Adiponectin binds to the surface of the B cells via adiponectin receptors (AR1/2), triggering intracellular signalling via an unknown pathway, and leading to the control of downstream PEPITEM production, possibly through regulation of B cell proteases. B cells constitutively release 14-3-3ζ via exosomes, which is subsequently cleaved by MMP-9 into a 17 amino acid peptide. An unknown protease further processes PEPITEM into smaller pharmacophore. These PEPITEM derivatives interact with endothelial cell cadherin 15 (CDH15), potentially in a complex with other proteins, inducing endothelial cell synthesis and release of sphingosine 1 phosphate (S1P) by sphingosine kinase-1 (SPHK1), transported By spinster homolog 2 (SPNS2). S1P binds to its receptors on the T cell surface (S1P1/4), inhibiting transmigration.

7.2 Future investigations:

Whist significant findings have been made in this thesis regarding the PEPITEM paradigm, much remains to be understood about this fascinating and unique pathway. Here, I summarise questions highlighted by this thesis requiring further investigation for a comprehensive understanding of the biology of PEPITEM, and to facilitate therapeutic development.

- **Investigations into PEPITEM function**

Is PEPITEM a 17 amino acid peptide, and does it undergo further processing?

A 17-amino acid sequence is now suspected to represent PEPITEM and must be synthesised and tested in the *in vitro* migration assay for function. We can further investigate its function through the use of inhibitors for glutamyl peptidase I, which we suspect is responsible for further cleavage into smaller pharmacophore. We must also synthesis these shorter peptide sequences and assess them for the ability to inhibit PBL transmigration *in vitro.*

How does PEPITEM interact with CDH15 on the endothelial cell surface?

We must study the interactions occurring at the endothelial cell surface, and how CDH15 is functioning as the PEPITEM receptor. The use of CDH15, 14-3-3ζ, MMP-9 and TSP-1 as “bait” to “fish” for interacting proteins may allow us to determine whether a complex of proteins assemble at the endothelial cell surface. Microarray data may elucidate how the endothelial transcriptome is affected by PEPITEM binding, as this is currently unknown.

How can we screen for PEPITEM function rapidly?

The *in vitro* migration assay has been central to this thesis but consists of many time-consuming elements unsuitable for high-throughput screening of PEPITEM function. It is important to develop a high-throughput assay as the measurement of calcium flux via a plate reader-based assay was not feasible. We must investigate the possibility of utilizing more sensitive calcium dyes or confocal microscopy to measure intracellular calcium flux. Alternatively, we can investigate the use commercially available kits for measuring sphingosine kinase 1 activity in endothelial cells.

Are other cell types capable of PEPITEM production?

While Chimen *et al.* (2015) demonstrated the ability of B cells to inhibit T cell transmigration via the production of PEPITEM, the potential for other cell types to produce PEPITEM has not been excluded. We must now determine which other cell types which express 14-3-3ζ can also produce PEPITEM, and what may be regulating its production.

- **Assessing the role of 14-3-3ζ in the PEPITEM paradigm**

Is 14-3-3ζ secreted specifically by B cells?

Preliminary results suggest that 14-3-3ζ is expressed in, and in fact secreted by B cells *in vitro*. However, these experiments must be repeated to ascertain validity. The presence or absence of 14-3-3ζ in the supernatants of EC or isolated T cells must also be confirmed. Since 14-3-3ζ dimerization can facilitate interaction with ligands, B cell-secreted 14-3-3ζ must be assessed for the presence of dimers using native western blotting. To confirm the *in vivo* relevance of 14-3-3ζ function in the context of

the PEPITEM paradigm, the generation of a B cell-specific 14-3-3ζ knock out mouse could be employed in *in vivo* mouse models of inflammatory diseases.

What mechanisms lead to14-3-3ζ export in B cells?

Our data suggested that 14-3-3ζ is released extracellularly by B cells, and this may be occurring via B cell exosomes. This mode of active export of 14-3-3ζ requires characterising, and the exosomes from B cells isolated from heathy donors must be assessed for the presence of 14-3-3ζ *ex-vivo*. Confirmation of the involvement of B cell exosomes in the release of extracellular 14-3-3ζ can be confirmed using commercially available exosome-specific inhibitors.

What is the role of other 14-3-3 family members in immunity?

The 14-3-3 family of proteins exhibited conserved protease recognition sites within the same residues corresponding to the location of PEPITEM. It is likely that the other peptide products resulting from cleavage at these sites have biological activity. We must examine whether these peptides are involved, like PEPITEM, in the inflammatory response, or whether they represent parts of other regulatory pathways.

- **Characterising the proteases involved in 14-3-3ζ processing**

Which protease(s) are involved in 14-3-3ζ processing?

To identify the involvement of specific proteases in the production of PEPITEM and derived peptides, the gene expression of proteases including MMP-9 and glutamyl peptidase I must be assessed in isolated T and B cell preparations, and in EC. Supernatants from these isolated cell types must be examined for protein expression of extracellular MMP-9 and glutamyl peptidase I by western blotting. Furthermore, the

role of AQ in the control of PEPITEM production must be explored, since AQ was previously shown to lead to the release of PEPITEM in B cell supernatants.

What is the source of proteases and how are they regulated?

While we have elucidated a role for proteases in the production of PEPITEM, we have not yet ascertained the cell type(s) responsible for them. The use of specific MMP-9 and glutamyl peptidase I inhibitors in the migration assay will establish protease involvement. By incubating either PBL or T cells with specific protease inhibitors, we will be able to narrow down the source of these proteases. Once the protease(s) and source(s) are defined, subsequent investigations into their regulation should be conducted. The use of MMP-$9^{-/-}$ mice, which are commercially available, will facilitate investigations into the importance of these protease(s) in the PEPITEM paradigm *in vivo*.

- **Development of PEPITEM as therapeutic agent**

How can we increase PEPITEM half-life?

It is essential that the half-life of PEPITEM is increased for successful use in the treatment of T cell-mediated chronic diseases. Pharmacological modifications, including the addition of higher molecular weight PEG and conjugation to albumin, must be synthesised and screened for functionality using the *in vitro* migration assay. Subsequent investigations must follow to assess *in vivo* half-life and pharmacokinetics. After the identification of suitable peptide modifications, *in vivo* models of chronic inflammatory disease must be employed to validate the effectiveness of PEPITEM as a therapeutic agent.

Chapter 8 - REFERENCES

Abraham, M., Shapiro, S., Karni, A., Weiner, H. L. & Miller, A. 2005. Gelatinases (MMP-2 and MMP-9) are preferentially expressed by Th1 vs. Th2 cells. *J Neuroimmunol,* 163**,** 157-64.

Ahmed, S. R., Mcgettrick, H. M., Yates, C. M., Buckley, C. D., Ratcliffe, M. J., Nash, G. B. & Rainger, G. E. 2011. Prostaglandin D2 regulates CD4+ memory T cell trafficking across blood vascular endothelium and primes these cells for clearance across lymphatic endothelium. *J Immunol,* 187**,** 1432-9.

Aird, W. C. 2005. Spatial and temporal dynamics of the endothelium. *J Thromb Haemost,* 3**,** 1392-406.

Ait-Oufella, H., Taleb, S., Mallat, Z. & Tedgui, A. 2009. Cytokine network and T cell immunity in atherosclerosis. *Semin Immunopathol,* 31**,** 23-33.

Alon, R., Hammer, D. A. & Springer, T. A. 1995. Lifetime of the P-selectin-carbohydrate bond and its response to tensile force in hydrodynamic flow. *Nature,* 374**,** 539-542.

An Haack, K., Narayan, S. B., Li, H., Warnock, A., Tan, L. & Bennett, M. J. 2011. Screening for calcium channel modulators in CLN3 siRNA knock down SH-SY5Y neuroblastoma cells reveals a significant decrease of intracellular calcium levels by selected L-type calcium channel blockers. *Biochim Biophys Acta,* 1810**,** 186-91.

Arita, Y., Kihara, S., Ouchi, N., Takahashi, M., Maeda, K., Miyagawa, J., Hotta, K., Shimomura, I., Nakamura, T., Miyaoka, K., Kuriyama, H., Nishida, M., Yamashita, S., Okubo, K., Matsubara, K., Muraguchi, M., Ohmoto, Y., Funahashi, T. & Matsuzawa, Y. 1999. Paradoxical decrease of an adipose-specific protein, adiponectin, in obesity. *Biochem Biophys Res Commun,* 257**,** 79-83.

Asdaghi, N., Kilani, R. T., Hosseini-Tabatabaei, A., Odemuyiwa, S. O., Hackett, T. L., Knight, D. A., Ghahary, A. & Moqbel, R. 2012. Extracellular 14-3-3 from human lung epithelial cells enhances MMP-1 expression. *Mol Cell Biochem,* 360**,** 261-70.

Bahra, P., Rainger, G. E., Wautier, J. L., Nguyet-Thin, L. & Nash, G. B. 1998. Each step during transendothelial migration of flowing neutrophils is regulated by the stimulatory concentration of tumour necrosis factor-alpha. *Cell Adhes Commun,* 6**,** 491-501.

Barrett, A. J. & Mcdonald, J. K. 1986. Nomenclature: protease, proteinase and peptidase. *Biochemical Journal,* 237**,** 935.

Berg, D., Holzmann, C. & Riess, O. 2003. 14-3-3 proteins in the nervous system. *Nat Rev Neurosci,* 4**,** 752-62.

Bevilacqua, M. P., Stengelin, S., Gimbrone, M. A., Jr. & Seed, B. 1989. Endothelial leukocyte adhesion molecule 1: an inducible receptor for neutrophils related to complement regulatory proteins and lectins. *Science,* 243**,** 1160-5.

Bortnick, A. & Allman, D. 2013. What is and what should always have been: long-lived plasma cells induced by T cell-independent antigens. *J Immunol,* 190**,** 5913-8.

Brezinschek, R. I., Lipsky, P. E., Galea, P., Vita, R. & Oppenheimer-Marks, N. 1995. Phenotypic characterization of CD4+ T cells that exhibit a transendothelial migratory capacity. *J Immunol,* 154**,** 3062-77.

Bridges, D. & Moorhead, G. B. 2005. 14-3-3 proteins: a number of functions for a numbered protein. *Sci STKE,* 2005**,** re10.

Broere, F., Apasov, S., Sitkovsky, M. & Van Eden, W. 2011. A2 T cell subsets and T cell-mediated immunity. *In:* NIJKAMP, F. P. & PARNHAM, M. J. (eds.) *Principles of Immunopharmacology.* Birkhäuser Basel.

Broux, B., Mizee, M. R., Vanheusden, M., Van Der Pol, S., Van Horssen, J., Van Wijmeersch, B., Somers, V., De Vries, H. E., Stinissen, P. & Hellings, N. 2015. IL-15 amplifies the pathogenic properties of CD4+CD28- T cells in multiple sclerosis. *J Immunol,* 194**,** 2099-109.

Browning, J. L. 2006. B cells move to centre stage: novel opportunities for autoimmune disease treatment. *Nat Rev Drug Discov,* 5**,** 564-76.

Brundula, V., Rewcastle, N. B., Metz, L. M., Bernard, C. C. & Yong, V. W. 2002. Targeting leukocyte MMPs and transmigration: minocycline as a potential therapy for multiple sclerosis. *Brain,* 125**,** 1297-308.

Brunger, A. T. 2007. Version 1.2 of the Crystallography and NMR system. *Nat. Protocols,* 2**,** 2728-2733.

Brunner, D., Frank, J., Appl, H., Schoffl, H., Pfaller, W. & Gstraunthaler, G. 2010. Serum-free cell culture: the serum-free media interactive online database. *Altex,* 27**,** 53-62.

Buschow, S. I., Van Balkom, B. W., Aalberts, M., Heck, A. J., Wauben, M. & Stoorvogel, W. 2010. MHC class II-associated proteins in B-cell exosomes and potential functional implications for exosome biogenesis. *Immunol Cell Biol,* 88**,** 851-6.

Cao, Y., Tao, L., Yuan, Y., Jiao, X., Lau, W. B., Wang, Y., Christopher, T., Lopez, B., Chan, L., Goldstein, B. & Ma, X. L. 2009. Endothelial dysfunction in adiponectin deficiency and its mechanisms involved. *J Mol Cell Cardiol,* 46**,** 413-9.

Celis, J. E., Gesser, B., Rasmussen, H. H., Madsen, P., Leffers, H., Dejgaard, K., Honore, B., Olsen, E., Ratz, G., Lauridsen, J. B. & Et Al. 1990. Comprehensive two-dimensional gel protein databases offer a global approach to the analysis of human cells: the transformed amnion cells (AMA) master database and its link to genome DNA sequence data. *Electrophoresis,* 11**,** 989-1071.

Chatenoud, L., Thervet, E., Primo, J. & Bach, J. F. 1994. Anti-CD3 antibody induces long-term remission of overt autoimmunity in nonobese diabetic mice. *Proc Natl Acad Sci U S A,* 91**,** 123-7.

Chen, R. F. 1967. Removal of Fatty Acids from Serum Albumin by Charcoal Treatment. *Journal of Biological Chemistry,* 242**,** 173-181.

Chimen, M., Mcgettrick, H. M., Apta, B., Kuravi, S. J., Yates, C. M., Kennedy, A., Odedra, A., Alassiri, M., Harrison, M., Martin, A., Barone, F., Nayar, S., Hitchcock, J. R., Cunningham, A. F., Raza, K., Filer, A., Copland, D. A., Dick, A. D., Robinson, J., Kalia, N., Walker, L. S. K., Buckley, C. D., Nash, G. B., Narendran, P. & Rainger, G. E. 2015. Homeostatic regulation of T cell trafficking by a B cell-derived peptide is impaired in autoimmune and chronic inflammatory disease. *Nat Med,* 21**,** 467-475.

Cole, K. E., Strick, C. A., Paradis, T. J., Ogborne, K. T., Loetscher, M., Gladue, R. P., Lin, W., Boyd, J. G., Moser, B., Wood, D. E., Sahagan, B. G. & Neote, K. 1998. Interferon–inducible T Cell Alpha Chemoattractant (I-TAC): A Novel Non-ELR CXC Chemokine with Potent Activity on Activated T Cells through Selective High Affinity Binding to CXCR3. *The Journal of Experimental Medicine,* 187**,** 2009-2021.

Craik, D. J., Fairlie, D. P., Liras, S. & Price, D. 2013. The future of peptide-based drugs. *Chem Biol Drug Des,* 81**,** 136-47.
Crotty, S., Felgner, P., Davies, H., Glidewell, J., Villarreal, L. & Ahmed, R. 2003. Cutting edge: long-term B cell memory in humans after smallpox vaccination. *J Immunol,* 171**,** 4969-73.
Cyster, J. G. 2005. Chemokines, sphingosine-1-phosphate, and cell migration in secondary lymphoid organs. *Annu Rev Immunol,* 23**,** 127-59.
Daneman, D. 2006. Type 1 diabetes. *The Lancet,* 367**,** 847-858.
Dansky, H. M., Charlton, S. A., Harper, M. M. & Smith, J. D. 1997. T and B lymphocytes play a minor role in atherosclerotic plaque formation in the apolipoprotein E-deficient mouse. *Proceedings of the National Academy of Sciences of the United States of America,* 94**,** 4642-4646.
De Sousa, M. a. B., Parrott, D. M. V. & Pantelouris, E. M. 1969. The lymphoid tissues in mice with congenital aplasia of the thymus. *Clin Exp Immunol,* 4**,** 637-44.
Delaglio, F., Grzesiek, S., Vuister, G. W., Zhu, G., Pfeifer, J. & Bax, A. 1995. NMRPipe: a multidimensional spectral processing system based on UNIX pipes. *J Biomol NMR,* 6**,** 277-93.
Delgado, M. B., Clark-Lewis, I., Loetscher, P., Langen, H., Thelen, M., Baggiolini, M. & Wolf, M. 2001. Rapid inactivation of stromal cell-derived factor-1 by cathepsin G associated with lymphocytes. *Eur J Immunol,* 31**,** 699-707.
Di Bartolo, V., Montagne, B., Salek, M., Jungwirth, B., Carrette, F., Fourtane, J., Sol-Foulon, N., Michel, F., Schwartz, O., Lehmann, W. D. & Acuto, O. 2007. A novel pathway down-modulating T cell activation involves HPK-1-dependent recruitment of 14-3-3 proteins on SLP-76. *J Exp Med,* 204**,** 681-91.
Di Girolamo, N., Tedla, N., Lloyd, A. & Wakefield, D. 1998. Expression of matrix metalloproteinases by human plasma cells and B lymphocytes. *Eur J Immunol,* 28**,** 1773-84.
Dougherty, M. K. & Morrison, D. K. 2004. Unlocking the code of 14-3-3. *J Cell Sci,* 117**,** 1875-84.
Duncan, R. 2003. The dawning era of polymer therapeutics. *Nat Rev Drug Discov,* 2**,** 347-60.
Eidhammer, I., Barsnes, H., Eide, G. E. & Martens, L. 2012. *Computational and Statistical Methods for Protein Quantification by Mass Spectrometry,* New Jersey, John Wiley & Sons.
Engel, P., Gomez-Puerta, J. A., Ramos-Casals, M., Lozano, F. & Bosch, X. 2011. Therapeutic targeting of B cells for rheumatic autoimmune diseases. *Pharmacol Rev,* 63**,** 127-56.
Fagarasan, S. & Honjo, T. 2000. T-Independent immune response: new aspects of B cell biology. *Science,* 290**,** 89-92.
Falk, E. 2006. Pathogenesis of atherosclerosis. *J Am Coll Cardiol,* 47**,** C7-12.
Faveeuw, C., Preece, G. & Ager, A. 2001. Transendothelial migration of lymphocytes across high endothelial venules into lymph nodes is affected by metalloproteinases. *Blood,* 98**,** 688-95.
Fda. 2010. *FDA approves first oral drug to reduce MS relapses* [Online]. Available: http://www.fda.gov/NewsEvents/Newsroom/PressAnnouncements/ucm226755.htm.
Ferguson, A. T., Evron, E., Umbricht, C. B., Pandita, T. K., Chan, T. A., Hermeking, H., Marks, J. R., Lambers, A. R., Futreal, P. A., Stampfer, M. R. & Sukumar, S. 2000. High frequency of hypermethylation at the 14-3-3 sigma locus leads to gene silencing in breast cancer. *Proc Natl Acad Sci U S A,* 97**,** 6049-54.

Filippi, C. M. & Von Herrath, M. G. 2008. Viral trigger for type 1 diabetes: pros and cons. *Diabetes,* 57**,** 2863-71.
Flanagan, S. P. 1966. 'Nude', a new hairless gene with pleiotropic effects in the mouse. *Genet Res,* 8**,** 295-309.
Fox, M. E., Szoka, F. C. & Frechet, J. M. 2009. Soluble polymer carriers for the treatment of cancer: the importance of molecular architecture. *Acc Chem Res,* 42**,** 1141-51.
Frucht, D. M., Fukao, T., Bogdan, C., Schindler, H., O'shea, J. J. & Koyasu, S. 2001. IFN-gamma production by antigen-presenting cells: mechanisms emerge. *Trends Immunol,* 22**,** 556-60.
Fu, H., Subramanian, R. R. & Masters, S. C. 2000. 14-3-3 proteins: structure, function, and regulation. *Annu Rev Pharmacol Toxicol,* 40**,** 617-47.
Fukuhara, S., Simmons, S., Kawamura, S., Inoue, A., Orba, Y., Tokudome, T., Sunden, Y., Arai, Y., Moriwaki, K., Ishida, J., Uemura, A., Kiyonari, H., Abe, T., Fukamizu, A., Hirashima, M., Sawa, H., Aoki, J., Ishii, M. & Mochizuki, N. 2012. The sphingosine-1-phosphate transporter Spns2 expressed on endothelial cells regulates lymphocyte trafficking in mice. *J Clin Invest,* 122**,** 1416-26.
Garcia-Guzman, M., Dolfi, F., Russello, M. & Vuori, K. 1999. Cell adhesion regulates the interaction between the docking protein p130(Cas) and the 14-3-3 proteins. *J Biol Chem,* 274**,** 5762-8.
Garris, C. S., Blaho, V. A., Hla, T. & Han, M. H. 2014. Sphingosine-1-phosphate receptor 1 signalling in T cells: trafficking and beyond. *Immunology,* 142**,** 347-353.
Ghahary, A., Karimi-Busheri, F., Marcoux, Y., Li, Y., Tredget, E. E., Taghi Kilani, R., Li, L., Zheng, J., Karami, A., Keller, B. O. & Weinfeld, M. 2004. Keratinocyte-Releasable Stratifin Functions as a Potent Collagenase-Stimulating Factor in Fibroblasts. *J Investig Dermatol,* 122**,** 1188-1197.
Giannoukakis, N. 2003. CJC-1131. ConjuChem. *Curr Opin Investig Drugs,* 4**,** 1245-9.
Good, K. L., Avery, D. T. & Tangye, S. G. 2009. Resting human memory B cells are intrinsically programmed for enhanced survival and responsiveness to diverse stimuli compared to naive B cells. *J Immunol,* 182**,** 890-901.
Gregori, S., Giarratana, N., Smiroldo, S. & Adorini, L. 2003. Dynamics of pathogenic and suppressor T cells in autoimmune diabetes development. *J Immunol,* 171**,** 4040-7.
Grisolano, J. L., Sclar, G. M. & Ley, T. J. 1994. Early myeloid cell-specific expression of the human cathepsin G gene in transgenic mice. *Proceedings of the National Academy of Sciences,* 91**,** 8989-8993.
Gürcan, H. M., Keskin, D. B., Stern, J. N. H., Nitzberg, M. A., Shekhani, H. & Ahmed, A. R. 2009. A review of the current use of rituximab in autoimmune diseases. *International Immunopharmacology,* 9**,** 10-25.
Han, D. C., Rodriguez, L. G. & Guan, J. L. 2001. Identification of a novel interaction between integrin beta1 and 14-3-3beta. *Oncogene,* 20**,** 346-57.
Hanemaaijer, R., Koolwijk, P., Le Clercq, L., De Vree, W. J. & Van Hinsbergh, V. W. 1993. Regulation of matrix metalloproteinase expression in human vein and microvascular endothelial cells. Effects of tumour necrosis factor alpha, interleukin 1 and phorbol ester. *Biochem J,* 296 (Pt 3)**,** 803-9.
Hansson, G. K., Libby, P., Schönbeck, U. & Yan, Z.-Q. 2002. Innate and Adaptive Immunity in the Pathogenesis of Atherosclerosis. *Circulation Research,* 91**,** 281-291.

Haugen, F. & Drevon, C. A. 2007. Activation of nuclear factor-kappaB by high molecular weight and globular adiponectin. *Endocrinology,* 148**,** 5478-86.
Herold, K. C., Hagopian, W., Auger, J. A., Poumian-Ruiz, E., Taylor, L., Donaldson, D., Gitelman, S. E., Harlan, D. M., Xu, D., Zivin, R. A. & Bluestone, J. A. 2002. Anti-CD3 monoclonal antibody in new-onset type 1 diabetes mellitus. *N Engl J Med,* 346**,** 1692-8.
Hla, T., Lee, M. J., Ancellin, N., Paik, J. H. & Kluk, M. J. 2001. Lysophospholipids--receptor revelations. *Science,* 294**,** 1875-8.
Hogg, N., Patzak, I. & Willenbrock, F. 2011. The insider's guide to leukocyte integrin signalling and function. *Nat Rev Immunol,* 11**,** 416-426.
Hori, S., Nomura, T. & Sakaguchi, S. 2003. Control of regulatory T cell development by the transcription factor Foxp3. *Science,* 299**,** 1057-61.
Imagawa, A., Hanafusa, T., Itoh, N., Waguri, M., Yamamoto, K., Miyagawa, J., Moriwaki, M., Yamagata, K., Iwahashi, H., Sada, M., Tsuji, T., Tamura, S., Kawata, S., Kuwajima, M., Nakajima, H., Namba, M. & Matsuzawa, Y. 1999. Immunological abnormalities in islets at diagnosis paralleled further deterioration of glycaemic control in patients with recent-onset Type I (insulin-dependent) diabetes mellitus. *Diabetologia,* 42**,** 574-8.
Inoue, Y., Izawa, K., Kiryu, S., Tojo, A. & Ohtomo, K. 2008. Diet and abdominal autofluorescence detected by in vivo fluorescence imaging of living mice. *Mol Imaging,* 7**,** 21-7.
Itagaki, K., Yun, J. K., Hengst, J. A., Yatani, A., Hauser, C. J., Spolarics, Z. & Deitch, E. A. 2007. Sphingosine 1-phosphate has dual functions in the regulation of endothelial cell permeability and Ca2+ metabolism. *J Pharmacol Exp Ther,* 323**,** 186-91.
Itoh, N., Hanafusa, T., Miyazaki, A., Miyagawa, J., Yamagata, K., Yamamoto, K., Waguri, M., Imagawa, A., Tamura, S., Inada, M. & Et Al. 1993. Mononuclear cell infiltration and its relation to the expression of major histocompatibility complex antigens and adhesion molecules in pancreas biopsy specimens from newly diagnosed insulin-dependent diabetes mellitus patients. *J Clin Invest,* 92**,** 2313-22.
Jacobsen, N. E. 2007. *NMR Spectroscopy Explained: Simplified Theory, Applications and Examples for Organic Chemistry and Structural Biology,* New Jersey, Wiley.
Jamin, C., Morva, A., Lemoine, S., Daridon, C., De Mendoza, A. R. & Youinou, P. 2008. Regulatory B lymphocytes in humans: A potential role in autoimmunity. *Arthritis & Rheumatism,* 58**,** 1900-1906.
Jensen, P. E. 2007. Recent advances in antigen processing and presentation. *Nat Immunol,* 8**,** 1041-8.
Johnston, B., Issekutz, T. B. & Kubes, P. 1996. The alpha 4-integrin supports leukocyte rolling and adhesion in chronically inflamed postcapillary venules in vivo. *J Exp Med,* 183**,** 1995-2006.
Juvenile Diabetes Research Foundation. 2010. *Type 1 Diabetes Facts* [Online]. Available: http://www.jdrft1.org.uk/page.asp?section=255&sectionTitle=Type+1+Diabetes+Facts.
Kadowaki, T. & Yamauchi, T. 2005. Adiponectin and adiponectin receptors. *Endocr Rev,* 26**,** 439-51.

Kadowaki, T., Yamauchi, T., Kubota, N., Hara, K., Ueki, K. & Tobe, K. 2006. Adiponectin and adiponectin receptors in insulin resistance, diabetes, and the metabolic syndrome. *J Clin Invest,* 116**,** 1784-92.

Kaech, S. M., Wherry, E. J. & Ahmed, R. 2002. Effector and memory T-cell differentiation: implications for vaccine development. *Nat Rev Immunol,* 2**,** 251-262.

Kase, H., Hattori, Y., Jojima, T., Okayasu, T., Tomizawa, A., Suzuki, K., Banba, N., Monden, T., Satoh, H., Akimoto, K. & Kasai, K. 2007. Globular adiponectin induces adhesion molecule expression through the sphingosine kinase pathway in vascular endothelial cells. *Life Sci,* 81**,** 939-43.

Kastin, A. 2013. *Handbook of Biologically Active Peptides*, Elsevier Science.

Keeler, J. 2013. *Understanding NMR Spectroscopy*, Wiley.

Keymeulen, B., Vandemeulebroucke, E., Ziegler, A. G., Mathieu, C., Kaufman, L., Hale, G., Gorus, F., Goldman, M., Walter, M., Candon, S., Schandene, L., Crenier, L., De Block, C., Seigneurin, J. M., De Pauw, P., Pierard, D., Weets, I., Rebello, P., Bird, P., Berrie, E., Frewin, M., Waldmann, H., Bach, J. F., Pipeleers, D. & Chatenoud, L. 2005. Insulin needs after CD3-antibody therapy in new-onset type 1 diabetes. *N Engl J Med,* 352**,** 2598-608.

Kitani, A., Nakashima, N., Izumihara, T., Inagaki, M., Baoui, X., Yu, S., Matsuda, T. & Matsuyama, T. 1998. Soluble VCAM-1 induces chemotaxis of Jurkat and synovial fluid T cells bearing high affinity very late antigen-4. *J Immunol,* 161**,** 4931-8.

Kobayashi, R., Deavers, M., Patenia, R., Rice-Stitt, T., Halbe, J., Gallardo, S. & Freedman, R. S. 2009. 14-3-3 zeta protein secreted by tumor associated monocytes/macrophages from ascites of epithelial ovarian cancer patients. *Cancer Immunol Immunother,* 58**,** 247-58.

Kohem, C. L., Brezinschek, R. I., Wisbey, H., Tortorella, C., Lipsky, P. E. & Oppenheimer-Marks, N. 1996. Enrichment of differentiated CD45RBdim,CD27- memory T cells in the peripheral blood, synovial fluid, and synovial tissue of patients with rheumatoid arthritis. *Arthritis Rheum,* 39**,** 844-54.

Komatsu, N. & Takayanagi, H. 2012. Inflammation and bone destruction in arthritis: synergistic activity of immune and mesenchymal cells in joints. *Front Immunol,* 3**,** 77.

Koshikawa, N., Nagashima, Y., Miyagi, Y., Mizushima, H., Yanoma, S., Yasumitsu, H. & Miyazaki, K. 1997. Expression of trypsin in vascular endothelial cells. *FEBS Letters,* 409**,** 442-448.

Kubo, M. & Motomura, Y. 2012. Transcriptional regulation of the anti-inflammatory cytokine IL-10 in acquired immune cells. *Front Immunol,* 3**,** 275.

Landon, L. A., Zou, J. & Deutscher, S. L. 2004. Is phage display technology on target for developing peptide-based cancer drugs? *Curr Drug Discov Technol,* 1**,** 113-32.

Lawson, J. M., Tremble, J., Dayan, C., Beyan, H., Leslie, R. D., Peakman, M. & Tree, T. I. 2008. Increased resistance to CD4+CD25hi regulatory T cell-mediated suppression in patients with type 1 diabetes. *Clin Exp Immunol,* 154**,** 353-9.

Layfield, R., Fergusson, J., Aitken, A., Lowe, J., Landon, M. & Mayer, R. J. 1996. Neurofibrillary tangles of Alzheimer's disease brains contain 14-3-3 proteins. *Neurosci Lett,* 209**,** 57-60.

Lebien, T. W. 2000. Fates of human B-cell precursors. *Blood,* 96**,** 9-23.

Ledgerwood, L. G., Lal, G., Zhang, N., Garin, A., Esses, S. J., Ginhoux, F., Merad, M., Peche, H., Lira, S. A., Ding, Y., Yang, Y., He, X., Schuchman, E. H., Allende, M. L., Ochando, J. C. & Bromberg, J. S. 2008. The sphingosine 1-phosphate receptor 1 causes tissue retention by inhibiting the entry of peripheral tissue T lymphocytes into afferent lymphatics. *Nat Immunol,* 9**,** 42-53.

Leger, R., Thibaudeau, K., Robitaille, M., Quraishi, O., Van Wyk, P., Bousquet-Gagnon, N., Carette, J., Castaigne, J. P. & Bridon, D. P. 2004. Identification of CJC-1131-albumin bioconjugate as a stable and bioactive GLP-1(7-36) analog. *Bioorg Med Chem Lett,* 14**,** 4395-8.

Ley, K. 2003. The role of selectins in inflammation and disease. *Trends in Molecular Medicine,* 9**,** 263-268.

Ley, K. & Kansas, G. S. 2004. Selectins in T-cell recruitment to non-lymphoid tissues and sites of inflammation. *Nat Rev Immunol,* 4**,** 325-35.

Ley, K., Laudanna, C., Cybulsky, M. I. & Nourshargh, S. 2007. Getting to the site of inflammation: the leukocyte adhesion cascade updated. *Nat Rev Immunol,* 7**,** 678-689.

Li, X., Zhang, X., Li, F., Chen, L., Li, L., Qin, X., Gao, J., Su, T., Zeng, Y. & Liao, D. 2010. 14-3-3 mediates apelin-13-induced enhancement of adhesion of monocytes to human umbilical vein endothelial cells. *Acta Biochim Biophys Sin (Shanghai),* 42**,** 403-9.

Lichtman, A. H., Ding, H., Henault, L., Vachino, G., Camphausen, R., Cumming, D. & Luscinskas, F. W. 1997. CD45RA-RO+ (memory) but not CD45RA+RO- (naive) T cells roll efficiently on E- and P-selectin and vascular cell adhesion molecule-1 under flow. *J Immunol,* 158**,** 3640-50.

Lidington, E. A., Moyes, D. L., Mccormack, A. M. & Rose, M. L. 1999. A comparison of primary endothelial cells and endothelial cell lines for studies of immune interactions. *Transpl Immunol,* 7**,** 239-46.

Lindley, S., Dayan, C. M., Bishop, A., Roep, B. O., Peakman, M. & Tree, T. I. 2005. Defective suppressor function in CD4(+)CD25(+) T-cells from patients with type 1 diabetes. *Diabetes,* 54**,** 92-9.

Liu, Y. C., Elly, C., Yoshida, H., Bonnefoy-Berard, N. & Altman, A. 1996. Activation-modulated association of 14-3-3 proteins with Cbl in T cells. *J Biol Chem,* 271**,** 14591-5.

Lodygin, D. & Hermeking, H. 2005. The role of epigenetic inactivation of 14-3-3sigma in human cancer. *Cell Res,* 15**,** 237-46.

Loetscher, M., Gerber, B., Loetscher, P., Jones, S. A., Piali, L., Clark-Lewis, I., Baggiolini, M. & Moser, B. 1996. Chemokine receptor specific for IP10 and mig: structure, function, and expression in activated T-lymphocytes. *The Journal of Experimental Medicine,* 184**,** 963-969.

Lojda, Z. & Gossrau, R. 1980. Study on aminopeptidase A. *Histochemistry,* 67**,** 267-290.

Lopez-Dee, Z., Pidcock, K. & Gutierrez, L. S. 2011. Thrombospondin-1: Multiple Paths to Inflammation. *Mediators of Inflammation,* 2011**,** 10.

Luo, J., Zhu, Y., Zhu, M. X. & Hu, H. 2011. Cell-based Calcium Assay for Medium to High Throughput Screening of TRP Channel Functions using FlexStation 3. *Journal of Visualized Experiments : JoVE***,** 3149.

Luscinskas, F. W., Ding, H. & Lichtman, A. H. 1995a. P-selectin and vascular cell adhesion molecule 1 mediate rolling and arrest, respectively, of CD4+ T lymphocytes on tumor necrosis factor alpha-activated vascular endothelium under flow. *J Exp Med,* 181**,** 1179-86.

Luscinskas, F. W., Ding, H. & Lichtman, A. H. 1995b. P-selectin and vascular cell adhesion molecule 1 mediate rolling and arrest, respectively, of CD4+ T lymphocytes on tumor necrosis factor alpha-activated vascular endothelium under flow. *The Journal of Experimental Medicine,* 181**,** 1179-1186.

Luster, A. D., Alon, R. & Von Andrian, U. H. 2005. Immune cell migration in inflammation: present and future therapeutic targets. *Nat Immunol,* 6**,** 1182-90.

Ma, Y. R. & Ma, Y. H. 2014. MIP-1alpha enhances Jurkat cell transendothelial migration by up-regulating endothelial adhesion molecules VCAM-1 and ICAM-1. *Leuk Res,* 38**,** 1327-31.

Mackay, A. R., Ballin, M., Pelina, M. D., Farina, A. R., Nason, A. M., Hartzler, J. L. & Thorgeirsson, U. P. 1992. Effect of phorbol ester and cytokines on matrix metalloproteinase and tissue inhibitor of metalloproteinase expression in tumor and normal cell lines. *Invasion Metastasis,* 12**,** 168-84.

Maclennan, I. C. M., Toellner, K.-M., Cunningham, A. F., Serre, K., Sze, D. M. Y., Zúñiga, E., Cook, M. C. & Vinuesa, C. G. 2003. Extrafollicular antibody responses. *Immunological Reviews,* 194**,** 8-18.

Maksymowych, W. P. & Marotta, A. 2014. 14-3-3eta: a novel biomarker platform for rheumatoid arthritis. *Clin Exp Rheumatol,* 32**,** S-35-9.

Mallat, Z., Ait-Oufella, H. & Tedgui, A. 2007. Regulatory T-cell immunity in atherosclerosis. *Trends Cardiovasc Med,* 17**,** 113-8.

Marracci, G. H., Jones, R. E., Mckeon, G. P. & Bourdette, D. N. 2002. Alpha lipoic acid inhibits T cell migration into the spinal cord and suppresses and treats experimental autoimmune encephalomyelitis. *J Neuroimmunol,* 131**,** 104-14.

Matloubian, M., Lo, C. G., Cinamon, G., Lesneski, M. J., Xu, Y., Brinkmann, V., Allende, M. L., Proia, R. L. & Cyster, J. G. 2004. Lymphocyte egress from thymus and peripheral lymphoid organs is dependent on S1P receptor 1. *Nature,* 427**,** 355-60.

Matsuda, M., Shimomura, I., Sata, M., Arita, Y., Nishida, M., Maeda, N., Kumada, M., Okamoto, Y., Nagaretani, H., Nishizawa, H., Kishida, K., Komuro, R., Ouchi, N., Kihara, S., Nagai, R., Funahashi, T. & Matsuzawa, Y. 2002. Role of adiponectin in preventing vascular stenosis. The missing link of adipo-vascular axis. *J Biol Chem,* 277**,** 37487-91.

Mauri, C. & Ehrenstein, M. R. 2008. The 'short' history of regulatory B cells. *Trends in Immunology,* 29**,** 34-40.

Mazanet, M. M., Neote, K. & Hughes, C. C. 2000. Expression of IFN-inducible T cell alpha chemoattractant by human endothelial cells is cyclosporin A-resistant and promotes T cell adhesion: implications for cyclosporin A-resistant immune inflammation. *J Immunol,* 164**,** 5383-8.

Mcgettrick, H. M., Hunter, K., Moss, P. A., Buckley, C. D., Rainger, G. E. & Nash, G. B. 2009. Direct observations of the kinetics of migrating T cells suggest active retention by endothelial cells with continual bidirectional migration. *J Leukoc Biol,* 85**,** 98-107.

Meir, K. S. & Leitersdorf, E. 2004. Atherosclerosis in the Apolipoprotein E–Deficient Mouse: A Decade of Progress. *Arteriosclerosis, Thrombosis, and Vascular Biology,* 24**,** 1006-1014.

Meller, N., Liu, Y. C., Collins, T. L., Bonnefoy-Berard, N., Baier, G., Isakov, N. & Altman, A. 1996. Direct interaction between protein kinase C theta (PKC theta) and 14-3-3 tau in T cells: 14-3-3 overexpression results in inhibition of PKC theta translocation and function. *Mol Cell Biol,* 16**,** 5782-91.

Mhawech, P. 2005. 14-3-3 proteins--an update. *Cell Res,* 15**,** 228-36.

Middleton, J., Patterson, A. M., Gardner, L., Schmutz, C. & Ashton, B. A. 2002. Leukocyte extravasation: chemokine transport and presentation by the endothelium. *Blood,* 100**,** 3853-60.
Millan, J., Hewlett, L., Glyn, M., Toomre, D., Clark, P. & Ridley, A. J. 2006. Lymphocyte transcellular migration occurs through recruitment of endothelial ICAM-1 to caveola- and F-actin-rich domains. *Nat Cell Biol,* 8**,** 113-23.
Mobley, J. L., Ennis, E. & Shimizu, Y. 1994. Differential activation-dependent regulation of integrin function in cultured human T-leukemic cell lines. *Blood,* 83**,** 1039-50.
Mohammad, D. K., Nore, B. F., Hussain, A., Gustafsson, M. O., Mohamed, A. J. & Smith, C. I. 2013. Dual phosphorylation of Btk by Akt/protein kinase b provides docking for 14-3-3zeta, regulates shuttling, and attenuates both tonic and induced signaling in B cells. *Mol Cell Biol,* 33**,** 3214-26.
Moroy, T. & Karsunky, H. 2000. Regulation of pre-T-cell development. *Cell Mol Life Sci,* 57**,** 957-75.
Muller, W. A. 2003. Leukocyte-endothelial-cell interactions in leukocyte transmigration and the inflammatory response. *Trends Immunol,* 24**,** 327-34.
Munn, L. L., Melder, R. J. & Jain, R. K. 1996. Role of erythrocytes in leukocyte-endothelial interactions: mathematical model and experimental validation. *Biophysical Journal,* 71**,** 466-478.
Muslin, A. J., Tanner, J. W., Allen, P. M. & Shaw, A. S. 1996. Interaction of 14-3-3 with signaling proteins is mediated by the recognition of phosphoserine. *Cell,* 84**,** 889-97.
Nakashima, Y., Plump, A. S., Raines, E. W., Breslow, J. L. & Ross, R. 1994. ApoE-deficient mice develop lesions of all phases of atherosclerosis throughout the arterial tree. *Arterioscler Thromb,* 14**,** 133-40.
Nelimarkka, L. O., Nikkari, S. T., Ravanti, L. S., Kahari, V. M. & Jarvelainen, H. T. 1998. Collagenase-1, stromelysin-1 and 92 kDa gelatinase are associated with tumor necrosis factor-alpha induced morphological change of human endothelial cells in vitro. *Matrix Biol,* 17**,** 293-304.
Neumeier, M., Weigert, J., Schaffler, A., Wehrwein, G., Muller-Ladner, U., Scholmerich, J., Wrede, C. & Buechler, C. 2006. Different effects of adiponectin isoforms in human monocytic cells. *J Leukoc Biol,* 79**,** 803-8.
Newton, K. & Dixit, V. M. 2012. Signaling in Innate Immunity and Inflammation. *Cold Spring Harbor Perspectives in Biology,* 4.
Nhs. 2015. *Electrolyte test: Introduction* [Online]. UK. [Accessed 15.10.2015.
Noelle, R. J., Ledbetter, J. A. & Aruffo, A. 1992. CD40 and its ligand, an essential ligand-receptor pair for thymus-dependent B-cell activation. *Immunology Today,* 13**,** 431-433.
Nurmi, S. M., Gahmberg, C. G. & Fagerholm, S. C. 2006. 14-3-3 proteins bind both filamin and alphaLbeta2 integrin in activated T cells. *Ann N Y Acad Sci,* 1090**,** 318-25.
O'banion, M. K. 1999. Cyclooxygenase-2: molecular biology, pharmacology, and neurobiology. *Crit Rev Neurobiol,* 13**,** 45-82.
Ohlson, M., Sorensson, J., Lindstrom, K., Blom, A. M., Fries, E. & Haraldsson, B. 2001. Effects of filtration rate on the glomerular barrier and clearance of four differently shaped molecules. *Am J Physiol Renal Physiol,* 281**,** F103-13.
Okamoto, Y., Kihara, S., Ouchi, N., Nishida, M., Arita, Y., Kumada, M., Ohashi, K., Sakai, N., Shimomura, I., Kobayashi, H., Terasaka, N., Inaba, T., Funahashi, T.

& Matsuzawa, Y. 2002. Adiponectin reduces atherosclerosis in apolipoprotein E-deficient mice. *Circulation,* 106**,** 2767-70.
Oliver, J. D., 3rd, Anderson, S., Troy, J. L., Brenner, B. M. & Deen, W. H. 1992. Determination of glomerular size-selectivity in the normal rat with Ficoll. *J Am Soc Nephrol,* 3**,** 214-28.
Ottmann, C., Yasmin, L., Weyand, M., Veesenmeyer, J. L., Diaz, M. H., Palmer, R. H., Francis, M. S., Hauser, A. R., Wittinghofer, A. & Hallberg, B. 2007. Phosphorylation-independent interaction between 14-3-3 and exoenzyme S: from structure to pathogenesis. *EMBO J,* 26**,** 902-13.
Ouchi, N., Parker, J. L., Lugus, J. J. & Walsh, K. 2011. Adipokines in inflammation and metabolic disease. *Nat Rev Immunol,* 11**,** 85-97.
Ouedraogo, R., Gong, Y., Berzins, B., Wu, X., Mahadev, K., Hough, K., Chan, L., Goldstein, B. J. & Scalia, R. 2007. Adiponectin deficiency increases leukocyte-endothelium interactions via upregulation of endothelial cell adhesion molecules in vivo. *J Clin Invest,* 117**,** 1718-26.
Owen, J. A., Punt, J., Stranford, S. A., Jones, P. P. & Kuby, J. 2007. *Kuby immunology,* New York, W. H. Freeman.
Pacholczyk, R. & Kern, J. 2008. The T-cell receptor repertoire of regulatory T cells. *Immunology,* 125**,** 450-8.
Patching, S. G. 2014. Surface plasmon resonance spectroscopy for characterisation of membrane protein–ligand interactions and its potential for drug discovery. *Biochimica et Biophysica Acta (BBA) - Biomembranes,* 1838**,** 43-55.
Paul, A., Calleja, L. A., Camps, J., Osada, J., Vilella, E., Ferré, N., Mayayo, E. & Joven, J. 2000. The continuous administration of aspirin attenuates atherosclerosis in apolipoprotein E-deficient mice. *Life Sciences,* 68**,** 457-465.
Peake, P. & Shen, Y. 2010. Factor H binds to the N-terminus of adiponectin and modulates complement activation. *Biochem Biophys Res Commun,* 397**,** 361-6.
Pescovitz, M. D., Greenbaum, C. J., Krause-Steinrauf, H., Becker, D. J., Gitelman, S. E., Goland, R., Gottlieb, P. A., Marks, J. B., Mcgee, P. F., Moran, A. M., Raskin, P., Rodriguez, H., Schatz, D. A., Wherrett, D., Wilson, D. M., Lachin, J. M. & Skyler, J. S. 2009. Rituximab, B-lymphocyte depletion, and preservation of beta-cell function. *N Engl J Med,* 361**,** 2143-52.
Pham, T. H., Baluk, P., Xu, Y., Grigorova, I., Bankovich, A. J., Pappu, R., Coughlin, S. R., Mcdonald, D. M., Schwab, S. R. & Cyster, J. G. 2010. Lymphatic endothelial cell sphingosine kinase activity is required for lymphocyte egress and lymphatic patterning. *J Exp Med,* 207**,** 17-27.
Pham, T. H. M., Okada, T., Matloubian, M., Lo, C. G. & Cyster, J. G. 2008. S1P(1) receptor signaling overrides retention mediated by Gα(i)-coupled receptors to promote T cell egress. *Immunity,* 28**,** 122-133.
Piali, L., Weber, C., Larosa, G., Mackay, C. R., Springer, T. A., Clark-Lewis, I. & Moser, B. 1998. The chemokine receptor CXCR3 mediates rapid and shear-resistant adhesion-induction of effector T lymphocytes by the chemokines IP10 and Mig. *European Journal of Immunology,* 28**,** 961-972.
Pietschmann, P., Cush, J. J., Lipsky, P. E. & Oppenheimer-Marks, N. 1992. Identification of subsets of human T cells capable of enhanced transendothelial migration. *The Journal of Immunology,* 149**,** 1170-8.
Plump, A. S., Smith, J. D., Hayek, T., Aalto-Setala, K., Walsh, A., Verstuyft, J. G., Rubin, E. M. & Breslow, J. L. 1992. Severe hypercholesterolemia and

atherosclerosis in apolipoprotein E-deficient mice created by homologous recombination in ES cells. *Cell,* 71**,** 343-53.
Potempa, J. & Pike, R. N. 2009. Corruption of innate immunity by bacterial proteases. *J Innate Immun,* 1**,** 70-87.
Pozuelo Rubio, M., Geraghty, K. M., Wong, B. H., Wood, N. T., Campbell, D. G., Morrice, N. & Mackintosh, C. 2004. 14-3-3-affinity purification of over 200 human phosphoproteins reveals new links to regulation of cellular metabolism, proliferation and trafficking. *Biochem J,* 379**,** 395-408.
Promocell 2015. HDBEC Quality Control Data lot 2012603.3. Heidelberg, Germany.
Qi, Z., Whitt, I., Mehta, A., Jin, J., Zhao, M., Harris, R. C., Fogo, A. B. & Breyer, M. D. 2004. Serial determination of glomerular filtration rate in conscious mice using FITC-inulin clearance. *American Journal of Physiology - Renal Physiology,* 286**,** F590-F596.
Rabe, K., Lehrke, M., Parhofer, K. G. & Broedl, U. C. 2008. Adipokines and insulin resistance. *Mol Med,* 14**,** 741-51.
Rainger, G. E., Stone, P., Morland, C. M. & Nash, G. B. 2001. A novel system for investigating the ability of smooth muscle cells and fibroblasts to regulate adhesion of flowing leukocytes to endothelial cells. *J Immunol Methods,* 255**,** 73-82.
Raposo, G. & Stoorvogel, W. 2013. Extracellular vesicles: Exosomes, microvesicles, and friends. *The Journal of Cell Biology,* 200**,** 373-383.
Reis, E. D., Roqué, M., Dansky, H., Fallon, J. T., Badimon, J. J., Cordon-Cardo, C., Shiff, S. J. & Fisher, E. A. 2000. Sulindac inhibits neointimal formation after arterial injury in wild-type and apolipoprotein E-deficient mice. *Proceedings of the National Academy of Sciences,* 97**,** 12764-12769.
Resovi, A., Pinessi, D., Chiorino, G. & Taraboletti, G. 2014. Current understanding of the thrombospondin-1 interactome. *Matrix Biology,* 37**,** 83-91.
Roberts, G. W., Baird, D., Gallagher, K., Jones, R. E., Pepper, C. J., Williams, J. D. & Topley, N. 2009. Functional effector memory T cells enrich the peritoneal cavity of patients treated with peritoneal dialysis. *J Am Soc Nephrol,* 20**,** 1895-900.
Rodriguez, L. G. & Guan, J. L. 2005. 14-3-3 regulation of cell spreading and migration requires a functional amphipathic groove. *J Cell Physiol,* 202**,** 285-94.
Rollins, B. J. 1997. Chemokines. *Blood,* 90**,** 909-928.
Roviezzo, F., Brancaleone, V., De Gruttola, L., Vellecco, V., Bucci, M., D'agostino, B., Cooper, D., Sorrentino, R., Perretti, M. & Cirino, G. 2011. Sphingosine-1-phosphate modulates vascular permeability and cell recruitment in acute inflammation in vivo. *J Pharmacol Exp Ther,* 337**,** 830-7.
Ruggiero, A., Villa, C. H., Bander, E., Rey, D. A., Bergkvist, M., Batt, C. A., Manova-Todorova, K., Deen, W. M., Scheinberg, D. A. & Mcdevitt, M. R. 2010. Paradoxical glomerular filtration of carbon nanotubes. *Proc Natl Acad Sci U S A,* 107**,** 12369-74.
Ryan, G. A., Wang, C. J., Chamberlain, J. L., Attridge, K., Schmidt, E. M., Kenefeck, R., Clough, L. E., Dunussi-Joannopoulos, K., Toellner, K. M. & Walker, L. S. 2010. B1 cells promote pancreas infiltration by autoreactive T cells. *J Immunol,* 185**,** 2800-7.
Sakaguchi, S., Sakaguchi, N., Asano, M., Itoh, M. & Toda, M. 1995. Immunologic self-tolerance maintained by activated T cells expressing IL-2 receptor alpha-

chains (CD25). Breakdown of a single mechanism of self-tolerance causes various autoimmune diseases. *J Immunol,* 155**,** 1151-64.
Sakaguchi, S., Wing, K. & Yamaguchi, T. 2009. Dynamics of peripheral tolerance and immune regulation mediated by Treg. *European Journal of Immunology,* 39**,** 2331-2336.
Sallusto, F., Geginat, J. & Lanzavecchia, A. 2004. Central memory and effector memory T cell subsets: function, generation, and maintenance. *Annu Rev Immunol,* 22**,** 745-63.
Sancho, D., Yáñez-Mó, M. A., Tejedor, R. & Sánchez-Madrid, F. 1999. Activation of Peripheral Blood T Cells by Interaction and Migration Through Endothelium: Role of Lymphocyte Function Antigen-1/Intercellular Adhesion Molecule-1 and Interleukin-15. *Blood,* 93**,** 886-896.
Scallon, B., Cai, A., Solowski, N., Rosenberg, A., Song, X.-Y., Shealy, D. & Wagner, C. 2002. Binding and Functional Comparisons of Two Types of Tumor Necrosis Factor Antagonists. *Journal of Pharmacology and Experimental Therapeutics,* 301**,** 418-426.
Schierwagen, R., Maybüchen, L., Zimmer, S., Hittatiya, K., Bäck, C., Klein, S., Uschner, F. E., Reul, W., Boor, P., Nickenig, G., Strassburg, C. P., Trautwein, C., Plat, J., Lütjohann, D., Sauerbruch, T., Tacke, F. & Trebicka, J. 2015. Seven weeks of Western diet in apolipoprotein-E-deficient mice induce metabolic syndrome and non-alcoholic steatohepatitis with liver fibrosis. *Scientific Reports,* 5**,** 12931.
Schmidt, S., Moser, M. & Sperandio, M. 2013. The molecular basis of leukocyte recruitment and its deficiencies. *Molecular Immunology,* 55**,** 49-58.
Schrödinger, L. The PyMOL Molecular Graphics System, Version 1.7.4.
Scott, D. L., Wolfe, F. & Huizinga, T. W. 2010. Rheumatoid arthritis. *Lancet,* 376**,** 1094-108.
Sen, G. C. 2001. Viruses and Interferons. *Annual Review of Microbiology,* 55**,** 255-281.
Seol, G. H., Kim, M. Y., Liang, G. H., Kim, J. A., Kim, Y. J., Oh, S. & Suh, S. H. 2005. Sphingosine-1-phosphate-induced intracellular Ca2+ mobilization in human endothelial cells. *Endothelium,* 12**,** 263-9.
Shapiro-Shelef, M. & Calame, K. 2005. Regulation of plasma-cell development. *Nat Rev Immunol,* 5**,** 230-242.
Sherry, N., Hagopian, W., Ludvigsson, J., Jain, S. M., Wahlen, J., Ferry, R. J., Bode, B., Aronoff, S., Holland, C., Carlin, D., King, K. L., Wilder, R. L., Pillemer, S., Bonvini, E., Johnson, S., Stein, K. E., Koenig, S., Herold, K. C. & Daifotis, A. G. 2011. Teplizumab for treatment of type 1 diabetes (Protégé study): 1-year results from a randomised, placebo-controlled trial. *Lancet,* 378**,** 487-497.
Shevach, E. M. 2009. Mechanisms of Foxp3+ T Regulatory Cell-Mediated Suppression. *Immunity,* 30**,** 636-645.
Shimizu, Y., Newman, W., Gopal, T. V., Horgan, K. J., Graber, N., Beall, L. D., Van Seventer, G. A. & Shaw, S. 1991. Four molecular pathways of T cell adhesion to endothelial cells: roles of LFA-1, VCAM-1, and ELAM-1 and changes in pathway hierarchy under different activation conditions. *J Cell Biol,* 113**,** 1203-12.
Song, J., Tan, H., Perry, A. J., Akutsu, T., Webb, G. I., Whisstock, J. C. & Pike, R. N. 2012. PROSPER: an integrated feature-based tool for predicting protease substrate cleavage sites. *PLoS One,* 7**,** e50300.

Springer, T. A. 1994. Traffic signals for lymphocyte recirculation and leukocyte emigration: the multistep paradigm. *Cell,* 76**,** 301-14.
Springer, T. A. 1995. Traffic signals on endothelium for lymphocyte recirculation and leukocyte emigration. *Annu Rev Physiol,* 57**,** 827-72.
Stead, R. B., Lambert, J., Wessels, D., Iwashita, J. S., Leuther, K. K., Woodburn, K. W., Schatz, P. J., Okamoto, D. M., Naso, R. & Duliege, A.-M. 2006. Evaluation of the safety and pharmacodynamics of Hematide, a novel erythropoietic agent, in a phase 1, double-blind, placebo-controlled, dose-escalation study in healthy volunteers. *Blood,* 108**,** 1830-1834.
Stebbins, K. J., Broadhead, A. R., Correa, L. D., Scott, J. M., Truong, Y. P., Stearns, B. A., Hutchinson, J. H., Prasit, P., Evans, J. F. & Lorrain, D. S. 2010. Therapeutic efficacy of AM156, a novel prostanoid DP2 receptor antagonist, in murine models of allergic rhinitis and house dust mite-induced pulmonary inflammation. *Eur J Pharmacol,* 638**,** 142-9.
Stemme, S., Holm, J. & Hansson, G. K. 1992. T lymphocytes in human atherosclerotic plaques are memory cells expressing CD45RO and the integrin VLA-1. *Arterioscler Thromb,* 12**,** 206-11.
Su, A. I., Wiltshire, T., Batalov, S., Lapp, H., Ching, K. A., Block, D., Zhang, J., Soden, R., Hayakawa, M., Kreiman, G., Cooke, M. P., Walker, J. R. & Hogenesch, J. B. 2004. A gene atlas of the mouse and human protein-encoding transcriptomes. *Proc Natl Acad Sci U S A,* 101**,** 6062-7.
Suri, A., Walters, J. J., Gross, M. L. & Unanue, E. R. 2005. Natural peptides selected by diabetogenic DQ8 and murine I-A(g7) molecules show common sequence specificity. *J Clin Invest,* 115**,** 2268-76.
Tang, Q. & Bluestone, J. A. 2008. The Foxp3(+) regulatory T cell: a jack of all trades, master of regulation. *Nat Immunol,* 9**,** 239-44.
Tangye, S. G. & Tarlinton, D. M. 2009. Memory B cells: effectors of long-lived immune responses. *Eur J Immunol,* 39**,** 2065-75.
Taraboletti, G., D'ascenzo, S., Borsotti, P., Giavazzi, R., Pavan, A. & Dolo, V. 2002. Shedding of the matrix metalloproteinases MMP-2, MMP-9, and MT1-MMP as membrane vesicle-associated components by endothelial cells. *Am J Pathol,* 160**,** 673-80.
Thornhill, M. H., Wellicome, S. M., Mahiouz, D. L., Lanchbury, J. S., Kyan-Aung, U. & Haskard, D. O. 1991. Tumor necrosis factor combines with IL-4 or IFN-gamma to selectively enhance endothelial cell adhesiveness for T cells. The contribution of vascular cell adhesion molecule-1-dependent and -independent binding mechanisms. *The Journal of Immunology,* 146**,** 592-8.
Thucydides, Crawley, R. & Thucydides 1910. *History of the Peloponnesian war,* London, J.M. Dent E.P. Dutton.
Ticchioni, M., Charvet, C., Noraz, N., Lamy, L., Steinberg, M., Bernard, A. & Deckert, M. 2002. Signaling through ZAP-70 is required for CXCL12-mediated T-cell transendothelial migration. *Blood,* 99**,** 3111-3118.
Tous, M., Ferre, N., Camps, J., Riu, F. & Joven, J. 2005. Feeding apolipoprotein E-knockout mice with cholesterol and fat enriched diets may be a model of non-alcoholic steatohepatitis. *Mol Cell Biochem,* 268**,** 53-8.
Trocmé, C., Gaudin, P., Berthier, S., Barro, C., Zaoui, P. & Morel, F. 1998. Human B Lymphocytes Synthesize the 92-kDa Gelatinase, Matrix Metalloproteinase-9. *Journal of Biological Chemistry,* 273**,** 20677-20684.
Tsatsanis, C., Zacharioudaki, V., Androulidaki, A., Dermitzaki, E., Charalampopoulos, I., Minas, V., Gravanis, A. & Margioris, A. N. 2005. Adiponectin induces TNF-

alpha and IL-6 in macrophages and promotes tolerance to itself and other pro-inflammatory stimuli. *Biochem Biophys Res Commun,* 335**,** 1254-63.

Tull, S. P., Yates, C. M., Maskrey, B. H., O'donnell, V. B., Madden, J., Grimble, R. F., Calder, P. C., Nash, G. B. & Rainger, G. E. 2009. Omega-3 Fatty acids and inflammation: novel interactions reveal a new step in neutrophil recruitment. *PLoS Biol,* 7**,** e1000177.

U.S. Food and Drug Administration. 2010. *FDA approves first oral drug to reduce MS relapses.* [Online]. Available: http://www.fda.gov/NewsEvents/Newsroom/PressAnnouncements/ucm226755.htm.

Umbricht, C. B., Evron, E., Gabrielson, E., Ferguson, A., Marks, J. & Sukumar, S. 2001. Hypermethylation of 14-3-3 sigma (stratifin) is an early event in breast cancer. *Oncogene,* 20**,** 3348-53.

Valentine, W. J. & Tigyi, G. 2012. High-throughput assays to measure intracellular Ca(2)(+) mobilization in cells that express recombinant S1P receptor subtypes. *Methods Mol Biol,* 874**,** 77-87.

Van Den Steen, P. E., Proost, P., Wuyts, A., Van Damme, J. & Opdenakker, G. 2000. Neutrophil gelatinase B potentiates interleukin-8 tenfold by aminoterminal processing, whereas it degrades CTAP-III, PF-4, and GRO-alpha and leaves RANTES and MCP-2 intact. *Blood,* 96**,** 2673-81.

Van Heusden, G. P. 2005. 14-3-3 proteins: regulators of numerous eukaryotic proteins. *IUBMB Life,* 57**,** 623-9.

Venkataraman, K., Lee, Y. M., Michaud, J., Thangada, S., Ai, Y., Bonkovsky, H. L., Parikh, N. S., Habrukowich, C. & Hla, T. 2008. Vascular endothelium as a contributor of plasma sphingosine 1-phosphate. *Circ Res,* 102**,** 669-76.

Veronese, F. M. & Pasut, G. 2005. PEGylation, successful approach to drug delivery. *Drug Discov Today,* 10**,** 1451-8.

Von Andrian, U. H., Chambers, J. D., Berg, E. L., Michie, S. A., Brown, D. A., Karolak, D., Ramezani, L., Berger, E. M., Arfors, K. E. & Butcher, E. C. 1993. L-selectin mediates neutrophil rolling in inflamed venules through sialyl LewisX-dependent and -independent recognition pathways. *Blood,* 82**,** 182-91.

Vranken, W. F., Boucher, W., Stevens, T. J., Fogh, R. H., Pajon, A., Llinas, M., Ulrich, E. L., Markley, J. L., Ionides, J. & Laue, E. D. 2005. The CCPN data model for NMR spectroscopy: development of a software pipeline. *Proteins,* 59**,** 687-96.

Weninger, W., Crowley, M. A., Manjunath, N. & Von Andrian, U. H. 2001. Migratory Properties of Naive, Effector, and Memory Cd8(+) T Cells. *J Exp Med,* 194**,** 953-66.

Werle, M. & Bernkop-Schnurch, A. 2006. Strategies to improve plasma half life time of peptide and protein drugs. *Amino Acids,* 30**,** 351-67.

Wilker, E. & Yaffe, M. B. 2004. 14-3-3 Proteins--a focus on cancer and human disease. *J Mol Cell Cardiol,* 37**,** 633-42.

Wu, B., Crampton, S. P. & Hughes, C. C. W. 2007. Wnt Signaling Induces Matrix Metalloproteinase Expression and Regulates T Cell Transmigration. *Immunity,* 26**,** 227-239.

Yamauchi, T., Kamon, J., Ito, Y., Tsuchida, A., Yokomizo, T., Kita, S., Sugiyama, T., Miyagishi, M., Hara, K., Tsunoda, M., Murakami, K., Ohteki, T., Uchida, S., Takekawa, S., Waki, H., Tsuno, N. H., Shibata, Y., Terauchi, Y., Froguel, P., Tobe, K., Koyasu, S., Taira, K., Kitamura, T., Shimizu, T., Nagai, R. & Kadowaki, T. 2003. Cloning of adiponectin receptors that mediate antidiabetic metabolic effects. *Nature,* 423**,** 762-9.

Yang, M., Rui, K., Wang, S. & Lu, L. 2013. Regulatory B cells in autoimmune diseases. *Cell Mol Immunol,* 10**,** 122-132.

Yoshimura, T., Robinson, E. A., Appella, E., Matsushima, K., Showalter, S. D., Skeel, A. & Leonard, E. J. 1989. Three forms of monocyte-derived neutrophil chemotactic factor (MDNCF) distinguished by different lengths of the amino-terminal sequence. *Mol Immunol,* 26**,** 87-93.

Zerr, I., Bodemer, M., Gefeller, O., Otto, M., Poser, S., Wiltfang, J., Windl, O., Kretzschmar, H. A. & Weber, T. 1998. Detection of 14-3-3 protein in the cerebrospinal fluid supports the diagnosis of Creutzfeldt-Jakob disease. *Ann Neurol,* 43**,** 32-40.

Zhang, X., Nakajima, T., Goronzy, J. J. & Weyand, C. M. 2005. Tissue trafficking patterns of effector memory CD4+ T cells in rheumatoid arthritis. *Arthritis Rheum,* 52**,** 3839-49.

Zhou, X., Nicoletti, A., Elhage, R. & Hansson, G. K. 2000. Transfer of CD4+ T Cells Aggravates Atherosclerosis in Immunodeficient Apolipoprotein E Knockout Mice. *Circulation,* 102**,** 2919-2922.

APPENDIX

Peer-reviewed articles

- M. Chimen*, H.M. McGettrick*, **B. Apta,** S.J. Kuravi, C. M. Yates, A. Kennedy, A. Odedra, M. Alassiri, M. Harrison, A. Martin, F. Barone, S. Nayar, J.R. Hitchcock, A.F. Cunningham, K. Raza, A. Filer, D.A. Copland, A.D. Dick, J. Robinson, N. Kalia, L.S.K. Walker, C.D. Buckley, G.B. Nash, P. Narendran, and G. Ed. Rainger (2015). Homeostatic regulation of T cell trafficking by a B cell derived peptide is impaired in autoimmune and chronic inflammatory disease. *Nature Medicine* (e-pub ahead of print - doi:10.1038/nm.3842) ** joint authorship,*

Published abstracts

- **B. Apta**, M. Chimen, M. Harrison, H.M. McGettrick, P. Narendran, P.F. Lalor and G.E. Rainger (2015) Investigating the pharmacokinetics and therapeutic potential of PEPITEM: a novel peptide inhibitor of T cell transmigration. *Immunology (ahead of press)* ***(£50 travel grant from PromoCell, Germany).***

Abstracts

- **B. Apta**, M. Chimen, M. Harrison, H.M. McGettrick, P. Narendran and G.E. Rainger (March 2015) Investigating the therapeutic potential of PEPITEM: a novel inhibitor of T cell trafficking. *Keystone Symposium: T cells: Regulation and effector function, Utah, USA* ***(£500 travel grant from University of Birmingham, £1000 travel grant from British Society for Immunology)***
- **B. Apta**, M. Chimen, M. Harrison, H.M. McGettrick, P. Narendran and G.E. Rainger (March 2015) Establishing the pharmacokinetic properties of PEPITEM: a novel inhibitor of T cell transmigration. *College of Medial & Dental Sciences Research Gala, University of Birmingham, UK*
- **B. Apta**, M. Chimen, M. Harrison, H.M. McGettrick, P. Narendran and G.E. Rainger (February 2015) Establishing the pharmacology of PEPITEM; Peptide Inhibitor of T-cell Transendothelial Migration. British Society for Immunology: 2nd *Leukocyte Migration Affinity Group meeting, University of Birmingham*, UK
- **Apta B,** Chimen, M., Harrison, M. J., McGettrick, H. M., Martin, A., Narandren P., Rainger, G. E. (2014) The development of PEPITEM, a novel peptide inhibitor of T cell trafficking, for therapeutic use. *16th Imperial College London Vascular Endothelium Symposium, Imperial College London, UK*
- **Apta B,** Chimen, M., Harrison, M. J., McGettrick, H. M., Martin, A., Narandren P., Rainger, G. E. (2013) The development of PEPITEM, a novel peptide inhibitor of T cell trafficking, for therapeutic use. *UK Adhesion Society Meeting, University of Birmingham, UK*